HYDROMETEOROLOGICAL REPORT NO. 36

INTERIM REPORT

PROBABLE MAXIMUM PRECIPITATION IN CALIFORNIA

REPRINTED WITH REVISIONS OF OCTOBER 1969

HYDROMETEOROLOGICAL REPORTS

(Nos. 6–22 Numbered Retroactively)

*No. 1. Maximum possible precipitation over the Ompompanoosuc Basin above Union Village, Vt. 1943.
*No. 2. Maximum possible precipitation over the Ohio River Basin above Pittsburgh, Pa. 1942.
*No. 3. Maximum possible precipitation over the Sacramento Basin of California. 1943.
*No. 4. Maximum possible precipitation over the Panama Canal Basin. 1943.
*No. 5. Thunderstorm rainfall. 1947.
*No. 6. A preliminary report on the probable occurrence of excessive precipitation over Fort Supply Basin, Okla. 1938.
*No. 7. Worst probable meteorological condition on Mill Creek, Butler and Hamilton Counties, Ohio. 1937. (Unpublished.) Supplement, 1938.
*No. 8. A hydrometeorological analysis of possible maximum precipitation over St. Francis River Basin above Wappapello, Mo. 1938.
*No. 9. A report on the possible occurrence of maximum precipitation over White River Basin above Mud Mountain Dam site, Wash. 1939.
*No. 10. Maximum possible rainfall over the Arkansas River Basin above Caddoa, Colo. 1939. Supplement, 1939.
*No. 11. A preliminary report on the maximum possible precipitation over the Dorena, Cottage Grove, and Fern Ridge Basins in the Willamette Basin, Oreg. 1939.
*No. 12. Maximum possible precipitation over the Red River Basin above Denison, Tex. 1939.
*No. 13. A report on the maximum possible precipitation over Cherry Creek Basin in Colorado. 1940.
*No. 14. The frequency of flood-producing rainfall over the Pajaro River Basin in California. 1940.
*No. 15. A report on depth-frequency relations of thunderstorm rainfall on the Sevier Basin, Utah. 1941.
*No. 16. A preliminary report on the maximum possible precipitation over the Potomac and Rappahannock River Basins. 1943.
*No. 17. Maximum possible precipitation over the Pecos Basin of New Mexico. 1944. (Unpublished.)
*No. 18. Tentative estimates of maximum possible flood-producing meteorological conditions in the Columbia River Basin. 1945.
*No. 19. Preliminary report on depth-duration-frequency characteristics of precipitation over the Muskingum Basin for 1- to 9-week periods. 1945.
*No. 20. An estimate of maximum possible flood-producing meteorological conditions in the Missouri River Basin above Garrison Dam site. 1945.
*No. 21. A hydrometeorological study of the Los Angeles area. 1939.
*No. 21A. Preliminary report on maximum possible precipitation, Los Angeles area, California. 1944.
*No. 21B. Revised report on maximum possible precipitation, Los Angeles area, California. 1945.
*No. 22. An estimate of maximum possible flood-producing meteorological conditions in the Missouri River Basin between Garrison and Fort Randall. 1946.
*No. 23. Generalized estimates of maximum possible precipitation over the United States east of the 105th meridian, for areas of 10, 200, and 500 square miles. 1947.
*No. 24. Maximum possible precipitation over the San Joaquin Basin, Calif. 1947.
*No. 25. Representative 12-hour dewpoints in major United States storms east of the Continental Divide. 1947.
*No. 25A. Representative 12-hour dewpoints in major United States storms east of the Continental Divide. 2d edition. 1949.
*No. 26. Analysis of winds over Lake Okeechobee during tropical storm of August 26–27, 1949. 1951.
*No. 27. Estimate of maximum possible precipitation, Rio Grande Basin, Fort Quitman to Zapata. 1951.
*No. 28. Generalized estimate of maximum possible precipitation over New England and New York. 1952.
*No. 29. Seasonal variation of the standard project storm for areas of 200 and 1,000 square miles east of 105th meridian. 1953.
No. 30. Meteorology of floods at St. Louis. 1953. (Unpublished.)
No. 31. Analysis and synthesis of hurricane wind patterns over Lake Okeechobee, Florida. 1954.
No. 32. Characteristics of United States hurricanes pertinent to levee design for Lake Okeechobee, Florida. 1954.
No. 33. Seasonal variation of the probable maximum precipitation east of the 105th meridian for areas from 10 to 1,000 square miles and durations of 6, 12, 24, and 48 hours. 1956.
No. 34. Meteorology of flood-producing storms in the Mississippi River Basin. 1956.
No. 35. Meteorology of hypothetical flood sequences in the Mississippi River Basin. 1959.
No. 36. Interim report—Probable maximum precipitation in California.
No. 37. Meteorology of hydrologically critical storms in California. (In preparation.)
No. 38. Meteorology of flood-producing storms in the Ohio River Basin. 1961.

---

* Out of print.

U.S. Department of Commerce
Weather Bureau

U.S. Department of Army
Corps of Engineers

HYDROMETEOROLOGICAL REPORT NO. 36

INTERIM REPORT

PROBABLE MAXIMUM PRECIPITATION IN CALIFORNIA

REPRINTED WITH REVISIONS OF OCTOBER 1969

Prepared by

Hydrometeorological Section
Hydrologic Services Division
U.S. Weather Bureau

Washington, D.C.
October 1961

TABLE OF CONTENTS

FIGURES

iv

FIGURES (Cont'd.)

*Please see the revision dated October 1969 of figure 5-35 that is included at the end of this publication.

Chapter I

AUTHORIZATION AND PURPOSE

Purpose of report

1.01. The purpose of this report is to present criteria for estimating probable maximum precipitation over basins above prospective flood-control structures in the Pacific drainage of California. Similar generalized criteria were previously prepared by the Hydrometeorological Section for the area of the United States east of the 105th meridian in Hydrometeorological Reports Nos. 23 and 33, (1) and (2), for the Corps of Engineers and by the Cooperative Studies Section of the Weather Bureau for the United States west of the 105th meridian in Weather Bureau Technical Paper No. 38 (3) for the Soil Conservation Service. The latter report includes California, but of necessity covers that area in less detail than the present report.

Authorization

1.02. The authorization for this study is contained in a memorandum from the Office of Chief of Engineers dated August 13, 1956, which states: "Work should be initiated in the immediate future as follows: (1) The Hydrometeorological Section will study orographic precipitation for the entire Pacific Coast area, applying the latest meteorological techniques and utilizing data from the latest storms, especially those of 1950 and 1955. The probable maximum precipitation studies by the Hydrometeorological Section will be concentrated primarily in the Sacramento-San Joaquin River Basin. Probable maximum precipitation, coincidental snow cover, and the temperatures and winds throughout the storm period will be furnished by the Hydrometeorological Section."

In later conferences between representatives of the Corps of Engineers and the Weather Bureau it was agreed that the studies should be extended to all of the Pacific drainage of California as the area of first priority, with a view to eventual further extension to derive consistent patterns of probable maximum precipitation values along the Pacific Coast from the Columbia Basin south to Los Angeles.

It was also agreed that studies had progressed to the point where this volume should be published as an interim report. It was intended that a final report later would encompass refinements of certain procedures. There were no apparent reasons for anticipating major changes in over-all results in the final report.

Scope of this report

1.03. Criteria are developed for obtaining estimates of probable maximum precipitation for storm durations up to 72 hours, for basin areas up to several thousand square miles throughout the Pacific drainage, by months through the primary precipitation season of October through April. The question of intense local storms outside the primary precipitation season exceeding these criteria is discussed in chapter II. The more general topographic features are taken into account to the extent feasible. The possible effects of lesser topographic variations on individual basins are discussed in chapter II.

Snowmelt is an important contributor to floods at some seasons over some basins in California. Values of wind and temperature that may be expected preceding and during probable maximum storm conditions at various elevations are derived for the purpose of computing snowmelt. The possible depth of the antecedent snow cover is not covered.

Organization of this report

1.04. Those problems incident to estimating probable maximum precipitation (PMP) in California which the user should take into account in evaluating the final PMP values are reviewed in chapter II. The meteorological characteristics of California storms that are most indicative of PMP conditions are summarized in chapter III and are analyzed in more detail in a separate report (see below). Those characteristics are applied to developing specific criteria for PMP storms of the two primary types, convergence and orographic (chapters IV and V) and are followed by the criteria for their combination into one storm event (chapter VII). A collection of checks on the PMP (chapter VIII) and comparison with other data give the user further aid in appraising the values. These include a discussion of the maximization steps as a whole, comparison with maximum observed values, statistical checks, relation to Standard Project values, and comparison with other PMP estimates. For convenience in computing PMP values for a specific basin from the various charts and nomograms, the requisite steps, discussed in detail at various places in the report, are collected together in a working list in chapter IX.

The special problems associated with spillover, the drift of precipitation with the wind across the crest of a mountain, are treated in chapter VI.

The final chapter covers dew point and wind criteria for snowmelt.

Relation to Hydrometeorological Report No. 37

1.05. Development of the California PMP required extensive analysis of the nature of precipitation storms that have affected the state in the past. Much of the results of this part of the investigation have been placed in a separate volume, Hydrometeorological Report No. 37, under the title "Meteorological Characteristics of Hydrologically-Critical Storms in California" (4). The frequent references to that report in the present volume are abbreviated "HMR 37."

Chapter II

APPRAISAL OF PROBABLE MAXIMUM PRECIPITATION PROBLEM

2.01. The purpose of this chapter is to point out the special characteristics of the PMP problem in California as compared with that in other areas, to indicate the physical, synoptic, and statistical facts and analyses that have been made and to give some perspective as to how these facts and analyses influence the estimates.

Elements of PMP estimates

2.02. <u>Maximum precipitation data in region</u>. The first basic data for probable maximum precipitation estimates in any region at any season are the greatest depths of precipitation that have been observed in that region or a climatologically and topographically similar region at that season. These values are sometimes viewed by the casual investigator as approaching the upper limit of precipitation potential for the region. In reality these data are an unequivocal <u>lower bound</u> to the estimate of the probable maximum precipitation.

2.03. <u>Maximum precipitation data in adjacent regions</u>. Maximum observed depths of precipitation in one place are not only obvious clues to the climate at that place but also are clues to the climate of adjacent regions. In estimates of probable maximum precipitation considerable reliance is placed on increasing the data applicable to a particular basin by <u>transposition</u> of observed maximum precipitation depths from one location or season to another location or season, with appropriate adjustments for topographic and meteorological differences. The limitation on this technique is the reliability with which the adjustment factors can be devised. In large quasi-homogeneous regions such as the Central Mississippi Valley simple adjustment factors suffice. More complex procedures are required in regions of rugged topography, such as most of California. In the development of criteria for Standard Project Storms, the Sacramento District of the Corps of Engineers transposed orographic storms by use of adjustment factors derived from a map of 3-day point precipitation depths with a mean recurrence interval of ten years (5) (6). The pattern of isopleths on this map is similar to that on a chart of mean annual precipitation. Transposition of orographic storms is indirect in the present report but nontheless is an inherent part of the procedure. Orographic PMP is hypothesized from a model which incorporates seasonal, latitudinal, and topographic variations. The model is then calibrated against selected major orographic storms. This procedure has the effect of transposing the selected storms to other areas with appropriate adjustments for latitude, season, and topography.

In a statistical approach referred to in chapter VIII the transposed factor is a statistical parameter related to rainfall variation.

2.04. <u>Maximization</u>. The storms are extended to probable maximum values after investigation has devised both a "how" and "how far."

The "how" consists of a storm model which relates extreme precipitation to measurable variables which may be regarded as causes of the precipitation. Present knowledge does not yet account for all aspects of precipitation formation in a quantitative way, therefore the model is a combination of established physical or statistical laws and judicious hypotheses. Development of the appropriate storm model for maximization is the most complex aspect of estimating probable maximum precipitation. The same basic model is used for storm transposition as for maximization. In application, parallel parts of both adjustments can be combined into a single computation.

The "how far" is the specification of the maximum values of the variables to which precipitation is related by the model. These limits are always based ultimately on observations of climatological parameters, appropriately organized and analyzed, and are therefore empirical. There are no purely theoretical limits. An example of an appropriate observed climatological parameter of a statistical character is the standard deviation of the series of the maximum annual point 24-hour depths at a station. Examples of parameters of a more physical character as employed in this report are maximum surface dew points and maximum wind speeds at various levels. Examples of other physical parameters not employed explicitly in this report that might be used with a different physical model are sea-surface temperature, length of wind fetch over water, and elevations of tops of cumulonimbus clouds.

The limiting values of each parameter must be set with due regard for compatibility with other parameters. This is discussed in paragraph 2.08.

2.05. <u>Relation of storm sample to maximization</u>. The number of precipitation storms that give useful clues to the precipitation potential over a particular basin is limited by several factors. These are the frequency and areal extent of severe storms, the density and length of record of precipitation gages, and the size of geographical areas and duration of season from which reliable transpositions can be made.

Severe limitation of storm sample pertain to intense local precipitation in California, both local storms and intense-precipitation centers of large-area storms. Insolation and low-level moisture are at a maximum during the summer but storm mechanisms (convergent windflows and instability) are infrequent during this dry season, and are most prevalent during cooler times of lesser specific humidity. Optimum combinations prevail only occasionally. Further, intense local storms in all but the middle of the Central Valley and a few plains in Southern California tend to be combined with orographic effects which becloud their transposability. The restricted sample of transposable values makes necessary a compensatory liberal degree of maximization of the sample storms, of the use of inferences from other regions, or both.

Other limitations on sample apply to major storms of a more orographic nature. These are the small windward-slope areas of California relative to accepted transposition areas in less rugged regions, complexity of transposition factors in mountainous regions, and the wide spacing of precipitation gages in relation to topographic variations. The last factor makes it likely that the highest centers of past storms are unrecorded. An indication of the effect of the first factor is presented in chapter VIII where maximum observed storm values in the eastern United States in areas the size and shape of the Pacific drainage of California are compared with accepted estimates of the PMP in the same areas.

2.06. <u>Objectives</u>. Appraisal of a generalized estimate of probable maximum precipitation is clarified if the objectives of the estimate are divided into two parts--creation of internal consistency and development of the appropriate general level of probable maximum precipitation. The distinction is particularly pertinent in California and other regions of rugged terrain.

2.07. <u>Internal consistency</u>. "Internal consistency" refers primarily to assessing the variation of the PMP within a geographical region as related to topographic and meteorological factors. Good internal consistency indirectly brings a large amount of data and thought to bear on the estimated value of PMP for a particular basin. It also supports consistency of design policy by tending to give equivalent safety factors for equivalent projects at differing locations. "Internal consistency" can also refer to consistency over storm duration, for example 6-hour duration vs. 24-hour duration, and over area, for example, 10 square miles vs. 500 square miles.

Consistency between adjacent topographic subdivisions is related to synoptic meteorological problems on the behavior of storms and geographical variations. For example Central Valley vs. windward Sierra slope areas involve the problem of relative roles of convergence and orographic precipitation, to be discussed later. San Gabriel Mountains in Southern California vs. Santa Lucia Range on the middle coast involves over-all latitudinal variations of storm intensities and tracks among other factors.

Refinement of internal consistency within each of the major topographic subdivisions of California in a generalized study such as this one is primarily limited by time and manpower for localized physical and statistical investigations of the response of wind, rainfall, temperature, and other meteorological variables to the local topography. In a particularized study for an individual basin the limitation would be the lack of closely spaced measurements on either rain or wind variations about local topographic features.

2.08. <u>General level</u>. The "general level" pertains to the over-all magnitude of the internally consistent values of PMP. It is the upper limit of precipitation produced by a complex natural process comprised of many

6

factors in optimum combination. Determination of the "optimum combination" is a matter of judgment taking into account a variety of factors.

The kinds of judgment required are suggested by describing a too-liberal and a too-restrictive maximization. The too-liberal maximization would combine the probable maximum values of each of several identifiable and measureable variables. This would compound probabilities excessively and might also introduce meteorological incompatibilities. By compounding probabilities excessively is meant combining events each so rare that their simultaneous occurrence clearly crosses from the ill-defined "probable" far into the zone of events so nearly impossible that man does not take measures against them. An example of a meteorological incompatibility would be combining maximum winds with maximum moisture in regions where one is characteristic only of northwest windflow and the other only of southwesterly or southerly flow. The too-restrictive maximization would attempt to insure realism by relating the optimum maximum combination of precipitation-producing variables to maximum observed combinations, for example, observed maximum simultaneous occurrence of high wind and high moisture. But the result of this approach if carried to its ultimate conclusion would be to equate the largest observed storm to the PMP!

Other factors influencing the judgment in the matter of general level are the exceedance over maximum observed values in comparison with other regions where PMP values have been adopted and the synoptic meteorological judgments relative to PMP that were made in the other regions.

2.09. Climatic trends. Changes or trends in climate throughout the world during the last several centuries have been so slight in comparison with other uncertainties in estimating probable maximum precipitation that they are entirely negligible. For spillway design purposes it is assumed with a high degree of confidence that the requirement is to assess the present climate with respect to potential for producing precipitation.

PMP methods

2.10. Physical-synoptic PMP method. The primary method of this report relates precipitation to other meteorological factors. The relationships are organized into a model. The relationships include the more simple known physical laws of precipitation formation and the characteristics of weather behavior in the particular geographic region revealed by synoptic weather maps. The model is extended to PMP values as described in paragraph 2.04. This method has been found to provide the broadest guidance in the crucial step of application of subjective judgment to "how far" and is the reason it is employed in this report and all previous PMP reports by the Hydrometeorological Section. Another advantage is the systematic accounting for the topography and the incorporation of a larger body of climatological data into the solution of the problem. Disadvantages are the multiplicity of hypotheses required and the extensive labor. Simple statistical procedures are used within the physical-synoptic method to analyze various climatological factors.

2.11. <u>Statistical PMP method</u>. In this report one statistical approach to PMP is used as a supplement and a check. This is covered in chapter VIII. Statistical approaches take into account each of the elements described in paragraphs 2.02-2.08 by statistical analysis of precipitation data. The most complex statistical theory that the data warrant may be used. A convenience of statistical methods is that a minimum number of hypotheses and assumptions are required. The precipitation data alone become the clues or indices of the behavior of the pertinent natural processes. The counterpart of a storm model is an assumed distribution of a statistical parameter. The statistical method provides an additional point of view in making the "how far" judgment. No provision has been made for estimating values between precipitation observing stations other than interpolation, though statistical relations of precipitation on PMP to topography are theoretically possible.

Limitation on storm types

2.12. <u>Cool-season storms</u>. Most flood-producing storms in California occur during the cool season from fall through spring and are associated with the existence offshore or the passage through California of cyclonic disturbances or Lows. This broad category, which releases both orographic rain from winds over the mountains and rain from meteorological processes not directly related to the mountains, is discussed in detail in chapter III. The specific values of PMP derived in this report are from the cool-season storm as the prototype, after due consideration of the other types described below.

2.13. <u>Tropical storm</u>. Tropical storms (hurricanes) occasionally invade California. The most recent to produce significant rain was in 1939, near Los Angeles. That the residual upper-level circulation of a hurricane can reach Northern California, though this is more rare, is shown by the storm of September 12-14, 1918, which was of essentially tropical origin. Both of these storms are described in HMR 37. It is the opinion of the authors of this report for the reasons set forth in the next chapter, that the total volume of precipitation from a tropical storm in any part of California would not appreciably exceed what could also occur in severe cool-season storms. Tropical storms can therefore be omitted from this report, which is primarily directed toward estimating the all-season probable maximum precipitation for basins. Tropical storms should not be overlooked if <u>summer</u> flows or volumes are of particular significance, especially in Southern California.

2.14. <u>Local summer convective storms</u>. Intense local summer-type thunderstorms are rare in California because of the dominance of the precipitation-inhibiting East Pacific High. However, the State is not entirely immune to this type of storm, as exemplified by a storm at Campo near the Mexican border that produced over eleven inches of rain in 80 minutes in August. Such storms can exist only during periods of sluggish general air flow when the East Pacific High has weakened or has been displaced from its normal position and are therefore not supported by strong inflows to replace precipitated moisture. Lacking such support they feed on the locally present instability and moisture and are therefore limited severely in the area and

duration they can encompass, and do not occur with an intensity equilavent
to the Campo storm as part of a more general storm. Such storms are the
prototype of the PMP only over very small watersheds for durations up to one
or two hours, during the summer season. These storms have not been assessed
in this report in order to concentrate on other problems. The user of this
report should obtain separate estimates of short-duration small-area summer
PMP for watersheds where such storms might produce more critical floods than
the generalized cool-season estimates of this report.

Characteristics of California storms and application to PMP

2.15. Large California storms require properly oriented pressure
gradients, adequate moisture, and lifting mechanisms, both topographic and
those inherent in the storm circulation itself.

2.16. _Pressure gradient and wind._ A large California storm requires a
strong persisting pressure gradient of favorable orientation for rapid lift-
ing of air over mountain barriers. The primary guides to onshore wind com-
ponents in a probable maximum storm are maximum observed winds at various
levels and maximum pressure gradients. The latter are related to wind by
the theoretical geostrophic relationship and also by empirical studies of
the interrelationship at California stations where the influence of the moun-
tains extends to considerable height. Development of maximum wind criteria
is covered in chapter V.

2.17. _Moisture._ Large California storms require an adequate supply of
moisture. The primary guides to maximum moisture content of the air in as-
sociation with maximum winds are maximum observed surface dew points. Maxi-
mum coastal dew points are applied to the Coast Range and Southern Califor-
nia. The maximum moisture criteria for the Central Valley and Sierras are
defined by Central Valley dew points. The development, use, and reasoning
behind the dew point criteria are covered in chapter IV.

2.18. _Lifting mechanisms._ Heavy precipitation requires that near-
saturated air be lifted on a vast scale. The lifted air cools adiabatically,
thus lowering its capacity to contain water vapor. This lifting can be as-
cribed to three causes: orographic, horizontal convergence including frontal
lifting, and instability. All are found in major California cool-season
storms.

1. Orographic lifting. The influence of topography as a lifting me-
chanism is obvious from a glance at charts of the geographical distribution
of mean annual precipitation; a similar effect is noted in most storms. Esti-
mates of maximum orographic effect are related to estimates of both maximum
component of wind normal to barriers and to moisture. The many complicating
factors are treated in chapter V.

2. Horizontal convergence. Stated in simple terms, when horizontal air
streams converge, vertical motion is required to carry off the air. Such
convergence takes place primarily in the vicinity of low pressure areas and

troughs. Convergence mechanisms may be identified by hourly rainfall measurements at the ground as patterns moving more or less independent of topography.

The primary guide to the magnitude of the precipitation possible from horizontal convergence is maximum observed point precipitation at stations in California where orographic influence is at a minimum and in storms where instability contribution (see next paragraph) is thought to be slight. Because of the paucity of such data, that from other regions must be considered also, especially with respect to variation of precipitation depth with size of basin.

3. Instability. The most impressive release of instability is in a thunderstorm. A lesser degree of instability facilitates moderate or heavy precipitation without thunder or lightning. Instability in California storms results primarily from offshore heating and moistening of air from below as it travels from a more northerly latitude over progressively warmer water. Lifting by horizontal convergence, fronts or orography may facilitate its release. Inflowing air in California storms from a more southerly latitude tends to be more stable as the trajectory is over progressively colder water. Thus the inflow direction favoring maximum moisture does not favor maximum instability.

2.19. Evaluation of orographic and convergence precipitation. In this report convergence PMP and orographic PMP are evaluated separately, then combined. It is intended that each of the separate evaluations be an index of processes existing in a combined storm. The definitions adopted to carry out this purpose are given in paragraph 3.01.

Separate evaluation of the orographic and convergence PMP permits separate definition of the respective variations with season, size of basin, geographical location, elevation, and storm duration.

2.20. Combination of orographic and convergence PMP. The two are combined by adding together. Care has been taken to minimize the contamination of the data used in the development of each by the opposite process.

Storm types which illustrate the simultaneous occurrence of orographic and convergence precipitation are described in chapter III. Further discussion of considerations for combination are contained in chapters IV and VII.

Use of report

2.21. Use related to method of development. Use of the values given in this report should be consistent with the methods employed to derive

them. It is again necessary to refer to the distinction between "general level" and "internal consistency." The applicability of each to the particular project should be considered separately.

2.22. Topographic detail. The design engineer would first assess the internal consistency as applied to his basin, that is, does the degree of detail in the report appear to adequately cover his basin in view of the real topographic variations and his requirements? The degree of topographic detail taken into account in this report is indicated by the orographic index map, figure 5-35. Basins with more critical topography than the general topographic variations indicated by figure 5-35 would be expected to have higher values of PMP than the report indicates while more sheltered, even with due regard for spillover, might have lesser values. In other words, no geographical safety factor has been introduced into the report to take care of localities that are topographically more critical than a generalized view of the topography would indicate and the user should consider this possibility, and whether further more detailed studies are needed.

2.23. General level. The designer would next consider the general level and its pertinence to his requirements. The meteorological aspect of the over-all PMP problem in California and the particular solutions presented in this report are covered in some detail for the necessary purpose of permitting the design engineer user to acquire some feel for the meteorological judgment factors involved. He will then be in a position to decide, in view of the degree to which risk has been eliminated in the PMP values furnished in the report, and in view of the particular requirement of his project, whether the PMP values should be adopted for his design, should be adjusted one way or the other, or whether further studies are required.

Relation to other PMP reports

2.24. This report is intended to serve purposes similar to those served by two previous Weather Bureau reports. These are Hydrometeorological Report No. 33, "Seasonal Variation of the Probable Maximum Precipitation East of the 105th Meridian for Areas from 10 to 1,000 Square Miles and Durations of 6, 12, 24 and 48 Hours" (2), and by Weather Bureau Technical Paper No. 38, "Generalized Estimates of Probable Maximum Precipitation West of the 105th Meridian for Areas to 400 Square Miles and Durations to 24 Hours" (3). Probable maximum precipitation is intended to be defined in the same way in the three reports. Technical Paper No. 38 and the early parts of the present report were in preparation at the same time, by different groups of meteorologists of the Weather Bureau but working in close consultation. Technical Paper No. 38 is restricted to maximum areas of 400 square miles and durations of 24 hours in accordance with the primary design problems of the supporting agency, the Soil Conservation Service. The present report extends to larger areas and longer durations in accordance with the needs of the supporting agency, the Corps of Engineers.

Comparisons are given in this report between the PMP values here and those presented in Technical Paper No. 38 for the zone of geographical overlap and corresponding storm areas and durations.

Numerical accuracy

2.25. Precipitation depths, windspeeds, dew points, and other variables are assigned numerical values to three significant figures throughout the report. Most of these numbers are indices of postulated natural conditions rather than measurements, and therefore no one of them has an absolute accuracy that is valid to three significant figures. The three significant figures are the convenient and common-sense method of portraying smooth variations geographically and over season, storm duration, and storm area.

Chapter III

TYPES AND CHARACTERISTICS OF MAJOR CALIFORNIA PRECIPITATION STORMS

3-A. INTRODUCTION

Definitions of orographic and convergence precipitation

3.01. Orographic precipitation is defined as that falling as a result of the lifting effect of a topographic feature on a flow of air passing over it. The induced vertical motions in the flow are primarily due to the slope of the ground but may also be related to the narrowing of the terrain. The latter effect is significant where valleys become constricted, such as in the northern Sacramento Valley. Orographic precipitation includes, in addition to that falling on upwind slopes, that blown across orographic barriers by the wind at the barrier, referred to in chapter VI as spillover.

Convergence precipitation in this report includes all precipitation resulting from lifting induced by atmospheric processes other than orographic. These are mainly horizontal convergence, frontal lifting and instability. Convergence and orographic precipitation occur simultaneously in mountain areas.

Condensation and precipitation

3.02. The lifting process, whether orographic or non-orographic, results in cooling of the air at the rate of 5.4 F. degrees per 1000 feet change in elevation until saturation is reached, then at 3 to 4 F. degrees, depending on temperature and pressure. The condensation process begins to take place as soon as saturation is attained. Minute water droplets or ice crystals are formed on various types of nuclei. These droplets and crystals are sustained by the vertical motion of the air. A net transport of moisture from water drops to ice particles takes place due to difference in vapor pressure, and from small to larger drops through collision. Precipitation results from inability of the upward motion of the air to sustain the hydrometeor (rain, snow, sleet, etc.) against the force of gravity. The size of hydrometeors is dependent on the magnitude of the vertical motions to which they are subjected. Their form on reaching the ground is largely dependent on air temperature.

The subject of condensation and precipitation is discussed in more detail in chapter I of Hydrometeorological Report No. 34 (7).

3-B. OROGRAPHIC STORMS

Definition

3.03. The term "major orographic storm" is used to denote storms which are important from the standpoint of sustained high intensity in orographic areas rather than in non-orographic areas. This definition serves to distinguish such storms from storms in which convergence precipitation (related to the storm mechanisms alone) is the more important feature. It recognizes that convergence precipitation is present in orographic storms as a contributing factor to total precipitation.

Factors in major orographic precipitation storms

3.04. Season. Seasonal controls limit California orographic precipitation to the cool months, roughly October to May. With the shift of the prevailing westerlies north of the latitude of California during summer months, the Pacific anticyclone dominates California with stable dry air, except for infrequent invasion of moisture from the Gulf of Mexico which results in showers and thunderstorms over the southeast desert areas and the Sierras and Southern California mountains.

Orographic storms similar to those of winter months do occur infrequently in the northern part of the state during September and into early June. Although these storms may have precipitation intensity comparable to that during the cool months their duration is restricted in these months by the transitory nature of offshore Lows and their runoff potential by dryness of the soil.

3.05. Intensity. The intensity of orographic precipitation depends on the strength of the wind normal to the mountain range and the moisture content of the air. California topography prescribes an optimum wind direction favorable to upslope motion varying from west-southwest to south. Optimum moisture content is contingent upon similar wind directions and upon storm trajectories from south of west, that is from a lower latitude. It follows that the storm of optimum orographic precipitation intensity in California is one in which the offshore trajectory of the airstream is south of west. This is the trajectory of the air during most of the storm duration in major orographic storms. It is also the trajectory of the storm center itself in most Northern California and some Southern California major orographic storms. Storms from a northerly latitude also may produce fairly heavy orographic precipitation in Southern California which are relatively less intense in Northern California because of the less favorable orientation of the flow and particularly because of more limited moisture.

The intensity of convergence precipitation superimposed on the orographic precipitation in mountain areas depends on moisture and strength of convergence mechanisms. These mechanisms may vary rapidly with time compared

to variations in upslope flow at a given location. Horizontal divergence may briefly decrease total precipitation in mountain areas.

3.06. Area. The areal extent of California orographic storms is usually large in comparison to size of drainage basins except for the two main Central Valley drainage basins. Thus orographic PMP criteria derived from relations based on major California storms is adequate for California basin sizes.

3.07. Duration. The feature of lengthy duration in major orographic storms is dependent upon a pressure pattern of such stability as to assure prolongation of vigorous upslope flow of moist air. Such a pattern can be stated in general terms as one involving low pressure in the eastern Pacific Ocean and high pressure over the mid-continent. High pressure may also dominate the central Pacific Ocean.

Basis for classification of major orographic storms

3.08. If more or less stationary anticyclones are of such strength as to interrupt the normal middle-latitude west-to-east flow or reroute it to low and/or high latitudes for a considerable period of time, the High is referred to as a blocking High. The resulting meridional flow from low to high latitudes and vice versa in such patterns permits maximum abnormalities of temperature and moisture. The major California orographic storms of this century are classified on the basis of this feature of blocking in HMR 37 as an aid in assessing the relationships of over-all weather map patterns to California cool-season precipitation. A summary of the classification is given here.

Storms are grouped under three main headings, Low, Middle or High-latitude types. This classification suggests the latitude relative to California from which storm centers move across the eastern Pacific, and depends on the longitude of blocking Highs which are effective prior to and/or during the course of the storm.

Low-latitude type (figure 3-1)

3.09. Storms of the Low-latitude type are nearly all centered in the northern two thirds of the state. The type involves a north-south blocking High in mid-Pacific between 160W and 180W. This High joins an intense High over Alaska which extends southeastward into the central United States. This pattern surrounds a Low of varying intensity and position in the southern Gulf of Alaska which is maintained by outbreaks of cold air from the interior of Alaska or across the eastern part of the Aleutian chain.

The main storm track from the western Pacific is diverted south of the block on its way to the Northern California coast. The storms following this trajectory, joined by a continuous frontal boundary, are forced to move rapidly in the strong flow under the periphery of the large Gulf of Alaska Low,

and have little opportunity to become large storm entities. Just south of
this frontal boundary a strong persistent flow of moist stable air from a
near tropical latitude is established around the eastern Pacific anticyclone.
The potential for orographic precipitation in this flow at the coast is ex-
tremely high. Convergence patterns in this flow have been shown to contrib-
ute significantly to rainfall totals at low elevations. Instability is min-
imized by cooling of lower layers in transit from a distant low latitude.

The duration of the above-described arrangement depends on the mainte-
nance and stability of position of the Gulf of Alaska Low as well as the
block to the west. The November 1950 and December 1955 flood storms are out-
standing examples of this storm type.

High-latitude type (figure 3-2)

3.10. Storms of the High-latitude type are more intense in Southern
California than farther north, with minor exceptions, because of the storm
trajectory. The Pacific block is east of 160W; it extends southward to low
latitudes and joins the High over Alaska and western Canada to form a cres-
cent-shaped ridge of shorter radius than in the Low-latitude type storms.
In most cases Low centers form off the British Columbia or Washington coasts
and deepen as they move southward. Off the Northern or Central California
coast they change direction toward northeast or north, depending on the ori-
entation of the crescent-shaped ridge. Offshore falling pressures on the
trailing cold front extend the trough of low pressure southward along the
Southern California coast, resulting in a strong flow from south and south-
west into Central and Southern California. Because of its limited trajectory
this air is not extremely moist. The orientation of the flow is particularly
favorable for orographic rain in parts of Southern California. Examples of
this storm type in which the Pacific block is complete and oriented north-
northwest-south-southeast as shown in figure 3-2 are the storms of Jan-
uary 16-19, 1916 and January 26-28, 1916.

A variation of this type is found in the January 20-23, 1943 storm (not
shown). Weakening of the Pacific block permitted breakthrough of a weak
storm from the west. As it moved eastward toward the coast rapid deepening
occurred when cold air flowing southward along the Washington coast entered
its circulation. This sequence was repeated at a lower latitude a day later.
This succession of deep Lows resulted in high pressure gradients over the en-
tire state. Orographic precipitation was particularly high in Southern Cal-
ifornia where dew points were fairly high.

Mid-latitude type

3.11. This type is characterized by low pressure in the central and
eastern Pacific with varying degrees of blocking over western North America.
The direction of approach of Lows near the coast is influenced by both the
general offshore circulation and the effectiveness of the continental block.

It is the basis for classing these storms as Southwest, Southerly or Westerly.

The Southwest subtype is the most common of Mid-latitude type storms. It is illustrated in figure 3-3 for Northern California. (In Southern California storms, the Low centers are shifted to the southeast.) Repeated entry of Lows into the eastern Pacific and cyclonic rotation around a mean offshore position in most storms brings weakening occluded frontal systems onshore and maintains a strong southwest flow there. The trajectory of this flow, originally from a distant polar source, over a low latitude results in high moisture content. Examples of Southwest Mid-latitude type storms in Northern California are February 25-29, 1940 and January 30-February 2, 1945; in Southern California, examples are April 4-8, 1926 and February 28-March 3, 1938.

The Southerly Mid-latitude type storms (not shown) are diverted northward by the continental block to a greater extent than are the Southwest type storms, permitting a more nearly southerly flow of very moist tropical air at the coast. An example in Northern California is the storm of December 9-11, 1937 and in Southern California that of December 30, 1933-January 1, 1934.

Westerly Mid-latitude type storms undergo little blocking at the coast as frontal systems move from west to east at rather infrequent intervals. Moisture is relatively low in air whose trajectory is essentially from west. Hence storms are comparatively minor. An example in Northern California is the storm of March 29-April 5, 1958.

3-C. CONVERGENCE STORMS

Factors in convergence precipitation

3.12. The three most important factors involved in convergence precipitation in California are reviewed below and discussed in more detail in chapter IV, HMR 37.

3.13. Ageostrophic convergence. The term "ageostrophic convergence" is used in this report to refer to horizontal convergence resulting from imbalance between horizontal pressure gradient and wind. It results from the time lag in response of an air particle to adjust its speed and direction to changes in magnitude and direction of pressure gradient forces. Its magnitude varies both with the pressure gradient changes encountered by the wind field and with the strength of the wind. It is the main cause of vertical motion not ascribed to orography in major winter California orographic storms. This motion is upward in that part of the air column which contains most of the moisture. The resulting precipitation may be noted on weather maps ahead of fronts, troughs, and in advance or to the right of moving Lows.

3.14. Frontal lifting. Vertical motions due to lifting of air over frontal surfaces, also a form of horizontal convergence, combine with those due to ageostrophic convergence as described above. Usually a large portion of the convergence rain in California winter storms occurs near and particularly in advance of the frontal systems; but most of this, particularly with warm fronts, is the result of the unbalanced wind-pressure gradient field associated with the frontal system rather than of lifting up the frontal slope. In most major California orographic storms frontal lifting is somewhat limited by lack of significant change in windspeed and direction at the fronts.

3.15. Instability. The importance of instability as a convergence precipitation mechanism lies in the capacity of unstable air to sustain large upward vertical motions over a limited area as a result of release of latent heat of condensation in ascending saturated air. Upward vertical motions due to instability, as observed in thunderstorms and large cumulus clouds, are large in comparison to possible values averaged over a larger area and resulting from ageostrophic convergence and frontal or orographic lifting. Yet they may combine, the latter causes of vertical motion tending to initiate the release of instability.

Instability is released as a result of increase of vertical gradient (commonly called 'lapse rate') of temperature and/or moisture. Three causes for this increase are surface heating, advection, and lifting. Heating in lower layers by a warmer ocean surface while the air is moving toward a lower latitude offshore steepens temperature and moisture lapse rates. Surface heating by the land increases temperature lapse rate in spring and fall, especially during the latter part of a storm during daylight hours when insolational heating of the ground surface is permitted by a breakup of the cloud deck. Vertical difference in horizontal advection of temperature and/or moisture can be an important factor in producing unstable lapse rates in major orographic storms. Lifting, either by orography or by convergence mechanisms, provides a means of release of convective instability by increase of temperature lapse rate.

Convective instability appears at the coast in major California orographic storms mainly near trough lines associated with cold or occluded fronts. In advance of the front, differences in temperature advection at different levels and vertical motion due to convergence, may cause a steepening of temperature lapse rate in the lower troposphere; behind the front a fairly steep temperature lapse rate may exist to the depth of the cooler air, especially if the front is the final one of the storm. However, the instability is hardly comparable to that which may be realized in large convergence storms.

Classification of large convergence storms

3.16. Large convergence storms are classified by season under the following headings:

1. Large cool-season convergence storms (approximately October through April) involving unusually heavy local convergence precipitation during a general storm. In assessing the level of convergence precipitation in such storms for comparison purposes it is necessary to account for or avoid contamination by orographic effects. Thus the preferred area for source material is the central part of the Central Valley. The 24-hour amounts at a point, provide the best means of comparing convergence precipitation in these storms and the most complete use of historical storm data because of the lengthy record of 24-hour rainfall measurements.

2. Large late spring and early fall convective storms. These storms, though usually associated with a general storm from the Pacific, are of short duration and very local. They depend primarily on instability and features of the nearby terrain for their intensity.

3. Large summer convective storms occurring in air from the Gulf of Mexico. These storms are also local short-duration storms depending primarily on instability and features of the nearby terrain.

Examples of each class are described briefly below. Fuller description of these storms is given in chapter V, HMR 37.

Examples of large cool-season convergence storms

3.17. In the first two storms discussed below, the offshore track (from northwest) favored instability as a factor in the heavy local rain but limited storm moisture. The reverse situation was the case in the third storm.

3.18. The April 20-21, 1880 storm at Sacramento. This storm is important because the 22-hour rainfall of 7.24 inches at Sacramento is a record during a general cool-season storm in an area of California free of orographic effects. A 1000-mb Low (figure 3-4) moved onshore from the northwest near Fort Bragg on the 20th and stagnated in the North Coastal area on the 21st before filling and then drifting southeastward on the 22d. Heavy rain was general over the northern half of California at low elevations; a low snow level resulted from the low temperatures prevailing in the recent polar air.

The 7.24 inches at Sacramento occurred mostly in the 18 hours after noon of the 20th as almost continuous rain, with three distinct bursts of very heavy rain. Despite absence of thunderstorm reports, instability is believed to have been an important factor in this extremely heavy local rainfall.

3.19. The December 20-21, 1866 storm at San Francisco. Like the above storm, instability in recent polar air flowing around a stagnant Low contributed to a heavy local rainfall. Two Lows moved inland near Point Arena from northwest, on December 18 and December 20, respectively. The second center stagnated about 50 miles north of San Francisco before moving northward and filling rapidly on the afternoon of the 21st. The storm was severe

at low elevations over the northern half of California. Because of the Low track from northwest, cold temperatures restricted precipitation at higher elevations to snow.

Between 1145 PST December 20 and 0815 PST December 21, 7.66 inches of rain was measured at one gage in San Francisco, a value substantiated by large amounts at several other locations within the city. The effect of instability as a factor in this heavy local rainfall is evident in the reports of many thunderstorms in and near the city on both days. (Local effect of topography added an orographic component to the above rainfall amount. Its magnitude in the average storm has been estimated at 23%, based on a comparison of rain at San Francisco and southeast Farallones.)

3.20. The Los Angeles area storm of January 25-26, 1956. This general storm over the southern half of California centered in the Southwest Plains area of the Los Angeles Basin. It involved passage of two occlusions across California from the west on the afternoons of the 25th and 26th. But the main feature of the storm was a warm front off the Southern California coast on the morning of the 26th. It had formed offshore on the trailing end of the first occlusion. Ageostrophic convergence in connection with the warm front is believed to have accounted for most of the 24-hour rainfall near the storm center in the Los Angeles Basin. An example of this high 24-hour intensity is the 7.42 inches west of Gardena. (This amount is thought to contain a slight orographic component, estimated as 0.9 inch). During the period of this rainfall, prior to approach of the second occlusion but including passage of the first occlusion, instability as indicated by raob data was not an important factor in rainfall intensity. Thus the convergence rainfall during this period is regarded as caused by factors compatible with those that might occur in the maximum orographic storm.

Examples of late spring and early fall convective storms

3.21. Local thunderstorms have been observed in certain parts of California during the months of May and September, the short-period intensity of which was higher than in the 1956, 1866 or 1880 storms described above. In these storms there was an unknown but probably minor direct orographic component in the rain total.

Topography apparently limits the location at which such storms may occur; thus in the Central Valley, records of the more intense thunderstorms come only from the extreme north end of the valley, from Red Bluff northward. The combination of lifting of a southerly surface flow in the north end of the valley (both by rise in elevation and by constriction of the width of the valley) and lifting of a southwesterly flow over the high coastal range to the west, appears to be essential to the storms' occurrence to the lee of the coastal range in the foothills at the north end of the valley.

The fact that these storms occurred in late spring and early fall months

partially explains their instability potential as the contribution of in-
solational heating during these periods. Transposition of the instability
features of the storm to the cool season is thus restricted.

The first two of the three storms described briefly below developed in
connection with, or as an aftermath of, a storm more or less typical of the
winter season. The name of each refers to the area near which it is thought
to have been centered. Kennet and Newton are located near Shasta Lake.

3.22. Kennet May 9, 1915. The Kennet storm, occurring during the aft-
ernoon, resulted in 8.25 inches in 8 hours. A Low moved from north of Hono-
lulu east-northeastward into Southern British Columbia. Its frontal system
did not become well occluded until it reached the Northern California coast;
rainfall was general over Northern California and northeastward into northern
Nevada and eastern Oregon. The intense thunderstorm development at Kennet
was a very local feature, as no other thunderstorms were reported in Califor-
nia on that date. Rain at nearby stations measured 1 to 2 inches for the
storm.

3.23. Newton September 18, 1959. In this thunderstorm an estimated
10.6 inches fell in 6 hours at Newton and 7 inches in the same period at
Toyon, about 2-1/2 miles away. This happened some 12 hours after a vigorous
winter-type storm, early for the season, moved in from west-northwest and
passed across Northern and Central California during the morning, leaving a
stationary trough offshore. Surface heating and lifting of the air in the
low-level southerly flow in transit up the narrowing Sacramento Valley, along
with cold advection in the upper-level flow superimposed on this southerly
low-level flow after being destabilized by lifting over the high coastal
mountains, apparently accounted for the instability release. During the aft-
ernoon, thunderstorms developed over the mountains to the west, later drift-
ing eastward over the foothills, where heaviest rain occurred.

3.24. Red Bluff September 14, 1918. This storm occurred as the after-
math of a general rain over the northern half of the state on the 12th and
13th from the circulation aloft about an old tropical storm. The latter had
been carried from the Mexican coast northward offshore in an elongated north-
south trough, moving inland aloft near Monterey and on up the Sacramento Val-
ley. The unstable nature of the tropical circulation above the level of the
stabilizing marine influence is evident in the 8.75-inch 24-hour rainfall at
Wrights in the Santa Cruz Mountains (elevation 1600 feet), largely from a
thunderstorm on the night of the 11th. It was not until a winter-type storm
from north-northwest became involved with the warm moist air from the tropi-
cal circulation, that the thunderstorm near Red Bluff developed on the night
of the 13th. With a surface dew point of 63, 4.70 inches fell in 3 hours and
5.70 inches in 6 hours.

Examples of summer-type convective storms

3.25. The following convective storms are typical of the summer season
when air from the Gulf of Mexico is the moisture source. Such a storm is in-
compatible with a winter-type orographic storm with moisture source from the
Pacific Ocean.

A storm at Encinitas, on the coast 12 miles south of Oceanside on October 12, 1889, resulted in 7.58 inches of rain in 8 hours. Seasonally it approaches the period of winter storms, but its origin was a typical summer-type flow of moist air from the Gulf of Mexico which moved unusually far to the west. It is apparent that the rainfall resulted from a very local intense thunderstorm, not evident at either San Diego or Los Angeles where 0.44 and 0.04 inches, respectively, were observed. Except for any upwind topographic effect of the coastal mountains in developing the thunderstorm, the rainfall amount can be considered as relatively free of orographic effects because of its occurrence on fairly level terrain.

The convective storm at Campo, in the coastal mountains near the Mexican border, in which 11.50 inches were reported in 80 minutes on August 12, 1891, involved a flow of air from the Gulf of Mexico westward over the coastal mountains of Southern California. Reports indicate that two thunderstorms merged in the area to produce the extremely high intensity. Because of the moisture source, the influence of terrain on the storm's development and the orographic component in the rainfall amount, its areal transposition is limited. A more detailed discussion of this storm is given in Weather Bureau Technical Paper No. 38, pp. 48-50. (3).

3-D. COMBINATION OF ELEMENTS OF OROGRAPHIC AND CONVERGENCE PRECIPITATION

Combination in observed storms

3.26. The cyclonic circulation inherent in all large orographic storms involves horizontal convergence and assures widespread convergence precipitation. Cool-season storms which cause heavy precipitation in orographic areas are often observed to cause heavy convergence precipitation in non-orographic areas. Convergence bursts are observed to occur during periods of heavy orographic rain (chapter IV-A, HMR 37). Thus combination of large values of convergence and orographic precipitation in the same storm is an established fact. In storms in which each factor assumes comparable importance, the classification of the storm as a convergence or orographic storm is arbitrary; both might be suitable. Further, a storm may have little convergence precipitation in one area compared to another, in both of which the orographic precipitation may be large.

The questions pertinent to PMP estimates is whether optimum values of convergence precipitation can occur in the optimum orographic storm and whether highest intensities can occur simultaneously. The following remarks draw on experience with past storms as a basis for combination of optimum values of most synoptic factors and for imposition of some restriction on the direct combination of other factors.

Synoptic factors in optimum combination

3.27. Combination of elements of orographic precipitation. Simultaneous occurrence of optimum values of moisture and favorably oriented pressure

gradient so as to cause optimum orographic precipitation is based on observed combination in large storms. Strong persisting gradients of an alignment most favorable to upslope flow over most California barriers have been observed to occur in storms whose general offshore circulation is conducive to a prolonged flow of moist air from a low latitude. Further, highest values of pressure gradient and dew point tend to occur simultaneously.

3.28. **Combination of elements of orographic precipitation with ageo-strophic convergence and frontal lifting.**

1. **Moisture.** Optimum moisture logically combines simultaneously with optimum values of ageostrophic convergence and frontal lifting, just as optimum moisture and upslope motion combine to produce optimum orographic precipitation.

2. **Pressure gradient.** Strong winds and large values of horizontal convergence are natural companions. This is so, first, because the vigorous cyclones which produce the high winds require convergence and the associated rising of warm air to high levels to maintain their energy source. Second, the higher the winds the greater the opportunity for large horizontal spatial variations. The total horizontal convergence at any one level is the sum of the wind velocity gradients in two directions:

$$C = - \frac{\partial V_x}{\partial x} - \frac{\partial V_y}{\partial y}$$

where V_x is the component of velocity in the x-direction, V_y the component in the y-direction, and C the convergence. A tendency for the simultaneous occurrence of high winds and high convergence (the latter is revealed by the rainfall) is illustrated by cyclonic storms throughout the world.

The procedure followed in developing the PMP criteria was to combine optimum moisture values with the highest values of horizontal convergence estimated to have occurred in selected cool-season storms in which instability was not an important factor. These values are regarded as appropriate convergence rain values to combine with the optimum orographic storm. No account was taken of the effect of pressure gradient on horizontal convergence, other than that inherent in the observed extreme values.

3.29. **Combination of elements of orographic precipitation with instability.**

1. **Moisture.** The role of instability in California cool-season storms tends to vary inversely with moisture supply: If moisture supply is limited by recent offshore air trajectory from north of west, then instability assumes importance in convergence precipitation because of the increased probability of an unstable lapse rate resulting from heating and addition of moisture to lower layers as air moves over warmer water toward the coast.

Thus instability precipitation may compensate for loss of convergence pre-
cipitation from factors other than instability, as moisture is limited by
trajectory. Larger cool-season convergence storms in California (measured
by 24-hour point rainfall) do not necessarily require high moisture, as is
the case in the eastern United States where high moisture and instability
are compatible in the same storm (chapter IV 3-E, HMR 37).

Since moisture requirements in the optimum orographic storm predicate
an offshore air trajectory which favors stability, it follows that the opti-
mum orographic storm cannot logically be combined with the optimum conver-
gence storm in which instability is an important contributor, as a result of
a recent offshore trajectory of the air from west or northwest.

2. Pressure gradient. Instability precipitation induced by orographic
lifting tends to be spread over an area, in the case of extreme upslope winds,
rather than concentrated at a point. Hence it is considered expedient to
limit the instability contribution to convergence to that inherent in the
highest observed values of convergence found in orographic storms, and max-
imize only for moisture.

In summary, optimum values of factors involved in combination of con-
vergence and orographic PMP are considered suitable for simultaneous combina-
tion, with the exception of moisture and instability. Combination of opti-
mum values of factors involved in convergence PMP only, is not restricted.

3-E. TROPICAL STORMS

History

3.30. Tropical storms originate off the coast of Central America or
southern Mexico at 10-20 degrees N. latitude, mainly from June to October
and particularly September. They frequently move northwestward along the
coast of lower Baja California before veering to northeast. On rare occa-
sions they move far enough north before veering to bring heavy rains to
southern mountain and southeast desert regions of California. On one occa-
sion, September 25, 1939, the center moved inland over Los Angeles with winds
of 30 knots at San Diego. On September 12-14, 1918 the upper circulation of
a former tropical storm brought heavy rains to Central and Northern Cali-
fornia, a prelude to the Red Bluff convective storm described above. More
detail on these two storms is found in HMR 37.

Requisite synoptic pattern

3.31. Tropical storms approach the latitude of Southern or Central Cal-
ifornia while still offshore only when a strong north-south trough is present
just off the coast between an unusually strong warm High southward from Colo-
rado and another north-south blocking High in the eastern Pacific. The

strength, orientation and persistence of this north-south trough influence the extent of northward penetration of the tropical storm before it moves onshore. Such a trough pattern is one which blocks wintertime Pacific storms from reaching the coast, except from a northwesterly direction.

Factors limiting precipitation potential

3.32. There are several limitations on precipitation potential from tropical storms in California. Probable maximum coastal wind velocity in a tropical storm is limited by the distance of California from storm source region. The energy of the storm is depleted by its northward movement over cooler water, a loss reflected most in reduction of surface wind velocity. Although winds to 115 knots have been observed along the coast of Baja California south of 30 degrees N. latitude, the highest surface velocity recorded in California was 30 knots at San Diego in the September 1939 storm. Coastal surface winds were light in the September 1918 storm when it moved onshore in Central California, although winds were strong aloft.

Surface friction resulting from the rough coastal mountain terrain rapidly erodes lower-level wind velocity in a tropical storm as it moves onshore. The small area of the circulation of the storm does not provide a continuing source of kinetic energy at lower levels.

Duration of orographic precipitation at any location is seriously limited by the rapid shift in wind direction as the storm moves by. With a movement of 200 miles per day (slow for a tropical storm at the latitude of Southern California) approximately a 90-degree change in wind direction at a local point would take place in that time. Rate of movement is not hampered by blocking Highs, as may occur in the eastern United States, since the arrival of the storm in California is dependent on the north-south trough extending northward into middle latitudes.

Instability release in coastal areas is restricted by environmental cooling of lowest layers. Instability may be an important factor in local convergence precipitation in inland areas or in the coastal mountains above the marine inversion.

Past experience indicates that the season of occurrence of tropical storms in California is limited to months when extratropical storms are at a minimum and when hydrologic factors such as soil moisture limit runoff.

The limitations on precipitation from tropical storms in California are such that the potential is estimated as less than that in some other storm types. The omission of these storms from the PMP criteria is discussed in paragraph 2.13.

Chapter IV

CONVERGENCE PROBABLE MAXIMUM PRECIPITATION CRITERIA

Purpose and procedure in maximizing convergence rain

4.01.   The purpose of this chapter is to develop a method of estimating probable maximum convergence precipitation so as to provide:

1.   Estimates of PMP for non-orographic areas.

2.   Estimates of the convergence portion of PMP to be combined with amounts computed by the orographic model in orographic areas.

The procedure employed is to develop, for durations through 72 hours:

1.   Seasonal curves of enveloping precipitation/moisture ratios (explained below) and

2.   Similar seasonal enveloping moisture curves.

These enveloping data are regarded as maximum values of the convergence precipitation parameters suitable for combination.   The next step is to combine corresponding values by multiplication:

$$\left(\frac{\text{Precipitation}}{\text{Moisture}}\right)_{\text{max}} \times \text{Moisture}_{\text{max}} = \text{convergence PMP.}$$

Values of convergence PMP are obtained for all months October through April and for all durations through 72 hours; these values are then distributed geographically.

4.02.   The enveloping precipitation/moisture (called P/M) ratio curves are indices of the highest observed efficiency of the storm processes, exclusive of orographic, which convert water vapor to precipitation, as discussed in chapter III.   They are expressed in terms of precipitation in a given length of time per unit of moisture in the air (that is, inches of precipitation per inch of precipitable water, W_p).   As a matter of convenience, ratios for all durations are ratios of precipitation for the various durations to 12-hour moisture values.   The term P/M ratio is synonymous with the term C-factor used in Hydrometeorological Preliminary Estimate No. 5004 (8) and by Fletcher (9).

4.03.   The enveloping moisture curves are based on envelopment of observed persisting 1000-mb dew points at low-level stations in California and the assumption of a moist-adiabatic lapse rate.

4-A. DEVELOPMENT OF ENVELOPING DEW POINTS

4.04. Surface dew points are used in this study as an index of the moisture which is processed both in probable maximum precipitation and in storms of record. Studies have been made showing that the surface dew point is, in general, representative of the moisture through depth during storm situations. One of the more recent studies is described in U. S. Weather Bureau Technical Paper No. 38, "Generalized Estimates of Probable Maximum Precipitation for the United States West of the 105th Meridian" (3). In both the orographic and convergence PMP components, observed storm depths are essentially maximized for moisture by multiplying by the ratio of the maximum moisture to the observed storm-moisture where the maximum moisture is that which is consistent with the storm type, the season, and the geographical location of the storm. The purpose of enveloping dew point charts is to provide these maximum moisture criteria.

4.05. The enveloping surface dew points provide other necessary information to the over-all problem. The height of the freezing level, which affects the amount of spillover beyond the crest, is set by the surface dew points and an assumed saturated pseudoadiabatic lapse rate of the air. Temperatures during the PMP storm at any basin elevation necessary to evaluate the snow-melt contribution to the PMP flood, are similarly established.

4.06. Basic dew point data. The highest persisting dew points of record for 12 hours duration for each month at first-order Weather Bureau stations, adjusted for elevation to 1000 mb, were the basic data used. By persisting is meant the dew point which was equaled or exceeded throughout the indicated duration. Use of persisting dew points allows including the considerable dew point data from older records when only 2 or 3 observations were taken in a 24-hour period. (For these early records, the concurrent minimum temperatures were also surveyed in order to take into account that the highest persisting dew point cannot be higher than the minimum temperature recorded during the period). If time-averaged dew points were used instead of the persisting values, higher dew points would usually result. A 12-hour duration was selected as being long enough to represent values which are consistent with a fairly broad general flow of warm moist air into a storm area. Dew points for a spectrum of durations are developed in paragraphs 4.21-4.25. The highest persisting dew points were adjusted to 1000 mb in order to have a common reference at which to compare the dew points observed at various elevations. This was done by reducing along the saturated pseudoadiabatic lapse rate. For the period 1905-1945 the highest persisting dew points are published in Weather Bureau Technical Paper No. 5, "Highest Persisting Dew Points in Western United States" (10). These published values are for midmonth and were taken from a seasonal envelope of observed values plotted at dates of occurrence. Durational consistency was obtained in these data by drawing a smooth dew point-duration curve. Changes were made in the published maximum 12-hour persisting values that were exceeded in the more recent years (1945-1959). For the Los Angeles area,

additional 12-hour persisting values were taken from a more complete survey made for Hydrometeorological Report No. 21B, "Revised Report on Maximum Possible Precipitation, Los Angeles Area, California" (11).

4.07. Rejection of unrepresentative dew point values. The procedure employed of simultaneous combination of maximum moisture with maximum pressure gradient in the maximum orographic storm imposes a slightly restricted definition of persisting dew point data, namely that they should come from a situation typical of a large cool-season storm and that they should occur during the storm rather than afterward. Therefore, some of the higher persisting 12-hour dew points were rejected. Examples of bases for rejection are described below.

4.08. In October, tropical or Gulf of Mexico air infrequently reaches Southern California and the Central Valley, resulting in high surface dew points. In October and April, high dew points occur along the Southern California coast with the approach of a weak cold front from the north down the east side of the Pacific High. High dew points are occasionally recorded there with a summer-type stratus condition in October and April. In the November 1950 storm, dew points in the San Joaquin Valley increased at the end of the storm which was terminated by a northward shift of the ridge over Southern California and of the storm track into Northern California on the 20th. Surface heating and evaporation along with maintenance of the moist flow from the southwest at lower levels accounted for the higher surface dew points after the rain ended. A similar situation occurs in the northern Sacramento Valley in late spring and early fall when a light southerly surface flow continues after the storm ends so that moisture and heat are added from the ground surface.

Envelope of maximum observed 12-hour persisting dew points

4.09. Two fundamental restrictions to an envelope of observed dew points are that it should largely envelop data observed during storm situations and that it should be smooth both seasonally and areally. The development of enveloping curves complying with these restrictions is described in the following paragraphs.

4.10. Maximum observed 12-hour persisting dew points. On figures 4-1a to 4-1d are plotted for first-order Weather Bureau stations the highest mid-month 12-hour persisting dew points taken from Technical Paper No. 5, (10) or any higher observed values, determined from hourly observations or more recent storms, which exceed those of Technical Paper No. 5. Those in parentheses were determined to result from non-storm situations as explained in paragraph 4.07 and therefore were not considered in the envelope. It may be seen that the great storms of November 1950 and December 1937 contribute many of the controlling points. Figures 4-2a and 4-2b show the highest 12-hour persisting values reduced to 1000 mb from all of the observation stations during these storms. (The highest _average_ 12-hour dew points for the same dates are about 1° higher than the highest 12-hour _persisting_ value

shown.) For the November 1950 storm, those south of 37°N latitude occurred after the intense rain and possibly are a degree or two too high to be representative of a storm situation. For example, the 64° at Fresno on the 20th was rejected and 63° dew point for the 19th used. These figures show that the first-order station dew points are representative of those in the general area and of large-scale flow of moisture.

4.11. Seasonal variation. Smooth seasonal variation from month to month is imposed by the gradual change in the meteorological parameters during the cool season. An envelope of highest observed storm dew points would therefore reasonably be an over-envelopment in some months which have not yet experienced the magnitude of storm that is potentially possible. For example, a close envelope of observed dew points constructed prior to November 1950 undoubtedly would have considerably undercut those attained in the storm of that month.

4.12. The shape of the seasonal curves of dew points at the key stations were determined from several guides, two of a statistical nature. For each first-order Weather Bureau station in California and southern Oregon the highest 12-hour persisting dew point for each month (October-April) was found for each of 25 years (1927-1945; 1950-1955). Dates of occurrence of the monthly maximum indicated little if any bias toward the beginning or ending of months; therefore each dew point was assigned to the mid-month day. Each set of dew points were then plotted on normal probability paper and a straight line of best fit drawn to the data. The fact that these data so plotted, quite readily fit a straight line indicates that they follow the normal probability distribution. The line of best fit then defines the 12-hour persisting dew point to be equaled or exceeded once in 2, 25, 50, etc. years. Figure 4-3 is an example of these plots of maximum 12-hour persisting values for Fresno for the month of October.

4.13. The dewpoints to be equaled or exceeded once in 2 years, termed the 2-year return period values, plotted for each station on figures 4-1a to 4-1d, show a fairly smooth progression through the season. The 100-year return period values on the other hand are not as stable since more weight is given to the higher values observed. In defining the line of best fit by eye on probability paper some variation in the 100-year return value results; therefore the 100-year return period dew points are indicated by vertical bars on the figures, representing the span of good fits of straight lines to the 25 years of data.

4.14. To serve its purpose as a guide, a smoothed 100-year return period curve was determined, shaped similar to the 2-year return period curve. This was done by plottings (not shown) of the 2-year value against the 100-year for each station, which gave fairly good correlations for most stations, and then adjusting the 100-year value to the line of best fit through each station's plot. The resulting smooth 100-year and 2-year return period values provide a guide to the shape of the enveloping dew point curve. (For comparison 10- and 50-year return period dew points are also

shown on figures 4-1a to 4-1d. These are smoothed similar to the 100-year values.)

4.15. Another guide is derived from mean sea-surface temperatures. Temperatures in the area of the source of moist flow to points along the California coast might be considered an index to the upper limit of moisture which is available to these points. Modifications in the air mass limit the amount of moisture that could reach the coast. However, the month-to-month variation in sea-surface temperatures upwind of the coast would appear to typify that of enveloping dew points. Such average monthly sea-surface temperatures are shown on figures 4-1a to 4-1d for points 600 nautical miles southwest of each station. In general, their variation with season is quite similar to the smooth seasonal variations of 2-year and 100-year return period dew points.

4.16. Enveloping seasonal 12-hour persisting dew point curves. An envelope for each station was drawn through the highest observed representative 12-hour persisting values and shaped after the 2- and 100-year return-period curves and the sea-surface temperature curve. These envelopes, shown on figures 4-1a to 4-1d by solid lines, include minor adjustments for geographic smoothing which is described in the next paragraph. The 1950 and 1937 storms control the curves for most stations.

4.17. Monthly maps of enveloping 12-hour persisting dew points. Seasonally smoothed enveloping dew points for each California and southern Oregon station were plotted on maps, month by month (figures 4-5a and 4-5b) and lines of enveloping dew points were drawn with some geographical smoothing. The maximum observed values for bordering states were also plotted to consider large-scale features over the Western States and to minimize discontinuities.

4.18. Mean seasonal variation of 12-hour moisture. The shape of the seasonal dew point curves of figures 4-1a to 4-1d differs somewhat from station to station. Therefore, the geographical variation of seasonal trend of 12-hour moisture was studied in order to decide whether a mean seasonal variation is permissible for the entire state. The difference in seasonal variation can be seen on figure 4-6 which shows the ratio (as a percentage) of the precipitable water (to the top of the column, assuming a saturated pseudoadiabatic lapse rate) corresponding to the maximum 12-hour persisting dew points for each month to the precipitable water for January at stations and grid points. Within the drainage areas of California with which this report is concerned the areal range in percentages is:

Oct.	Nov.	Dec.	Feb.	Mar.	Apr.
12%	5%	2%	3%	4%	6%

The large October areal range is explained as follows: the latitudinal dew point gradient in October in Northern California is relaxed because of October storm tracks being such as to bring warm moist air to the Pacific Northwest.

4.19. Considering the relatively small areal range shown above, it is reasonable to adopt one seasonal variation of moisture for the California area of concern. Averaging the percentages at the stations and grid points, and expressing them in terms of percentages of February (month of lowest average moisture), the following percentages result:

Oct.	Nov.	Dec.	Jan.	Feb.	Mar.	Apr.
121	110	105	100+	100	101	104

Smoothed values from a curve drawn to these data give:

Table 4-1

SEASONAL VARIATION OF MAXIMUM MOISTURE. PERCENT OF FEBRUARY

Oct.	Nov.	Dec.	Jan.	Feb.	Mar.	Apr.
121	111	104	100	100	101	104

These ratios, if applied to the precipitable water for the dew point on the February map at any location, will give the seasonal variation of moisture for that location. The mean seasonal variation when applied to January dew points at key stations results in the dotted curves in figures 4-1a to 4-1d. It is seen that adjustment for the geographically-averaged seasonal trend makes changes of less than 1°F from the station envelope at most stations.

Comparison of enveloping with 100-year return period dew points

4.20. Because 100-year return period dew points have been determined, it is of interest to see the effect on the PMP if they alone had been used to define the moisture criteria. The average difference between the enveloping and 100-year return period dew points for the eight key stations for each month is a measure of the difference between the two over the whole area. These differences are given in table 4-2 for each month.

Table 4-2

EXCEEDANCE OF ENVELOPING OVER 100-YEAR RETURN PERIOD DEW POINTS (°F)
(Average of Eight Key Stations)

Oct.	Nov.	Dec.	Jan.	Feb.	Mar.	Apr.
0.4	0.8	1.1	1.2	1.3	0.9	0.5

Individual 100-year return period values range from over 3°F lower at San Francisco to 2°F higher at Eureka than the enveloping criteria. A 1°F change in dew point affects convergence PMP by 5 to 6 percent and orographic PMP by 2-1/2 to 3 percent.

In assessing the exceedance of the enveloping curves over "100-yr" values it should be taken into account that the 100-yr values are for a month only. Thus, on the average over a span of 100 years, at each station the October value would be equaled or exceeded once, the November value once, etc., that is seven exceedances for the October-April season.

Moisture criteria for other durations

4.21. Thus far we have dealt only with 12-hour dew points. Variation of dew point with storm duration is useful in defining the moisture that is processed during the 72-hour PMP storm. Such variations were obtained by plotting, for each station, the precipitable water W_p corresponding to the highest persisting California dew point values for the 12, 24, 36, 48, 60 and 72 hours published in Weather Bureau Technical Paper No. 5 (10) and drawing a smooth curve, extrapolated to 1 hour. These curves, called 'decay' curves, permit expressing W_p for any duration in terms of the 12-hour W_p.

4.22. In order to determine if a composite or mean decay curve can be adopted for all areas and seasons, it is necessary to study the geographical and seasonal variation in the curves.

4.23. Geographical variation of decay rate. For each California station and each month (October-April) the ratios of the W_p for the 12-hour dew point to that for the 24, 36, 48, 60 and 72-hour dew point were computed. The largest range in these ratios, from station to station within each month, showed up in those for 12/72 hours, mainly because of high ratios (less decay) at Red Bluff, especially for winter months - about 10% less decay in moisture from 12 to 72 hours than at adjacent stations. This singularity may be due to the trapping of the lower level inflow moisture at the head of the Sacramento Valley at the end of storms, resulting in an overestimate of the precipitable water for longer durations. Because this effect is restricted to lower level moisture and to a small area no geographical variation of the decay rate of moisture has been introduced.

4.24. Seasonal variation of decay rate. The monthly decay rates were determined by averaging the decays at the California stations. These decays showed very little seasonal variation, the ratios of the W_p for 12 hours to that for 24, 36, and 48 hours varying by 0.02 and ratios of the W_p for 12 hours to that for 60 and 72 hours by 0.03.

4.25. Composite decay rate. The above studies justify use of a composite variation of moisture with duration for all areas and months. In terms of the precipitable water for a saturated pseudoadiabatic column it is given in the following table.

Table 4-3

DURATIONAL VARIATION OF MAXIMUM MOISTURE

Duration (hours)

1	3	6	12	18	24	30	36	42	48	54	60	66	72

Percent of 12-hour precipitable water

107	106	104	100	97	95	93	91	89	88	86	85	84	83

This average durational decay of persisting moisture has been compared with some observed decays in major storms and is shown in figure 4-4. The adopted moisture decay for PMP computations is similar to that in observed storms.

Enveloping moisture criteria as indices of maximum moisture

4.26. In the development of moisture criteria, a few observed values for some stations and months were used as key points on a general seasonal envelope of 12-hour persisting moisture which in turn was extended to other durations by use of observed relations. The purpose of the enveloping moisture criteria thus developed is to provide an index of moisture suitable for combination with other maximized parameters involved in the PMP storm. Though not representative of absolute maximum values, the above enveloping criteria are regarded as adequate for use in combining with other maximized parameters in the PMP storm, in line with the presentation of maximization in chapter II. For this reason, a smoothed envelope of observed values of moisture are referred to as maximum moisture values.

4-B. DEVELOPMENT OF ENVELOPES OF PRECIPITATION/MOISTURE RATIOS

4.27. The precipitation/moisture ratio is defined in paragraph 4.02.

4.28. Limitations of P/M ratio data applicable to California

1. Areal restriction of P/M ratio evaluation, necessary to avoid orographic contamination in point rainfall by upslope or spillover effects, limits data selection in California mainly to stations in the central portion of the Central Valley, between Red Bluff and Bakersfield.

2. Length of record of observations in this area is very limited for durations other than 24 hours, except for a few stations, so that enveloping P/M ratios for other durations must be obtained mostly by indirect means.

3. Maximum P/M ratios from the non-orographic parts of the eastern United States are not directly transposable to California and are too high. In the East there is a positive correlation between P/M ratio and dew point, high moisture seeming to promote storm efficiency. In California this

correlation is absent because of differences in trajectories that favor high moisture and marked instability (paragraph 3.29). In other words, in California, winds with a southerly component generally are accompanied by less instability than at times prevails in the Eastern States.

Classification of storms for development of P/M ratios

4.29. The minor contribution of instability toward convergence precipitation in the orographic storm as compared to that in the pure convergence storm, discussed in chapter III, leads to classifying convergence storms into two groups on that basis for obtaining P/M ratios, namely:

1. Convergence storms in which instability is a minor factor.
2. Convergence storms in which instability is an important factor.

Enveloping P/M ratios are developed from (1) for convergence PMP to be combined with orographic PMP and from (2) for convergence PMP not combined with orographic PMP. The largest P/M ratios come from Group 2.

Enveloping P/M ratios to combine with the maximum orographic storm

4.30. Applicable data. Only storms in Group 1 of paragraph 4.29 are used to develop P/M ratios for the convergence part of orographic storms. Group 2 storms, as well as local convective storms which are seasonally unsuitable, are eliminated. For short durations, such as 1 hour, the instability restriction on data in Group 1 is relaxed since short period instability is not uncommon in major storms.

Storm values were found from three sources: (a) The extensive precipitation compilations during major orographic storms; (b) the published extreme 24-hour station values in Weather Bureau Technical Paper No. 16 (12) for Central Valley stations; (c) high 2-day totals from Climatological Data (13). Storms from the last two sources were subjected to a qualitative synoptic appraisal intended to insure that they fell in the required Group 1. For the two-day totals, maximum values for 24 consecutive hours were estimated by constructing mass curves for stations in the vicinity.

Two of the daily values were reduced to durations of less than 24 hours, also on the basis of comparative mass curves. The larger P/M ratios are listed with pertinent data on figure 4-7.

4.31. All-season envelope of 24-hour P/M ratio. Envelopment of the Central Valley P/M ratios on figure 4-7 yields a 24-hour maximum of 6.4.

A computed ratio of 7.4 at Colusa for 24 hours is undercut by the envelope. This was done because original records leave some possibility that the reported 24-hour precipitation may have occurred in a longer period of time.

The next highest effective value is at Willows, during a storm involving a deep occluding Low from the southwest with an apparently minor instability effect. The 22-hour assigned duration is an estimate supported by the Red Bluff recorder and several other mass curves. The third highest effective value comes from the Southern California storm of January 25-27, 1956. This storm is discussed in detail in HMR 37.

4.32. <u>Seasonal variation of 24-hour P/M ratio</u>. There are insufficient values to define the seasonal variation of maximum 24-hour P/M ratios directly. Extensive seasonal plots of maximum values of 24-hour precipitation for numerous stations in general indicate no trend in any region of California at non-orographic stations for higher values in one month than another, within the October-May cool season. The 24-hour duration is the approximate "cross-over" point. For shorter durations, the higher values occur in spring and fall. For longer durations the mid-winter maxima are the largest. This variation is indicated by figures 4-9 and 4-10, discussed in subsequent paragraphs.

4.33. The conclusion from the precipitation plots is that <u>for the 24-hour duration</u> the seasonal trends of maximum moisture and P/M ratio must counteract each other. The seasonal variation of the maximum P/M ratio is then the reciprocal of the seasonal trend of maximum moisture (table 4-1). Applying this concept, the enveloping value of 6.4 of 24-hour P/M ratio is assigned to the driest month, February, in figure 4-7. The enveloping 24-hour P/M ratios for the other months are calculated from the indicated reciprocals.

4.34. <u>P/M ratios for other durations</u>. The durational variations of the P/M ratio, like the seasonal variation, is based primarily on the observed variation of precipitation. Since the denominator of the P/M ratio, for convenience, is always the 12-hour moisture, in this report (paragraph 4.02), the durational variation of P/M is the same as the durational variation of precipitation, P. The 24-hour enveloping P/M ratios for the various months in figure 4-7 are extended to other durations by use of 1/6-, 6/24-, and 72/24-hour precipitation ratios in large storms. The resulting P/M ratio curves envelop satisfactorily the highest P/M ratios found for durations other than 24 hours.

4.35. <u>Enveloping P/M ratios for 6 hours</u>. A seasonal variation of 6/24-hour precipitation ratios was obtained by averaging the ratios from the highest monthly 6-hour and 24-hour storms for 21 Central Valley recorder stations, most of them with short records. This seasonal trend is similar to that for eastern data, as shown in figure 4-9. An average mid-winter ratio of 0.55 was assigned to February and fall value of 0.70 to October; intermediate ratios were interpolated. Use of a California seasonal trend of 6/24-hour precipitation in this way distributes enveloping 6-hour P/M ratios in a symmetrical manner.

4.36. <u>Enveloping ratios for 1 hour</u>. A seasonal variation of 1/6-hour rain ratio was obtained by study of highest monthly 1- and 6-hour rainfall values for 30 Central Valley stations for approximately 14 years. It indicates 1-hour to 6-hour ratios ranging from .40 in midwinter to .48 in October. These values were used in extending the 6-hour P/M ratios to 1 hour.

4.37. <u>Enveloping values for 72 hours</u>. A seasonal variation of 72/24-hour rain ratios was obtained by averaging ratios of 72/24-hour rain from the 10 highest 24-hour rains and 10 highest 72-hour rains for each month from 50 representative stations, mostly in the Central Valley. This seasonal 72/24-hour rain ratio curve is shown in figure 4-10. For each month the ratio from this curve was multiplied by the 24-hour P/M ratio for the corresponding month to obtain monthly 72-hour P/M ratios.

Monthly P/M-ratio enveloping curves for 0 to 72 hours were drawn through the 1-, 6-, 24-, and 72-hour values (figure 4-7). The approximate envelopment of the highest observed 24-hour values by the February curve results in approximate envelopment of values for all durations in any month of occurrence.

<u>Enveloping P/M ratios for the maximum convergence storm</u>

4.38. The purpose of the curves in figure 4-8 is to provide enveloping P/M ratios which, when combined with maximum moisture, will yield pure convergence PMP for non-orographic areas. (It also yields pure convergence PMP for foothill areas if it is greater than the total PMP obtained by combination of orographic PMP and convergence PMP based on the P/M ratio curve developed for orographic storms, figure 4-7.)

4.39. Storm data applicable to this envelopment are from storms excluded from the curves in figure 4-7, namely those with a storm trajectory from north of west or those with high instability precipitation due to cold air intrusion from northwest during much of the storm. The two storms used in the 24-hour envelopment are those at Sacramento in April, 1880 and at San Francisco in December, 1866. Not used in the envelopment but plotted for reference purposes only were a summer-type storm in a moist flow from the Gulf of Mexico (Encinitas, October 12, 1889) and spring and fall local convective storms peculiar to the foothills in the north end of the Sacramento Valley (Red Bluff, September 14, 1918; Newton, September 18, 1959; Kennet, May 9, 1915). Storms entered in figure 4-8 are described in some detail in chapter V of HMR 37.

4.40. The procedure in constructing these curves is the same as that for the curves in figure 4-7. The highest observed P/M ratio near 24-hours is enveloped and assigned to February. The same seasonal variation of 24-hour values as in figure 4-7 was assumed. The same 1/6-, 6/24-, and 72/24-hour precipitation ratios were used to obtain 1-, 6-, and 72-hour seasonal P/M ratios since those ratios were determined without regard to the off-shore trajectory of the storm.

4.41. The seasonal envelopes drawn to these 1-, 6-, 24-, and 72-hour computed values (figure 4-8) slightly undercut the highest observed 24-hour value in month of occurrence. However, envelopment in month of occurrence in the case of the 1880 storm is not considered necessary inasmuch as it was in most respects typical of a cold midwinter storm.

The enveloping P/M ratios for non-orographic storms, figure 4-8, have a constant ratio of 1.33 to the P/M ratio values for convergence rain in orographic storms, figure 4-7.

Enveloping P/M ratios as maximum ratios

4.42. The enveloping P/M ratios are regarded as maximum values in the same sense as enveloping moisture values are regarded as maximum values, namely, suitable values for combination with other maximized variables. Occurrence of higher values of P/M ratio than those enveloped is probable in view of the extremely limited sampling area for non-orographic rain in California and the short period of record at most stations.

4.43. The convergence part of the PMP is directly proportional to the adopted P/M ratios. Different assumptions as to enveloping P/M ratios would make corresponding changes in the convergence PMP.

4-C. GENERALIZED CONVERGENCE PMP CHARTS

Combination of parameters of convergence PMP

4.44. Multiplication of the enveloping P/M ratios (derived in 4-B) by the enveloping moisture criteria (derived in 4-A) gives convergence PMP. Since the P/M ratio curves of figures 4-7 and 4-8 are in terms of 12-hour persisting moisture, the convergence PMP for any duration is the product of P/M for that duration and the 12-hour persisting moisture. Two sets of values of convergence PMP result from this combination of the two sets of P/M ratio curves with moisture. Since the P/M ratios are based on precipitation at a point, the convergence PMP values are referred to as point values.

Reduction of convergence PMP for elevation and coastal barrier

4.45. Reduction for effective elevation. For slopes not affected by an upwind barrier, the reduction in convergence PMP with elevation is assumed to be proportional to the reduction of W_p in a saturated column. Thus no account is taken of variation with elevation of the convergence mechanisms such as release of instability precipitation by orographic lifting. The effective elevation is taken as the height of the ground 5 miles upwind of a given location because raindrops or snowflakes are carried forward in the wind stream.

4.46. <u>Reduction for effective coastal barrier</u>. The convergence mecha-
nisms that produce the heaviest point rainfalls in California in winter
storms approaching probable maximum proportions require the interplay of
vigorous horizontal wind systems and horizontal pressure gradient forces
that are not in balance with these wind systems. Thus, in the sense of con-
tributing to convergence precipitation, air lying below the crest of the
Coast Range in the southernmost part of the Central Valley is considered as
virtually dead air since the strength of horizontal wind components in this
layer is limited. On this basis the effective elevation for computing con-
vergence PMP in that region is taken as the minimum elevation of the coastal
barrier over which wind might be expected to flow. East of San Francisco
Bay there is an opportunity for low-level winds to penetrate into the north-
ern end of the Sacramento Valley, and contribute to a convergence mechanism.
Taking these factors into account, effective barriers have been estimated for
reducing (by moisture depletion) the above convergence PMP values for the
floor of the Central Valley, slopes to the lee of the coastal mountains and
the Sierra foothills. In the southern San Joaquin Basin the effective barri-
er is equal to the actual barrier; in the Sacramento Basin the effective
barrier is much less than the actual barrier. A map of estimated effective
barrier heights (figure 4-11) was constructed for basin sizes of 200 square
miles and greater. Local topographic features that would affect very small
basins were necessarily smoothed out.

4.47. Reduction of convergence PMP for elevation and coastal barrier is
accomplished by the same elevation and barrier profiles in both the combined
convergence and orographic storm and the pure convergence storm. The greater
relative role of instability in the pure convergence storm, not reduced to
the same extent by the shadow effect of the Coastal Range as is the effect of
unbalanced pressure fields, suggests a less stringent barrier reduction.
Since this difference does not lend itself to evaluation, it was not taken
into account.

<u>Reduction of 10-square-mile convergence PMP for basin size</u>

4.48. The variation of California convergence PMP with basin size was
made similar to that in selected areas of the eastern United States from
Hydrometeorological Report No. 33 (2). Zones were selected on the basis of
latitude and season. This procedure eliminated the most southerly zones (5,
8 and 9) and the east coastal zones during the hurricane season. For each
month (October-April) in each of the remaining zones, the 6-hour incremental
maximum precipitation for standard-sized areas was expressed as a percent of
the 10-square-mile value. Then an average of the areal variation (percents
of 10-square-mile values) was obtained for each month in the selected zones
for each 6-hour increment to 72 hours. Since the relations in Hydrometeoro-
logical Report No. 33 extend only to 1000 square miles, values to 5000 square
miles were obtained by smooth-line extrapolation. The percents showed little
areal variation beyond the third 6-hour increment. This eastern United States
basin size reduction relation was used to convert California 10-square-mile
values of convergence PMP to other basin sizes.

Construction of a 6-hour 200-square-mile January-February probable maximum convergence precipitation index map

4.49. The steps taken in combining the factors involved in an index map of probable maximum convergence precipitation for the first 6 hours for January or February for a 200-square-mile basin size are outlined in 1 to 5 below.

1. The 6-hour increments of P/M ratio (for a point or 10 square miles) were read from figure 4-7 for each month and plotted for smoothing.

2. These 6-hour smoothed values were expressed as percentages of the 1st 6-hour February value. They refer to a point or 10 square miles. This gives combined seasonal and durational variation of P/M ratio.

3. The barrier and elevation reduction map (figure 4-11) was used to reduce geographically the moisture criteria for mid-February (month of lowest dew point) on figure 4-4b, expressed as precipitable water.

4. These reduced values of W_p were multiplied by the first 6-hour 10-square-miles February P/M ratio from figure 4-7 to give 6-hour 10-square-mile February probable maximum convergence precipitation.

5. From the eastern United States basin-size reduction relation, described in paragraph 4.48, a factor 0.80 was applied to the 10-square mile probable maximum convergence precipitation values in step (4), to reduce to a basin size of 200 square miles. Figure 4-12 shows the resulting 1st 6-hour 200-square-mile February probable maximum convergence precipitation index map for California areas of concern in this report. As the differences are insignificant, the map also applies to January.

4.50. This map, referred to as the probable maximum convergence precipitation index map, gives values from which may be derived values of convergence PMP for different sizes of areas and durations for combination with corresponding values of orographic PMP to obtain the total PMP. Values of convergence PMP for the maximum convergence storm are obtained by multiplying by 1.33 and are applicable to non-orographic areas and to foothill areas where total PMP values obtained by the above combination are smaller.

Monthly charts of variation of convergence index with basin size and duration

4.51. The variation of convergence PMP for basin size and duration was incorporated into monthly charts of percentage of index (figures 4-13a to 4-13c). These relations are derived by combining (a) Seasonal variation of moisture, table 4-1, (b) Seasonal and durational variation of P/M ratio, figure 4-7, and (c) Basin-size reduction relation described in paragraph 4.48.

Convergence PMP for 1 and 3 hours

4.52. For small basins it may be necessary to define the PMP for durations less than 6 hours, therefore the convergence PMP for one hour for areas up to 100 sq. mi. and for 3 hours for areas up to 500 sq. mi. have been included in this report.

4.53. The areal variations of rainfall for these durations were based on all convergence type storms contained in "Storm Rainfall" (14) for which the 1- and 3-hr maximum depths had been determined. The depths for standard sized areas were expressed in percent of the depth at 10 sq. mi. for each storm. Averaging the percentage decrease of depth with area for all the available storms and smoothing with area resulted in the following percentages.

Table 4-3

AREAL VARIATION OF SHORT-DURATION CONVERGENCE PMP

Duration (hrs)	Area (sq. mi.)					
	10	30	50	100	200	500
	Percentage of 10 sq.-mi. depth					
1	100	90	84	76		
3	100	94	90	84	78	71

This defined the basin-size reduction for 1 and 3 hours (similar to that described in paragraph 4.49 step 5 for 6-hour increments) and enabled combining with the seasonal variation of moisture and P/M ratios to obtain the depth-areal 1- and 3-hour duration curves of figures 4-13a to 4-13c.

Chapter V

CRITERIA FOR PROBABLE MAXIMUM OROGRAPHIC PRECIPITATION ON WINDWARD SLOPES

5-A. OROGRAPHIC PRECIPITATION

Definition

5.01. Precipitation which results from the forced lift imparted to moist air by its motion over a solid barrier is called orographic precipitation. It does not include that component of the total precipitation which would have occurred had the barrier not been there (i.e., caused by the dynamics of the general weather situation).

Treatment

5.02. The orographic component of the total precipitation, its formation, path of descent, distribution on windward slopes including loss to leeward by spillover, variation with time, and finally its maximization are the subjects of this chapter.

5-B. THE OROGRAPHIC MODEL

Introduction

Basic characteristics

5.03. The 2-dimensional orographic model used in the Los Angeles and San Joaquin Reports (11) and (15) is also applied in this report, but with some modifications. There are different formulations of this basic model, but the following features are common to each:

1. The 2-dimensional model (length along the current and height) is expanded to 3 dimensions by averaging the parameters across the current, i.e., wind, moisture, topography, etc.

2. Precipitation is conceived of as the difference between inflow and outflow moisture in a specified volume.

3. There is no convergence or divergence of the air. Except for the water vapor precipitated, which amounts to a few percent at most, conservation of mass is realized.

4. As a closely associated condition, laminar flow is assumed, i.e., the air moves smoothly in nearly parallel streamlines, with no turbulent motion.

5. At some great height (low pressure) above the mountain called the nodal surface the atmospheric flow is horizontal.

6. The air is saturated.

7. A steady state is assumed, i.e., velocities at all points are independent of time.

Formulas

5.04. The basic condensation model formulas, derived in the Los Angeles Report (11), are:

$$\frac{R}{t} = \frac{.4\ V_1\ \bar{q}_1 \Delta P_1 - .4\ V_2\ \bar{q}_2\ \Delta P_2}{Y} \tag{1}$$

and

$$\frac{R}{t} = \frac{V_1\ (W_{p1} - \dfrac{\Delta P_1}{\Delta P_2}\ W_{p2})}{Y} \tag{2}$$

Since from mass continuity considerations: $V_2\ \Delta P_2 = V_1\ \Delta P_1$ (3)

(1) may be written:

$$\frac{R}{t} = \frac{.4\ V_1\ \bar{q}_1\ \Delta P_1 - .4 V_1 \Delta P_1 \bar{q}_2}{Y} = \frac{.4\ V_1 \Delta P_1\ (\bar{q}_1 - \bar{q}_2)}{Y} \tag{4}$$

Equation (4) is the form used most in the report.

Symbols

5.05. A list of symbols used in the above equations and in the rest of this chapter follows:

R - precipitation (inches); also gas constant for air
R_o - observed precipitation
R_c - computed precipitation
t - time (hours)
V - windspeed (mph)
V_1 - speed of air at inflow
V_2 - speed of air at outflow

V_c - component of the wind

V_{gc} - component of the geostrophic wind

V_g - geostrophic windspeed

W_{p1} - precipitable water at inflow (inches)

W_{p2} - precipitable water at outflow

Y - distance, inflow to outflow (miles)

X - distance, normal to Y

$\bar{q}$ - specific humidity

$\bar{q}_1$ - average specific humidity at inflow (gm/gm)

$\bar{q}_2$ - average specific humidity at outflow

P - pressure (mb)

ΔP_1 - pressure difference at inflow

ΔP_2 - pressure difference at outflow

g - acceleration of gravity (cm sec^{-2})

Z - height (geopotential meters)

$\dfrac{\partial Z}{\partial n}$ - slope of isobaric surface normal to contour lines

$\dfrac{\partial P}{\partial n}$ - pressure change per unit horizontal distance

f - coriolis parameter ($2\omega \sin\phi$), a function of latitude

ω - angular velocity of the earth

ϕ - latitude

λ - model coefficient

C - temperature, °Centigrade

F - temperature, °Fahrenheit

T - temperature, °Absolute

T_v - virtual temperature (°C)

S - indicator for an air streamline

A - area on thermodynamic diagram (figure 5-7)

R.H.   - relative humidity

k - an arbitrary frictional coefficient, dimensionless

ρ - air density

n - subscript indicating nodal surface

1, 2, 3, 4, etc. Subscripts applied to other variables. All odd-numbered subscripts refer to values above the foot of a ridge or mountain (inflow). All even numbered subscripts refer to values above the crest of the mountain (outflow).

The Inflow Wind (V_1)

The inflow wind profile

5.06. A reasonably accurate portrayal of the inflow wind profile is of great importance in the estimation of orographic precipitation. The inflow wind is one factor (and an important one) in determining the outflow wind. In combination these profiles determine the amount of air available to be processed and the degree to which it is lifted.

Referring to the schematic diagram, figure 5-1, the inflow face is $X\Delta P_1$ and the component of the windflow against this face is shown by the hatched area formed by connecting the surface, 500 mb and nodal surface wind vectors. It is seen that the more wind vectors used to construct the inflow wind profile, the better the approximation to the true rate of inflow. Winds at 100-mb intervals were used for construction of the inflow profiles, except for two 50-mb layers at the bottom of the atmosphere where the wind turns fastest with height.

The geostrophic wind approximation

5.07. Because of an almost complete lack of upper air wind observations in storms over most of California an approximation to the real wind is made by the use of the geostrophic wind and empirical relations between the two.

The geostrophic wind is defined as the theoretical horizontal wind velocity for which the coriolis acceleration would balance the horizontal pressure force. At sufficiently great heights above the ground the airflow is normally close to geostrophic. Thus the geostrophic formula has great utility in estimating winds. Its speed is given by:

$$V_g = - \frac{1}{f\rho} \frac{\partial P}{\partial n} \quad \text{(for constant level chart, e.g.,} \atop \text{sea-level map)} \tag{5}$$

$$V_g = - \frac{g}{f} \frac{\partial Z}{\partial n} \quad \text{(for constant pressure chart,} \atop \text{e.g., 500 mb)} \tag{6}$$

Its direction is parallel to the isobars or height lines.

The formula which gives the geostrophic windspeed in mph when the pressure gradient is expressed in millibars per mile is:

$$V_g = (1.39 \times 10^{-4}) \frac{1}{f\rho} \frac{\partial P}{\partial n} \tag{7}$$

Here f and ρ are in the usual units of $\sec^{-1}$ and gm/cm^3, respectively.

Relation of wind to geostrophic wind

5.08. On the average over land the wind and geostrophic wind approximate each other above about 4000 feet with sub-geostrophic windspeeds and more or less cross-isobar flow toward lower pressure below 4000 feet. The rougher the terrain the deeper the friction layer. (Under certain weather conditions, e.g., rapidly changing pressure, the wind may depart significantly from the geostrophic at any level).

In order to establish quantitatively the deviations from geostrophic conditions over the rough terrain of California a series of wind studies was undertaken. Pilot balloon and rawin (radio wind sounding) reporting stations used for these studies were: Bishop, Inyokern, Los Angeles, Merced, Oakland, Red Bluff, Sacramento and Santa Maria, Calif.; Medford, Ore.; and Reno, Nev. At each of these stations 3 to 6 seasons (October through April, inclusive) of data were processed. Cases were selected for study when a) the wind aloft observation extended to sufficient height and b) the direction of the geostrophic wind at the time was within a span typical of storms and the speed was in excess of certain minimum values.

A sample comparative plot of actual and geostrophic wind for one station, Oakland, Calif., is presented in figure 5-2. This example is based on 5 seasons of record (1951-1955 inclusive). Each dot represents one observation unless otherwise indicated. The figure shows the ratio of the actual wind component against the Coast Range, V_c, to the geostrophic component, V_{gc}. (The component in all study cases was taken normal to the mountain range in the vicinity of the station.) It will be noted that the mean value of V_c/V_{gc} rises from a very low value at the surface to near geostrophic conditions at 500 mb. This result is fairly typical of all stations. Similar data for other stations are shown in HMR 37.

Figures 5-3 and 5-4 show the mean profiles of V_c/V_{gc} for the study stations. The grouping of curves into Coastal and Central Valley was suggested by the generally higher values along the coast up to the 500-mb level.

A single average V_c/V_{gc} curve was adopted for the Coast Range and is shown by the heavier line on figure 5-3. The coastal relation is based primarily on Oakland and Santa Maria and to a lesser extent on Long Beach.*

---

*The curve for Long Beach appears to be low compared with Oakland and Santa Maria. A possible reason for this difference is a bias due to the small number of cases suitable for study at Long Beach. Although 5 years of data were searched only 4 cases were found to meet selection specifications. At Oakland and Santa Maria 25 and 12 cases respectively were found for an equal length of record.

The rapid rise to three fourths of the geostrophic at 900 mb shows the effect of sea proximity, since at this level approximately 90% of the geostrophic speed is attained over the ocean. Full geostrophic windspeed is not attained till 500 mb, due to the impedance of the Coast Range.

The Central Valley relation proved to be more complicated than the Coastal. Three stations were studied in the Valley; Red Bluff, Sacramento and Merced. The three curves at the higher levels were generalized to one valley prototype shown by the heavier line on figure 5-4. Below 800 mb Red Bluff and Merced were very similar and therefore combined. Results of the Sacramento wind study indicated that the lower elevation of the Coastal Range around the San Francisco region is responsible for higher V_c/V_{gc} ratios below 850 mb. It is estimated that when the wind is from the southwesterly quadrant this influence is felt from about Stockton to Chico, with fullest effect near Sacramento. Figure 5-5 shows the adopted areal distribution of the V_c/V_{gc} ratio at 1000, 950 and 900 mb.

Obtaining the inflow wind profile

5.09. In this report inflow wind profile in a storm is obtained from geostrophic winds and the V_c/V_{gc} ratio. A short survey indicated that the vertical profile of the geostrophic wind could be approximated to a sufficiently accurate degree by only 2 measurements, the surface and 500-mb geostrophic wind and the assumption of a linear relation between the two. The appropriate V_c/V_{gc} ratio from figures 5-3, 5-4 or 5-5 is then applied to the geostrophic wind profile to obtain the "real" wind profile.

In some storm cases the 500-mb wind is not known. In these, the 500-mb wind is estimated by indirect means, discussed in paragraph 5.27. The 300-mb wind was derived by extrapolation from the 500-mb wind by the following relation:

$$V_{300} = 1.30 \ V_{500} \tag{8}$$

This relation was derived from an empirical study of observed winds in storm or near-storm situations.

The Outflow Wind (V_2) and Pressure (P_2)

Flow over slopes

5.10. The amount of orographic precipitation is related to the decrease in pressure experienced by each part of the flow. The windflow that would yield the maximum of orographic precipitation would be for the entire flow at each level to rise and fall parallel to the ground, so as to be lifted by an amount equal to the height of the barrier. Such a flow, however, is never obtained in the atmosphere. Rather there is a tendency for a leveling off of

the airflow at some great height above the ridge; thus the amount of lift decreases upward from the ground. The lift is equal to the height of the ridge only at the ground and decreases to zero at the elevation where the flow essentially levels off.

The nodal surface

5.11. The outflow pressures required for computing orographic precipitation are found in two steps. The first is the choice of the pressure at which the flow is level, called the nodal pressure. The other is determining the spacing of the streamlines on a pressure scale between the ground and this nodal surface. These pressures could be computed rather simply from requirements for continuity of mass if an observed vertical profile of the windspeed above the crest of the ridge were available. However, such observations are non-existent and the entire flow above the slope and crest of the mountain must be estimated from the given inflow at the foot of the mountain by application of pertinent laws.

The assumption of an upper level of near-horizontal flow derives from several considerations. Foremost is the analogy to flows that can be directly observed. The flow of water in a river levels off above an obstacle on the bottom. Similar effects are observed in model experiments with fluids. Second is the stability of the stratosphere. The near-isothermal vertical distribution of temperature in the base of the stratosphere is an extremely stable stratification. Such stable layers are quite resistant to being lifted. There is much less resistance to lifting in the upper portion of the troposphere where a condition of near-neutral equilibrium in the vertical stratification is often approached. It would be expected that the winds above a large ridge would exhibit some tendency to level off no higher than the lower portion of the stratosphere. These and other considerations suggest that the windflow in an orographic precipitation storm can be approximated by placing a nodal surface near the tropopause. In this study a nodal surface is considered to exist at 300 mb in observed storms, at the same level in a probable maximum storm over the Coast Range, and at 250 mb in a probable maximum storm over the Sierra Range.

Physical laws of airflow

5.12. In a frictionless, laminar-flow, two-dimensional model in which there is no transverse convergence of the airstream, four laws which govern the flow are:

1. Continuity equation. This is expressed by equation (3) or, in differential form,

$$\int_{S_1}^{S_3} V dP = \text{constant} \tag{9}$$

where the integration is vertically between any two streamlines, S_1 and S_3.

2. Bernoulli's equation for motion along a streamline

$$\frac{1}{\rho} dP + \frac{1}{2}d(V^2) + gdZ = 0 \tag{10}$$

3. Hydrostatic equation.

$$dP = -\rho gdZ \tag{11}$$

4. Adiabatic laws. For air not reaching saturation the adiabatic law is

$$\frac{T_1}{T_2} = \left(\frac{P_1}{P_2}\right)^{.286} \tag{12}$$

where the subscripts refer to successive values of the same air parcel along a streamline. The law describing the temperature variation of saturated air undergoing adiabatic expansion is not stated explicitly because of its complexity but is solved graphically on a thermodynamic diagram (pseudo-adiabatic chart).

Application of laws

5.13. How these four laws control the flow will be discussed with reference to the schematic flow diagram of figure 5-6.

Start with any assumed distribution of windspeeds. First the spacing between any two streamlines above B, in millibars, must represent a contraction of the spacing between the same streamlines above A in relation to the increase in windspeed as given by the continuity equation. Thus the continuity equation, for the particular windspeed field, and the known pressure at point 2, will yield the pressure on each streamline above B.

Second, the temperature changes along a streamline are known from the adiabatic laws. The changes, subtracted from the initial temperatures above A, yield temperatures on each streamline at B. These temperatures in combination with the pressure in turn, through the hydrostatic equation, fix the height of each streamline above B. (The height of the various streamlines at designated pressure levels above A are also known through the hydrostatic equation.) But, the resulting differences in height and pressure from A to B along any streamline, through the Bernoulli equation, permit only a specific change in the square of the windspeed between the same two points. If this difference does not agree with the postulated windflow, the flow is dynamically inconsistent.

For a specified ground profile, nodal surface, and distribution of atmospheric variables above A, there is a unique wind field that will satisfy the physical requirements when analyzed in the above fashion.

48

Computation of outflow pressure and winds

5.14. To compute the required outflow wind and pressure above a ridge the flow was divided into layers, bounded by streamlines, as in figure 5-6. The four laws were then combined into two equations. In the following discussion subscripts are used that apply to the layer nearest the ground in figure 5-6. The equations also apply to any other layer by changing the subscripts. The continuity of mass equation, (9), may be written

$$(V_1 + V_3)(P_1 - P_3) = (V_2 + V_4)(P_2 - P_4). \tag{13}$$

It can be shown (16) that the three remaining laws, Bernoulli, hydrostatic, and adiabatic are all satisfied for frictionless flow if the following square-of-speed relationship is fulfilled:

$$(V_4^2 - V_3^2)(V_2^2 - V_1^2) = 2RA \tag{14}$$

Here R is the gas constant for air and A is the area, shown schematically in figure 5-7, on a thermodynamic diagram bounded by the pressure-temperature curves between the points 1, 2, 3, and 4 (of figure 5-6). The constant R is in units of speed squared divided by degrees, A is in units of degrees; thus 2RA is in units of velocity squared and conforms to the left side of equation 14.

Taking friction into account, (14) becomes

$$k_3(V_4^2 - V_3^2) - k_1(V_2^2 - V_1^2) = 2RA \tag{15}$$

where the k's are friction coefficients at the upper and lower streamlines of the layer respectively, as discussed in paragraph 5.16.

Utilizing (13) and (15) in combination, a solution for any two unknowns for a layer may be obtained where the remaining variables are specified. As applied in this report, the two unknowns are always V_4 and P_4, the outflow speed and pressure at the top of a layer. The steps to obtain the required outflow profiles over a ridge are to assign a tentative outflow speed at the ground, compute V_4 and P_4 for the first layer by simultaneous solution of (13) and (15), introduce these values as the outflow at the bottom of the next layer, and compute the outflow variables at the top of that layer from the equations. This procedure is continued layer by layer into the stratosphere. The resulting outflow profile will not necessarily reflect the nodal pressure previously decided upon. Trials are continued, determining complete outflows for a succession of assigned ground outflow speeds, until the flow is found that reflects the desired nodal pressure. (In practice, two judiciously chosen outflows, followed by interpolation between them, usually suffices). A sample outflow is shown in table 5-1.

Table 5-1

SAMPLE OF OUTFLOW WINDS AND RELATED DATA

	Inflow				Outflow			
$P_{1, 3, 5...}$	$V_{1, 3, 5...}$	$(V_{1, 3, 5...})^2$		$P_{2, 4, 6...}$	$V_{2, 4, 6...}$	$(V_{2, 4, 6...})^2$	ΔV^2	k
mb	mph	$(\text{mph})^2$		mb	mph	$(\text{mph})^2$	$(\text{mph})^2$	
1000	18	324		800	50	2544	2220	0.5
950	42	1764		777	72	5252	3488	0.75
900	55	3025		747	88	7779	4754	1.0
800	74	5476		679	103	10,529	5053	1.0
700	87	7569		605	114	12,902	5332	1.0
600	100	10,000		527	125	15,589	5589	1.0
500	100	10,000		447	126	15,813	5813	1.0
400	100	10,000		367	126.5	15,991	5991	1.0
300	100	10,000		289	126.9	16,099	6100	1.0
250	100	10,000		250	127.0	16,166	6116	1.0

See text, paragraph 5.14, for interpretation.

Stability considerations

5.15. The stability of the inflowing air has a marked effect on the computed outflow (16). The effect of stability in the simultaneous solution of equations (13) and (15) as described in the preceding paragraph is exercised on "A" in equation (15). "A" in each computation is evaluated from a plot like figure 5-7. The more stable the inflow the larger the value of "A", other factors being fixed. "A"'s are positive in rising stable air up to the nodal surface and the effects of the "A"'s in the successive layers accumulate. Thus the difference in the squares of the inflow and outflow speeds increases up to the nodal surface, as in table 5-1.

For reproduction of observed storms, the vertical temperature variation at inflow was assumed to be 1°C per 100 mb more stable than the moist adiabatic lapse rate, while 1/2°C/100 mb was assumed for the PMP storm. These assumed temperature lapse rates are based on observed lapse rates at Oakland during the more intense part of several orographic storms, which tend to run from 0.75 to 1.0°C/100 mb more stable than the moist adiabatic lapse rate. Adoption of the higher value for observed storms has the effect of allowing for the stabilizing effect of slightly less than saturated conditions in some layers. The adoption of 1/2°C/100 mb for PMP storms is in accordance with facilitating maximum simultaneous convergence rain, which is favored by near-neutral stability.

The foregoing assumptions of a moderate degree of stability are not at variance for the purpose of computing precipitation with the practice elsewhere in the report of computing the moisture distribution in the vertical from the exact moist adiabatic lapse rate. One is a stability index, the other a moisture index, of the average conditions through great vertical depth, which represent the natural conditions within certain limits.

Surface friction

5.16. Friction imposes a significant impedance to an airflow near the ground. The frictional effect is at a maximum at the ground and diminishes with height. It is impossible to evaluate the exact effect of friction over the rugged terrain of the California mountains. Certain approximate allowances that appeared to yield reasonable results were adopted. It was assumed that, along each streamline near the ground:

$$(V_2{}^2 - V_1{}^2)_{frictional} = k(V_2{}^2 - V_1{}^2)_{frictionless} \tag{14}$$

The coefficient k was assigned arbitrary values. These were 0.5 at the ground, increasing to 1.0 at the top of the friction layer. For convenience the top of the friction layer was placed along a streamline, thus closer to the ground at the top of the ridge than at the base, probably a realistic

assumption. For flow over the Coast Range k was given a value of 1.0 at the streamline passing through 950 mb at inflow. Over the Sierras the values of k were 0.75 at the 950-mb streamline and 1.0 at the 900 mb streamline and above.

Inflow Moisture

Dew point control

5.17. The index of moisture charge used for all storm computations and in the hypothetical maximum storm is the persisting surface dew point. The upper air moisture is then assumed to be equal to and distributed like the moisture contained in a saturated pseudoadiabatic atmosphere, the 1000-mb temperature of which is equal to the persisting surface dew point.

The maximum surface dew points (used for the maximum storm) are to be found in chapter IV, along with the method of derivation. These dew points were used without modification for coastal PMP computations. For Sierra PMP estimates a barrier depletion was used described in the following section.

Upwind barrier depletion for Sierra estimates

5.18. Consideration of the moisture-depleting effect of the coastal barrier is necessary for Sierra estimates. Air reaching the southern Sierras generally must come completely over the Coast Range while for the middle and northern Sierras the inflowing air is a combination of air through the gap in the Coast Range in the San Francisco Bay area and air from over the Coast Range. The increase in the mean seasonal precipitation in the Sierra foothills over that of the Central Valley floor at elevations lower than the top of the Coast Range, demonstrates that the effective barrier depletion of moisture is less than what a full barrier depletion would give. This is due to a recharge of the valley air by evaporation of precipitation.

The degree of saturation of Central Valley air for Sierra probable maximum precipitation estimates was determined by a consideration of moisture through depth and a study of differences between surface dew points and surface temperatures at Central Valley stations in major storms. The latter consisted of relating hourly values of temperature-dew point spread to the associated hourly rainfall amounts in the January 1943, January-February 1945, November 1950 and December 1955 storms.

Figure 5-8 summarizes the results of the Central Valley surface relative humidity study. In addition to the humidity values a corresponding elevation scale is shown along the right margin of the figure. A discussion of this figure will serve to clarify the choice of the adopted relative humidity curve (labeled "C"). Two limiting curves are shown on the figure. A minimum humidity curve labeled "B" is a "no-evaporation" curve and represents the

surface relative humidity that would result by moist adiabatic ascent of coastal air to the crest of the Coast Range with dry adiabatic descent leeward to the floor of the Central Valley. The straight line labeled "A" is a 100% relative humidity line and simply represents complete recharge of the air by evaporation of precipitation in the lee of the Coast Range.

The adopted humidity line, "C", on figure 5-8 represents a compromise between unrepresentatively high observed storm data and curve B. It was felt that an increased barrier depletion effect could be expected in the PMP case (compared to storm cases) due to the prevalence of higher wind speeds. The more stagnant the air (i.e., lighter winds) the greater is the opportunity for a recharging by falling precipitation. The adopted curve was drawn relatively closer to the no-evaporation curve in the San Joaquin than in the Sacramento since the winds in the PMP storm would exert a more pronounced depleting effect in the San Joaquin Valley where a source of low-level moisture, such as provided by the break in the Coast Range in the San Francisco Bay region, is lacking.

Figure 5-9 gives empirical support for adopting a mean humidity curve between the two extremes of a no-evaporation recharge curve and a full-evaporation recharge curve. The data for this figure concerns a two-day period in the January-February 1945 storm. Curves "C" and "D" are based on three-hourly dew points for Bakersfield and Taft. Curve A is a "full-evaporation" curve and curve B a "no-evaporation" curve based on lifting of the air at Santa Barbara across a 5370-foot barrier before descent to Bakersfield. The six-hourly rainfall amounts at Bakersfield are also shown on the figure. The San Joaquin Valley dew points show a tendency to approach the full-evaporation curve during periods of significant rain while periods of slackening or stopping of precipitation cause the dew point to drop toward the no-evaporation curve. During the 12-hour period beginning 2130Z on February 1, 1945 the Taft dew point depression indicated approximately dry adiabatic descent of air from the coastal barrier. Considerably stronger winds prevailed at Taft during this period emphasizing the increased tendency toward greater barrier depletion effect with stronger winds.

Figure 5-10 is an adaptation of the humidity curve (C) of figure 5-8. The humidity lines on figure 5-10 were used as the basis for determination of surface relative humidity for Sierra PMP computations. The relative humidity was increased from the indicated ground value with increasing height by the following rule: The specific humidity equivalent to the surface dew point was kept constant with height while the temperature decreased dry adiabatically to the level of saturation.

Precipitation Trajectories

Significance of trajectories

5.19. Precipitation particles are carried forward by the moving airstream through which they are falling. To be realistic a precipitation model

must take this motion into account. The distribution of rainfall on the slope cannot be determined accurately without knowing the area of formation of the precipitation and its subsequent path. It is especially important to study the path of the precipitation element that hits the ridge line in order to separate the precipitation into its upslope and spillover components.

Terminal velocity of raindrops

5.20. Based on the results of a survey of the literature on drop sizes and associated fall velocities a raindrop size of slightly under 0.20 cm diameter (fall velocity of 6 m/sec) was selected as appropriate for computations of orographic precipitation. Studies by Laws and Parsons (17) and Gunn and Kinzer (18) appear to have withstood the test of time regarding their conclusions on raindrop sizes and fall velocities. Results of laboratory experiments concerning relationships of fall velocities with drop size reported by Gunn and Kinzer in 1949 (18) substantially verified previous work by Laws in 1941 (19) who at that time also demonstrated a close correspondence of his laboratory values with actual storm condition measurements. Additional work by Laws and Parsons reported in 1943 (17) indicated that for a rainfall rate of 0.5 inch per hour drops with a diameter of about 0.18 cm were the primary contributor to the rainfall. Furthermore their work showed that for an intense rainfall rate of four inches per hour the primary drop size is one which falls around 8 meters per second.

Since the computations using trajectories involved orographic rainfall only it was important to pick a drop size (and fall velocity) for raindrops appropriate to orographic rainfall. Studies in orographic regions by Anderson (20) and more recently by Blanchard (21) substantiated the choice of a drop size near 0.20 cm in diameter as a good average value to use for orographic computations.

Terminal velocity of snowflakes

5.21. The fall velocity for snowflakes adopted in this study was one and one-half meters per second and is a mean value for the first 200 mb above the freezing level. The results of several studies support this choice particularly when we recognize that, in the probable maximum storm the higher levels (above 500 mb) are not a significant contributor to either upslope or close-to-ridge spillover precipitation. Langleben (22) in three case studies computed fall velocities of slightly over one meter per second and concluded a one and one-half meter per second fall velocity is likely for "rimed" flakes. Langleben also pointed out that significant agglomeration (clustering together of crystals) can occur at temperatures well below freezing. Marshall and others (23), using radar measurements concluded snowflake terminal velocities ranged from one to six feet per second. Reported terminal velocities higher than this in the below-freezing layer would imply the existence of large supercooled raindrops, snow in an almost melted condition, or hail of some form.

A 50-mb "wet snow" layer above the freezing level is introduced for probable maximum precipitation computations to allow for a transition zone where the raindrops are carried upward into the snow area by the stronger vertical velocities in probable maximum storm conditions. This layer is handled in the computations by using a fall velocity that is intermediate between those for rain and snow separately.

Construction of trajectories

5.22. Figure 5-11 shows schematically the main features of precipitation trajectory construction. In addition to the terminal fall velocities, the construction of trajectories requires a simplified smoothed approximation to the topographic profile above which is drawn the field of air streamlines. The positioning of the air streamlines is described under paragraph 5.14. Based on the adopted terminal fall velocities, the time required for the precipitation to fall a given distance (in millibars) is then used in determining the vertical component of the precipitation trajectory. The horizontal component of the trajectory is obtained by noting that the raindrop or snowflake moves horizontally with the speed of the wind.

The slope of the trajectories is a function of windspeed, ground slope, terminal velocity of precipitation elements and the elevation of the freezing level or level at which snowflakes melt to raindrops. The distribution of precipitation along the ground is influenced by the slope of the precipitation trajectories. The orographic model assumes a saturated atmosphere with close approximation to the pseudoadiabatic lapse rate. The pseudoadiabatic assumption also fixes the freezing level. The precipitation particles are assumed to form and fall (or be "swept out" by falling raindrops) as soon as the air is lifted. Storage of water as cloud droplets is neglected so that the rate of precipitation is equal to the rate of condensation.

Computation of Precipitation

5.23. The computation of orographic precipitation was based on the complete orographic model with generalized ground profile, air streamlines, moisture distribution, freezing level, and trajectories of precipitation particles. Precipitation was computed by layers bounded by streamlines. For example consider the layer bounded by the streamlines starting at 800 mb and 700 mb in figure 5-11, with S as the center streamline of the layer. The entire orographic precipitation formation within this layer, from equation (4) is:

$$\frac{R}{t} = \frac{.4 \ V_a(100) \ (q_a - q_e)}{Y} \tag{17a}$$

Here ΔP is 100 mb and the letter subscripts refer to labeled points along S in figure 5-11. Different portions of the orographic precipitation are determined by changing the specific humidity difference and the Y distance as follows:

Total precipitation falling to windward from this layer:

$$\frac{R}{t} = \frac{.4V_a(100) \ (q_a - q_d)}{Y} \tag{17b}$$

Total precipitation falling to leeward from this layer:

$$\frac{R}{t} = \frac{.4V_a(100) \ (q_d - q_e)}{Y''} \tag{17c}$$

where Y'' is the distance over which it is dispersed.

Total windward precipitation formed as rain, below freezing level from this layer:

$$\frac{R}{t} = \frac{.4V_a(100) \ (q_a - q_b)}{Y} \tag{17d}$$

Total windward precipitation formed as snow, above freezing level from this layer:

$$\frac{R}{t} = \frac{.4V_a(100) \ (q_b - q_d)}{Y} \tag{17e}$$

Total precipitation reaching ground between C and D from this layer:

$$\frac{R}{t} = \frac{.4V_a(100) \ (q_c - q_d)}{Y'} \tag{17f}$$

The several formulas are used in this report as follows: The total windward orographic precipitation in storms is obtained for model coefficient determinations, by applying (17b) to each layer. (17f) is used for determinations of orographic precipitation for various segments of the windward slope, in a test of precipitation distribution, to be described. For the PMP, the rain formation and snow formations were computed separately, by (17d) and (17e) for reasons to be given later.

Test of Trajectory Model on Storms

The test

5.24. The orographic model was tested by 6-hour periods on a group of major California storms of predominantly orographic character. These storms were: December 21-23, 1955; November 17-20, 1950; January 31-February 2, 1945; January 20-23, 1943; February 24-29, 1940; and December 9-12, 1937. The tests were conducted for 8 areas covering a wide range of California orography (figure 5-12). Basically the test consisted of comparing observed orographic precipitation (defined in paragraphs 5.01 and 3.01) on the 8 windward

slopes with the amount predicted by the model. The orographic spillover precipitation could also be compared, but to a lesser degree of reliability owing to the greater difficulty of judging the convergent rain component on the lee slopes. In addition, the observed precipitation on the lee side is not as well defined because of the sparse network of stations.

The model can also be used to calculate the distribution of precipitation within upslope or downslope areas, but this degree of refinement did not seem justified because large differences in distribution could be due to small differences in wind direction. A limited test was conducted, however, on the distribution within two test strips, one on the Coast Range, the other on the Sierras. The results of this test are given in paragraph 5.30.

Storm test areas

5.25. The test areas (figure 5-12) were chosen for their nearness to weather stations having hourly pressure records in the large storms of the region. The outflow side of the area was determined by the generalized topographic ridge line, the sides by parallel lines that pass through weather reporting stations. The inflow side was generally parallel to the outflow and about 5 miles upwind from the first significant rise in ground level (or the seacoast). This distance was chosen to include any upwind effect. The inflow or (outflow) side need not be one straight segment if the average distance from inflow to outflow (Y) is used in the computations.

Storm moisture

5.26. The index of moisture for all tests (except tests of distribution within areas) is the surface dew point. A saturated pseudoadiabatic atmosphere is assumed. At most times of heavy rainfall this index is probably reasonably close to a true measure. During lulls in the storm when drier air may slip in above moist surface air, the surface dew point is an overestimate of moisture in depth. But since lower layers are usually the most important rain contributors, this situation is not very serious. A bias toward moisture underestimation comes about at times of a surface temperature inversion. This effect is apt to be most important in the earlier portion of a storm when, for example, residual polar air still covers the Central Valley. The model coefficient, discussed in paragraph 5.29 is an attempt to take care of these and other deficiencies.

Storm winds

5.27. Inflow winds are, in all cases, estimated from geostrophic winds. The geostrophic winds are then converted to "real" winds by the wind-geostrophic wind relation discussed in paragraph 5.08 and as applied in 5.09.

In the storms prior to 1945, the upper air geostrophic wind could not be obtained for many storm periods. In these cases the 500 mb-geostrophic wind

had to be estimated from surface data only. A relation involving the surface pressure and temperature gradient was developed to do this. The surface temperature gradient is, in effect, substituted for the mean surface-to-500-mb temperature gradient which, if known, would give the 500-mb geostrophic wind exactly. It was found that the best relationships between the surface temperature gradient and upper air temperature gradient was obtained when the surface stations from which the gradient was measured were latitudinally far apart. For example, the Medford-Oakland surface temperature difference was used for the Northern California relation and San Diego-Oakland for Southern California.

Storm outflow winds are entirely theoretical and are based upon mass continuity and energy balance considerations. Computational details of the energy balanced model for outflow winds were taken up in paragraph 5.14.

Storm orographic rainfall

5.28. Average storm rainfall depths over the test areas were determined by the percent of normal annual rainfall (29) method. Six-hourly increments at each available rain reporting station were expressed in percent of the normal annual. The average percent of the normal annual for each six hours for each area was then determined, and multiplied by the normal annual over the area to obtain the 6-hour average storm rainfall depths.

The observed storm rainfall is a combination of orographic and convergence types. The observed rainfall must therefore be depleted by an estimate of the convergence rainfall. The convergence rain in each storm period was estimated from observed rainfall values at nearby stations considered relatively free of orographic influence.

The Sierra area estimates were based on average observed amounts at stations near the zero orographic precipitation line in the Central Valley. This average convergence rainfall amount was then depleted for average storm test area effective elevation by a moisture reduction factor based on ratios of precipitable waters. For example, in an area whose average pressure is 900 mbs, the upwind precipitation average is reduced by a factor surface-to-900-mb precipitable water over total column precipitable water. (A moist adiabatic lapse rate is assumed for reduction factor purposes.)

On the coast, the same kind of elevation reduction procedure was applied, but more attention was given to orographic contamination of the index stations. In some cases stations to the lee of the Coast Range were used in addition to coastal stations to compensate for coastal orographic effect. The amount of compensation required depended on the moisture flow across the barrier. For Southern California areas, as well as some other coastal areas where no suitable inland stations are available, percentage reductions were made for orographic effect, depending on station and strength of upslope flow.

An attempt was made to compensate for precipitation bursts oriented parallel to the coast which were apparent at the coast during the last part of a 6-hour period but over most of the basin during the following period.

In storms involving semi-stationary convergence patterns, such as ahead of slow-moving warm fronts, large geographical variation of convergence precipitation over the area introduces errors in the use of upwind values for area values. Also in a few cases, low-level divergence occurred over large regions, resulting in negligible rain upwind of the area during the 6-hour period, which only partially reflects the depletion of orographic rain over the area. These effects, not compensated for, play a part in the poor computed-observed orographic precipitation relation in some periods.

Table 5-2 contains the estimated convergence precipitation, estimated orographic and the total precipitation. The convergence precipitation, depleted for elevation appears in the table as a positive quantity additive to the orographic rain to equal the total observed precipitation.

In a few storm periods the index stations showed short periods of no rain between intense precipitation bursts. In this situation it is logical to assume that these short no-rain periods were associated with divergence between regions of intense convergence. Further it is assumed that these divergence areas are operative over the nearby slopes causing the orographic rain to be less than what would occur without the divergence. A correction was therefore applied in these periods, analagous to the convergent correction. The amount of the divergence correction was determined by a plot of the time-intensity bursts at the non-orographic index stations. The amplitude of the negative portion of the time-intensity profile was arbitrarily made one-third of the average amplitude of the preceding and following bursts. These corrections appear as negative numbers in the convergent precipitation column of table 5-2. This amount is subtracted from the orographic precipitation to give the observed total. A depletion for elevation was also applied here.

Test results

5.29. Table 5-2 contains the basic storm data that went into the model, the observed total rainfall, the adjustment to "observed orographic", the computed orographic, and the ratio observed to computed (λ). The ratio of observed to computed rain (λ) is a measure of the efficacy of the model in duplicating the rain. It is by the study of this ratio that the results are evaluated.

A total of 111 cases in the eight test areas were computed. Not all storm periods within a given storm were done because of time limitations. The 1st, 2nd, 3rd, 4th, 6th, 8th and 12th period, in order of observed orographic precipitation intensity, were chosen for computation.

Table 5-2

BASIC STORM DATA, COMPUTED WINDWARD OROGRAPHIC PRECIPITATION AND MODEL COEFFICIENT

Period No.	Date	Time 6-hr end (PST)	Surface Dew point (°F)	V_g Sea-level (mph)	V_g 500 mb (mph)	Precipitation Observed Conv. (in.)	Oro. (in.)	Total (in.)	Computed Oro. (in.)	λ (R_o/R_c)
				Test Area No. 1						
				January 1943 Storm						
1	21	12	45.0	26	24	-	-	.02	n.c.	-
2		18	51.3	26	36	0	.12	.12	.41	0.29
3		24	54.3	45	58	.04	.13	.17	n.c.	-
4	22	06	55.3	53	72	.16	.85	1.01	.81	1.05
5		12	56.4	49	59	.10	.83	0.93	n.c.	-
6		18	56.1	64	74	.10	.85	0.95	.93	0.91
7		24	56.6	70	93	.20	1.16	1.36	1.02	1.14
8	23	06	56.0	39	58	.23	1.14	1.37	.74	1.54
9		12	55.1	29	55	-.03	.42	0.39	.64	0.66
				Test Area No. 2						
				January 1943 Storm						
1	20	24	41.0	15	34	0	.04	.04	0.24	0.17
2	21	06	43.0	38	48	.04	.10	.14	n.c.	-
3		12	47.0	59	57	.16	.22	.38	n.c.	-
4		18	52.5	63	73	.20	.76	.96	n.c.	-
5		24	56.0	46	59	.44	2.00	2.44	1.05	1.90
6	22	06	57.0	28	47	.20	1.11	1.31	0.82	1.35
7		12	57.0	40	50	.04	.55	.59	0.99	0.56
8		18	57.5	65	75	.28	1.36	1.64	1.24	1.10
9		24	58.0	55	78	.24	1.58	1.82	1.19	1.33
10	23	06	56.5	42	61	.04	.57	.61	0.94	0.61
11		12	55.5	27	53	0	.48	.48	0.72	0.67
12		18	54.5	2	25	.04	.20	.24	n.c.	-

n.c. - not computed

Table 5-2 Continued

Period No.	Date	Time 6-hr end (PST)	Surface Dew point (°F)	V_g Sea-level (mph)	V_g 500 mb (mph)	Precipitation Observed Conv. (in.)	Oro. (in.)	Total (in.)	Computed Oro. (in.)	λ (R_o/R_c)
					Test Area No. 3					
					December 1937 Storm					
1	9	06	52.0	45	74	0.00	0.18	0.18	0.51	0.35
2		12	54.0	53	88	0.07	0.41	0.48	0.66	0.62
3		18	56.0	59	88	0.13	0.58	0.71	0.73	0.79
4		24	59.0	68	78	0.25	0.48	0.73	0.90	0.53
5	10	06	-	84	91	0.42	0.13	0.55	n.c.	-
6		12	-	84	88	0.06	0.10	0.16	n.c.	-
7		18	-	78	88	0.09	0.44	0.53	n.c.	-
8		24	64.0	78	82	0.10	0.75	0.85	1.16	0.65
9	11	06	61.0	78	82	0.35	0.56	0.91	1.02	0.55
10		12	-	62	78	0.38	0.19	0.57	n.c.	-
11		18	-	53	85	0.14	0.08	0.22	n.c.	-
12		24	57.0	45	74	0.02	0.02	0.04	0.70	0.03
					November 1950 Storm					
1	18	12	57.5	52	46	0.06	0.10	0.16	0.72	0.14
2		18	60.1	46	50	0.01	0.03	0.04	n.c.	-
3		24	60.6	65	62	0.02	0.13	0.15	0.88	0.15
4	19	6	59.8	52	68	0.08	0.39	0.47	0.84	0.46
5		12	60.7	31	60	0.08	0.35	0.43	0.74	0.47
					December 1955 Storm					
1	22	6	57.1	65	58	0.12	0.41	0.53	0.76	0.54
2		12	57.4	54	58	0.14	0.22	0.36	n.c.	-
3		18	59.1	56	57	-0.14	0.29	0.15	0.78	0.37
4		24	59.0	78	73	0.43	1.31	1.74	0.94	1.39
5	23	6	59.1	59	84	0.44	1.35	1.79	0.76	1.78
6		12	56.7	69	89	0.27	0.62	0.89	0.79	0.78
7		18	54.9	37	91	0.20	0.60	0.80	0.53	1.13
8		24	51.9	13	92	0.35	0.47	0.82	n.c.	-

Table 5-2 Continued

Period No.	Date	Time 6-hr end (PST)	Surface Dew point (°F)	V_g Sea-level (mph)	V_g 500 mb (mph)	Precipitation Observed Conv. (in.)	Oro. (in.)	Total (in.)	Computed Oro. (in.)	λ (R_o/R_c)
				Test Area No. 4						
				December 1937 Storm						
1	9	6	46.4	30	98	0.00	0.00	0.00	0.25	0
2		12	51.8	30	63	0.27	0.22	0.49	n.c.	-
3		18	51.8	15	12	0.25	0.38	0.63	0.25	1.52
4		24	53.1	39	53	0.45	0.73	1.18	0.48	1.52
5	10	6	56.8	57	88	0.39	0.87	1.26	0.59	1.47
6		12	58.6	60	97	0.25	0.62	0.87	n.c.	-
7		18	58.2	59	104	0.13	0.62	0.75	0.68	0.91
8		24	57.3	41	82	0.36	0.66	1.02	0.58	1.14
9	11	6	57.7	54	90	0.27	0.78	1.05	0.66	1.18
10		12	56.6	30	67	0.02	0.38	0.40	n.c.	-
11		18	55.5	0	23	0.00	0.06	0.06	n.c.	-
12		24	54.9	0	38	0.02	0.10	0.12	n.c.	-
				November 1950 Storm						
1	17	18	53.8	17	49	0.22	0.26	0.48	n.c.	-
2		24	55.8	23	43	0.03	0.16	0.19	n.c.	-
3	18	6	55.6	15	42	0.08	0.22	0.30	0.26	0.85
4		12	55.0	1	68	0.36	0.41	0.77	0.14	2.93
5		18	55.3	22	83	0.34	0.70	1.04	0.44	1.59
6		24	57.2	29	69	0.20	0.82	1.02	0.51	1.61
7	19	6	56.3	17	54	0.11	0.34	0.45	0.34	1.00
				December 1955 Storm						
1	21	12	56.8	30	63	0.06	0.15	0.21	0.46	0.33
2		18	58.0	41	72	0.45	0.50	0.95	n.c.	-
3		24	57.1	38	78	0.95	0.99	1.94	0.51	1.94
4	22	6	56.1	29	82	0.14	1.23	1.37	0.40	3.08
5		12	57.3	13	78	0.09	0.39	0.48	n.c.	-

Table 5-2 Continued

Period No.	Date	Time 6-hr end (PST)	Surface Dew point (°F)	V_g Sea-level (mph)	V_g 500 mb (mph)	Precipitation Observed Conv. (in.)	Oro. (in.)	Total (in.)	Computed Oro. (in.)	λ (R_o/R_c)
						Test Area No. 4 Cont'd				
						December 1955 Storm Cont'd.				
6		18	57.3	27	83	0.23	0.12	0.35	n.c.	-
7		24	58.0	57	108	0.77	0.79	1.56	0.57	1.39
8	23	6	57.1	30	102	-0.10	0.48	0.38	0.41	1.17
9		12	56.0	4	94	0.27	0.56	0.83	0.20	2.80
10		18	52.3	3	92	0.00	0.14	0.14	n.c.	-
						Test Area No. 5				
						December 1955 Storm				
1	21	12	55.5	71	80	0.13	0.45	0.58	1.03	0.44
2		18	56.9	72	76	0.33	1.27	1.60	0.97	1.31
3		24	56.4	72	75	0.26	1.37	1.63	1.01	1.36
4	22	6	56.5	59	129	0.07	0.91	0.98	0.98	0.93
5		12	54.3	26	122	0.06	1.29	1.35	0.53	2.43
6		18	52.8	23	98	0.13	0.18	0.31	0.56	0.32
7		24	51.9	54	108	0.33	0.46	0.79	n.c.	-
8	23	6	50.2	14	129	0.04	0.21	0.25	n.c.	-
9		12	46.7	12	145	0.04	0.01	0.05	n.c.	-
						Test Area No. 6				
						December 1937 Storm				
1	9	6	44.0	7	75	0.00	0.04	0.04	0.37	0.11
2		12	45.7	6	39	0.15	0.12	0.27	n.c.	-
3		18	48.4	0	0	0.22	0.52	0.74	0.00	inf.
4		24	51.2	16	30	0.21	1.21	1.42	n.c.	-
5	10	6	53.7	45	76	0.32	1.20	1.52	0.90	1.33
6		12	58.9	56	93	0.40	1.01	1.41	1.40	0.72
7		18	62.2	60	105	0.03	0.70	0.73	n.c.	-

Table 5-2 Continued

Period No.	Date	Time 6-hr end (PST)	Surface Dew point (°F)	V_g Sea-level (mph)	V_g 500 mb (mph)	Precipitation Observed Conv. (in.)	Oro. (in.)	Total (in.)	Computed Oro. (in.)	λ (R_o/R_c)
				Test Area No. 6 Cont'd						
				December 1937 Storm Cont'd						
8		24	61.3	49	90	0.36	0.96	1.32	n.c.	-
9	11	6	58.7	41	77	0.57	1.03	1.60	1.09	0.94
10		12	57.4	54	91	0.13	0.88	1.01	1.20	0.73
11		18	53.3	40	63	0.00	0.27	0.27	n.c.	-
12		24	51.4	17	55	0.02	0.12	0.14	n.c.	-
				February 1940 Storm						
1	24	24	55.8	2	36	0.05	0.08	0.13	n.c.	-
2	25	6	55.2	10	48	0.12	0.31	0.43	n.c.	-
3		12	54.8	5	39	0.27	0.35	0.62	0.40	0.88
4		18	55.4	15	15	0.05	0.17	0.22	n.c.	-
5		24	53.9	22	42	0.03	0.09	0.12	n.c.	-
6	26	6	53.9	48	79	0.00	0.14	0.14	n.c.	-
7		12	53.7	46	63	0.12	0.54	0.66	n.c.	-
8		18	55.2	45	31	0.35	0.65	1.00	1.11	0.59
9		24	55.0	57	86	0.39	0.85	1.24	1.34	0.63
10	27	6	54.3	56	92	0.41	1.01	1.42	1.07	0.94
11		12	53.9	39	63	0.14	0.50	0.64	n.c.	-
12		18	54.3	32	40	0.47	0.89	1.36	0.85	1.05
13		24	53.6	31	41	0.14	0.42	0.56	n.c.	-
14	28	6	52.1	47	60	0.29	0.53	0.82	0.98	0.54
15		12	52.8	60	90	0.04	0.41	0.45	n.c.	-
16		18	49.5	35	65	0.02	0.25	0.27	n.c.	-
17		24	49.2	42	73	0.18	0.43	0.61	0.84	0.51
18	29	6	48.2	34	67	0.03	0.42	0.45	n.c.	-
				November 1950 Storm						
1	17	6	52.6	22	66	0.05	0.18	0.23	n.c.	-
2		12	55.1	22	60	0.14	0.35	0.49	0.78	0.45
3		18	58.3	28	55	0.08	0.50	0.58	n.c.	-

Table 5-2 Continued

64

Period No.	Date	Time 6-hr end (PST)	Surface Dew point (°F)	V_g Sea-level (mph)	V_g 500 mb (mph)	Precipitation Observed Conv. (in.)	Oro. (in.)	Total (in.)	Computed Oro. (in.)	λ (R_o/R_c)
					Test Area No. 6 Cont'd					
					November 1950 Storm Cont'd					
4		24	57.8	35	59	0.10	0.66	0.76	1.03	0.64
5	18	6	56.2	14	80	0.31	0.83	1.14	n.c.	-
6		12	61.8	8	91	0.19	0.93	1.12	0.81	1.15
7		18	58.2	15	80	0.08	0.94	1.02	n.c.	-
8		24	56.9	4	71	0.03	0.66	0.69	n.c.	-
9	19	6	53.4	0	77	0.00	0.21	0.21	n.c.	-
10		12	53.3	0	78	0.00	0.07	0.07	n.c.	-
11		18	57.3	7	66	0.00	0.09	0.09	n.c.	-
12		24	58.5	8	59	0.04	0.41	0.45	n.c.	-
13	20	6	60.6	12	71	0.27	1.01	1.28	0.74	1.36
14		12	61.0	17	83	0.13	1.17	1.30	0.87	1.35
15		18	63.8	12	75	0.13	1.18	1.31	0.88	1.34
16		24	60.5	7	69	0.14	0.95	1.09	0.72	1.32
					December 1955 Storm					
1	21	12	53.8	37	51	0.02	0.09	0.11	n.c.	-
2		18	56.0	66	76	0.13	0.80	0.93	n.c.	-
3		24	57.2	71	80	0.36	1.53	1.89	1.52	1.01
4	22	6	56.7	77	72	0.13	1.41	1.54	1.50	0.94
5		12	57.3	56	86	0.02	0.93	0.95	n.c.	-
6		18	58.3	59	72	-0.16	0.54	0.38	n.c.	-
7		24	58.0	76	105	0.27	1.27	1.54	1.56	0.81
8	23	6	57.8	104	141	-0.12	0.66	0.54	1.73	0.38
9		12	54.0	54	127	0.24	1.34	1.58	1.05	1.28
10		18	48.2	33	136	0.06	0.84	0.90	0.84	1.00
					Test Area No. 7					
					December 1937 Storm					
1	9	6	41.7	1	49	0.00	0.07	0.07	0.30	0.23
2		12	45.3	22	56	0.09	0.17	0.26	n.c.	-

Table 5-2 Continued

Period No.	Date	Time 6-hr end (PST)	Surface Dew point (°F)	V_g Sea-level (mph)	V_g 500 mb (mph)	Precipitation Observed Conv. (in.)	Oro. (in.)	Total (in.)	Computed Oro. (in.)	λ (R_o/R_c)
				Test Area No. 7 Cont'd						
				December 1937 Storm Cont'd						
3		18	49.2	36	49	0.15	0.48	0.63	n.c.	-
4		24	54.2	48	60	0.22	0.97	1.19	1.01	0.96
5	10	6	58.3	58	77	0.21	0.99	1.20	1.22	0.81
6		12	60.2	58	78	0.18	0.88	1.06	n.c.	-
7		18	61.3	53	80	0.06	0.31	0.37	n.c.	-
8		24	61.0	60	82	0.18	0.78	0.96	1.42	0.55
9	11	6	60.8	54	74	0.27	1.30	1.57	1.35	0.96
10		12	60.0	34	60	0.29	1.08	1.37	1.04	1.04
11		18	57.8	9	36	0.07	0.41	0.48	0.50	0.82
12		24	54.5	12	45	0.00	0.16	0.16	n.c.	-
				November 1950 Storm						
1	17	6	52.2	18	53	0.00	0.10	0.10	n.c.	-
2		12	55.8	22	53	0.06	0.14	0.20	0.76	0.18
3		18	58.3	22	47	0.01	0.41	0.42	n.c.	-
4		24	58.2	8	50	0.11	0.64	0.75	0.62	1.03
5	18	6	57.3	17	72	0.32	1.22	1.54	0.85	1.44
6		12	59.2	47	77	0.30	1.66	1.96	1.09	1.52
7		18	60.8	45	67	0.27	1.79	2.06	1.27	1.41
8		24	60.1	36	56	0.15	1.43	1.58	1.04	1.37
9	19	6	58.6	21	49	0.01	0.49	0.50	n.c.	-
10		12	57.8	13	50	0.03	0.04	0.07	n.c.	-
11		18	60.6	13	55	0.00	0.06	0.06	n.c.	-
12		24	61.0	12	60	0.10	0.26	0.36	n.c.	-
13	20	6	62.8	32	63	0.14	0.85	0.99	1.22	0.70
14		12	63.7	34	63	0.06	0.91	0.97	n.c.	-
15		18	64.9	24	58	0.01	0.62	0.63	n.c.	-
16		24	62.3	19	50	0.01	0.65	0.66	n.c.	-

Table 5-2 Continued

Period No.	Date	Time 6-hr end (PST)	Surface Dew point (°F)	V_g Sea-level (mph)	V_g 500 mb (mph)	Precipitation Observed Conv. (in.)	Oro. (in.)	Total (in.)	Computed Oro. (in.)	λ (R_o/R_c)

Test Area No. 7 Cont'd

December 1955 Storm

Period No.	Date	Time 6-hr end (PST)	Surface Dew point (°F)	V_g Sea-level (mph)	V_g 500 mb (mph)	Conv. (in.)	Oro. (in.)	Total (in.)	Computed Oro. (in.)	λ (R_o/R_c)
1	21	18	56.3	32	54	0.01	0.16	0.17	n.c.	-
2		24	57.0	32	61	0.11	0.62	0.73	0.95	0.65
3	22	6	56.7	31	67	0.28	1.52	1.80	0.92	1.65
4		12	57.2	32	67	0.06	1.42	1.48	n.c.	-
5		18	59.4	35	73	-0.13	0.74	0.61	n.c.	-
6		24	59.2	57	83	0.60	1.73	2.33	1.26	1.37
7	23	6	58.5	68	88	0.27	1.68	1.95	1.29	1.30
8		12	56.7	61	99	0.25	1.40	1.65	1.20	1.17
9		18	53.1	25	122	0.21	1.47	1.68	0.86	1.71

Test Area No. 8

November 1950 Storm

Period No.	Date	Time 6-hr end (PST)	Surface Dew point (°F)	V_g Sea-level (mph)	V_g 500 mb (mph)	Conv. (in.)	Oro. (in.)	Total (in.)	Computed Oro. (in.)	λ (R_o/R_c)
1	18	6	56.5	15	31	0.06	0.38	0.44	0.78	0.49
2		12	58.9	21	39	0.02	1.05	1.07	0.96	1.09
3		18	59.2	31	57	0.00	0.86	0.86	1.03	0.83
4		24	57.2	22	61	0.07	1.20	1.27	0.87	1.38
5	19	6	57.1	6	53	0.04	0.97	1.01	0.66	1.47
6		12	61.3	7	47	0.00	0.48	0.48	n.c.	-
7		18	63.3	5	41	0.00	0.04	0.04	n.c.	-
8		24	63.9	4	39	0.01	0.03	0.04	n.c.	-
9	20	6	62.9	1	39	0.02	0.05	0.07	0.53	0.09
10		12	62.8	6	38	0.00	0.06	0.06	n.c.	-

December 1955 Storm

Period No.	Date	Time 6-hr end (PST)	Surface Dew point (°F)	V_g Sea-level (mph)	V_g 500 mb (mph)	Conv. (in.)	Oro. (in.)	Total (in.)	Computed Oro. (in.)	λ (R_o/R_c)
1	22	6	51.2	9	43	0.09	0.16	0.25	n.c.	-
2		12	55.2	8	45	0.09	0.71	0.80	0.64	1.11
3		18	58.5	12	56	-0.25	0.39	0.14	n.c.	-
4		24	58.5	17	70	-0.06	0.89	0.83	1.03	0.86
5	23	6	58.6	12	82	0.18	1.23	1.41	0.85	1.45
6		12	57.2	1	84	0.09	0.76	0.85	0.72	1.06
7		18	57.0	0	95	0.03	0.32	0.35	0.79	0.41

The over-all average observed divided by computed precipitation (λ) for the 111 cases was 0.994 with one case eliminated, the infinite value for the third period of the December 1937 storm in Test Area No. 6. (This odd result is due to a breakdown of the method for estimating the 500-mb geostrophic wind. The surface temperature gradient method yielded the unrealistic value of zero for this level.)

While the trajectory model as applied to these storms gives a very good approximation in the mean, there is a wide variation in individual cases. λ varies from zero to slightly over three. In an effort to account for some of this variability it was observed that if λ is ordered by magnitude of the observed 6-hour precipitation, high values occurred during the heavy rain periods and lower λ values in the light rain periods. A plot of these curves for the individual storms by Coast Range and Sierra appear in figure 5-13a and b. High peaks and troughs are a feature of most individual storms but the general trend of the relation is unmistakable. λ for the Coast Range and Sierras was plotted separately to see whether there was significant difference. Average decay curves for each Range (figure 5-14) seemed to be similar enough to combine. The final adopted combined Coast Range and Sierra curve is shown on the same figure. (The matter of statistical bias introduced by the ordering process when this curve is used in the maximum case is examined in paragraph 5.43.)

The dropoff of λ is so pronounced that it is more effective in reducing the rainfall than the wind and moisture dropoff with time combined. The question arises as to why λ varies and why it drops off with observed rain. To answer these questions a list of sources of error in both computed and observed rain is instructive.

1. Sources of error in computed orographic precipitation.

    a) Unrepresentativeness of surface dew point especially in lighter rain situations.

    b) Estimate of upper wind from upper geostrophic wind in error (from V_c/V_{gc} relation scatter).

    c) Estimate of upper-level geostrophic wind from thermal wind relation in error.

    d) Error in outflow winds due to error of inflow wind.

    e) Effect of wind error on spillover percentage.

    f) Error in choice of average effective nodal surface.

    g) Simplification of the terrain profile.

    h) Error in assumed lapse rate of temperature and/or moisture.

2. Sources of error in "observed" orographic precipitation.

    a) Gage catch error due to wind.

    b) Error in estimate of total precipitation over test area from gages.

    c) Error in estimate of convergent component of total observed precipitation.

Model coefficients over 1.0 are probably due to an underestimation of the inflow of water vapor or an overestimation in the orographic rain, or both. The inflow profiles are derived from empirically determined averages and represent the <u>most probable</u> wind with a given geostrophic gradient, thus part of the time it is an underestimate of the wind.

The low values of λ when the observed rainfall is light may result largely from lack of saturation aloft. In this situation the surface dew point would be too high, i.e., not representative of the entire column. The decay curve of λ measures the departure from saturation aloft when the storm sequence is reordered by 6-hour observed amounts. Another possible reason for low λ values with light rain is divergence aloft, which results in zero precipitation at the convergence rain index stations but tends to rob the orographic precipitation on the slopes.

In estimating the convergence component of the total precipitation from index stations, the convergence rainfall was depleted for elevation as described in paragraph 5.28. This procedure most nearly replicates with the test storms the procedure followed later in computing PMP. There is, on the average, less moisture available to be processed in the air column over the slope than over the low elevation convergence index stations. Complicating factors, very difficult to evaluate, tend to augment or diminish the convergence rain estimate from index stations. These factors include the stability of the air, the degree of saturation and its distribution in the vertical, and lateral variations of the convergence rain bursts. Although it is theoretically possible to take these effects into consideration to some extent, little over-all confidence can be placed in such corrections for a particular storm and/or area. For this reason the depletion which probably occurs on the average over the slopes was used, i.e., based on the ratio of the depths of precipitable water. The adopted model coefficient curve shown in figure 5-14 results from this concept.

If the convergence component is not depleted for elevation, the model coefficient curve is somewhat lower for the first 24 hours. This curve is shown on figure 5-14 for comparison, marked A. The effect on PMP estimates would be to reduce them by the ratio of the two curves, i.e., curve A divided by adopted curve value.

Distribution within windward areas

5.30. A stringent test of the trajectory model is to compare the observed with computed orographic rain <u>within</u> windward areas. The December 1955 storm was chosen as a favorable one for such a test. Knox (24) has made a similar test of his model on the December 1955 storm in the Feather River Basin. For our distribution test, two strips 20 miles wide were chosen, one on the Coast Range and one on the Sierra. Figure 5-15 shows the location of these strips, the placement of which was chosen partly on the basis of recorder gages in operation at the time. The Coast Range test area extends northeast from Point Arena to the main ridge (5900 feet) 65 miles from the coastline. The generalized topographic profile (see figure 5-16a) shows a sharp rise between 40 and 50 miles from the coast but does not show a short abrupt rise near the coast. The Sierra test area is in the vicinity of Blue Canyon. The generalized topographic profile (see figure 5-16b) shows an almost continuous rise to 7700 feet at a distance of 53 miles from the entrance. The rise is somewhat steeper beyond 44 miles. There is a second ridge (also to 7700 feet) 10 miles east of the first ridge. The ground between them is shown generalized as a level plateau.

The test was conducted for two 6-hour periods ending at 1800 and 2400 PST December 21, 1955 for both the Coast Range and Sierra sites. The two 6-hour periods were combined in order to smooth out random irregularities, and because the estimation of the convergence rainfall is quite uncertain over such a small area in a given 6-hour period.

In the Coast Range test the moisture charge and its vertical distribution was determined by the surface dew point and an assumed saturated pseudo-adiabatic atmosphere. Moisture for the Sierra test was taken from the observed Oakland sounding and included lack of saturation, where present. The inflow wind profiles used for the Coast Range test were the same as used for Test Area No. 5, i.e., from the geostrophic winds and V_c/V_{gc} relationship. Sierra inflow winds were taken from observed rawins at Oakland modified by Sacramento winds aloft and the surface winds at Blue Canyon Airport.

The distribution of observed precipitation was accomplished by means of the percent of normal annual precipitation method, using all recorders and non-recorders within and in the vicinity of the strip. The precipitation was then averaged at 10-mile intervals along the strip up the slope. The resulting precipitation profiles were corrected for convergence effects by use of index stations where orographic influence was at a minimum.

Figures 5-16a and b show the comparative computed and observed precipitation profiles in inches per 6 hours. Both the Coast Range and Sierra computed distributions are, in general, consistent with the observed, i.e., the precipitation increases with increased slope and is of about the right order of magnitude. The Sierra test shows better agreement, as expected, since more observed data are entered into the model. Also the topography is less

broken up and can therefore be better generalized. The computed precipitation of the Coast Range test falls short of the observed for the 40 miles near the coast. This discrepancy may be due at least in part to the lack of a proper estimate of the convergence component of the observed precipitation in this area. This is due to a tendency for the orography to set off convection, thus concentrating the convergence component in the lower portion of the slope.

5-C. MAXIMIZATION OF OROGRAPHIC PRECIPITATION

Maximum Moisture

5.31. The maximum orographic storm is conceived of by extension from the most intense predominantly orographic storms of record. These storms have moisture sources from low latitudes (see figure 3-1, for example, showing path of warm air).

The maximum 12-hour dew points during midwinter are about 62°F along the Southern California coast (see figure 4-5a). This is about 7° higher than the offshore water temperature. Trajectories in some of the major storms show that the moist air comes from south of 25°N latitude where the water temperature is 72°F or more. (Sea surface temperatures sometimes are regarded as the index of maximum potential of the atmosphere to contain moisture. Actually the maximum moisture is somewhat less than the sea surface temperatures in the source region would indicate as there must be gradient from sea surface vapor pressure to air vapor pressure for evaporation to take place). Most of the water vapor apparently lost in transit from the Tropics to California is distributed in depth or stored in heavy cloud layers. A small portion is lost by condensation back to the sea. Even so, the air is probably not saturated to the nodal surface as this would require a greater amount of instability than is usually found in the orographic storm. Some mixing of the tropical air with drier peripheral air at higher latitudes undoubtedly takes place also.

The index of maximum moisture used in the orographic storm is the maximum observed surface dew point found in storm situations. The surface dew point is more representative of the whole column of air during this type of storm than in most other weather situations. Lack of complete saturation mentioned earlier is very often compensated for by a slight surface temperature inversion.

There is some reason to think that observed moisture might be higher in the maximum case than the adopted criteria as stronger southwesterly winds would tend to raise the dew point and moisture content of the air over California (less time for condensation of water vapor on sea surface). The maximum dew points used to compute the maximum orographic storm rainfall are the same as those used for the maximum convergence storm, including geographical, seasonal and durational variation. The dew points are described in detail in chapter IV.

Maximum Winds

Approaches

5.32. Estimates of maximum winds may be approached from two angles,
1) from maximum pressure gradients converted to winds and 2) the statistical
extrapolation of observed winds. Both of these avenues have been used to
form a final judgment on PMP winds.

Estimation by pressure gradients

5.33. 1. Surface. Sea-level pressure gradients as an index for maximum
winds have definite advantages, but must be used with caution. The relative-
ly great length of record, the large number of observing points and the con-
tinuous nature of the record (barograph traces) make them an indispensable
aid. Their disadvantage is that local distortions of the pressure field due
to dynamic effects sometimes give erroneous indications of the wind. Very
often in periods of strong winds a dynamic trough forms in the lee of a moun-
tain range. This effect may persist for long periods of time in storm situa-
tions but with varying strength due to changes in wind direction and speed.
It is generally difficult and not too reliable to correct for this effect.
Winds based on dynamically-affected pressure gradients are fictitiously high
or low since the actual wind does not have to accelerate to the value the
pressure gradients indicate.

Almost all stations in California are subject to some dynamic effect,
being either in a downslope trough or upslope ridge at times of high winds.
The choice of cases for inclusion is therefore partly a matter judgment. The
difficulty can be mitigated somewhat by choosing pairs of pressure-observing
stations with similar dynamic effect, but this becomes more difficult with
increasing distance between them. In most instances high pressure gradient
cases in which dynamic effects were strong have been discarded.

Geostrophic winds were computed from pressure differences between sta-
tions oriented approximately parallel to the mountains. The record covered
by the pressure gradient survey is listed in table 5-3, and comes mainly
from severe stormy periods.

Persisting large pressure differences were extracted from the records
for durations of 1, 3, 6, 12.....72 hours with station separations of about
20 to 600 miles. After investigation for dynamic effect, the accepted pres-
sure gradients were converted to geostrophic winds, adjusted for season (to
February 1) and for latitude (to 38°N). The maximum geostrophic winds were
then plotted (figure 5-17) and enveloping lines drawn. One value, that for
Red Bluff to Chico in the January 1943 storm at 54 hours, was undercut
slightly for smoothing purposes.

Table 5-3

PRESSURE GRADIENT SURVEY DATES

Dec. 21-23, 1955	March 22-27, 1928
Nov. 17-20, 1950	Feb. 14-16, 1927
Oct. 27-29, 1945	April 3-5, 1926
Jan. 30-Feb. 2, 1945	Dec. 18-26, 1921
March 6-8, 1943	Jan. 26-28, 1916
Jan. 19-24, 1943	Dec. 16-18, 1914
Feb. 24-29, 1940	Dec. 29, 1913-Jan. 3, 1914
Feb. 28-March 2, 1938	Jan. 12-16, 1909
Dec. 9-11, 1937	March 16-20, 1907
April 6-8, 1935	Jan. 11-19, 1906
Oct. 15-17, 1934	Oct. 18-20, 1899
Dec. 8-16, 1929	

2. Upper air. The 500-mb geostrophic wind is uniquely determined by the surface geostrophic wind and the surface-to-500-mb thermal wind. The thermal wind in turn is directly proportional to the horizontal temperature gradient averaged between the two levels. It is obvious that with a given surface geostrophic wind the 500-mb geostrophic wind is strictly limited by the possible thermal gradients consistent with the climatology of the region and the storm type.

An empirical study was conducted to determine the limiting value of the 500-mb wind when the surface geostrophic wind approaches the highest observed values. The data were taken from the upper wind studies of Oakland, Long Beach, Santa Maria, Merced and Red Bluff. Figure 5-18 shows a plot of surface geostrophic wind vs the ratio of 500 mb-to-surface geostrophic wind. The data show that the higher the surface geostrophic wind, the smaller the ratio of 500 mb-to-surface geostrophic wind. The thin curving lines on the chart are the horizontal temperature gradients (in degrees Fahrenheit per degree latitude) averaged from the surface to 500 mb, necessary to produce the ratio of surface to 500-mb wind, at given surface geostrophic windspeed These lines show that at higher surface geostrophic speeds more temperature gradient is needed to produce the same 500 mb-to-surface ratio. For example, to double a surface geostrophic wind of 50 mph at the 500-mb level only 1.4 °F/°latitude is needed while about 4.2°F is required at 150 mph. This effect accounts for the observed low ratios at the higher surface geostrophic speeds since the moist air of tropical origin is characteristically homogeneous and has relatively weak temperature fields.

The adopted 500 mb-to-surface relationship (heavy dashed curve on figure 5-18) envelops about 85% of the points and is shaped in part by the curvature of the temperature-gradient lines. The adopted curve becomes coincident with the 1.0 ratio line above 165 mph. The ratios, since they were

developed from individual observations, are assumed to apply for 1 hour's time.

Figure 5-19 shows the maximum wind profiles derived by using maximum surface and 500-mb geostrophic winds and the V_c/V_{gc} ratios for coastal California. The light dashed straight lines connect surface and 500-mb geostrophic winds. (It is assumed that the geostrophic wind varies linearly between the surface and 500 mb). The surface geostrophic winds are taken from the envelope of maximum geostrophic winds (see figure 5-17) at the 30-mile width. The surface decay with time is from the same curve.

The 500-mb 1-hour geostrophic wind of 200 mph is derived from the surface geostrophic wind and the ratio of surface-to-500-mb geostrophic wind of 1:1 (from figure 5-18). The decay with duration of the 500-mb geostrophic wind is assumed the same as the decay of the actual wind at that level, to be discussed later (par. 5.37).

The "actual" winds between 1000 and 500 mb are found by using the V_c/V_{gc} ratios from figure 5-3. The 300-mb wind is derived from the $V_{300} = 1.30 \ V_{500}$ relationship.

Statistical estimate of maximum winds

5.34. The statistical approach to the estimate of maximum winds is in a sense the most direct one. Several severe limitations, however, preclude the possibility of basing estimates on such extrapolations alone. One obvious limitation is the short length of record. Oakland, which has the best record of upper wind data on the West Coast, had no rawin before 1949. This means that before 1949 upper winds were almost always lacking during rainy periods. Between 1949 and October 1954 rawin soundings were made twice a day but wind data above 3000 m. were very sparce when surface winds were strong. For a period of about 3 years starting in October 1954 four rawins a day were taken. These have been very satisfactory in obtaining winds at all levels during rainy and windy periods. Estimates of maximum winds aloft have to come primarily from the 5-year record 1954-1958, with a little help from the period 1947-1953.

Both the short period of record and the tendency for missing observations during periods of strong surface winds have a biasing effect toward lowering of estimates of maximum winds.

Still another bias toward lower estimates is the non-continuous nature of upper air observations. The chance of observing the maximum wind at a particular level is small since the balloon is at or near it only a small fraction of a day. It is assumed that each upper air observation is representative of about one hour's time.

With aforementioned limitations in mind, an analysis has been made of the Oakland maximum winds at selected levels for the November through February

period. It was thought that this period would contain almost all of the highest yearly values. The 12-year period 1947-1958 was used, with no corrections attempted for missing reports or number of observations per day. Highest winds were tabulated: a) regardless of direction and b) within certain restricted directions, typical of precipitation storms. Wind direction restrictions are as follows: surface, no restriction; 950 mb, SSE through W; 900 mb, S through W; and 850 mb through 300 mb, SSW through W. A similar study was made for Santa Maria for three levels.

Figures 5-20 and 5-21 show some results of these studies. Oakland and Santa Maria maximum winds from the restricted directions were plotted on extreme probability paper and straight lines fitted. Fifty-year mean return internal winds were read from the fitted lines and plotted as vertical wind profiles. These appear on figure 5-22.

Comparison of statistical and geostrophically-derived winds

5.35. In order to compare the two methods, the 50-year return period winds at Oakland and Santa Maria are shown on figure 5-22 along with the geostrophically-derived 1-hour maximum wind from figure 5-19. (Fifty years was chosen because it roughly corresponds with the pressure record). It will be recalled that the geostrophic wind is on a component basis, while the statistical winds are total winds. On the other hand, the geostrophic winds are from scores of station records, while the statistical are from but two. These two biases are in opposing directions, though not necessarily of the same magnitude.

The 50-year Oakland wind and the one-hour geostrophically-derived wind are regarded as bracketing the probable maximum winds. The geostrophic winds are undoubtedly an overestimate due to inevitable dynamic effects and possible overestimate of the surface - 500 mb V_c/V_{gc} ratio at 200 mph. The 50-year winds, on the other hand, barely exceed certain observed values, which are derived from short records with sampling biases toward lighter winds.

Compromise solution

5.36. Because of possible differences between component and total winds it was decided to study component winds also but to augment the record by including all West Coast stations*. The resulting composite profile of

---

*Stations used and record searched are as follows:

Oakland, Calif.	1946-1958, incl.;	Nov.-Feb., incl.
Santa Maria, Calif.	1946-1958, incl.;	Nov.-Feb., incl.
Long Beach, Calif.	1953-1958, incl.;	Jan.-April, Oct.-Dec., incl.
Medford, Oregon	1953-1958, incl.;	Jan.-April, Oct.-Dec., incl.
Seattle, Wash.	1953-1958, incl.;	Jan.-April, Oct.-Dec., incl.

component winds is shown in figure 5-23, curve A. The station providing the record wind at each level is indicated. Also shown on figure 5-23 are the geostrophically-derived winds from figure 5-19, curve B, the 50-year Oakland winds, curve D, and the adopted curve C. The adopted curve represents a compromise based on the following: 1) The speeds are everywhere between the observed winds and geostrophically-derived winds. 2) The adopted curve (C) is a slight maximization beyond the 50-year Oakland winds (except at the surface and 300 mb) thus taking into consideration the fact that the curve is based on only one station. 3) At 300 mb it was thought desirable to maintain the 300-500-mb wind ratio of 1.3, even though the 50-year Oakland wind exceeds this value slightly. Winds at this level are near the jet stream maximum. In large orographic storms it is probable that the jet stream maximum would lie somewhat north of California. 4) At the surface the adopted maximum 1-hour speed of 35 mph is an average of the observed maximum wind at Oakland and the geostrophically-derived maximum wind. This speed maintains the same 1000 to 950-mb ratio as that shown by the adopted coastal V_c/V_{gc} relationship (figure 5-3). 5) The adopted curve has been smoothed to resemble the long record geostrophic wind profile (B) and the combined station observed wind profile (A).

Variation of Maximum Windspeed with Time

Upper air

5.37. Characteristic diminution of the onshore wind with increasing duration of the orographic storm was determined from selected periods of strong winds from the southwest quadrant at Oakland. Oakland winds aloft observations were selected as the most suitable for study, because of its most frequent observations, central location, length of record, and minimum topographic effect. December, January and February winds for the years 1946-1956 were searched. Study was restricted to the 900-, 700-, and 500-mb levels. Selection of cases was made on the basis of wind direction and speed. Direction limits were: 900 mb, SSE through W; 700 mb, S through W; and 500 mb, S through W. For speeds at least 2 successive observations at one or more levels exceeded the following lower limits: 900 mb, 15 mps (34 mph); 700 mb, 25 mps (56 mph); 500 mb, 35 mps (78 mph).

Twelve cases at 900 and 700 mb and thirteen at 500 mb were finally selected. Times and dates of these are tabulated in table 5-4.

Four rawin observations were taken daily during the years 1955-1957 and twice daily in other years. In order to make the record comparable, six-hourly values were linearly interpolated for the windy periods occurring during years of 12-hourly observations.

First, for each of the periods of strong winds at Oakland, the highest individual windspeed at each of several levels was recorded, the highest average that could be formed by taking the mean of two successive observations

Table 5-4

WINDY PERIODS AT OAKLAND

		Beginning		End	
Period No.	Date	Time (GMT)	Date		Time (GMT)
1	Feb. 3, 1950	03	Feb. 7, 1950		15
2	Feb. 7, 1951	03	Feb. 11, 1951		15
3	Jan. 12, 1952	03	Jan. 17, 1952		15
4	Jan. 23, 1952	03	Jan. 26, 1952		15
5	Jan. 14, 1954	03	Jan. 19, 1954		15
6	Nov. 30, 1954	15	Dec. 6, 1954		21
7	Dec. 18, 1955	03	Dec. 23, 1955		21
8	Jan. 23, 1956	03	Jan. 28, 1956		03
9	Feb. 18, 1956	21	Feb. 24, 1956		03
10	Jan. 10, 1957	15	Jan. 15, 1957		15
11	Feb. 22, 1957	21	Feb. 27, 1957		09
12	Jan. 23, 1958	00	Jan. 27, 1958		00
13	Feb. 1, 1958	00	Feb. 6, 1958		00
14	Feb. 24, 1958	00	Feb. 26, 1958		00

6 hours apart, and similarly for increasing number of successive observations out to twelve successive 6-hour observations. In many instances, but not all, the periods yielding the highest average for short durations were contained within the periods yielding the highest average for longer durations. Not all storms furnished data for the complete array out to eight successive six-hour periods. Figure 5-24a shows the decay at 900 mb.

Second, the foregoing values were averaged over storms, resulting in a single decay curve at each level. The average decay curve at 900 mb is shown in figure 5-24b.

Third, the average durational values from these curves were converted to a 6-hour incremental basis. For example, if at a particular level the maximum average for three, four, and five successive observations are 65, 60, and 56 mph respectively, then the corresponding speed at the fourth and fifth observation compatible with these numbers must be 45 mph and 40 mph, respectively:

$$\frac{(3 \times 65) + 45}{4} = 60$$

$$\frac{(3 \times 65) + 45 + 40}{5} = 56$$

The purpose of converting to incremental speeds is to facilitate the computation of orographic PMP, which is carried out separately for successive 6-hour periods. The purpose of deriving average values from the wind data first, instead of incremental values, is to introduce an optimum of smoothing.

Finally, the incremental speeds were converted to ratios of the speed at each increment to the speed for the highest six-hour period and smoothed. The resulting curves for the several levels are shown in figure 5-25.

Surface

5.38. Since surface winds are taken hourly, the estimate of surface decay is theoretically more precise than the upper air, but due to local influences cannot be used except for comparative purposes.

The storm periods investigated for surface decay rates were: December 9-12, 1937; February 24-29, 1940; January 20-23, 1943; January 31-February 2, 1945; November 17-20, 1950; and December 21-23, 1955. All observations were taken from Oakland airport except during the 1937 storm when they were taken from the San Francisco City Office. Hourly windspeeds for directions southeast through west were plotted against time. Highest average values for 1, 6, 12, 18...72 hours were noted. The final surface incremental decay curve was obtained in the same manner as the upper air decays and is also shown in figure 5-25.

Adopted maximum windspeed variation

5.39. _Surface._ The decay of the geostrophic wind (at 30 miles) was selected as a more reliable index than the decay of the surface wind itself, although the two decays turned out to be quite similar (see figure 5-25 for comparison). The surface wind decay was thought too susceptible to extraneous influences such as, e.g. differential friction due to wind direction changes.

Upper air. The decay of the 500-mb wind taken from the Oakland study was adopted. The adopted decay of the wind at intermediate levels is based on a direct linear interpolation (by pressure) between the adopted decays at the surface and 500 mb. This was done for the sake of simplicity after a check was made showing that the decay of the observed winds was very close to the interpolated decays, there being less than 3 mph difference at any level or time in the resulting maximum winds. The two sets of decays are shown on figure 5-25.

Adopted Maximum Winds

5.40. The final maximum wind profiles are shown in figures 5-26 (Coast Range) and 5-27 (Sierra). The one-hour coastal wind profile is taken from figure 5-23, the profiles at other durations were obtained by applying the

adopted variation of windspeed with duration as shown in figure 5-25. The Sierra profiles were obtained in similar fashion except for the use of Sierra V_c/V_{gc} ratios.

The Coastal winds can be used anywhere along the coast after suitable seasonal and latitudinal adjustments have been applied. The Central Valley winds need a further barrier correction downwind from the San Francisco Bay region the areal distribution of which is shown in figure 5-5a, b and c.

Comparison of Adopted Maximum Winds with Previous Estimate

5.41. Maximum windspeeds in the present estimate average about 30% higher than the comparable maximum winds in Hydrometeorological Report No. 3 (25). Figure 5-28 shows the pertinent speed-duration curves. Report No. 3 winds are based on maximum surface winds at Pt. Reyes, Calif. which were shown to be a good estimate of winds at the 4000-foot level. Due to increased storm history and greatly expanded upper wind coverage (due mainly to rawin observations) our estimate of maximum winds has necessarily been raised.

Combination of Maximum Moisture, Winds and Model Coefficient

Wind and moisture

5.42. In the rainfall maximizing process it is assumed that the highest dew point will occur with the highest wind. This is a reasonable assumption since the maximum dew points are derived from storm situations, (see chapter IV and HMR 37) and high winds make more effective the transport of moisture from low latitudes.

Model coefficient

5.43. The model coefficients listed in table 5-2, are derived from the largest storms of record. It would be unreasonable, however, to use the very highest coefficients observed in these storms since these are usually associated with the lower winds and dew points. A possibility of bias therefore exists when the λ decay curve, based on observed precipitation order, is used in the maximizing process. The average highest λ values are used together with highest dew point and winds. Accordingly, the model coefficient was also plotted ordering by the computed 6-hour precipitation instead of the observed. Here the computed precipitation is a good measure of wind and moisture potential. Figure 5-29a shows the results. There is no discernible relationship.

The most reliable model coefficients for short duration PMP it could be argued would derive from instances of simultaneous high computed and high observed precipitation. To apply this concept the model coefficients were ordered by the average of the ranks of computed and observed, (see figure 5-29b, for the Sierras). The figure is quite definite in indicating that

for high values of both computed and observed the model coefficient substantially exceeds 1.0. An eye-fitted curve to figure 5-29b is transcribed to figure 5-14 and tends to support the latter.

A value of the model coefficient of 1.35 adopted for the first 6 hours (the average model coefficient for the heaviest observed 6-hour period rain) appears to be a reasonable figure in the light of the above analysis as a conservative maximization beyond the record.

Delineation of Maximum Orographic Precipitation

Probable maximum orographic precipitation over areas

5.44. 1. Description of areas. The first step toward obtaining the probable maximum orographic precipitation (generalized) is its computation over contiguous quasi-homogeneous areas along the Coast Range and Sierras. Figure 5-30 shows the location and Y distance of the PMP areas (as distinct from test areas shown elsewhere). These areas were chosen for the following characteristics:

a) the inflow boundary was located 5 miles upwind from the first significant upslope (or seacoast) and generalized to a straight line.

b) the outflow boundary was a generalized ridge line along which the elevation was not widely variable.

c) the sides of the areas were parallel and oriented into storm wind directions (between south and west-southwest) but favored a near-normal to the ridge-line orientation.

d) intermediate ridges were oriented in directions appropriate to their position between the inflow and outflow boundaries, and of relatively uniform height.

The profiles of PMP areas were derived by joining with straight lines the following: the average inflow height, the average height of significant intermediate ridges and the average height of outflow. If no intermediate ridges existed, a point marking the position of a generalized contour line was substituted. Adopted generalized profiles for all PMP areas appear in figure 5-31.

2. Latitudinal variation. A relation between surface winds and latitude was obtained by an analysis of maximum geostrophic winds along the West Coast for 15 Januarys (1943-1957). The maximum geostrophic wind was found for each year from sea-level pressure differences between the following stations: Tatoosh Island, Washington; North Bend, Oregon; Eureka, San Francisco, Los Angeles, and San Diego, California. The 100-year mesa return interval wind was computed by the Gumbel method for each of these line segments.

Maximum observed upper winds were also investigated for latitudinal variation. For Medford, Oakland, Santa Maria, and Long Beach the maximum annual twice-a-day observed winds from the southwest quadrant at the 300-, 500-, 700-, 850-, and 950-mb levels were tabulated. The years of record were from 1953 to 1957, inclusive. The average of the maximum annual values for each level at each station was then compared on a latitudinal basis. Between Medford (above the level of the upwind barrier) and Oakland the averages are quite comparable, level for level. From Oakland to Long Beach, there is a trend toward lower winds at all levels except the 300-mb level. At this height the higher winds at the lower latitude are probably due to the positioning of the jet stream during the winter season, and are not representative of orographic storm conditions.

The average of the maximum annual upper winds and 100-year return period surface geostrophic winds were plotted in percent of Oakland's winds on a latitudinal scale. Considerable scatter was shown for the upper air winds probably because of having only 5 years of maximum annual values. The latitudinal variation was adjusted slightly to maintain the same relative wind variation with height at all latitudes. This was done to avoid an overwhelming amount of numerical computations. The resulting latitudinal variation is given in figure 5-32.

3. Computation of orographic PMP. The computation of orographic precipitation is carried through by use of the orographic model in a similar fashion to that used in the test on storm periods. Procedural differences include:

1) Use of maximum winds and dew points.
2) Inclusion of latitudinal variation of winds.
3) Inclusion of model coefficient factor.
4) A simplified computation of snow formation described in the next paragraph.

Orographic precipitation for a windward slope is affected by two opposite influences in the snow layer. These are, the rate of precipitation formation per unit volume increases with windspeed, but the ratio of precipitation intercepted by the windward slope to that lost by spillover decreases. These effects were found to be very nearly in balance over the durational and latitudinal range of PMP winds. The explanation is clarified by figure 5-11. The area of the cross section bounded by the freezing level and the precipitation trajectory at the top decreases in proportion to the windspeed increase, because of the change in slope of the upper bounding trajectory. This is the area of the snow zone which contributes precipitation to the windward slope and its change offsets the increase in precipitation formation per unit volume.

In view of this lack of dependence of effective snow formation on wind speed, the following procedure was used. The portion of the orographic PMP

formed as snow was determined from a simplified nomogram which did not take
the exact speed into account. The portion formed below the freezing level as
rain was determined, 6-hour period by 6-hour period, by exact application of
equation 17d to the respective winds.

Index map *

5.45. A map of 6-hour January orographic PMP was developed by distrib-
uting the PMP values for the areas of figure 5-30 with respect to the local
topography. This map is the basic index map for orographic PMP and is shown
in figure 5-35. The adopted guide to these local topographic influences was
the chart of 10-year 3-day point storm precipitation, figure 5-33a, prepared
by the Corps of Engineers (6), with convergence precipitation removed. The
3-day 10-year map is closely related to the normal seasonal precipitation map
and synthesizes the effects of topography on past storms.

1. Convergence component of 3-day 10-year map. The convergence com-
ponent of the 3-day 10-year map was estimated in the same manner as the con-
vergence component of 6-hour rainfall in storms. That is, the values at
low-level stations were used as a base. These base values, reduced for mois-
ture depletion of elevation, were then subtracted from the total slope pre-
cipitation. Along the coast, values in regions of relatively flat terrain
were given more weight than those close to precipitous rises, the latter be-
ing assumed to contain some orographic component. The estimated convergence
component of the 3-day 10-year map is shown for information in figure 5-33b.
Its sole purpose is to derive the orographic component, described below.

2. Orographic component of 3-day 10-year map. The orographic component
of the 3-day 10-year map was derived by graphical subtraction of the con-
vergence component from the total. This is shown in figure 5-33c. The posi-
tion of the zero line on this chart determines the position of the zero line
on the orographic PMP index map, and careful attention was given to the
placement of this line and values in the foothills on the two component maps.

3. Distribution of orographic PMP by orographic component of 3-day
10-year map. Generalized distribution of orographic PMP was accomplished by
taking ratios, for each PMP area, of the computed 6-hour orographic PMP to
the orographic component of the 3-day 10-year storm averaged over the area.
The latter values were obtained by planimetering the orographic component of
the 3-day 10-year map (figure 5-33c) in the relevant PMP area. The ratios
were then plotted against latitude (figure 5-34) and smoothed somewhat. Many
different parameters were tried to reduce the scatter of points of this re-
lation. No significant improvement was attained. The scatter of the points
about the adopted relation line is not explainable.

Finally, the orographic component of the 3-day 10-year storm map (fig-
ure 5-33c) was multiplied by the smoothed ratios in the respective computation-
al areas and isopleths drawn. The result constitutes the orographic PMP index
map and is shown in figure 5-35.

*Please see the revision dated October 1969 of figure 5-35
that is included at the end of this publication.

The ratios for PMP areas Nos. 23, 24 and 25 in figure 5-34 are based on that part of the areas at elevations lower than 10,000 feet. Above this elevation the maximum 6-hour winter orographic PMP storm is in the snow form and there is a relatively large fraction of spillover. The ratios obtained for the area below 10,000 feet were carried into the area above 10,000 feet but centers were modified downward subjectively in constructing figure 5-35.

Variation of Orographic PMP

5.46. This section will discuss procedures for obtaining orographic PMP specifications from the index chart. The index map itself integrates the effect of topography on 6-hour orographic PMP winds and moisture and contains the latitudinal variation of the winds. The effect of topography is assumed constant throughout the PMP storm. Variations of the following parameters are not taken into consideration by the index map, and must be applied after the index map answer is obtained.

1. Wind variation with time.
2. Moisture variation with time.
3. Variation of model coefficient with time.
4. Basin width variation.
5. Seasonal variation.

5.47. Wind variation. The adopted wind decay with time at 4 levels is shown in figure 5-25. The manner in which the decays were derived is described in paragraphs 5.37-5.39.

The rate at which the rainfall decreases with time due to wind variation alone is dependent upon the integrated variations of the wind at all levels and their effect in turn on the outflow wind. If one wishes to assess roughly the effect of this variable alone, more weight should be given to the variation of the winds at the lower levels.

5.48. Moisture variation. The development of the adopted moisture decay curve and its test for geographical and seasonal applicability appear in chapter IV. Table 4-2 and figure 4-5 show the variation of this parameter for 1 through 72 hours.

5.49. Variation of model coefficient. The model coefficient decay curve, developed in section 5-28 of this chapter can be used in any orographic area in California. The curve appears in figure 5-14.

5.50. Combined wind, moisture and model coefficient variation. The wind and moisture variation each give twelve 6-hour incremental values, from the highest to lowest through a total of 72 hours duration. These were combined, highest wind with highest moisture, 2nd highest with 2nd highest, etc. The rain portion of the orographic PMP was computed by 6-hourly increments from

these combinations of wind and moisture for each of the PMP areas. The snow portion of the PMP showed only slight variation from 6-hour period to 6-hour period for any given area and therefore was assumed constant throughout the 72-hour storm. It was added to each 6-hourly orographic rain PMP increment and the resulting increments were multiplied by the appropriate 6-hour model coefficient. For representative areas covering the Sierra and Coast Ranges, the resulting variations of 6-hourly total orographic PMP, in percent of the 1st or maximum 6-hour value were determined. This showed that there were only small differences in the resulting variations of orographic PMP with area; therefore the percentages were averaged to give one durational variation of orographic PMP for all regions. This variation is given in figure 5-36.

Criteria for small drainage basins require a breakdown of PMP into durations of less than 6 hours. The orographic PMP was computed for 1 and 3 hours, similar to the computations for longer durations for numerous orographic PMP areas on the Coast and Sierra Ranges. One-hour winds were taken from figures 5-26 and 5-27 and the 3-hour winds were interpolated. Dew points were obtained from the adopted mean dew point-duration relation, figure 4-5. The model coefficient for 6 hours was used for both 1-and 3-hour durations. To the computed rain portion of the orographic PMP was added the snow contribution. The total orographic PMP (in percent of the 1st 6 hours) showed only slight variation with geographic location. Therefore it was averaged, resulting in 20 percent of 6 hours for 1 hour and 54 percent for 3 hours. The inset on figure 5-36 gives the variation of orographic PMP within the maximum 6-hour period.

5.51. Seasonal variation of orographic PMP. The seasonal variation of orographic PMP is controlled by the seasonal variations of 1) moisture and 2) windspeed. The moisture factor has been described in detail in chapter IV; briefly recapitulating it is based on smooth seasonal curves of the 12-hour persisting surface dew points at stations. It was shown that a single seasonal variation is adequate for California. The figures are shown in table 4-1.

The seasonal variation of surface windspeed is based on the following data at the indicated stations for the months of October through April inclusive.

1) Maximum observed 5-minute surface winds for each month at Eureka, San Francisco and San Luis Obispo (1905-1927).

2) Maximum observed 6-hour average winds for each month at Eureka, San Francisco and San Luis Obispo (1905-1927).

3) Maximum observed 24-hour average winds for each month at Eureka, San Francisco and San Luis Obispo (1905-1927).

4) Maximum observed instantaneous surface pressure differences for each
   month between Eureka-San Francisco, San Francisco-San Luis Obispo
   (1901-1927).

For each of these items at each station and each month, the maximum
values were arrayed and the 100-year return period value determined from a
Gumbel distribution. The seasonal trend of each item was obtained by ex-
pressing the monthly 100-year return values in percent of the highest monthly
100-year return value. This gave 14 somewhat differing seasonal variations
of windspeed which were averaged.

For upper-level winds, 5 years of record at Seattle, Medford, Oakland,
and Long Beach for the 950-, 850-, 700-, 500-, and 300-mb levels were sur-
veyed. The maximum observed speed at each level from the southwest quadrant
for each month (October through April) for each year was extracted from the
records for each station. These maximum values (five for each month, level
and station) were averaged to give the average maximum monthly windspeed.
By combining the data for all stations, seasonal trends at each upper level
were obtained. While considerable scatter resulted, the data show less sea-
sonal change at higher levels than at lower levels. The change of windspeeds
with duration shows a similar variation, that is, less change with duration
for the higher levels. This similarity has been utilized in drawing the
seasonal curve at the different levels; in other words, the seasonal curves
are such that the variation with elevation does not change with season. Fig-
ure 5-37 shows the adopted set of windspeed seasonal curves.

Having determined the factors which will adjust the wind and moisture
for season, computations by the orographic model give the resulting variation
of the rain portion of the orographic PMP with season. To this was added the
snow contributions to the orographic PMP and the seasonal variation of total
PMP determined for representative areas covering the orographic regions of
California. This displayed a varying seasonal curve depending on the height
of the outflow barrier in the specific orographic area. The higher the bar-
rier the greater the October orographic PMP, relative to January; this effect
is due to the height of the freezing level, as rain contribution to the PMP
is more effective than snow. For the areas of highest barrier the computed
October PMP slightly exceeded the January value. While such a seasonal trend
may be correct for the highest elevations, it is not reasonable for this to
be maintained for individual basins, sometimes far removed from a high bar-
rier. Furthermore, all our experience with orographic storms indicates a
lesser storm in October than in midwinter. For these reasons, the height of
the mean Coastal and Sierra barriers was the basis for adopting two mean sea-
sonal curves--one for the Coastal orographic region, the other for the Sier-
ras. These are given in figure 5-38.

5.52.[*] Adjustment of orographic PMP for duration and season. The dura-
tional decay of orographic PMP given in figure 5-36 is combined with the

*Please see revision dated October 1969 to section 5.52
 that is included at the end of this publication.

seasonal variations of figure 5-38 by multiplying the corresponding ratios. The combined seasonal and moisture variation is shown in table 5-5. These percentages when multiplied by the average 6-hour PMP over a particular basin, taken from the orographic index map (figure 5-35), give the 6-hourly increments of PMP for the October through April season.

Table 5-5 *

COMBINED SEASONAL AND MOISTURE VARIATION OF OROGRAPHIC PMP
(In percent of basin average orographic index)

6-hr period

	Month	1	2	3	4	5	6	7	8	9	10	11	12
	Oct	92	72	58	48	41	34	28	24	20	17	13	10
	Nov	94	73	59	49	41	35	29	24	21	17	13	10
Coastal	Dec	98	77	62	51	43	36	30	26	22	18	14	11
Range	Jan-Feb	100	78	63	52	44	37	31	26	22	18	14	11
Basins	Mar	94	74	60	49	42	35	29	25	21	17	13	10
	Apr	87	68	55	45	38	32	27	23	19	16	12	10
	Oct	97	76	61	50	43	36	30	25	21	17	14	11
	Nov	98	76	62	51	43	36	30	25	22	18	14	11
Sierra	Dec	99	77	62	52	44	37	31	26	22	18	14	11
Range	Jan-Feb	100	78	63	52	44	37	31	26	22	18	14	11
Basins	Mar	96	75	60	50	42	35	30	25	21	17	13	11
	Apr	90	70	56	47	40	34	28	24	20	16	13	10

For 1- and 3-hour durations the factors of .20 and .54 are applied to the first 6-hour period value of table 5-5 for the appropriate month.

The Sierra factors are to be used for any basin to the east of the Central Valley between Redding and Bakersfield, and the Coastal factors for the remaining areas of interest in California.

5.53. Basin width variation. In the orographic storm, basin width takes the place of area in investigations of volumes of storm precipitation. The basin width variation is based primarily upon the pressure gradient variation with distance, shown in figure 5-17. This variation, put through the orographic formula for various barrier heights, dew points and months is generalized into a single curve shown in figure 5-39. Since the rainfall is nearly proportional to the wind, these percentages may be used to reduce each increment of rainfall depending on its position in the storm. For basins less than 30 miles in width, the variation is assumed constant and equal to

*Please see revision dated October 1969 at end of this publication for use of this table.

the 30-mile value. Although a somewhat stronger windstream is possible over basins less than 30 miles in width, the possibility of it remaining over the basin for an appreciable time is thought to be negligible.

5.54. <u>Summary of variations</u>. Ordinarily, the variation of orographic PMP can be determined in three steps after the index map value is obtained. The combined wind, moisture and model coefficient variation is determined first. The seasonal and basin width variations are applied as necessary afterwards.

A complete step-by-step procedure to obtain the orographic and convergent components of the probable maximum precipitation storm and their combination is taken up in chapter IX.

Chapter VI

CRITERIA FOR PROBABLE MAXIMUM SPILLOVER PRECIPITATION

A. INTRODUCTION

Purpose of spillover chapter

6.01. The geographical distribution of orographic precipitation in California is primarily a function of the orography and wind variations. The results of spillover computations, as presented in this chapter, have provided one guide to adjusting the leeward areas of the orographic index chart (figure 5-35) so as to reflect the effects of these factors on the spillover precipitation. Extrapolation from the windward slopes by use of the orographic component 10-year map (figure 5-33c) provides another guide. The orographic and convergence components of spillover are considered separately following the general procedure of this report.

Limitations of observed spillover data

6.02. There is some observational control on the broad outlines of the magnitude of the total spillover effect. Observations show that, in the major storms giving precipitation on the windward slopes, large amounts are not observed at distances of 20 miles or more beyond the ridge. Also, streamflow observations show that the precipitation must be much less at distances of about 20 miles to the lee than it is on the windward slopes. However, we do not have a dense enough network of rain gages located in the lee areas near the crest to accurately evaluate spillover directly by empirical means. Indices for leeward areas based on the normal seasonal precipitation, etc., suffer from this same deficiency since they are not derived from closely-spaced observational data. They, of course, do show the general drop off that takes place within distances of about 20 miles.

Computational limitations

6.03. Probable values of orographic spillover can be computed by physical considerations based on the rate of raindrop and snowflake fall, the horizontal wind speed, and rates of evaporation of precipitation in descending air. Such computed values fall within the broad limits set by the observational evidence as indicated above. The assumptions of smooth laminar flow of air, fixed rate of fall of precipitation elements, and standardized evaporation rate, as well as other assumptions, limit the precision of the computed values. Detailed refinement of the PMP spillover beyond the maximum 6-hour period was not considered warranted.

B. CONVERGENCE SPILLOVER

6.04. The spillover of convergence precipitation has been incorporated into the convergence PMP index map (figure 4-12) through the use of effective barriers shown in figure 4-11. The drift of the raindrops and snowflakes with the wind does not of itself have much effect on the potential for convergence precipitation at any one selected point on the ground. The concentration of convergence of the air could just as well occur at the location in the atmosphere from which the precipitation would fall to the selected spot on the ground rather than vertically above that place. There are, however, two modifying effects in downslope leeward areas. First, the depth of the air column increases along the wind stream as the ground gets lower, giving more air for a convergence mechanism to operate on. Second, downslope motion would have some inhibiting effect on the convergence mechanism as compared with adjacent regions. These two effects cannot be evaluated explicitly and are assumed to cancel each other, on the average, in a PMP storm.

C. PLATEAU OROGRAPHIC SPILLOVER

Basic approach

6.05. The orographic model with precipitation trajectories described in chapter V was used for spillover computations. Prior to consideration of evaporation it was necessary to determine the spillover distribution along a fictitious plateau to the lee of a ridge, which would require no evaporation. This spillover was termed the plateau orographic spillover.

The procedure followed was aimed at deriving spillover values which would be based primarily on the maximum 6-hour PMP conditions. However, it was also intended that, in combination with the derived decay of upslope orographic precipitation as shown in table 5-5 representative leeward area total storm precipitation depths would result for other durations. To accomplish this more than fifty individual spillover computations were made. In these computations, constant winds above the 600-mb level and an upslope 50-mb "wet snow" layer above the freezing level were assumed. Although this latter assumption acts to decrease the total spillover, at the same time it serves to augment the important "close-up" spillover.

Computations of spillover were limited mainly to the consideration of the effects of slope, moisture, and wind. Other effects which were given some consideration included those of freezing-level variation and drop-size variation. Smoothed plateau spillover curves, figures 6-1 and 6-2, were derived primarily from consideration of 37 spillover computations using a 700-mb freezing level (i.e. representative of PMP storm conditions for the middle latitude of California for January). Higher freezing levels were used with high barriers (with more pronounced upslopes) to allow for the effect of stronger vertical velocities in carrying liquid water to higher levels. In

deriving the final smooth curves, consideration had to be given to eliminating discontinuities such as the one due to the change from wet snow to rain. Using the same pressure-height relationship used in the upslope computations, the final spillover values were determined for barrier heights of 1000, 2000, etc. up to 7000 feet.

Relation of plateau spillover to variables

6.06. To generalize the rather involved effects due to joint variation of the pertinent parameters, one can say that the more important close-up spillover (i.e., say up to 10 miles) is greatest for relatively strong winds, high moisture content, steep upslopes, high freezing levels, and moderate barrier heights. If the barriers are low, spillover is restricted by the limited production of precipitation due to lesser slopes for a fixed Y distance, while for high barriers the spillover is less, due to the precipitation source being in the higher, less productive levels. In general, beyond the first 15 miles, the computations indicate spillover to be relatively unimportant.

Computations for wind and moisture conditions appropriate to durations other than the maximum 6-hour PMP indicate that the spillover at a particular distance from the ridge decreases less with duration than does the upslope precipitation. This is explained by the less horizontal trajectories of the precipitation elements with increased storm duration, which partially offsets the decreased spillover due to lessened condensation. However, the differences from the decay rates adopted for upslope precipitation in table 5-5 are prominent only at spillover distances where amounts are light. Table 5-5 therefore is considered representative for the spillover regions.

Interpretation of final plateau spillover

6.07. The spillover figures 6-1 and 6-2 give computed PMP plateau spillover precipitation values for upslope Y distances of up to 40 miles. For instances where the upslope Y distance is greater than 40 miles, the curve for 40 miles should be used. This is considered an appropriate simplification since the less extreme vertical motion associated with gentler upslopes would provide a compensating factor toward increased spillover due to smaller precipitation elements with smaller fall velocities.

D. EVAPORATION CONSIDERATIONS

Description of approach, including underlying assumptions

6.08. Given the plateau spillover of orographic precipitation, a fundamental problem of application becomes one of determining the effectiveness of evaporation in descending air to leeward in depleting the spillover precipitation reaching the ground.

In order to provide a practical solution to the evaporation problem, the simplifying assumption is made that the downslope regions are occupied by two distinct bodies of air. A certain upper layer of this air is assumed to be subjected to a drying, foehn effect (requiring the evaporation of liquid water to maintain saturation) while the remaining lower portion remains essentially undisturbed by the foehn motion above. In effect, the lower layers of air occupying the areas to the lee of ridges are considered therefore to inhibit the drying foehn effect. This inhibiting effect is handled in the form of an assumption regarding the descent of the leeward air compared to that indicated by the ground downslope alone. What the assumption should be regarding the descent of the leeward air must, in part, be determined empirically.

Relation of evaporation to downslope and other variables

6.09. Evaporation values computed for a one-third assumption are shown in figure 6-3. Numerous evaporation computations with varying downslope assumptions indicated that the evaporation amounts at the distances of consequential spillover were proportional to the downslope. Proportionality between the evaporation and downslope was applied in making the simplified presentation shown in figure 6-3.

The winds used in the evaporation computations are the base winds applicable to 38° north latitude for the maximum 6-hour period of the PMP storm. Relatively minor increases or decreases in evaporation due to variations in height of freezing level etc. were not considered.

The leeward wind profile for a particular vertical in the foehn downslope region is assumed to be the same as the profile above the same level on the upslope side. Variations from such a profile might be considerable, especially when one considers that eddies in the lee current are undoubtedly more likely than a strictly laminar flow. Such uncertainties, presently not amenable to theoretical or empirical resolution, serve to emphasize the need for a simplified presentation.

E. ADJUSTMENT OF SPILLOVER

Purpose

6.10. Due to the uncertainties in the theoretical spillover procedure, some empirical adjustments are considered essential. In the adjustment procedure used, the degree of foehn effect is adjusted so that the computed spillover reaching the ground comes the closest to approximating the observed precipitation.

Storm comparisons

6.11. The two twenty-mile strips shown in figure 5-15 were used for spillover comparisons. Generalized profiles of the ground were determined and leeward precipitation trajectories were constructed for the same storm periods used in the windward comparisons described in chapter V. The computed spillover was then compared to the observed, using means of the two six-hour periods. Figures 6-4 and 6-5 show the results of these storm case comparisons.

A second method of comparison with storm data consisted of using the leeward distribution of maximum observed 24-hour precipitation. An average minimum non-orographic value appropriate to the valley floor was subtracted from the analyzed drop-off curve. For comparative purpose the leeward values were put in terms of percent of ridge value, and are shown by one of the curves of figure 6-6.

PMP criteria comparisons

6.12. The distribution of leeward precipitation was computed for ten of the PMP blocks of figure 5-30 and then compared to the leeward distribution of orographic precipitation as given by a tentative generalized orographic index map based on the orographic component of the 10-year 3-day map. In obtaining values of the leeward precipitation, generalized downslopes of the terrain were determined for use with figure 6-3 in estimating the evaporation to be subtracted from the plateau spillover distribution as determined from the appropriate figure 6-1 or 6-2.

An auxiliary PMP comparison consisted of an analysis of the leeward drop off in the statistically-determined estimate of probable maximum 24-hour point precipitation data used in the construction of figure 8-3. As in the above maximum observed 24-hour case, a non-orographic minimum value was subtracted from the analyzed drop-off curve and percentages of ridge value were determined. Figure 6-6 shows a comparison of these various computations along with the adjusted and unadjusted orographic index values.

Adopted foehn-effect assumption and application

6.13. Model computations for the extreme northern portion of the Sacramento Valley region (see above under "adjustment of spillover") seem to indicate that practically no lee downslope motion exists in this region, at least in some storms. This is realistic when one considers that the low-level southerly winds in storm situations not only help to saturate the lee air by some upslope motion but also these winds pile up the air in this region due to the forced transverse convergence resulting from the topographic narrowing of the valley. This piling up of the air should inhibit downward motion to the lee of the Coast Range. In the southern portion of the San Joaquin Valley, however, opposite effects would be indicated. An air downslope of one third the ground downslope is considered reasonable in this region.

The adopted assumption involving the degree of foehn effect is the following: In the extreme southern portion of the San Joaquin Valley the one-third assumption is considered applicable.   It is considered to decrease linearly from there northward through the San Joaquin and Sacramento Valleys to a zero effect in the extreme northern end of the Sacramento Valley.   Using this varying foehn assumption, spillover computations were used as a guide in drawing the orographic index map in applicable lee areas.

Spillover PMP

6.14.   Probable maximum precipitation estimates for basins in spillover regions are to be computed by the procedure covered in chapter IX.   This follows first from the fact that spillover computations were incorporated into the generalized orographic index map and secondly from the assumption that the durational decay of precipitation, derived for upwind slopes, is also applicable to the spillover region.

Chapter VII

COMBINATION OF CONVERGENCE AND OROGRAPHIC PROBABLE MAXIMUM PRECIPITATION

Summary of synoptic aspects

7.01. The simultaneous occurrence of convergence and orographic pre-
cipitation in the same storm, and at the same place, is characteristic of
major California storms. This is amply demonstrated in HMR 37. Further, as
discussed in paragraphs 3.26 - 3.28 of this report, most factors favoring
high precipitation rates may occur together and should be combined for an
estimate of PMP. Maximum instability does not combine with maximum moisture
(par. 3.29).

Approach in this report

7.02. In simulation of the characteristics of storms, convergence and
orographic PMP are estimated separately as a practical procedure, with due
regard for the differing seasonal, geographical, storm-duration, and areal
variation of the two precipitation-producing mechanisms. Orographic and con-
vergence precipitation are defined in certain ways with the end in view of
combining (2.19). The next section summarizes the concepts in the separa-
tion and then recombination, while subsequent paragraphs cover aspects of the
actual treatment of the data.

Summary of basis for index charts

7.03. The purpose of this section is to summarize the basis for the
convergence and orographic PMP index charts (figures 4-12 and 5-35). This
section will also show that the procedures are one method of adjusting and
transposing observed storms, with numerous intervening smoothing steps. The
various steps will be symbolized in algebraic form using the symbols listed
below.

$$PMP = \text{probable maximum precipitation}$$
$$P = \text{precipitation}$$
$$W_p = \text{precipitable water}$$
$$(P_c/W_p) = \text{precipitation/moisture ratio}$$
$$X = \text{multiply}$$
$$\underline{/X/} = \text{symbolic multiplication, i.e., combined in a relation}$$
more complex than straight multiplication, such as
subdividing into layers
$$B = \text{all topographic factors controlling orographic pre-}$$
cipitation
$$\lambda = \text{orographic model coefficient}$$
$$V = \text{inflow wind in orographic storm}$$
$$Q = \text{inflow moisture in orographic storm}$$

Subscripts

   c - convergence
   o - orographic
   t - total (convergence + orographic)
   i - index
  6, 24 - storm duration, hours
 10, 200 - storm area, sq. mi.
   x - maximum
   s - storm (observed)
   m - sea level
   e - effective elevation of basin
   p - used only in "W_p," see above
   1 - location of a storm
   2 - location of a basin
   d - computed by orographic model, before coefficient adjustment
  av. - average

  7.04. **Convergence PMP.** The three basic relationships for the convergence index map are given below, with an explanation following.

  Index relation:

  Max.   Max.   Average
                    of storms

$$(P_c/W_p)_{x,6,10,Jan,m} \quad X \; (W_p)_{x,6,Jan,e} \quad X \frac{P_{c,200}}{P_{c,10}} = (PMP)_{c,i} \quad (1)$$

  Maximization for moisture at storm location:

$$(PMP)_{c,1} = \underset{\text{envelope}}{\bigg|\bigg|} \; P_{c,s} \frac{(W_p)_{x,1}}{(W_p)_s} \; \bigg|\bigg| \quad (2)$$

  Transposition relation:

$$(PMP)_{c,2} = (PMP)_{c,1} \frac{(W_p)_{x,2}}{(W_p)_{x,1}} \quad (3)$$

  The **index relation**, (1), symbolizes the steps followed in this report. It represents the multiplication of enveloping precipitation/moisture ratios for 6 hours in January at sea level (from figure 4-7 or 4-8) by the maximum precipitable water for January at the effective basin elevation to obtain the 6-hour convergence PMP index at any part of the map. The precipitation/moisture ratios determined at points are considered to apply to an area of 10 sq. mi. The precipitable water is derived from the January dew point chart

(figure 4-5a). For basins with effective elevation different from sea level the maximum precipitable water is obtained from $(W_p)_{x,m}$ that portion of the precipitable water above the effective elevation.

Relations (2) and (3) are presented to demonstrate that (1) is equivalent to the method of direct maximization of storm precipitation values in their places of occurrence, combined with transposition, that has been used for the eastern United States in previous reports (1) (2).

The <u>maximization for moisture relation</u>, (2), symbolizes adjustment of storms by multiplying storm precipitation depths by the ratio of maximum to storm precipitable water. Resulting moisture-maximized values at any one place are then enveloped.

The <u>transposition relation</u>, (3), symbolizes adjustment for relocation, again on the basis of a moisture ratio.

Combining (2) and (3) yields:

Maximization-transposition relation:

$$
(PMP)_{c,2} = \underset{\text{envelope}}{\left|\left| P_{c,s} \frac{(W_p)_{x,1}}{(W_p)_s} \right| \left| \frac{(W_p)_{x,2}}{(W_p)_{x,1}} \right|\right|}
$$

$$
= \underset{\text{envelope}}{\left|\left| \frac{P_{c,s}}{(W_p)_s} (W_p)_{x,2} \right|\right|}
$$

$$
= (P_c/W_p)_x (W_p)_{x,2} \tag{4}
$$

The maximization-transposition relation, (4), is the same as the index relation, (1) when: the enveloping precipitation/moisture ratio, $(P_c/W_p)_x$, is for 10 square miles and 6 hours in January, is adjusted to 200 square miles by an average relationship, and $(W_p)_{x,2}$ is for 6 hours in January.

7.05. <u>Orographic PMP</u>. The basic relationships for orographic PMP are:

Index relation:

$$
V_{x,6,Jan,2} \; \underline{/\bar{\bar{X}}/} \; Q_{x,6,Jan,2} \; \underline{/\bar{\bar{X}}/B_2} \; X \; (\lambda_6)_{av.} = (PMP)_{o,i} \tag{5}
$$

Maximization relation at storm location:

$$(PMP)_{o,1} = \text{average} \left| P_{o,s} \; \underline{/\bar{X}/} \; \frac{Q_{x,1}}{Q_{s,1}} \; \underline{/\bar{X}/} \; \frac{V_{x,1}}{V_{s,1}} \right| \qquad (6)$$

Transposition relation:

$$(PMP)_{o,2} = (PMP)_{o,1} \; \underline{/\bar{X}/} \; \frac{Q_{x,2}}{Q_{x,1}} \; \underline{/\bar{X}/} \; \frac{V_{x,2}}{V_{x,1}} \; \underline{/\bar{X}/} \; \frac{B_2}{B_1} \qquad (7)$$

Model coefficient relation:

$$\lambda_s = \text{average} \left| \frac{P_{o,2}}{P_{o,d}} \right| = \text{average} \left| \frac{P_{o,s}}{Q_s \; \underline{/\bar{X}/} \; V_s \; \underline{/\bar{X}/} \; B_1} \right| \qquad (8)$$

Relation (5) symbolizes the steps by which orographic PMP index precipitation (for the blocks of figure 5-30) is obtained in this report. Maximum winds are combined with maximum moisture and the topographic factors, then adjusted by the model coefficient, in a direct synthesis of the precipitation. The equivalence of this to moisture and wind adjustment, plus transposition, is shown by the other relationships.

Relation (6) symbolizes the manner, in effect, by which the PMP estimate is obtained at centers of orographic precipitation storms. The observed values are adjusted upward to maximum moisture and maximum wind. These adjusted values are then _averaged_ (not enveloped).

Relation (7) indicates the manner in which the PMP estimate is made, in effect, for regions which have not experienced extreme orographic precipitation values during the period of record, or where there are no observations. The PMP "in place of occurrence" values from (6) are relocated with corresponding moisture, wind, and topographic corrections.

The model coefficient, λ, is defined by (8) and is the ratio of observed to computed orographic precipitation, averaged over several cases.

A combined maximization-transposition relation is obtained by substituting (6) in (7):

Maximization-transposition relation:

$$(PMP)_{o,2} = \text{average} \left| P_{o,s} \; \underline{/\bar{X}/} \; \frac{Q_{x,1}}{Q_{s,1}} \; \underline{/\bar{X}/} \; \frac{V_{x,1}}{V_{s,1}} \; \right| \underline{/\bar{X}/} \; \frac{Q_{x,2}}{Q_{x,1}} \; \underline{/\bar{X}/} \; \frac{V_{x,2}}{V_{x,1}} \; \underline{/\bar{X}/} \; \frac{B_2}{B_1}$$

$$= \text{average} \left| P_{o,s} \; \underline{/\bar{X}/} \; \frac{Q_{x,2}}{Q_{s,1}} \; \underline{/\bar{X}/} \; \frac{V_{x,2}}{V_{s,1}} \; \underline{/\bar{X}/} \; \frac{B_2}{B_1} \right| \qquad (9)$$

Now substituting the definition of the model coefficient, (8), in (9), the coefficient-adjusted maximization-transposition relation is

$$(\text{PMP})_{0,2} = Q_{x,2} \; \overline{/X/} \; V_{x,2} \; \overline{/X/} \; B_2 \; X \; \lambda_{av}. \tag{10}$$

It is now apparent that where the values of Q and V in relation (10) are for 6 hours in January and λ is for 6 hours that (10) is the same as relation (5). This means that the orographic index map is by and large a composite of moisture-adjusted and wind-adjusted transposed orographic storm values. It is not an envelope of such values but rather an average of selected high values.

The convergence PMP index was derived by enveloping storm values with one maximization adjustment. The orographic PMP index is derived by averaging storm values with two maximization adjustments.

7.06. Total PMP. Finally the total PMP for 6 hours and 200 square miles in January is obtained from

$$(\text{PMP})_{t,6,200,\text{Jan}} = (\text{PMP})_{c,i} + (\text{PMP})_{o,i}. \tag{11}$$

In anticipation of this combination, $P_{o,s}$, which enters into the orographic PMP, was derived from

$$P_{o,s} = P_{t,s} - P_{c,s}. \tag{12}$$

$P_{c,s}$, which enters into the convergence PMP through the precipitation/moisture ratio, was derived from

$$P_{c,s} = P_{t,s} - P_{o,s}. \tag{13}$$

Here values of $P_{c,s}$ were mostly obtained by restricting the selection to cases where $P_{o,s}$ was equal to zero.

Safeguards

7.07. Steps were taken to minimize contamination of the basic orographic storm precipitation data by convergence rain and conversely. The safeguards are explained in detail in chapters IV and V, respectively, and will be summarized here. In estimating the convergence PMP, the measure of intensity of the storm mechanism is the P/M ratio in outstanding past storms. The first safeguard was the separation of the controlling P/M ratios in two classes, those compatible with orographic precipitation, and those not, because of characteristics of the individual storm. The two resulting envelopes of P/M ratios are, respectively, indices of the maximum convergence mechanism that would be expected without restriction, and of the maximum that would be expected as part of an orographic storm. The other safeguard was in the location of storms selected to provide the P/M ratios. These were restricted to the Central Valley of California at some distance from either of the principal ranges. One exception was a San Francisco value, which was corrected for minor orographic influence by comparison with Farallon Islands.

In deriving the criteria for orographic PMP the following safeguards were applied. First, in calibrating the orographic precipitation model against observed storms, an estimate of the convergence precipitation was subtracted from the total observed precipitation over the mountain slopes in each storm period to yield an estimate of the orographic precipitation in the storm. The last was used in the calibration. The estimate of the convergence precipitation was based on observed rainfall catches at low-level stations relatively free of orographic influence.

A similar refinement was introduced in use of the 3-day 10-year point precipitation map as an index for the distribution of orographic PMP with large blocks. The 3-day 10-year map was divided into an estimated convergence component and orographic component throughout region of the study, again by using values at low-lying stations as guided to the convergence rain on adjacent slopes. The orographic component was then used for the distribution step.

Airflow in combined storm

7.08. A clue as to the nature of the combined convergence and orographic storm may be derived from figure 7-1, a schematic cross section through the Yuba Basin. Idealized air streamlines are shown for pure orographic flow (solid curves) and for combined orographic and convergence flow. Also shown are the corresponding trajectories of fall of precipitation elements. The air streamlines for the combined storm are derived by superimposing convergence on the orographic flow. The rate of convergence is uniform from the ground to the 750-mb streamline with compensating divergence between there and the nodal surface. The convergence value superimposed is that required to produce convergence rainfall throughout the area at a rate of 2 inches per 6 hours. This is comparable to the winter convergence PMP in the Sierras during the 2nd 6-hour period of the PMP storm. The superimposed convergence is from an unspecified combination of longitudinal convergence, and transverse convergence. The net result, as can be seen from the dashed lines, is for greater lift of all air parcels and greater crowding of the streamlines toward the nodal surface. It should be emphasized that the dashed curves are _average_ streamlines. It would be anticipated that in the storm more severe lifts would be experienced for shorter periods of time, averaged with lesser lifts at intervening times.

The two inches in six hours is an average over a large area. It can be envisioned that more intense local cells would double the convergence component over small areas, thus yielding the convergence PMP values of this report.

Sample trajectories of precipitation elements are shown schematically in figure 7-1. Those labeled "orographic storm" are constructed according to the criteria for orographic PMP in chapter V. The trajectories of precipitation elements for the combined storm apply to the more severe conditions resulting from the more vigorous convergence activity, larger raindrops

and larger and wetter snowflakes resulting in greater rates of fall. The effective freezing level is placed higher to take greater cognizance of liquid condensation processes that occur at temperatures colder than 0°C. The steeper precipitation element trajectories yield more precipitation over a given area at the ground than the other set. Such differences are not estimated explicitly in this report. They are included in the convergence rain, which is defined as all effects other than the orographic rain.

Summary of procedure for obtaining total PMP

7.09. The orographic PMP is computed for a project basin six-hour period by six-hour period, for each month of interest, and the same for convergence PMP. The two are then combined by simple addition. The highest monthly total at each duration is then the all-season PMP. Thus, for example, the highest 6-hour value may occur in October, while the highest 24-hour value pertains to January. The January 24-hour value does not contain the 6-hour PMP, which was in October, but rather the somewhat smaller January 6-hour PMP. A list of the computational steps to derive the total PMP for a particular basin is given in chapter IX with examples.

Time distribution

7.10. Requirements for time distribution. To compute a flood hydrograph for the probable maximum storm it is necessary to specify the time sequence of the precipitation. The estimate of PMP is derived by six-hour increments. In the text and figures of the report the "first" 6-hour period means the first in order of magnitude rather than the first in time sequence. Nomenclature for the other increments is similar. It is intended that the increments be arranged in a sequence that will result in a critical flood hydrograph and which is meteorologically reasonable.

There are two meteorological factors to be taken into account in devising the time sequence for the PMP storm. First is the time sequence in observed storms. The PMP time sequence should be modeled somewhat after observed storms in order to simulate natural conditions. Samples of observed hyetographs both for points and for areal averages are depicted in figure 7-2. There is some tendency for the two or three highest 6-hour increments in a storm to bunch together, as that length of time is required for the influence of a severe precipitation-producing situation to pass a given region. Otherwise the hyetographs for observed storms are quite varied.

The second factor to take into account derives from the manner of developing the theoretical PMP data. The maximum dew points by 6-hour increments are derived from envelopes of persisting values. Thus in a series of dew points a second peak has no influence on the maximum value for various durations. The treatment of pressure gradients is identical. Maximum observed wind, P/M ratios, and storm rainfall data are analyzed on a basis of enveloping values of total accumulation or averages for consecutive 6-hour

periods. The foregoing method of developing the parameters from which the PMP is computed leads to the following principle: For consistency in maintaining critical PMP conditions for each duration, the 6-hour increments that make up the PMP for that duration must be adjacent to each other in time. For example, the second highest increment must be adjacent to the highest in order to provide the critical combination for 12 hours, the third highest should be immediately before or after this 12-hour sequence to provide the maximum 18-hour total, and the fourth highest should be before or after the 18-hour sequence to give 24-hour PMP, etc. Sample pattern PMP time sequences that conform strictly to the foregoing principle are shown in figures 7-3a and b.

Review of the observed hyetographs will show that 3-day storms typically have two or more peaks or bursts. Time sequence patterns which show this characteristic storm behavior and which conform to the sequential requirement described in the preceding paragraph within practical limits, though not strictly adhering to it 6-hour period by 6-hour period, are obtained by application of the following rules:

(a) Group the four heaviest 6-hour increments of the 72-hour PMP in a 24-hour sequence, the middle four increments in a 24-hour sequence, and the smallest four increments in a 24-hour sequence.

(b) Within each of these 24-hour sequences arrange the four increments in accordance with the sequential requirements. That is, the second highest next to the highest, the third highest adjacent to these, and the fourth highest at either end.

(c) Arrange the three 24-hour sequences in accordance with the sequential requirement, that is, the second highest 24-hour period next to the highest with the third at either end. Any of the possible combinations to the three 24-hour periods is acceptable with the exception of placing the lightest 24-hour period in the middle.

7.11 <u>Examples</u>. Figure 7-3c, d, and e depict sequences arranged in accordance with the foregoing rules. The 24-hour grouping is in accordance with a general practice of the Corps of Engineers. It is intended that the hydrologist experiment with different time sequences to uncover any factors that would make one more critical than another in his basin.

Within the limits of the rules for time distribution the hydrologist may wish to give preference to patterns of distribution most similar to the hyetographs of one or more past major storms in the vicinity of his basin, this may be done provided other time distribution patterns do not yield appreciably more critical flood hydrographs.

7.12. <u>Snowmelt winds and dew points</u>. The time distribution of 6-hour dew points and windspeeds for snowmelt computations is explained in chapter X of this report. The arrangement of these is fixed by the adopted time distribution of the rain, that is the highest dew point and wind coincident with the highest period of rainfall, etc. The corresponding dew points have been entered on figure 7-3 to illustrate this point.

Chapter VIII

CHECKS ON PROBABLE MAXIMUM PRECIPITATION

8.01. Checks on the magnitude of the derived PMP of this report are obtained in two ways; first, by a review of the maximization incorporated in each variable and secondly, by comparing the PMP with observed precipitation and statistically derived values.

Maximization of meteorological factors

8.02. An important aspect in appraising an estimate of probable maximum precipitation is to view the degree of maximization in the aggregate. It is necessary to choose degrees of maximization for each factor which, in combination, are representative of a probable maximum storm. General principles and guide lines on maximization were discussed in chapter II.

8.03. Maximization of the important meteorological factors used in this report are summarized below. In order to give some perspective, three degrees of maximization are listed. The "extreme" maximization might be used to estimate something comparable to a probable maximum value of that variable alone. The "intermediate" maximization in each instance is a description of the procedure used in this report and is considered suitable for combination with the other maximizations to estimate probable maximum precipitation. The "minimal" assumption is a lesser criterion than used in this report and ranges between PMP and Standard Project conditions.

1. ## Surface dew point

Extreme: Equate to offshore sea-surface temperature at a source latitude; or extrapolate past record for all stations to allow for future events that will exceed past record.

Intermediate: Envelop long records at key stations but with some undercutting of higher values, especially those during periods of sluggish airflow. Smooth seasonally and areally to compensate for small sample of great storms.

Minimal: Use highest values during selected major storms without search of long record.

2. ## Relation of upper-air moisture to surface dew point

Extreme: Envelop relation of upper level moisture to surface dew point in storms for which upper-air data are available. Such an envelope would

show higher dew points aloft than at the surface on account of the surface inversion effect.

Intermediate: Assume saturated pseudoadiabatic atmosphere.

Minimal: Make some allowance for non-saturated layers aloft. (The model coefficient factors for later durations of the probable maximum precipitation are in part due to this effect.)

3. Storm mechanism, convergence component of PMP

Extreme: Envelop precipitation/moisture ratios throughout the United States; transpose precipitation/moisture ratios without adjustment throughout season.

Intermediate: Restrict envelope of precipitation/moisture ratios primarily to storms in the Central Valley of California. Undercut Campo, Calif. storm considerably; undercut slightly P/M ratios of certain storms in northern Central Valley where there are special topographic effects.

Have sufficient downward trend in precipitation/moisture ratios from winter toward summer to compensate for the upward trend in moisture at 24-hour duration.

Determine separate sets of precipitation/moisture ratios; one set for combining with orographic precipitation, the other not so limited.

Minimal: The "intermediate" degree of maximization approaches a "minimal" character for point precipitation. There is some compensation toward higher values for areas larger than a point, covered in item 9.

4. Wind, orographic component of PMP

Extreme: Wait for accumulation of 25 years of rawin observations (which are carried out regardless of cloudiness) at several California stations; extrapolate beyond the record to more severe future events by a Gumbel frequency analysis or equivalent.

Determine maximum surface geostrophic winds from the long period of surface pressure observations and suitably extrapolate to upper levels in the atmosphere.

Intermediate: Select wind values characteristic of the probable maximum precipitation storm intermediate between a and b that follow.

   a. Maximum observed geostrophic winds at the various levels
       corrected for mountain frictional effects by mean ratios
       of observed wind to geostrophic wind.

b. Frequency extrapolation of maximum winds found in the fragmentary record of upper wind observations, including those during cloudy weather, at Oakland and other stations. Restrict such winds to the southwest quadrant.

Minimal: Envelop the wind record.

5. Raindrop and snowflake terminal velocities

Note: The higher the assumed terminal velocity the greater the collection of orographic precipitation on the windward slope. The smaller the terminal velocities the greater the total spillover; however optimum precipitation a few miles beyond the crest is associated with fairly high terminal velocities.

Extreme: Neglect spillover precipitation as a loss to the windward slopes in view of the various uncertainties.

Intermediate: Adopt as terminal velocities values near the highest, but not the absolute largest values, of those observed in laboratory experiments.

Assume a wet snow layer for a space extending a couple of thousand feet upward from the freezing level, in which the terminal velocity is intermediate between rain and dry snow.

Minimal: Assume dry snow above 34°F level, and an average terminal velocity for all raindrop sizes below.

6. Orographic model coefficient

Extreme: Envelop model coefficients determined from major storms, undercutting a few extreme values.

Intermediate: Average model coefficients arrayed for each storm in decreasing order of precipitation intensity.

Minimal: Set an arbitrary ceiling of 1.0 on model coefficient. Or use the over-all average model coefficient irrespective of storm duration. Introduce a characteristic decay of precipitation with duration over and above the moisture and wind decays in some other fashion.

7. Combination of orographic and convergence components of precipitation

Extreme: In view of the predilection of thunderstorms to occur more frequently and possibly more severely in mountainous areas, superimpose the extreme convergence rain on the extreme orographic rain that might be expected in any one season.

Intermediate: Add maximum values of a convergence PMP and an orographic PMP, each derived for compatibility with the other, 6-hour period by 6-hour period.

Minimal: As a Standard Project type of approach, combine the above 6-hour increments in some other arrangement than maximum with maximum, etc.

Or, base criteria on observed total precipitation only.

8. Upwind barrier depletion for Sierras

Extreme: Neglect any upwind barrier effects. This would be supported by the facts that the air is nearly saturated during periods of precipitation at Merced and other valley stations, that maximum valley dew points are in general as high as coastal dew points at the corresponding latitudes, and that the mean annual precipitation increases rapidly at fairly low elevations in the foothills of the Sierras.

Intermediate: Apply a fairly severe barrier depletion to convergence rain and a more moderate depletion to orographic rain as a balance. Deplete convergence PMP by ratio of precipitable water in column above elevation of crest of Coast Range to precipitable water in column above sea level. For orographic PMP make some allowance for recharge of valley air with moisture by evaporation of falling precipitation. (Per figure 5-8.)

Minimal: Lesser recharge than assumed above.

9. Areal variations

This item refers to adjustments to index map values for area of basin.

Extreme: The precipitation/moisture ratios are for the most part based on point values. Use a flat relationship in going from point values of convergence rain to a 200-square-mile index. Such a relationship would be supported by the considerable scatter of the data and by the high probability that the observed point samples are not the largest values that actually occurred in each storm.

For orographic PMP, do not correct for areal variation.

Intermediate: Derive an average depth-area relationship from many storms to go from a point to a 200-square-mile index.

Assume in general that point values of precipitation are representative of 10 square miles, except for a few extreme events which may be undercut by a 10-square-mile enveloping curve.

For orographic PMP deplete the index for basins wider than 30 miles in proportion to the distribution of extreme pressure gradients.

Minimal: The foregoing approaches minimal values.

10. Durational variations

Extreme: Base durational variation of moisture on all-station envelope of observed decays since a flat decay is as reasonable at any one station as at any other. The same reasoning is apropos to the wind decay used for orographic precipitation.

Intermediate: Use an average durational decay of moisture determined from envelopes of persisting dew points at key stations. For winds use an average of observed decays during strong wind situations.

Minimal: The intermediate criterion approaches minimal standards.

Comparison of PMP with maximum observed precipitation

8.04. The most obvious comparison of PMP estimates with other data is with the maximum observed storm precipitation depth of the region. Tables 8-1, 8-2, 8-3, and 8-4 list maximum known precipitation depths in the Central Valley, the Sierra slopes, the Coastal slopes, and Southern California respectively, together with the PMP derived from the criteria of this report at the corresponding locations. The PMP values are given both for the month of occurrence of the observed storm and the maximum for the October-April season. A few September and May storm values are compared with October and April PMP respectively. Point observed depths are compared with 10-square mile PMP unless indicated otherwise.

8.05. The closest approach of an observed value to PMP in the Central Valley is at Newton in the September 18, 1959, convective storm. The 3-hour and 6-hour point values were estimated from a mass rainfall curve reconstructed for Newton by use of observers' notes and surrounding measurements. The 3-hour estimated point value of 8.1 inches is slightly higher than the 3-hour 10-square mile PMP for Newton. An isohyetal map was drawn for this period which gave a reduction of 17 percent from point to an area of 10 square miles. This results in a 10-square mile depth of 6.7 inches in 3 hours which is 85 percent of the PMP. Point values at three other stations, (Red Bluff, Fresno and Sacramento) are near or exceed 50 percent of the 10-square mile PMP at some duration (Reference table 8-1.)

8.06. In the Sierras, the March 1907 storm yielded 59 percent of the PMP over 1100 square miles of the Feather River and Yuba Basins and 56 percent over 90 square miles in the Feather River Basin. Other instances of storm precipitation reaching more than 50 percent of the probable maximum were the 24-hour point value at Cathay Bull Run Ranch in the November 1950 storm, and the December 1913-January 1914 storm over 419 square miles of the Feather River Basin. (Reference table 8-2)

8.07. In the coastal region, the November 22, 1874 point rain at Ft.
Ross was over 80 percent of the 10-square mile PMP. This extreme rain was
measured near the base of an abrupt slope of about 1500 feet elevation, and
although the observer had only shortly prior to this storm started to take
precipitation measurements he has a long history of accurate records and the
extreme rain is quite probably correct. Other observed point amounts reaching
50 percent of the 10-square mile PMP occurred at Hobergs, December 10-11,
1937; San Francisco, December 20, 1866; Orick Prairie Creek, November 20,
1950; and Upper Matole, January 30, 1888. (Reference table 8-3)

8.08. In Southern California, the Campo measurement of 11.5 inches in
80 minutes on August 12, 1891 greatly exceeds the 10-square mile PMP for the
October-April season as does the 7.1 inches of July 18, 1922 in 2 hours. Ex-
clusion of storms of this type has been discussed in chapter II of this re-
port. The very localized nature of such severe summer convective rains leads
one to suspect that the 10-square mile average value was considerably less
than the point value in each storm. However, if hydrologic problems in these
areas arise in spite of the dry ground conditions, they must be dealt with
individually. (Reference table 8-4)

Significance of size of sampling area on ratio of observed precipitation to
PMP

8.09. Two factors that must be given important weight when assessing
PMP relative to maximum observed precipitation values are the length of pre-
cipitation records and the size of region (sampling area) over which compari-
sons are made. The larger the region, the more nearly will the biggest
observed storms approach PMP proportions. The non-orographic Central Valley
and few coastal regions of California are examples of small sampling areas
for non-orographic rains. Thus, if observations were available for the ad-
joining ocean region, it is most probable that ratios of maximum observed to
PMP would be larger than those shown in table 8-1. Examples of large sampling
areas are regions in the Central and Eastern States where a relatively few
widely spaced storms, such as Thrall, Texas and Smethport, Pennsylvania of
1921 and 1942, respectively, are considered to come near to PMP proportions
for certain durations and sizes of areas.

Table 8-5 has been prepared to illustrate the sampling area effect and
is somewhat analogous to the preceding tables (8-1, -2, -3, and -4) for Cal-
ifornia. Table 8-5 compares PMP values as derived from Hydrometeorological
Report No. 33 (2) with maximum observed values from "Storm Rainfall in the
United States" (14) for six areas in the Central and Eastern States which are
the size and shape of the San Joaquin and Sacramento drainage of California.
The respective areas are depicted in figure 8-1. No attempt was made to place
them either on or between major storms; therefore, they are randomly spaced.
None of the observed/PMP ratios within the six test areas are as large as some
that can be found outside these areas, illustrating that areas of this size
can "miss" big values. The ratios of table 8-5 are of about the same order of

Table 8-1

COMPARISON OF MAXIMUM OBSERVED CENTRAL VALLEY PRECIPITATION WITH PMP
(Point rainfall compared with 10-sq.-mi. PMP
unless indicated otherwise)

Location	Date	Observed pcpn (inches)	Duration (hours)	PMP for month of storm (inches)	Ratio: Obs. Value PMP (storm mo.)	PMP Oct-Apr Season (inches)	Ratio: Obs. Value PMP (season)
Fresno	4/8/26	1.4	1	2.4	.58	2.9	.48
Fresno	4/8/26	1.7	2	4.0	.42	4.8	.35
Fresno	11/16/00	2.9	24	9.3	.31	9.4	.31
Kennet	5/9/15	8.3	8	16.5(Apr)	.50	18.2	.46
Newton	9/18/59	8.1#	3	7.9(Oct)	1.02	7.9	1.02
Newton	9/18/59	10.6#	6	12.5(Oct)	.85	12.5	.85
Newton (10 sq. mi.)	9/18/59	6.7*	3	7.9(Oct)	.85	7.9	.85
Newton (10 sq. mi.)	9/18/59	8.8*	6	12.5(Oct)	.70	12.5	.70
Red Bluff	9/13/18	4.7	3	6.0(Oct)	.78	6.0	.78
Red Bluff	9/13/18	5.7	6	7.7(Oct)	.74	7.7	.74
Red Bluff	9/13/18	5.9	12	9.8(Oct)	.60	9.8	.60
Red Bluff	9/13/18	6.1	24	13.0(Oct)	.47	13.1	.47
Sacramento	4/7/35	1.7	1	5.4	.32	6.6	.26
Sacramento	4/20/80	6.4	16	10.7	.60	11.4	.56
Sacramento	4/20/80	7.2	24	12.5	.58	12.8	.56
Sacramento	4/19-21/80	8.8	72	17.3	.51	18.1	.49
Tulare	9/26/98	3.8	24	9.1(Oct)	.42	9.1	.42
Wasco	1/20/21	2.8	24	8.7	.32	9.1	.31

\# Estimated from constructed mass rainfall curve.
* Reduced from point to 10 sq. mi. by storm isohyetal map.

Table 8-2

COMPARISON OF MAXIMUM OBSERVED SIERRA SLOPE PRECIPITATION WITH PMP
(Point rainfall compared with 10-sq.-mi. PMP unless indicated otherwise)

Location	Date	Observed Pcpn (inches)	Duration (hours)	Area (sq.mi.)	PMP for Month of Storm (inches)	Ratio: Obs. Value / PMP (storm mo.)	PMP Oct-Apr Season (inches)	Ratio: Obs. Value / PMP (season)
Blue Canyon	12/21-22/55	9.3	24	point	24.9	.37	25.1	.37
Brush Creek	12/11/37	11.6	24	point	27.2	.43	27.4	.42
Cathay Bull Run	11/19/50	6.3	24	point	11.4	.55	11.4	.55
Giant Forest	11/18/50	13.2	24	point	33.0	.40	33.3	.40
Huntington Lake	11/18-19/50	9.1	24	point	20.6	.44	20.7	.44
Feather Basin	Mar. 1907	27.7	72	90	47.9	.58	49.9	.56
Feather Basin	Dec. 1913-Jan. 1914	5.7	6	419	10.4	.55	10.7	.53
Feather Basin	Dec. 1913-Jan. 1914	8.8	12	419	17.7	.50	17.7	.50
Feather Basin	Dec. 1913-Jan. 1914	10.8	18	419	23.5	.46	23.6	.46
Feather Basin	Dec. 1913-Jan. 1914	17.0	48	419	41.0	.41	41.1	.41
Feather, Yuba Basins	Mar. 1907	23.7	72	1100	38.5	.62	40.1	.59
Fresno, Merced "	Dec. 1937	16.4	36	312	37.5	.44	37.8	.43
Fresno, Merced "	Dec. 1937	21.0	48	312	43.0	.49	43.0	.49
Fresno, Merced and Tuolumne Basins	Dec. 1937	13.1	36	1173	30.2	.43	30.6	.43
Fresno, Merced and Tuolumne Basins	Dec. 1937	17.0	48	1173	34.8	.49	34.8	.49
Kaweah Basin	Nov. 1950	14.6	24	110	29.8	.49	30.3	.48
Kaweah, Tule Basins	Nov. 1950	13.2	24	408	27.4	.48	27.8	.48
Kaweah, Tule and Kings Basins	Nov. 1950	11.8	24	908	23.5	.50	23.9	.49

Table 8-3

COMPARISON OF MAXIMUM OBSERVED COASTAL SLOPE PRECIPITATION WITH PMP
(Point rainfall compared with 10-sq.-mi. PMP unless
indicated otherwise)

Location	Date	Observed Pcpn (inches)	Duration (hours)	Area (sq.mi.)	PMP for Month of Storm (inches)	Ratio: Obs. Value / PMP (storm mo.)	PMP Oct-Apr Season (inches)	Ratio: Obs. Value / PMP (season)
Ben Lomond	1/31/45	11.8	24	point	41.8	.28	41.8	.28
Boulder Creek Locatelli	12/23/55	5.8	6	point	15.5	.37	16.0	.36
Branscomb	1/18/06	9.8	24	point	22.7	.43	22.7	.43
China Flat	2/1/15	7.1	24	point	14.4	.49	14.4	.49
Cummings	12/8/52	10.1	24	point	21.6	.47	21.9	.46
Ft. Ross	11/22/74	12.1	12	point	14.4	.84	14.6	.83
Ft. Ross	11/22/74	18+	24	point	20.7	.87+	20.9	.86+
Hayward	11/20/50	7.2	24	point	15.7	.46	15.8	.46
Highland	11/18/50	11.9	24	point	25.6	.47	26.3	.45
Hobergs	12/10-11/37	5.7	6	point	10.3	.55	10.8	.53
Hobergs	12/10-11/37	14.8	24	point	24.6	.60	24.8	.60
Klamath	10/29/50	3.7	6	point	8.6	.43	8.6	.43
Los Gatos	12/23/55	8.5	24	point	28.7	.30	29.1	.29
Mt. Hamilton	12/22-23/55	8.6	24	point	18.7	.46	18.9	.45
Orick Prairie Crk.	11/20/50	11.5	24	point	16.5	.70	16.7	.69
San Francisco	12/20/66	4.2	8	point	8.2	.51	9.5	.44
San Francisco	12/19-20/66	7.8	21	point	12.4	.63	13.0	.60
San Francisco	12/18-20/66	10.2	72	point	21.3	.48	21.8	.47
Upper Matole	1/30/88	10.0	24	point	20.1	.50	20.1	.50
Centered at Hobergs	Dec. 1937	2.6	6	313	8.7	.30	9.1	.29
Centered at Hobergs	Dec. 1937	4.7	12	313	14.2	.33	14.3	.33
Centered at Hobergs	Dec. 1937	8.8	24	313	21.9	.40	22.1	.40
Centered at Hobergs	Dec. 1937	14.0	48	313	31.1	.45	31.6	.44

Table 8-4

COMPARISON OF MAXIMUM OBSERVED SOUTHERN CALIFORNIA PRECIPITATION WITH PMP
(Point rainfall compared with 10-sq.-mi. PMP unless indicated otherwise)

Location	Date	Observed pcpn (inches)	Duration (hours)	Area (sq. mi.)	PMP for month of storm (inches)	Ratio: Obs. Value PMP (storm mo.)	PMP Oct-Apr Season (inches)	Ratio: Obs. Value PMP (season)
Azusa	1/1/34	9.2	24	point	23.7	.39	23.7	.39
Bennet Ranch	1/23/43	15.3	24	point	25.1	.61	25.1	.61
Big Bear Lake Dam	3/3/38	15.1	24	point	27.1	.56	28.1	.54
Campo	7/18/22	7.1	2	point	4.2(Oct)	1.69*	4.2	1.69*
Campo	8/12/91	11.5	80 min.	point	3.6(Oct)	3.28*	3.6	3.28*
Chatsworth Hughes	12/31/33	8.1	24	point	15.8	.51	15.9	.51
Covina	2/17/27	10.6	24	point	22.2	.48	22.2	.48
Encinitas	10/12/89	7.6	8	point	9.8	.78	9.8	.78
Fullerton City Res.	3/14/41	2.5	1	point	2.9	.86	4.0	.63
Garrett Winery Cucamonga	9/29/46	3.5	80 min.	point	4.2(Oct)	.83	4.2	.83
Hoegee's Camp	1/22/43	7.4	6	point	13.3	.56	14.5	.51
Hoegee's Camp	1/22/43	26.1	24	point	37.2	.70	37.2	.70
Lechuza Patrol Station	12/31/33	10.3	24	point	21.2	.48	21.5	.48
Sierra Madre Carter	3/4/43	2.7	1	point	3.0	.90	3.9	.69
Sierra Madre Carter	3/4/43	3.5	3	point	6.0	.58	6.9	.51
Centered at Hoegee's Camp	Jan. 1943	5.5	6	300	14.1	.39	14.1	.39
Centered at Hoegee's Camp	Jan. 1943	9.6	12	300	24.1	.40	24.1	.40
Centered at Hoegee's Camp	Jan. 1943	17.5	24	300	38.4	.46	38.4	.46
Centered at Hoegee's Camp	Jan. 1943	24.5	48	300	55.8	.44	55.8	.44
Centered at Hoegee's Camp	Jan. 1943	4.8	6	702	10.5	.46	10.6	.45
Centered at Hoegee's Camp	Jan. 1943	8.3	12	702	17.7	.47	17.7	.47
Centered at Hoegee's Camp	Jan. 1943	15.1	24	702	28.4	.53	28.4	.53
Centered at Hoegee's Camp	Jan. 1943	21.1	48	702	42.0	.50	42.0	.50

*October 10 square mile compared with summer point.

Table 8-5

COMPARISON OF MAXIMUM STORM VALUES WITH PMP FOR AREAS THE SIZE AND SHAPE OF
SAN JOAQUIN AND SACRAMENTO DRAINAGE OF CALIFORNIA (Ref. fig. 8-1)

Duration (hrs)	Area (sq. mi.)	Maximum Observed (in.)	Storm Assignment No.	PMP (in.)	Ratio (Obs./PMP)
		Test Area No. 1			
6	10	12.0	MR 4-3	22.9	.52
6	200	11.2	MR 4-3	18.2	.62
6	1000	8.7	MR 4-3	14.3	.61
24	10	12.3	MR 4-3	30.0	.41
24	200	11.5	MR 4-3	22.4	.51
24	1000	9.2	MR 4-3	18.4	.50
		Test Area No. 2			
6	10	8.5	UMV 1-22	23.8	.36
6	200	7.8	UMV 1-22	16.2	.48
6	1000	5.6	UMV 1-22	12.6	.44
24	10	12.4	GL 2-29	28.6	.43
24	200	11.3	GL 2-29	20.3	.56
24	1000	9.2	GL 2-29	16.2	.57
		Test Area No. 3			
6	10	20.1	NA 2-4	26.9	.75
6	200	15.0	NA 2-4	19.5	.77
6	1000	8.8	NA 2-4	15.2	.58
24	10	22.7	NA 2-4	31.4	.72
24	200	16.5	NA 2-4	23.8	.69
24	1000	12.4	NA 2-22A	16.2	.77
		Test Area No. 4			
6	10	17.3	SW 2-11	29.1	.59
6	200	13.3	SW 2-11	21.3	.62
6	1000	9.1	SW 2-11	17.7	.51
24	10	21.3	SW 2-11	34.3	.62
24	200	16.4	SW 2-11	26.5	.63
24	1000	11.1	SW 2-11	22.1	.50
		Test Area No. 5			
6	10	7.9	GM 2-25	30.0	.26
6	200	6.4	LMV 2-5	22.2	.29
6	1000	5.5	LMV 2-5	17.9	.31
24	10	12.6	LMV 2-5	37.9	.33
24	200	12.2	LMV 2-5	30.8	.40
24	1000	11.3	LMV 2-5	26.5	.43
		Test Area No. 6			
6	10	8.4	SA 3-20	28.9	.29
6	200	7.9	SA 3-20	21.7	.36
6	1000	7.1	SA 3-20	17.5	.41
24	10	16.0	SA 3-20	37.0	.43
24	200	14.9	SA 2-9A	28.3	.53
24	1000	13.5	SA 2-9A	21.4	.60

magnitude (for six randomly-selected areas in the East) as the ratios in tables 8-1 through 8-4. The largest ratios are in California, not considering the special-category storms at Newton and Campo. This comparison suggests that the California PMP in the present report is at a comparable general level to Report No. 33 for the East, or possibly that the California PMP is at a slightly lower level.

Statistical approach to PMP

8.10. A statistical approach to estimating PMP has recently been devised. It is explained briefly in the following paragraphs and results from its application in California compared with this report. Further details of the method are in a paper by Hershfield (26).

8.11. There are two factors which at this time suggest a statistical approach to the PMP problem: the large quantity of available rainfall data and new statistical techniques. As a by-product of the many rainfall-frequency studies made by the Weather Bureau during the past decade, records from several thousand stations are in a form amenable to probability analysis; i.e., the annual maxima of daily rainfall have been extracted from climatological publications.

8.12. In 1951, Chow (27) demonstrated that the only difference between the theoretical distributions which lend themselves to the analysis of extreme-value hydrologic data is the value of the factor K in the following equation

$$X_T = \bar{x} + K \, s_N \qquad (1)$$

where X_T is the rainfall for return-period T, $\bar{x}$ is the sample mean of a series of annual maxima, s_N is the sample standard deviation, and N is the size of the sample. If the maximum observed rainfall, X_M, is substituted for X_T in equation (1) K becomes K_M, the number of standard deviations that have to be added to the mean to obtain that maximum:

$$X_M = \bar{x} + K_M \, s_N \qquad (2)$$

K_M's were determined for the series of annual maximum 24-hour rainfall depths for each of more than 2600 stations from several countries. An enveloping value of 15 for K_M was considered appropriate for estimating PMP. The parent paper (26) shows that K_M is both independent and random with respect to rainfall magnitude, storm that produced the maxima, and geographical location. This is another way of saying the K_M's are transferable. Therefore, to determine a statistically derived PMP for a station, one need only calculate the $\bar{x}$ and s_N from the series of annual maxima at that station to solve equation (2).

8.13. A statistical map with $K_M = 15$ is illustrated in figure 8-2 for eastern United States along with the Hydrometeorological Report No. 33 (2) isolines for 24 hours and 10 square miles. The statistical PMP isolines of this figure are based on the 100 long-record Weather Bureau First Order and 100 Cooperative stations shown on the chart. Agreement between the Report No. 33 and the statistical map is excellent along the Gulf of Mexico. They diverge rapidly to the north and west with the Report No. 33 map sometimes showing results twice as large as the statistical map.

8.14. A similar analysis was performed in California where orography has a great influence on the rainfall regime. The statistical map is shown in figure 8-3 along with the points (solid dots) from more than 400 stations which were used to define the position of the isolines. No consideration was given to orography in the construction of the isolines--just simple linear interpolation between the points with some degree of smoothing between closely-spaced points.

8.15. Statistical values for California are compared with 24-hour 10-square-mile PMP from this report in figure 8-4. The map shows values from both sources plotted on a grid. The upper number is interpolated from the lines of figure 8-3. The lower number is the highest of the monthly PMP's for October through April, by the steps in chapter IX. Some values are from the convergence-only criteria, others from orographic-plus convergence criteria. In each instance the higher value is used.

8.16. The relative level of the two methods may be compared in the scatter diagram of figure 8-4. The statistical value from the map for each grid point has been plotted against the corresponding PMP of this report. The position of the points with respect to a 45° line suggests that the general level of the physical - synoptic values is a little lower.

8.17. The level of the statistical method can be adjusted by changing K_M. A value of 15 was shown to yield results comparable to Hydrometeorological Report No. 33 (2) in the southern United States, but relatively lower values farther north. The inference is that, if there is any difference, the PMP values of this report for points are less conservative than Report No. 33.

Comparison of PMP with SPS

8.18. The PMP of this report is compared with the Standard Project Storm values derived by the Sacramento District Corps of Engineers for the Sacramento-San Joaquin Valley (5). The comparison may extend the scope of the SPS report, however storms that were used in its derivation encompass the coastal drainage of California. The comparisons are shown on figures 8-5 through 8-9. For 6 hours, 10 and 200 square miles; 24 hours, 200 and 1000 square miles; and 72 hours, 1000 square miles the SPS and PMP values are plotted on a 1/2° grid and a separate map provided showing the computed ratio of SPS to PMP at each grid point for each of the duration and area combinations. It can be seen that in general the SPS runs from 40 to 60 percent of

the PMP. There is also a trend from relatively lower ratios of SPS to PMP in
drier regions to higher ratios in regions of greater storm frequency. This
is climatologically correct. Some scattered anomalous high or low ratios
derive from differences in generalization of topographic influences in the
respective reports.

Comparison of SPS and PMP for certain selected basins is shown on fig-
ure 8-12.

8.19. The values for different sizes of areas on figure 8-5 through
8-9 are obtained by applying the appropriate areal relationship to the index
values at each respective grid point for both PMP and SPS and therefore will
differ somewhat from the value that would be obtained for a basin of that
size in that vicinity where the index values throughout the basin would be
weighted. This difference is of no consequence for the comparisons. The
SPS values and ratios on the charts that are in parentheses are derived from
the "local" SPS criteria (5) for small areas and short durations.

Comparison of PMP with precipitation for various return periods

8.20. The PMP in this report is derived primarily by generalizing from
a few large storms in California on a synoptic, physical, and topographic
basis. The long-term precipitation records of the individual stations also
contain a measure of the synoptic, physical and topographic effects. Grid
comparisons of 2-year 24-hour values (24-hour point depth with a mean re-
currence interval of 2 years), and 100-year 24-hour values with the PMP for
24-hour 10-square miles are shown in figure 8-10. Ten-year 72-hour values
are compared with the 72-hour 10-square mile PMP in figure 8-11. At each
grid point the ratio of the return period value to the PMP is plotted in per-
cent. The 2-year and 100-year return period values were derived from Weather
Bureau Technical Paper 40, (28) charts 44 and 49. The 10-year 72-hour values
are from chart No. 6 of Technical Bulletin No. 4, "Ten Year Storm Precipita-
tion in California and Oregon Coastal Basins", Sacramento District Corps of
Engineers (6). Figures in the referenced studies show isolines drawn rather
closely to a large number of station values.

8.21. The primary significance of these comparisons is of geographical
consistency (see "internal consistency" in chapter II) rather than of the gen-
eral level of the PMP. It can be seen that generally the percentages of PMP
fall into reasonable patterns and that they are lower in dry regions than in
regions of greater storm frequency.

Comparison of PMP of this report with Weather Bureau Technical Paper No. 38, "Generalized Estimates of Probable Maximum Precipitation for the United States West of the 105th Meridian."

8.22. Selected comparisons between the PMP values of this report and
those from Weather Bureau Technical Paper No. 38 (3) are shown in figures
8-12 through 8-14, in a manner similar to the comparison with SPS values.

Figures 8-13 and 8-14 include differences at the high spots on the respective index maps (figure 5-35 of this report and figures 6-1 and 6-4 of Weather Bureau Technical Paper No. 38). The differences at these points, of course, are biased by the method of selection, while the grid point comparisons may be regarded as random.

8.23. Some differences between the two reports result from different but reasonable approaches to making PMP estimates and thus are a measure of the uncertainty in estimates of PMP. Other differences and reasons for them are as follows. In this paragraph the reports are referred to as "TP 38" and "HMR 36" respectively. (a) On the San Joaquin Valley floor and in other arid regions HMR 36 values are lower than TP 38 because further studies have given more confidence in relying on the desiccating effects of downslope motions which inhibit rain. (b) TP 38 includes small-area intense local warm-season storms, while HMR 36 is restricted to cool-season storms, as discussed elsewhere. This accounts for the large differences on the charts in Southern California. (c) HMR 36 values exceed TP 38 along the crest of the Sierras at 24 hours. This results in part from closer drawing to topography on larger scale maps made possible by the more detailed study. (d) A single 6/24-hour duration ratio (for each size area) was adopted throughout the study-region of TP 38 that is characteristic of the intense local storms that control most of the PMP values. Somewhat lower 6/24-hour ratios were adopted for California in HMR 36, as characteristic of the cool-season storms of primary emphasis. This accounts for the difference in shape of the comparative depth-duration curves in figure 8-12.

Chapter IX

SUMMARY OF STEPS IN OBTAINING PROBABLE MAXIMUM PRECIPITATION
FOR A BASIN

9.01. The steps necessary to obtain generalized values of PMP have been
kept to a minimum. For computing the orographic component of PMP, the proba-
ble maximum orographic precipitation index map (figure 5-35)*, the orographic
PMP computation areas (figure 5-30), the basin-width variation (figure 5-39)
and the seasonal-duration variation (table 5-5)*are used. The restricted
convergence PMP (to be combined with the orographic PMP) requires the proba-
ble maximum convergence precipitation index map (figure 4-12), and the vari-
ation of convergence PMP with basin size and duration (figures 4-13a, b, and
c). The unrestricted convergence PMP (which is used if it exceeds the com-
bined orographic and restricted convergence values) is 133 percent of the re-
stricted convergence component of PMP.

A detailed step-by-step procedure in determining PMP for a basin follows,
after which several examples are given.

9-A. PROCEDURE FOR COMPUTING PMP

9.02.* Steps in determining orographic PMP

1. Determine average probable maximum precipitation index within basin out-
line from figure 5-35. (A grid average is adequate.)

2. Determine the basin representative width perpendicular to the optimum in-
flow direction. This is measured perpendicular to the sides of the orograph-
ic PMP computation areas shown on figure 5-30. (Narrow extensions of the
basin perpendicular to the inflow would not be considered in determining the
basin representative width.)

3. Determine basin-width adjustment factor from figure 5-39.

4. Multiply the basin average probable maximum orographic precipitation in-
dex from step 1, by the basin-width adjustment factor. This will give the
January 6-hour maximum orographic PMP.

5. To obtain all 6-hourly increments of orographic PMP for each month use
percentages given in table 5-5. If the basin is in the Sierra Range east of
a line through the middle of Central Valley multiply the width-adjusted ba-
sin-average probable maximum orographic precipitation index from step 4 by
the Sierra Range percentages. For a basin in any other area, multiply the
width-adjusted basin-average probable maximum orographic precipitation index
from step 4 by the Coastal Range percentages.

*Please see the revision dated October 1969 to the appropriate figure, table,
and section that is included at the end of this publication.

6. For small basins, the 1- and 3-hour duration orographic PMP values are 20 and 54 percent respectively (see paragraph 5.50) of the 1st (maximum) 6-hour orographic PMP.

9.03. Steps in determining convergence PMP

A. Restricted convergence PMP to be combined with orographic PMP.

1. Determine average probable maximum convergence precipitation index within basin outline from figure 4-12. (A grid average is adequate.)

2. Tabulate the 6-hour incremental percentages of convergence PMP index for the area of the basin for each month, October through April (figures 4-13a, b, and c). After the 3rd or 4th 6-hour increment, there is no areal variation so the percentages are given on the figures. For small basins, the 1- and 3-hour duration percentages are obtained from the same figures.

3. Multiply the basin-average probable maximum convergence precipitation index from step 1 by the percentages determined in step 2. The results are the 1- and 3-hour duration and 6-hourly incremental restricted convergence PMP values that are added to the orographic PMP month for month.

B. Unrestricted convergence PMP for basins with zero or a relatively small probable maximum orographic precipitation index.

1. Multiply the restricted convergence PMP from 9.03 A3 by 1.33 to obtain the unrestricted convergence PMP increments.

2. Accumulate the 6-hourly increments to obtain the 6-, 12-, 18-, etc. hour duration unrestricted convergence PMP.

9.04. Total PMP

1. Add the 6-hourly increments of orographic PMP from 9.02.5 to the 6-hourly increments of restricted convergence PMP from 9.03 A3 month for month; 1st 6-hour orographic to 1st 6-hour convergence, 2nd 6-hour orographic to 2nd 6-hour convergence, etc. For small basins also add the 1- and 3-hour duration orographic and convergence values.

2. Accumulate the 6-hourly incremental values of combined restricted convergence PMP and orographic PMP for each month to obtain the 6-, 12-, 18-, etc. hour duration values.

3. For pronounced orographic areas the combined orographic and restricted convergence PMP will exceed the unrestricted convergence PMP month for month. For basins in non-orographic regions, the unrestricted convergence is the

total PMP. For foothill areas, the combined orographic and restricted convergence PMP (9.04.2) and unrestricted convergence PMP (9.03 B2) may be compared and the most critical selected dependent upon critical duration and other hydrologic factors. For any basin the PMP values for the various months should be evaluated on the basis of snowmelt contribution, (ref. chapter X for snowmelt winds and temperatures) size of basin, etc. in order to select the most hydrologically critical precipitation.

9.05. Time distribution

Arrange 6-hour increments of selected PMP into a critical storm sequence (ref. chapter VII paragraphs 7.10 to 7.12). Figure 7-3 gives examples of such sequences. Winds and temperatures for computing snowmelt should be arranged in the same sequence.

9-B. EXAMPLES OF PMP COMPUTATIONS

I. Large Sierra Slope Basin

Tuolumne River above LaGrange, California. Basin Area: 1540 square miles

9.06. Orographic PMP for Tuolumne Basin

1. Basin average probable maximum orographic precipitation index (figure 5-35): 4.86 inches
2. Basin representative width (figure 5-30): 30 miles
3. Basin-width adjustment factor (figure 5-39): 1.00
4. Basin-width adjusted probable maximum precipitation index:
   4.86 X 1.00 = 4.86 inches
5. All 6-hourly increments of orographic PMP: 4.86 times Sierra Range percentages from table 5-5

6-Hour Period

Mid-month	1	2	3	4	5	6	7	8	9	10	11	12
	6-hourly incremental orographic PMP in inches											
Oct.	4.71	3.69	2.96	2.43	2.09	1.75	1.46	1.21	1.02	.83	.68	.53
Nov.	4.76	3.69	3.01	2.48	2.09	1.75	1.46	1.21	1.07	.87	.68	.53
Dec.	4.81	3.74	3.01	2.53	2.14	1.80	1.51	1.26	1.07	.87	.68	.53
Jan.-Feb.	4.86	3.79	3.06	2.53	2.14	1.80	1.51	1.26	1.07	.87	.68	.53
Mar.	4.66	3.64	2.92	2.43	2.04	1.70	1.46	1.21	1.02	.83	.63	.53
Apr.	4.37	3.40	2.72	2.28	1.94	1.65	1.36	1.17	.97	.78	.63	.49

Note: 1- and 3-hour duration PMP values were not computed for this large-area basin.

9.07. Convergence PMP for Tuolumne Basin

(Restricted convergence PMP to be combined with orographic PMP.)

1. Basin average probable maximum convergence precipitation index (figure 4-12): 2.26 inches
2. 6-hourly incremental percents of convergence PMP index (figures 4-13a, b, and c)

6-Hour Period

Mid-month	1	2	3	4	5	6	7	8	9	10	11	12
	Percents of convergence PMP index											
Oct.	94	30	20	16	14	12	11	10	9	9	8	8
Nov.	85	38	26	20	16	14	13	11	10	10	10	10
Dec.	79	37	26	21	18	16	13	12	11	11	10	10
Jan.-Feb.	74	40	28	23	19	16	14	13	12	11	11	11
Mar.	76	39	28	22	19	16	13	11	10	10	9	9
Apr.	78	36	27	21	18	14	12	10	9	9	8	8

3. 6-hourly incremental restricted convergence PMP: 2.26 times percents of convergence PMP index

6-Hour Period

Mid-month	1	2	3	4	5	6	7	8	9	10	11	12
	6-hourly incremental restricted convergence PMP in inches											
Oct.	2.12	.68	.45	.36	.32	.27	.25	.23	.20	.20	.18	.18
Nov.	1.92	.86	.59	.44	.36	.32	.29	.25	.23	.23	.23	.23
Dec.	1.79	.84	.59	.48	.41	.36	.29	.27	.25	.25	.23	.23
Jan.-Feb.	1.67	.91	.63	.52	.43	.36	.32	.29	.27	.25	.25	.25
Mar.	1.71	.88	.63	.50	.43	.36	.29	.25	.23	.23	.20	.20
Apr.	1.77	.81	.61	.48	.41	.32	.27	.23	.20	.20	.18	.18

Note: Because of pronounced orographic index for this basin, unrestricted convergence was not computed.

9.08. Total PMP for Tuolumne Basin

1. 6-hourly orographic PMP increments from 9.06.5 added to 6-hourly re-
    stricted convergence PMP increments from 9.07.3 (inches)

6-Hour Period

Mid-month	1	2	3	4	5	6	7	8	9	10	11	12
	6-hourly incremental convergence and orographic PMP in inches											
Oct.	6.8	4.4	3.4	2.8	2.4	2.0	1.7	1.4	1.2	1.0	.9	.7
Nov.	6.7	4.5	3.6	2.9	2.5	2.1	1.8	1.5	1.3	1.1	.9	.8
Dec.	6.6	4.6	3.6	3.0	2.6	2.2	1.8	1.5	1.3	1.1	.9	.8
Jan.-Feb.	6.5	4.7	3.7	3.0	2.6	2.2	1.8	1.6	1.3	1.1	.9	.8
Mar.	6.4	4.5	3.6	2.9	2.5	2.1	1.8	1.5	1.2	1.1	.8	.7
Apr.	6.1	4.2	3.3	2.8	2.4	2.0	1.6	1.4	1.2	1.0	.8	.7

2. Combined orographic PMP and restricted convergence PMP accumulated

Duration (hrs)

Mid-month	6	12	18	24	30	36	42	48	54	60	66	72
	Convergence and orographic PMP in inches											
Oct.	6.8	11.2	14.6	17.4	19.8	21.8	23.5	24.9	26.1	27.1	28.0	28.7
Nov.	6.7	11.2	14.8	17.7	20.2	22.3	24.1	25.6	26.9	28.0	28.9	29.7
Dec.	6.6	11.2	14.8	17.8	20.4	22.6	24.4	25.9	27.2	28.3	29.2	30.0
Jan.-Feb.	6.5	11.2	14.9	17.9	20.5	22.7	24.5	26.1	27.4	28.5	29.4	30.2
Mar.	6.4	10.9	14.5	17.4	19.9	22.0	23.8	25.3	26.5	27.6	28.4	29.1
Apr.	6.1	10.3	13.6	16.4	18.8	20.8	22.4	23.8	25.0	26.0	26.8	27.5

3. Select month of critical PMP on basis of hydrologic factors. Winds and
    temperatures for computing snowmelt contribution to probable maximum
    flood are given in chapter X. Arrangement of selected 6-hourly PMP in-
    crements and similar arrangement of accompanying winds and temperatures
    is covered in chapter VII.

II. Small Coastal Basin

San Lorenzo Creek above Palomares, California. Basin Area: 20 square miles

9.09. Orographic PMP for San Lorenzo Basin

1. Basin average probable maximum orographic precipitation index (figure 5-35): 2.00 inches
2. Basin representative width (figure 5-30): 12 miles
3. Basin-width adjustment factor (figure 5-39): 1.00
4. Basin-width adjusted probable maximum orographic precipitation index: 2.00 X 1.00 = 2.00 inches
5. All 6-hourly increments of orographic PMP: 2.00 times Coastal Range percentages from table 5-5

6-hour Period

Mid-month	1	2	3	4	5	6	7	8	9	10	11	12
	6-hourly incremental orographic PMP in inches											
Oct.	1.84	1.44	1.16	.96	.82	.68	.56	.48	.40	.34	.26	.20
Nov.	1.88	1.46	1.18	.98	.82	.70	.58	.48	.42	.34	.26	.20
Dec.	1.96	1.54	1.24	1.02	.86	.72	.60	.52	.44	.36	.28	.22
Jan.-Feb.	2.00	1.56	1.26	1.04	.88	.74	.62	.52	.44	.36	.28	.22
Mar.	1.88	1.48	1.20	.98	.84	.70	.58	.50	.42	.34	.26	.20
Apr.	1.74	1.36	1.10	.90	.76	.64	.54	.46	.38	.32	.24	.20

6. Multiply the 1st 6-hour orographic PMP by 20 and 54 percent to obtain orographic PMP for 1 and 3 hours, respectively

Mid-month

Duration	Oct.	Nov.	Dec.	Jan. Feb.	Mar.	Apr.
	Orographic PMP in inches					
1 hr	.37	.38	.39	.40	.38	.35
3 hrs	.99	1.02	1.06	1.08	1.02	.94

9.10. Restricted convergence PMP to be combined with orographic PMP

1. Basin average probable maximum convergence precipitation index (figure 4-12): 4.21 inches
2. 1- and 3-hour percentages and 6-hourly incremental percentages of convergence PMP index (figures 4-13a, b and c)

Mid-month	Duration (hrs) 1	3	6-Hour Period 1	2	3	4	5	6	7	8	9	10	11	12
			Percents of convergence PMP index											
Oct.	69	118	155	36	23	17	14	12	11	10	9	9	8	8
Nov.	62	105	141	42	27	20	16	14	13	11	10	10	10	10
Dec.	56	96	129	43	29	21	18	16	13	12	11	11	10	10
Jan.- Feb.	52	89	122	45	30	23	19	16	14	13	12	11	11	11
Mar.	53	90	125	47	31	23	19	16	13	11	10	10	9	9
Apr.	55	96	130	44	30	23	18	14	12	10	9	9	8	8

3. 1- and 3-hour duration and 6-hourly incremental restricted convergence PMP: 4.21 times percents of convergence PMP index

Mid-month	Duration (hrs) 1	3	6-Hour Period 1	2	3	4	5	6	7	8	9	10	11	12
			Restricted convergence PMP in inches											
Oct.	2.90	4.97	6.52	1.52	.97	.72	.59	.51	.46	.42	.38	.38	.34	.34
Nov.	2.61	4.42	5.94	1.77	1.14	.84	.67	.59	.55	.46	.42	.42	.42	.42
Dec.	2.36	4.05	5.44	1.81	1.22	.89	.76	.67	.55	.51	.46	.46	.42	.42
Jan.- Feb.	2.19	3.75	5.14	1.89	1.31	.97	.80	.67	.59	.55	.51	.46	.46	.46
Mar.	2.23	3.79	5.26	1.98	1.31	.97	.80	.67	.55	.46	.42	.42	.38	.38
Apr.	2.32	4.05	5.48	1.85	1.26	.97	.76	.59	.51	.42	.38	.38	.34	.34

9.11. Unrestricted convergence PMP

1. 1- and 3-hour duration and 6-hourly incremental unrestricted convergence
   PMP. Restricted convergence PMP times 1.33

Mid- month	Duration (hrs) 1	3	6-Hour Period 1	2	3	4	5	6	7	8	9	10	11	12
			Unrestricted convergence PMP in inches											
Oct.	3.9	6.6	8.7	2.0	1.3	1.0	.8	.7	.6	.6	.5	.5	.5	.5
Nov.	3.5	5.9	7.9	2.4	1.5	1.1	.9	.8	.7	.6	.6	.6	.6	.6
Dec.	3.1	5.4	7.2	2.4	1.6	1.2	1.0	.9	.7	.7	.6	.6	.6	.6
Jan.- Feb.	2.9	5.0	6.8	2.5	1.7	1.3	1.1	.9	.8	.7	.7	.6	.6	.6
Mar.	3.0	5.0	7.0	2.6	1.7	1.3	1.1	.9	.7	.6	.6	.6	.5	.5
Apr.	3.1	5.4	7.3	2.5	1.7	1.3	1.0	.8	.7	.6	.5	.5	.5	.5

2. Accumulated unrestricted convergence PMP

Mid- month	Duration (hrs) 1	3	6	12	18	24	30	36	42	48	54	60	66	72
					Unrestricted convergence PMP in inches									
Oct.	3.9	6.6	8.7	10.7	12.0	13.0	13.8	14.5	15.1	15.7	16.2	16.7	17.2	17.7
Nov.	3.5	5.9	7.9	10.3	11.8	12.9	13.8	14.6	15.3	15.9	16.5	17.1	17.7	18.3
Dec.	3.1	5.4	7.2	9.6	11.2	12.4	13.4	14.3	15.0	15.7	16.3	16.9	17.5	18.1
Jan.- Feb.	2.9	5.0	6.8	9.3	11.0	12.3	13.4	14.3	15.1	15.8	16.5	17.1	17.7	18.3
Mar.	3.0	5.0	7.0	9.6	11.3	12.6	13.7	14.6	15.3	15.9	16.5	17.1	17.6	18.1
Apr.	3.1	5.4	7.3	9.8	11.5	12.8	13.8	14.6	15.3	15.9	16.4	16.9	17.4	17.9

9.12. Total PMP

1. 6-hourly orographic PMP increments from 9.09.5 added to 6-hourly re-
    stricted convergence PMP increments from 9.10.3. 1- and 3-hour values
    similarly added

Mid-month	Duration (hrs)		6-Hour Period											
	1	3	1	2	3	4	5	6	7	8	9	10	11	12

1- and 3-hour duration and 6-hourly increments of orographic and
convergence PMP in inches

Mid-month	1	3	1	2	3	4	5	6	7	8	9	10	11	12
Oct.	3.3	6.0	8.4	3.0	2.1	1.7	1.4	1.2	1.0	.9	.8	.7	.6	.5
Nov.	3.0	5.4	7.8	3.2	2.3	1.8	1.5	1.3	1.1	.9	.8	.8	.7	.6
Dec.	2.8	5.1	7.4	3.4	2.5	1.9	1.6	1.4	1.2	1.0	.9	.8	.7	.6
Jan.-Feb.	2.6	4.8	7.1	3.4	2.5	2.0	1.7	1.4	1.2	1.1	1.0	.8	.7	.7
Mar.	2.6	4.8	7.1	3.5	2.5	2.0	1.6	1.4	1.1	1.0	.8	.8	.6	.6
Apr.	2.7	5.0	7.2	3.2	2.4	1.9	1.5	1.2	1.1	.9	.8	.7	.6	.5

2. Combined orographic PMP and restricted convergence PMP accumulated

Duration (hrs)

Mid-month	1	3	6	12	18	24	30	36	42	48	54	60	66	72
					Orographic and convergence PMP in inches									
Oct.	3.3	6.0	8.4	11.4	13.5	15.2	16.6	17.8	18.8	19.7	20.5	21.2	21.8	22.3
Nov.	3.0	5.4	7.8	11.0	13.5	15.1	16.6	17.9	19.0	19.9	20.7	21.5	22.2	22.8
Dec.	2.8	5.1	7.4	10.8	13.3	15.2	16.8	18.2	19.4	20.4	21.3	22.1	22.8	23.4
Jan.-Feb.	2.6	4.8	7.1	10.5	13.0	15.0	16.7	18.1	19.3	20.4	21.4	22.2	22.9	23.6
Mar.	2.6	4.8	7.1	10.6	13.1	15.1	16.7	18.1	19.2	20.2	21.0	21.8	22.4	23.0
Apr.	2.7	5.0	7.2	10.4	12.8	14.7	16.2	17.4	18.5	19.4	20.2	20.9	21.5	22.0

3. Comparison of unrestricted convergence PMP (9.11.2) with combined oro-
    graphic PMP and restricted convergence PMP (9.12.2) shows that the un-
    restricted convergence PMP is greater for 1 and 3 hours duration for
    each month; at 6 hours duration, the combined orographic and restricted
    convergence PMP is greater than the unrestricted convergence PMP in the
    winter season; for 12 hours and longer durations the combined values are
    greater in each month. Hydrologic factors will determine which storm
    type and month is most critical. Snowmelt winds and temperatures, if
    applicable, are given in chapter X. Arrangements of winds, temperatures,
    and PMP increments in the same critical storm sequences are given in
    chapter VII.

Chapter X

TEMPERATURE AND WIND CRITERIA FOR SNOWMELT

10.01. Temperatures and winds associated with probable maximum precipitation are two important snowmelt factors amenable to generalization for snowmelt computations. Other items which need to be considered in determining basin melt such as optimum depth, areal extent and type of snowpack as well as vegetal cover are integral characteristics of each drainage basin and cannot readily be generalized over the State.

The derivation of generalized winds and temperatures for a PMP storm and how they may be obtained for a basin are given in this chapter. An example of derived winds and temperatures for a specific location is also presented.

Temperature during PMP storm

10.02. Enveloping 1000-mb (sea level) 12-hour persisting dew points for February developed in chapter IV (figure 4-5b) and the average seasonal variation of moisture (table 4-1) establish the 12-hour temperature using the assumption of a saturated pseudoadiabatic atmosphere during the PMP storm. Likewise the sea-level temperatures for each 6-hour increment for the 72-hour storm are determined from the adopted moisture variation with duration given in table 4-3. The variations in both tables are expressed in terms of precipitable water (W_p).

The 6-hour incremental sea-level temperatures (1000 mb) for an area for a particular month may be obtained from figure 4-5b and tables 4-1 and 4-3 through the use of auxiliary figure 10-1, by the following steps:

1) Read the 12-hour February dew point (temperature) at the area of interest from figure 4-5b.

2) Obtain the W_p corresponding to this temperature from figure 10-1. Enter this figure with the 12-hour February temperature on the abscissa, read the corresponding W_p on the ordinate.

3) Multiply the W_p by the appropriate percent of February (table 4-1) for the month of interest.

4) Multiply the resulting W_p by the percentages of table 4-3 to obtain W_p for each 6-hour increment.

5) Obtain 6-hour temperatures from figure 10-1 by reading the temperature corresponding to each 6-hour W_p of step 4.

These temperatures then are adjusted to the elevation of the area of interest by using the variation of temperature with height in a saturated

pseudoadiabatic atmosphere. This is given in figure 10-2 and is used by starting on the abscissa with each sea-level temperature, proceeding parallel to the sloping line to the basin elevation, and reading the adjusted temperature that is vertically downward on the abscissa.

10.03. Height of the freezing level during the PMP storm may be determined, under the saturated pseudoadiabatic atmosphere assumption, from 6-hourly sea-level temperatures. Enter figure 10-2 with sea-level temperature on the abscissa, proceed parallel to the sloping line and read the elevation at the 32°F isotherm.

Temperatures prior to the PMP storm

10.04. Temperatures prior to the onset of the PMP storm are a factor in determining the availability and condition of the snowpack. High antecedent temperatures could bring snowmelt runoff to the stream concurrently with the probable maximum precipitation. Below-freezing antecedent temperatures on the other hand, will avoid depletion of the available snowpack. Whether warm or cold temperatures are critical will depend on the magnitude of the snowpack. Since this varies greatly from place to place, a range of possible antecedent temperatures have been determined which will give the hydrologist the general limits of temperatures for snowmelt computations. These limits were derived from a survey of observed temperatures antecedent to major California storms.

10.05. Figure 10-3 shows the wide range in temperatures observed prior to the maximum 3-day precipitation in recent great California storms. Curves labeled A_1 and A_2 are the upper and lower envelopes of differences between the mean daily temperatures on the day of onset of a 3-day storm and 1 and 2 days prior to the day of onset at key Central Valley stations. Curve B envelops the largest day-to-day increases in temperatures observed during snow cover periods between 1949 and 1958 at Mt. Wilson, Mt. Hamilton, Blue Canyon, and Mt. Shasta.

10.06. Antecedent temperatures given in figure 10-3 are used in the following manner. After the initial 6-hour temperature (or dew point) at the onset of the PMP storm is determined, (dependent on the selected PMP storm time sequence, reference paragraphs 7.10-12) and assuming highest antecedent temperatures are most critical in this particular instance, add the temperature differences obtained from curve A_1 in figure 10-3 for each time before beginning of PMP storm to the temperature at the storm onset.

Dew points during and prior to PMP storm

10.07. Dew points, for computing condensation melt, during the 3-day PMP storm are the same at each elevation as the temperature. Prior to the storm, the dew points associated with the lower limit of temperatures (curve A_2 or B) should be 2 or 3 degrees colder. If high temperatures are critical

(curve A_1) the appropriate corresponding dew points are indicated by curve C. This curve is derived from the mean variation of maximum persisting dew points in California for durations up to 5 days.

Snowmelt winds during the PMP storm

10.08. Free-air windspeeds derived for computing orographic PMP are used, with adjustment, for defining the windspeeds over a snow cover. These maximum winds are shown on figures 5-26 and 5-27 by solid lines for January at 38°N for the Coast and Sierra Ranges respectively. Seasonal and latitudinal variations, of the maximum winds, shown in figures 5-37 and 5-32 respectively, should be applied. Figure 10-4 is provided to conveniently convert from pressures to heights.

10.09. In order to determine a factor for reducing free-air winds to those which would be expected at the surface of a snowpack, a comparison study was made of free-air winds from the Oakland sounding and simultaneous Blue Canyon (station elevation 5280 feet) anemometer-level winds, at the same elevation above mean sea level. Periods of strong winds at each location were considered. The mean ratio of the Blue Canyon anemometer wind to the free-air wind was found to be 0.75. This reduction may be used for arriving at winds for other locations which have exposure and topographic features similar to that of Blue Canyon. The Blue Canyon Weather Bureau Station is well exposed toward the southwest. The anemometer is 50 feet above the ground level and downwind from the landing field during the average southerly storm winds. There is relatively little reduction of wind by nearby forest.

10.10. Areas more sheltered than the Blue Canyon site should have correspondingly greater reduction to be estimated by the user.

10.11. A check on the magnitude of the computed winds for the PMP storm is shown in table 10-1.

Table 10-1

COMPARISON OF REDUCED PMP WINDS FROM FIGURE 5-27 WITH MAXIMUM
OBSERVED WINDS AT BLUE CANYON

	Duration (hours)				
	6	12	24	48	72
	Speed (mph)				
January computed winds	61	54	46	39	36
Maximum observed Blue Canyon winds	49	42	35	29	23

In table 10-1 maximum observed Blue Canyon persisting winds, for the durations indicated, from a survey of two complete winter seasons and selected major storms are compared with computed winds derived by multiplying speeds from figure 5-27 by 0.75.

The two winter seasons surveyed for observed Blue Canyon winds were 1954 and 1955. The major storms surveyed in other seasons were November 1950, January, February 1945, January 1943, January 1940, and December 1937.

Snowmelt winds prior to PMP storm

10.12. Winds prior to the PMP storm could vary even more than the temperatures prior to the onset. As an expedient which gives a reasonably critical wind, the wind for the 72-hour duration may be extended for two days prior to the storm.

Example of computed snowmelt winds and temperatures

10.13. An example of computed snowmelt winds, temperatures, and dew points prior to and during a PMP storm is given for a hypothetical basin on the following pages.

Example of computed snowmelt winds and temperatures

Hypothetical basin: near Blue Canyon. Average elevation: 7000 feet
Month: mid-November.

A. Temperatures and dew points during PMP storm

1) Average 12-hour February sea level dew point over basin (figure 4-5b): 59.0°F.

2) Precipitable water (W_p) for 59.0°F (figure 10-1): 1.31 inches.

3) W_p for February times seasonal adjustment for November (table 4-1):
   1.31 times 111 = 1.45 inches.

	6-hour period											
	1	2	3	4	5	6	7	8	9	10	11	12
4) W_p corresponding to 6-hour temperature increments during PMP storm. 1.45 x %'s of table 4-3 (inches)	1.51	1.45	1.41	1.38	1.35	1.32	1.29	1.27	1.25	1.23	1.22	1.21
5) 6-hour incremental sea-level temperatures and dew points from figure 10-1 (°F)	61.8	61.0	60.5	60.0	59.6	59.2	58.8	58.4	58.1	57.8	57.6	57.5
6) Sea-level temperatures and dew points adjusted to 7000 feet elevation. Figure 10-2 (°F)	43.1	42.0	41.4	40.8	40.3	39.8	39.3	38.8	38.3	38.0	37.7	37.6
7) Height of 32°F above mean sea level. Figure 10-2 (1000's feet)	10.7	10.3	10.1	9.9	9.7	9.5	9.3	9.2	9.1	8.9	8.8	8.8

8) The temperatures and elevations in steps 6 and 7 should be arranged in time sequence corresponding to the selected PMP storm sequence. (see E)

B. <u>Temperatures prior to PMP storm</u>

(For this example highest temperatures are considered critical.)

	Hours prior to storm onset							
	48	42	36	30	24	18	12	6
1) Differences between temperature at beginning of storm and at indicated hours prior to storm. From figure 10-3, curve A_1 (°F)	10.0	9.5	9.0	8.0	7.0	6.0	4.5	3.5

2) The above differences are added to the initial temperature determined in step 10.13 A8.

C. <u>Dew points prior to PMP storm</u>

	Hours prior to storm onset							
	48	42	36	30	24	18	12	6
1) Differences between dew point at beginning of storm and at indicated hours prior to storm. Figure 10-3, curve C (°F)	3.0	2.5	2.0	2.0	1.5	1.0	1.0	0.5

2) The above differences are subtracted from the initial temperature (dew point) determined in step 10.13 A8.

D. <u>Snowmelt winds</u>

	6-hour period											
	1	2	3	4	5	6	7	8	9	10	11	12
1) Winds from figure 5-27 and interpolations at 7000 ft msl (7000 ft = 775 mb) ref. figure 10-4 (mph)	87	78	72	68	65	62	60	58	56	55	54	54
2) Winds reduced to surface conditions similar to Blue Canyon. Step 1 winds x 0.75 (mph)	65	59	54	51	49	47	45	43	42	41	40	40
3) Surface winds adjusted to November. Step 2 winds x 0.84 (from figure 5-37)(mph)	55	50	45	43	41	39	38	36	35	34	34	34

4) Arrange 6-hour winds (step 3) in time sequence similar to arrangement of precipitation and temperatures in PMP storm (see E).

132

E. Time sequence of temperatures, winds and precipitation during PMP storm

	6-hour period											
	1	2	3	4	5	6	7	8	9	10	11	12
1) November 6-hourly PMP increments for hypothetical basin near Blue Canyon obtained by procedures of chapter IX. (inches)	9.2	5.8	4.6	3.8	3.2	2.6	2.2	1.9	1.6	1.4	1.1	0.9

	Time in hours from beginning of storm											
	6	12	18	24	30	36	42	48	54	60	66	72
2) 6-hour PMP increments arranged according to sequence (c) of figure 7-3. (inches)	0.9	1.4	1.6	1.1	3.8	5.8	9.2	4.6	1.9	2.6	3.2	2.2
3) 6-hour temperatures from 10.13 A6 arranged in same sequence (°F)	37.6	38.0	38.3	37.7	40.8	42.0	43.1	41.4	38.8	39.8	40.3	39.3
4) 6-hour winds from 10.13 D3 arranged in same sequence (mph)	34	34	35	34	43	50	55	45	36	39	41	38
5) Height of freezing level from 10.13 A7 in same sequence (1000's ft)	8.8	8.9	9.1	8.8	9.9	10.3	10.7	10.1	9.2	9.5	9.7	9.3

	Hours prior to storm onset								
	48	42	36	30	24	18	12	6	0
6) Temperatures prior to storm. Differences of 10.13 B1 added to 37.6 (°F).	47.6	47.1	46.6	45.6	44.6	43.6	42.1	41.1	37.6
7) Dew points prior to storm. Differences of 10.13 C1 subtracted from 37.6 (°F).	34.6	35.1	35.6	35.6	36.1	36.6	36.6	37.1	37.6

8) Winds prior to storm may be assumed to be 34 mph (ref. paragraph 10.12) for two days prior to storm.

ACKNOWLEDGMENTS

REFERENCES

1. U. S. Weather Bureau, "Generalized Estimates of Maximum Possible
    Precipitation over the United States East of the 105th Meridian
    for Areas of 10, 200, and 500 Square Miles", Hydrometeorological
    Report No. 23, Washington, 1947.

2. U. S. Weather Bureau, "Seasonal Variation of Probable Maximum
    Precipitation East of the 105th Meridian for Areas from 10 to
    1000 Square Miles and Durations of 6, 12, 24 and 48 Hours",
    Hydrometeorological Report No. 33, Washington, 1956.

3. U. S. Weather Bureau, "Generalized Estimates of Probable Maximum
    Precipitation West of the 105th Meridian", Weather Bureau Technical
    Paper No. 38, Washington, 1960.

4. U. S. Weather Bureau, "Meteorological Characteristics of Hydrologi-
    cally-Critical Storms in California", Hydrometeorological Report No. 37.
    (In preparation).

5. Corps of Engineers, U. S. Army, "Standard Project Rain-Flood Criteria,
    Sacramento-San Joaquin Valley, California", Sacramento, 1957.

6. Corps of Engineers, U. S. Army, "Ten-Year Storm Precipitation in
    California and Oregon Coastal Basins", Technical Bulletin No. 4,
    Sacramento, 1957.

7. U. S. Weather Bureau, "Meteorology of Flood-Producing Storms in the
    Mississippi River Basin", Hydrometeorological Report No. 34, Wash-
    ington, 1956.

8. U. S. Weather Bureau, "Maximum Possible Precipitation, Small Basins
    in the Los Angeles Area During the Winter Season", Preliminary
    Estimate HMS 5004, Washington, 1951.

9. Fletcher, R. D., "Computation of Thunderstorm Rainfall", Transactions
    of American Geophysical Union, Vol. 29, No. 1, pp. 41-50, February
    1948.

10. U. S. Weather Bureau, "Highest Persisting Dewpoints in Western United
    States", Weather Bureau Technical Paper No. 5, Washington, 1948.

11. U. S. Weather Bureau, "Revised Report on Maximum Possible Precipi-
    tation, Los Angeles Area, California", Hydrometeorological Report
    No. 21B, Washington, 1945.

12. U. S. Weather Bureau, "Maximum 24-Hour Precipitation in the United
    States", Weather Bureau Technical Paper No. 16, Washington, 1952.

13. U. S. Weather Bureau, "Climatological Data for the United States by Sections", Washington, Series.

14. Corps of Engineers, U. S. Army, "Storm Rainfall in the United States", Washington, 1945-.

15. U. S. Weather Bureau, "Maximum Possible Precipitation, San Joaquin Basin, California", Hydrometeorological Report No. 24, Washington, 1947.

16. Myers, Vance A., "Airflow on the Windward Side of a Large Ridge", U.S. Weather Bureau, Washington, (In preparation).

17. Laws, J. O. and D. A. Parsons, "The Relation of Raindrop Size to Intensity", Transactions of American Geophysical Union, Part II, pp. 452-459, 1943.

18. Gunn, R. and G. D. Kinzer, "The Terminal Velocity of Fall for Water Droplets in Stagnant Air", Journal of Meteorology, Vol. 6, No. 4, pp. 243-248, August 1949.

19. Laws, J. Otis, "Measurements of the Fall-Velocities of Waterdrops and Raindrops", Transactions of American Geophysical Union, pp. 709-712, 1941.

20. Anderson, L. J., "Drop-Size Distribution Measurements in Orographic Rain", Bulletin of the American Meteorological Society, Vol. 29, pp. 362-366, 1948.

21. Blanchard, D. C., "Raindrop Size-Distribution in Hawaiian Rains", Journal of Meteorology, Vol. 10, No. 6, pp. 457-473, December 1953.

22. Langleben, M. P., "Terminal Velocity of Snowflakes", Quarterly Journal of Royal Meteorological Society, Vol. 80, No. 344, pp. 174-181, 1954.

23. Douglas, R. H., K.L.S. Gunn and J. S. Marshall, "Pattern in the Vertical of Snow Generation", Journal of Meteorology, Vol. 14, No. 2, pp. 95-114, April 1957.

24. Knox, Joseph B., "Procedures for Estimating Maximum Possible Precipitation", Bulletin 88, California State Department of Water Resources, May 1960.

25. U. S. Weather Bureau, "Maximum Possible Precipitation, Sacramento River Basin", Hydrometeorological Report No. 3, Washington, 1943.

26. Hershfield, D. M., "Estimating the Probable Maximum Precipitation", Journal of the Hydraulics Division, Proceedings of the ASCE, Vol. 87, No. HY 5, pp. 99-116, September 1961, Part 1.

27. Chow, V. T., "A General Formula for Hydrologic Frequency Analysis", Transactions of American Geophysical Union, Vol. 32, No. 2, pp. 231-237, April 1951.

28. U. S. Weather Bureau, "Rainfall Frequency Atlas of the U. S. for Durations from 30 Minutes to 24 Hours and Return Periods from 1 to 100 Years", Weather Bureau Technical Paper No. 40, Washington, 1961.

29. Corps of Engineers, U. S. Army, "Sacramento Method of Correlating Storm Precipitation with Normal Seasonal Precipitation and Runoff", Sacramento, 1941.
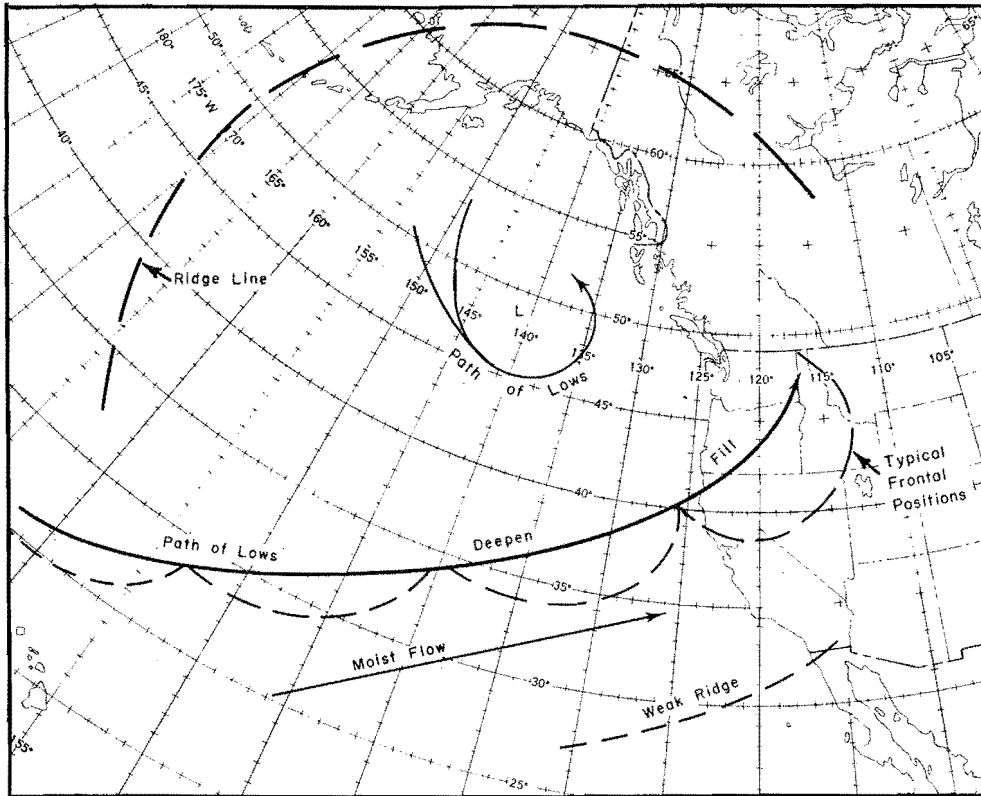
FIG. 3-1. LOW-LATITUDE-TYPE MAJOR OROGRAPHIC STORM
(NORTHERN AND CENTRAL CALIFORNIA)
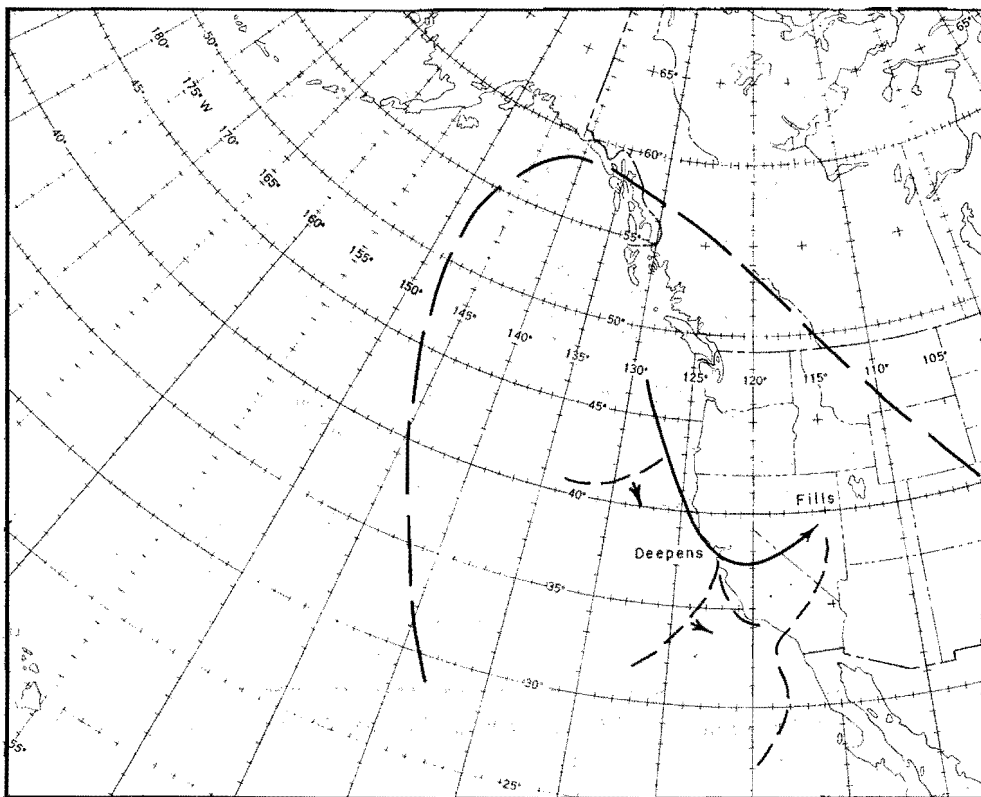
FIG. 3-2. HIGH-LATITUDE TYPE (SOUTHERN CALIFORNIA)

138
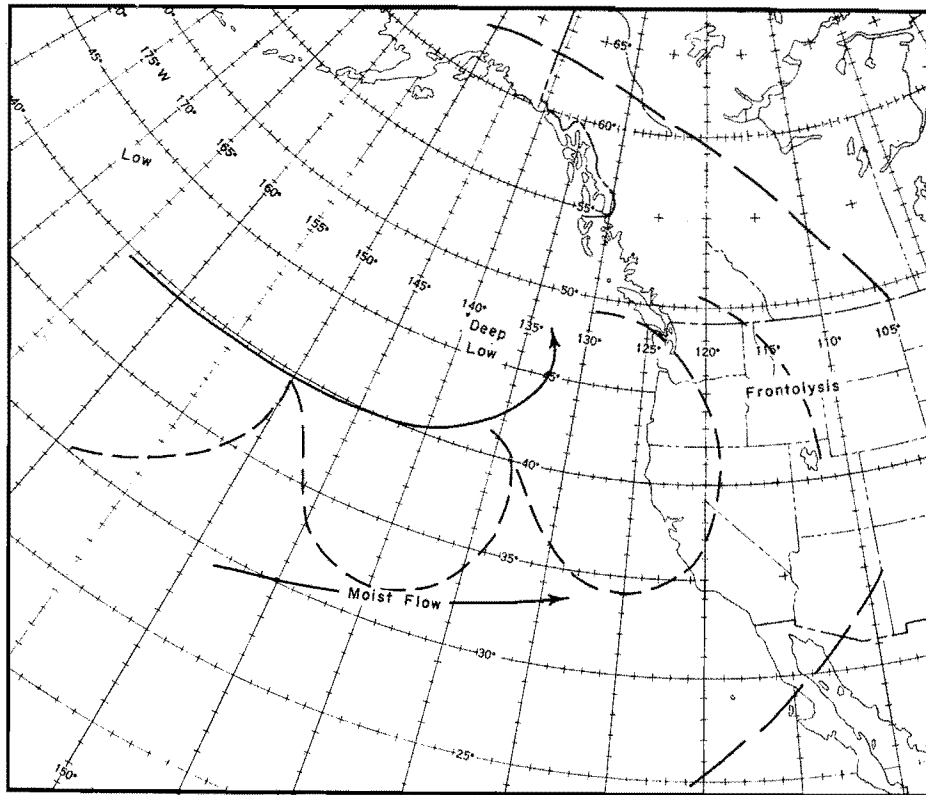
FIG. 3-3. MID-LATITUDE-TYPE, SOUTHWESTERLY APPROACH
(NORTHERN AND CENTRAL CALIFORNIA)
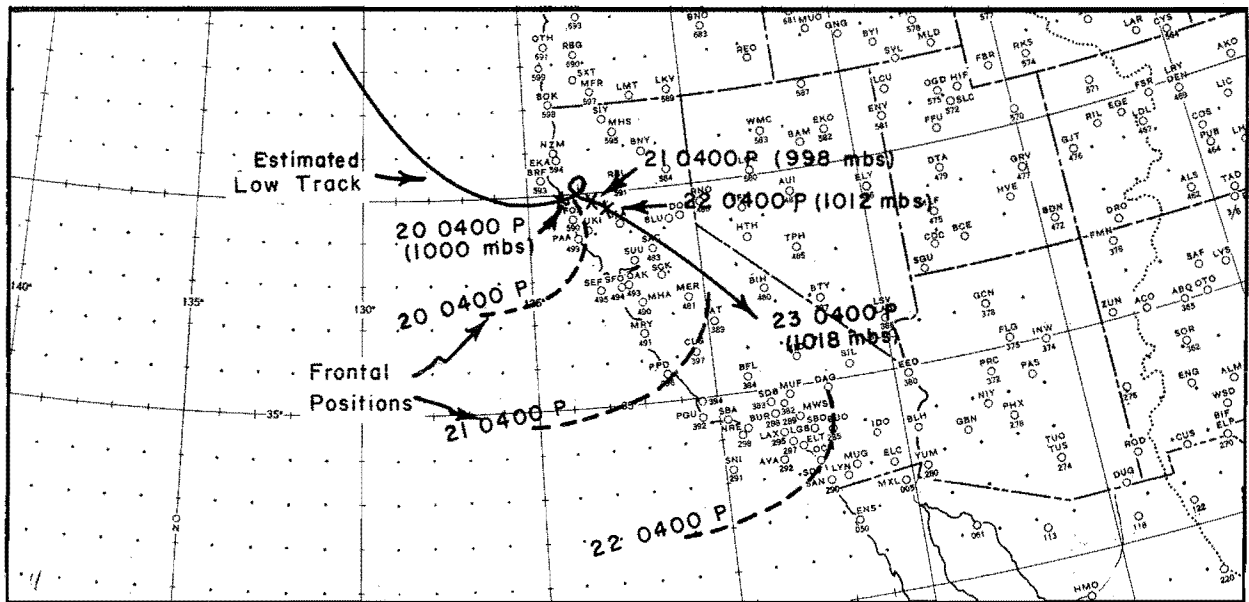
FIG. 3-4. COOL-SEASON CONVERGENCE STORM CENTERED AT SACRAMENTO
APRIL 20-21, 1880
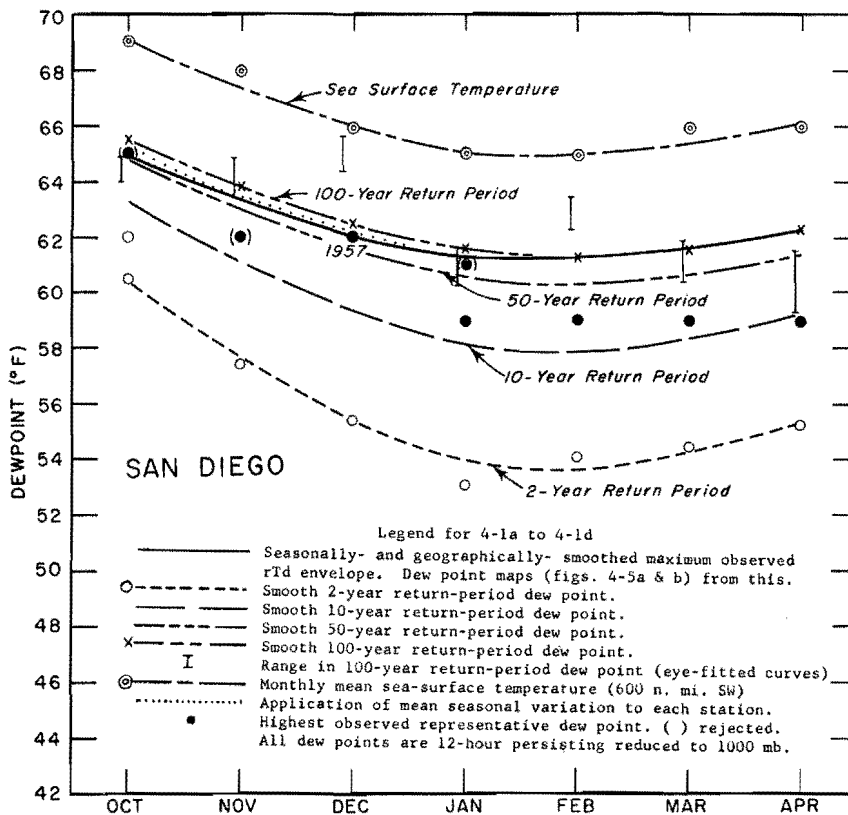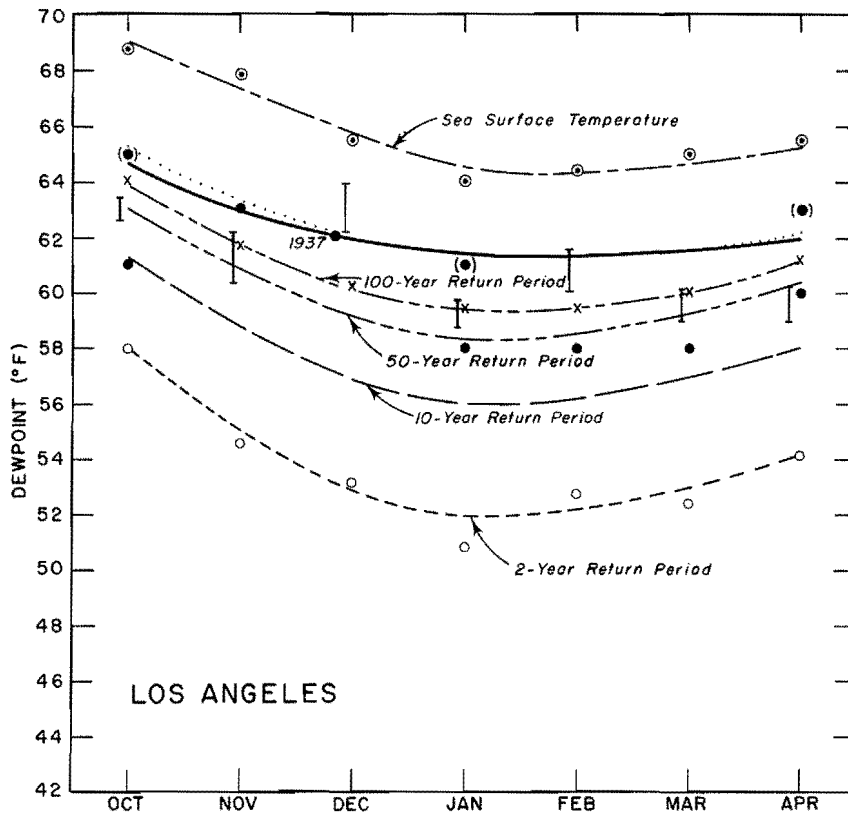
FIG. 4-1a. SEASONAL ENVELOPE OF MAXIMUM OBSERVED DEW POINTS
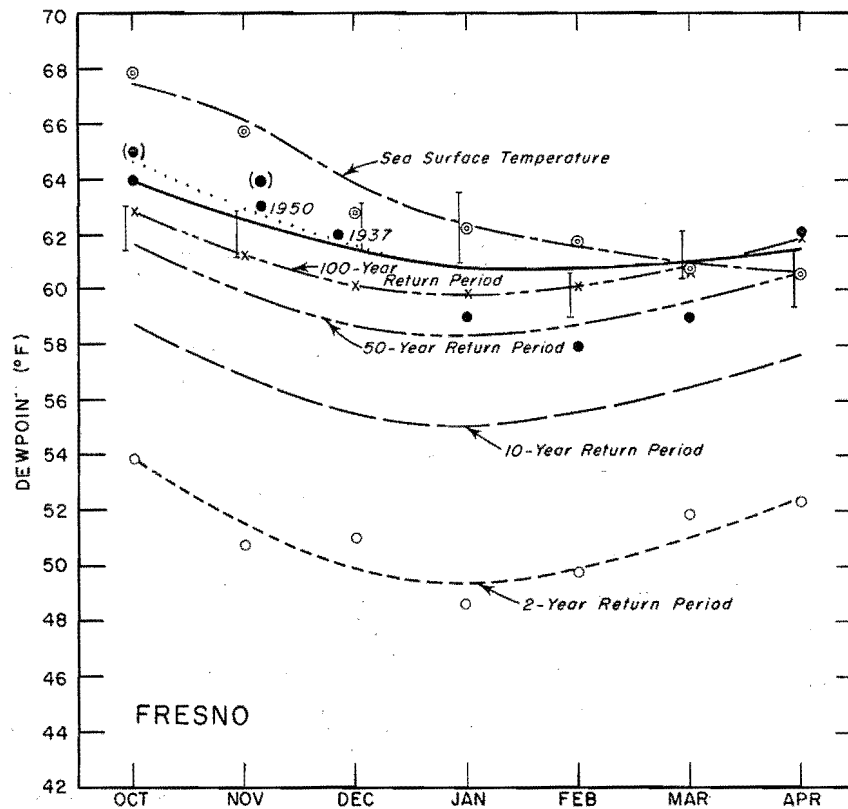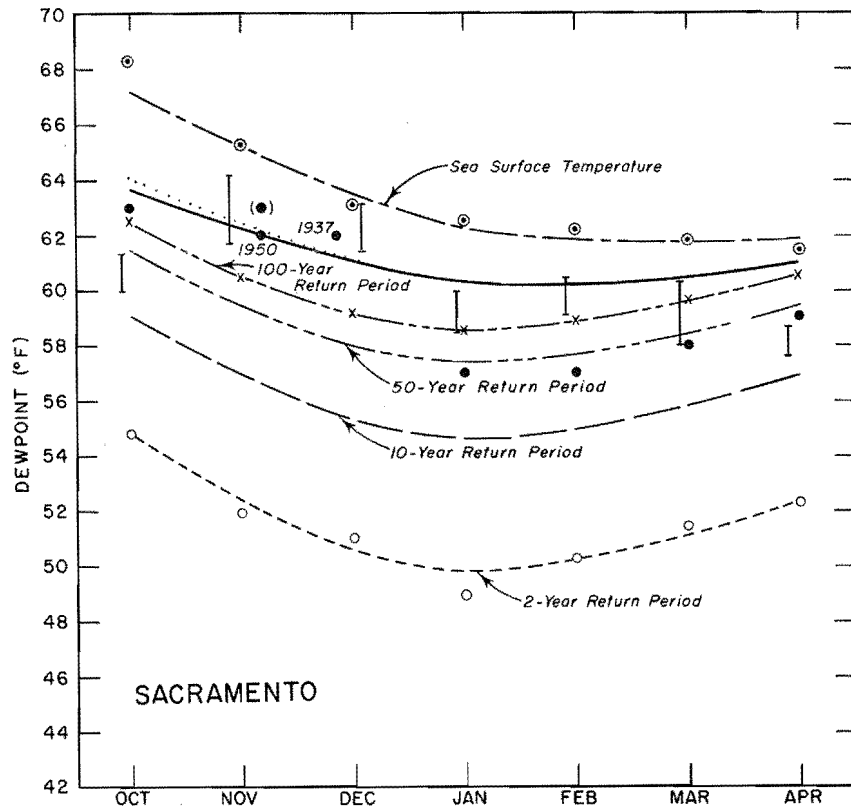
FIG. 4-1b. SEASONAL ENVELOPE OF MAXIMUM OBSERVED DEW POINTS (CONT'D)
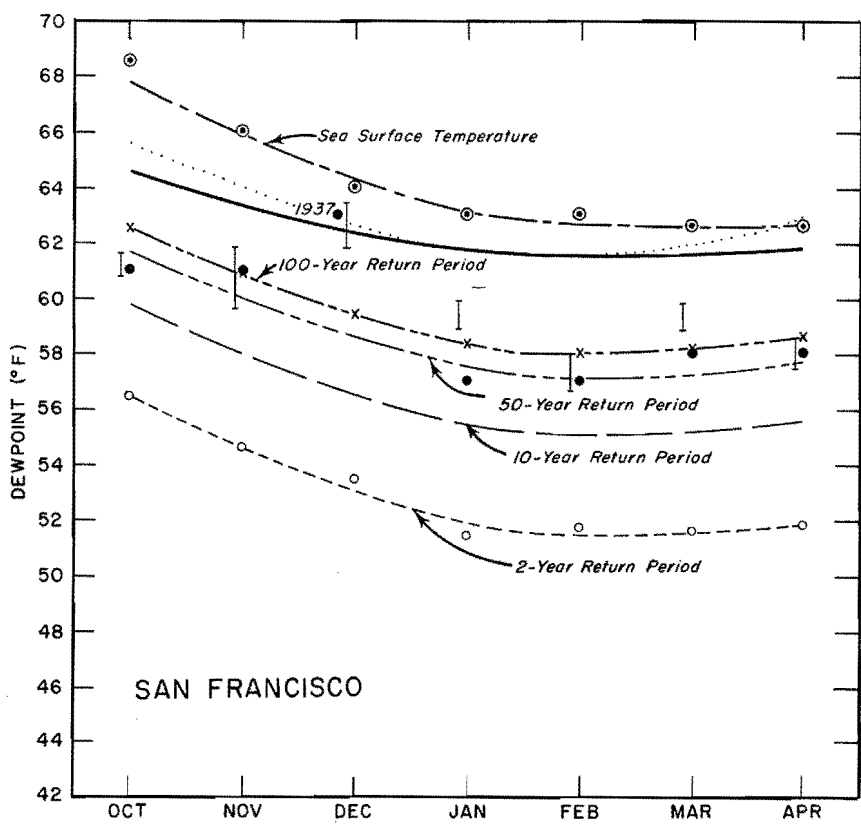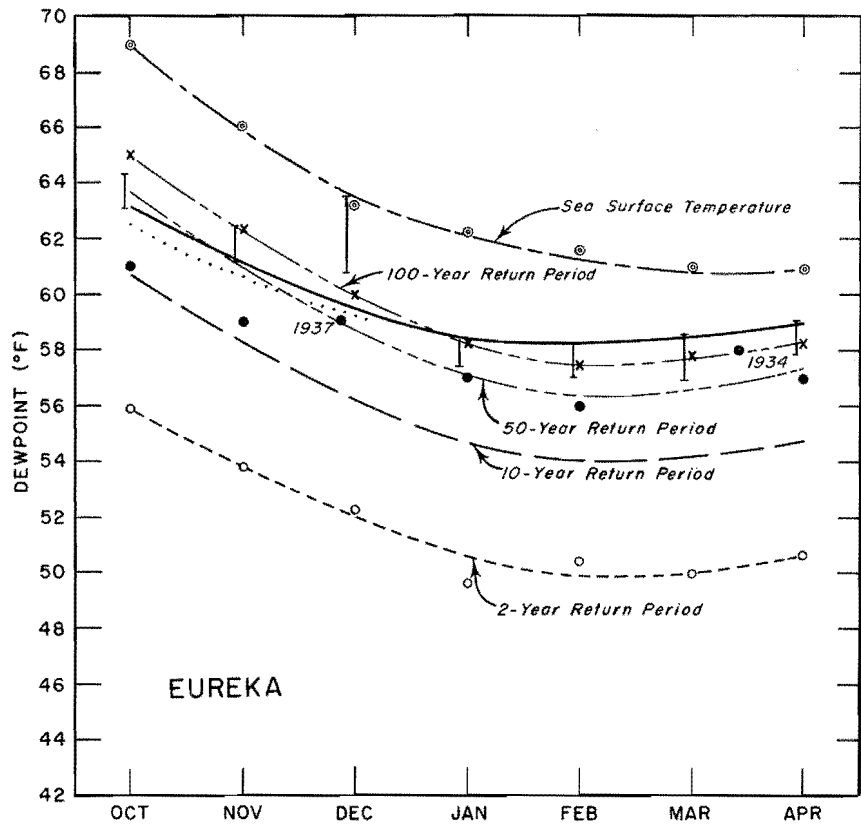
FIG. 4-1c. SEASONAL ENVELOPE OF MAXIMUM OBSERVED DEW POINTS (CONT'D)
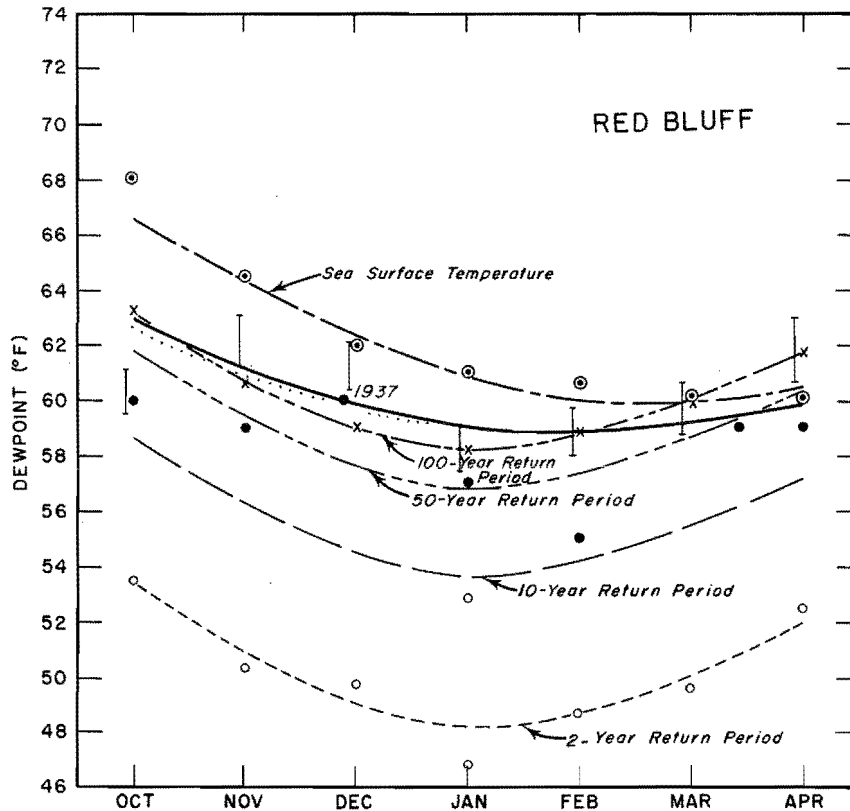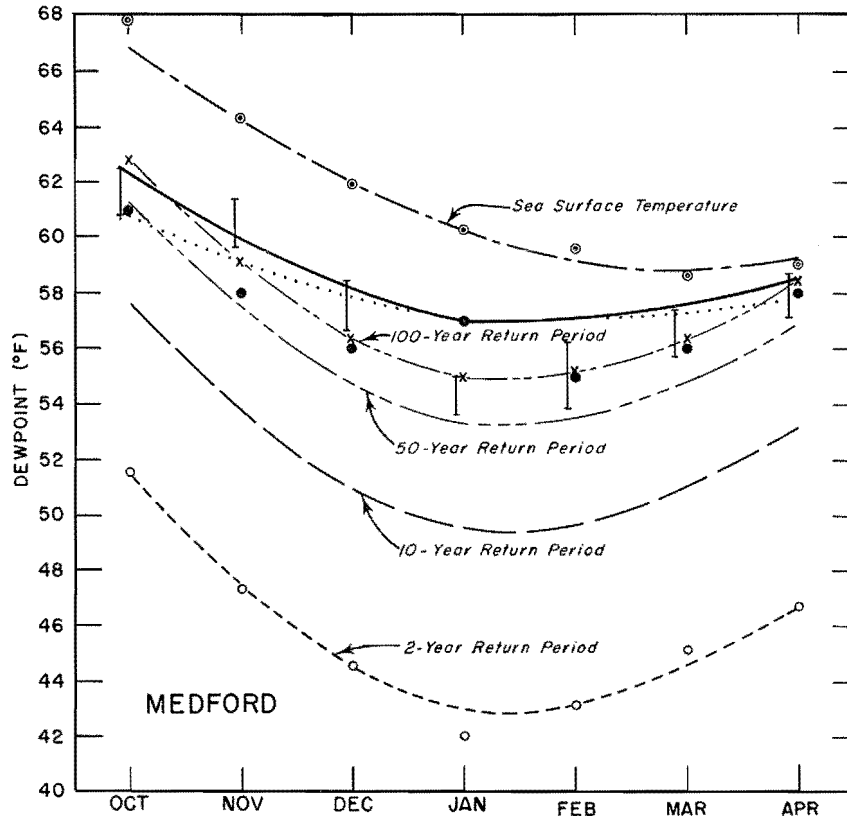
FIG. 4-1d. SEASONAL ENVELOPE OF MAXIMUM OBSERVED DEW POINTS (CONT'D)
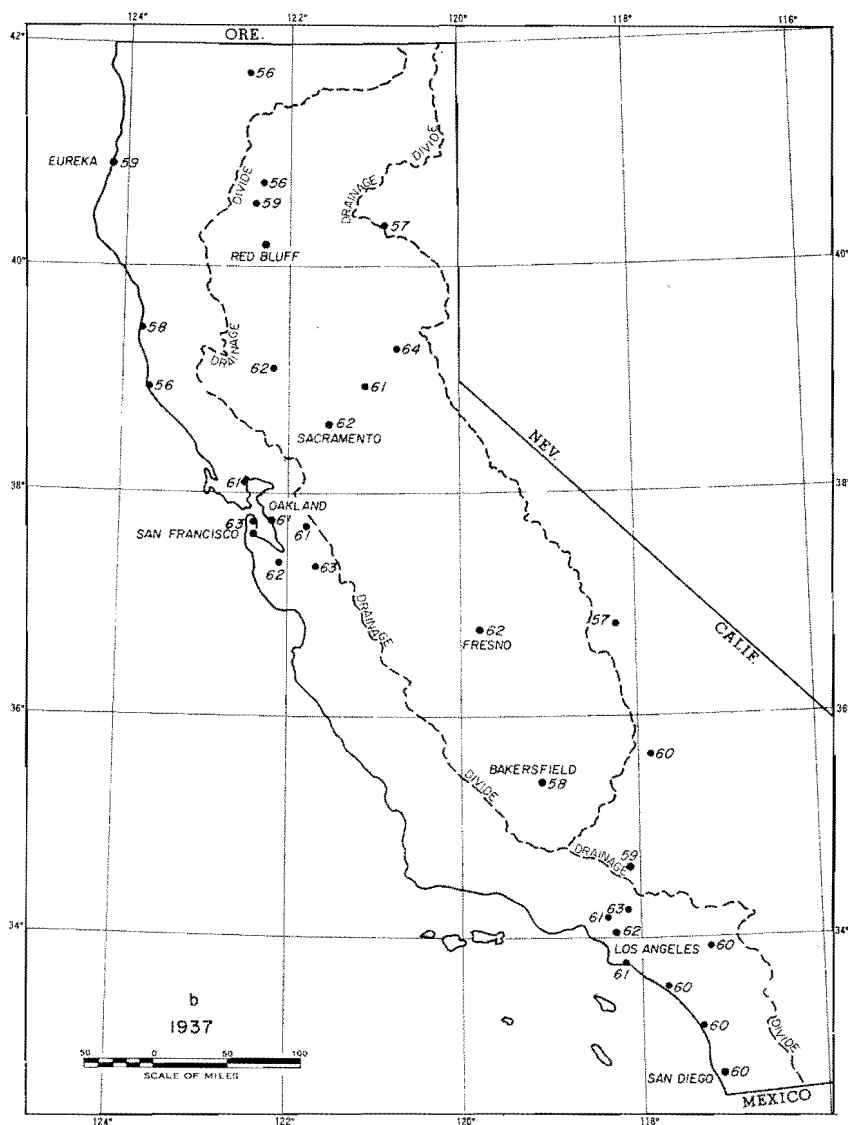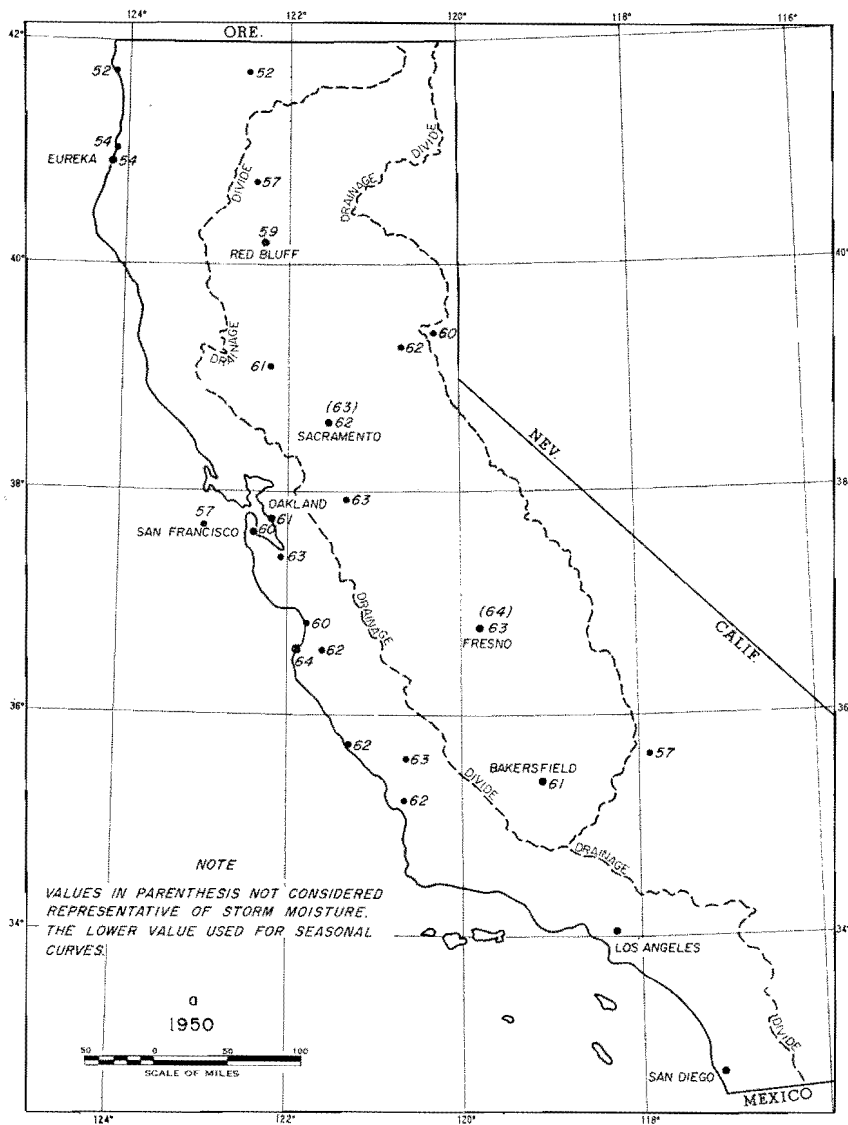
FIG. 4-2. HIGHEST 12-HOUR PERSISTING 1000-MB DEW POINTS, (°F) NOVEMBER 18-20, 1950 AND DECEMBER 10-11, 1937
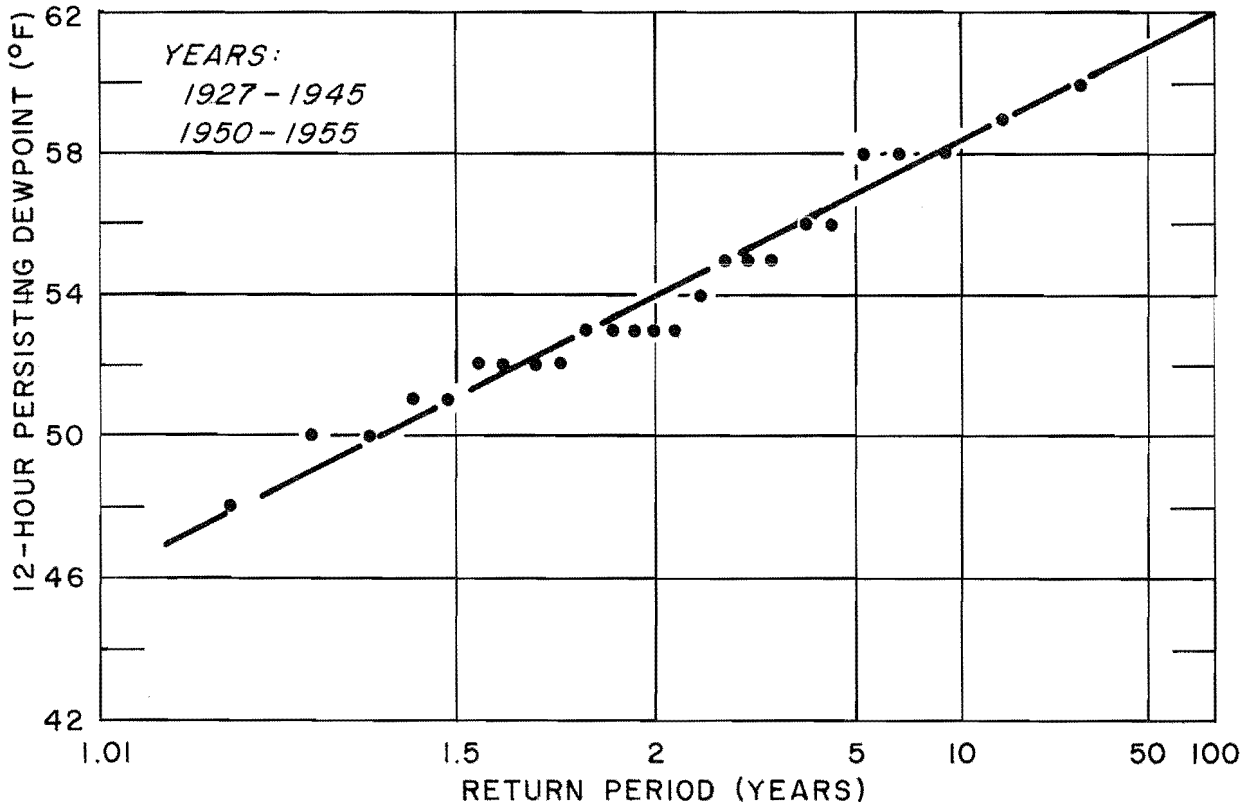
FIG. 4-3. MAXIMUM ANNUAL OCTOBER 12-HOUR PERSISTING DEW POINT, FRESNO
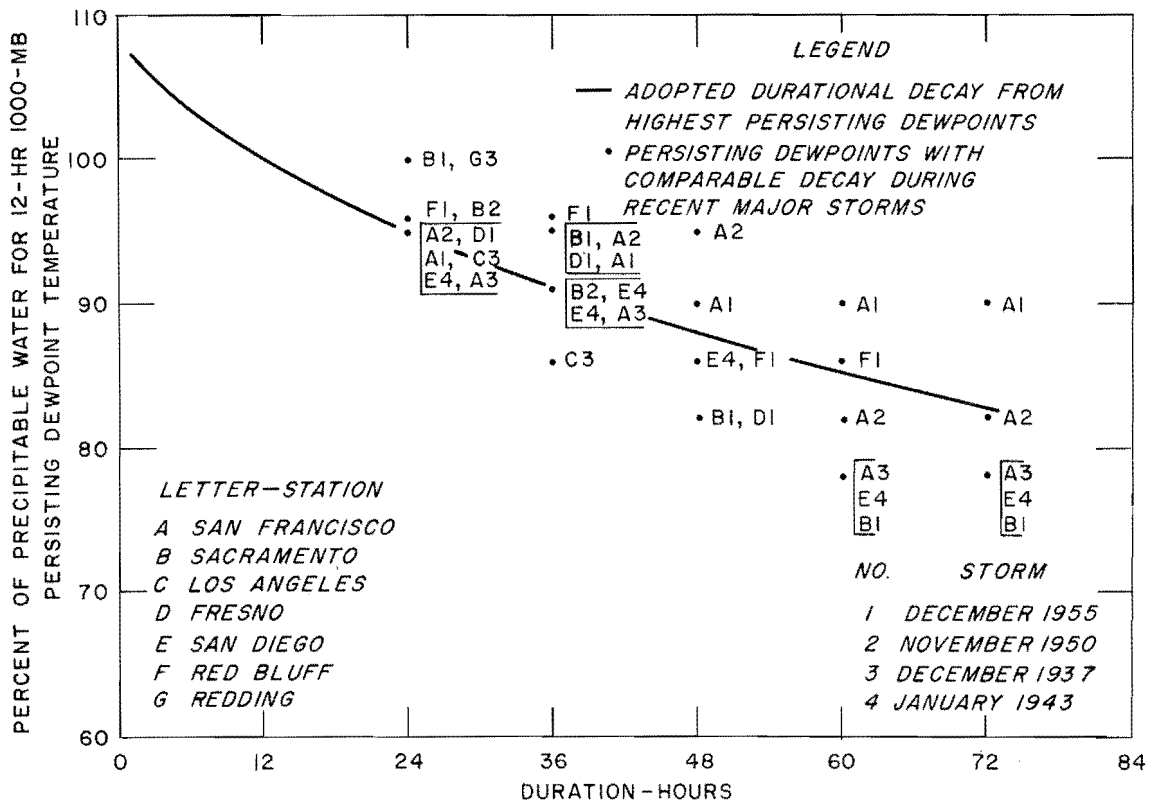
FIG. 4-4. COMPARISON OF OBSERVED AND ADOPTED MOISTURE DECAYS
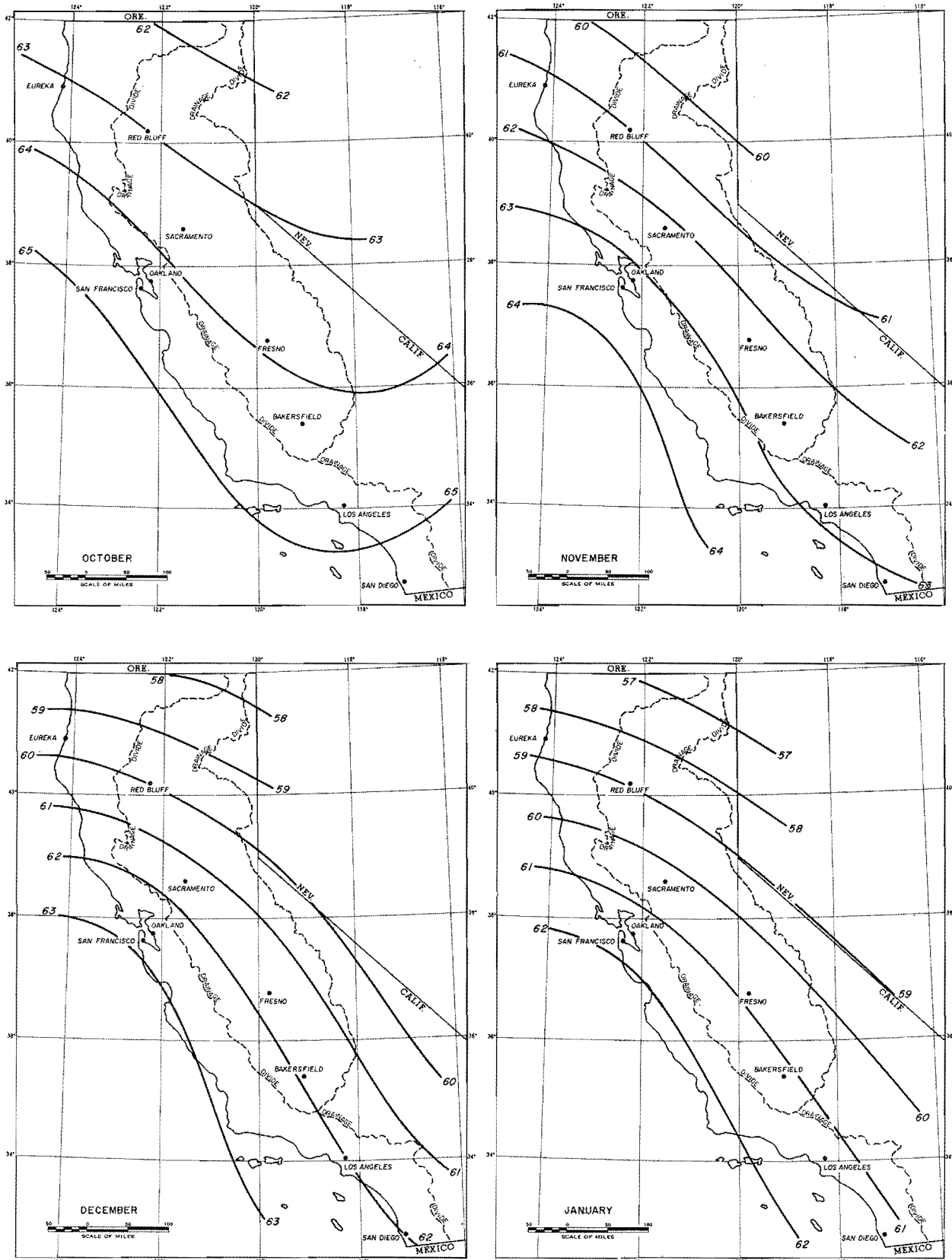
FIG. 4-5a. ENVELOPING 12-HOUR PERSISTING 1000-MB DEW POINT MAPS(°F)

146
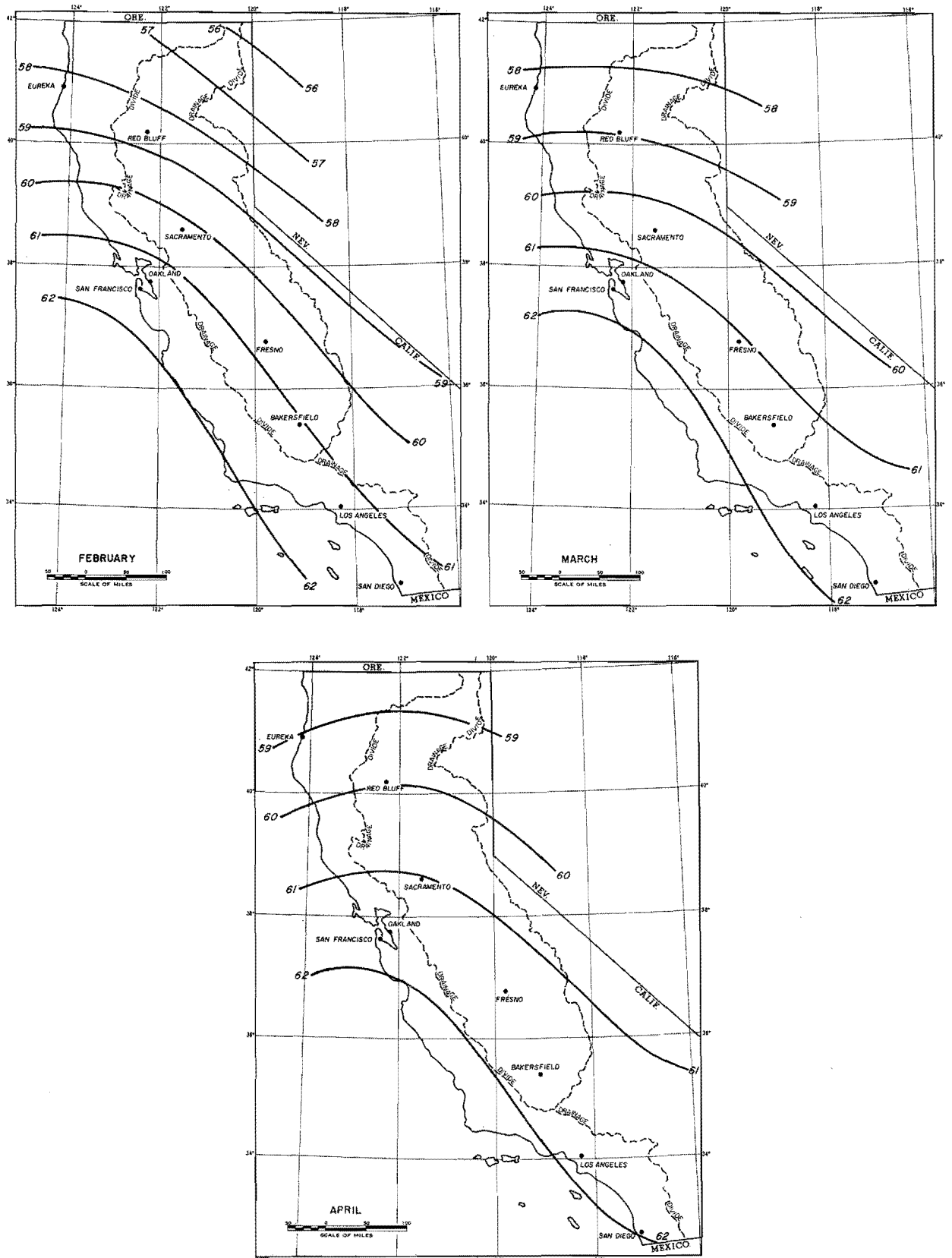
FIG. 4-5b. ENVELOPING 12-HOUR PERSISTING 1000-MB DEW POINT MAPS(°F)(CONT'D)
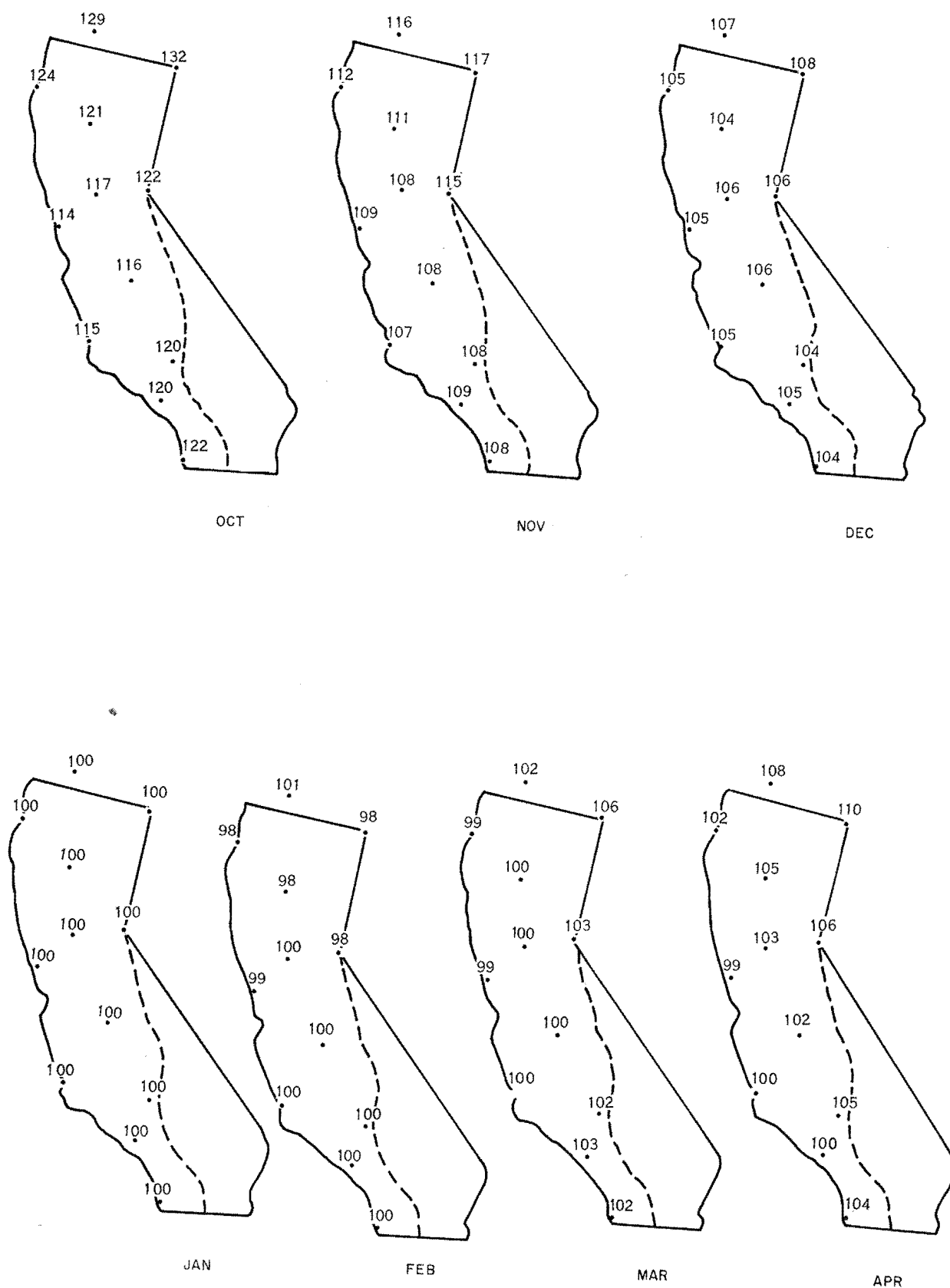
FIG. 4-6. ENVELOPING PRECIPITABLE WATER IN PERCENT OF JANUARY

Point No.	Duration (hrs)	P/M Ratio	Station	Date	Rain (in)	rTd (°F)	W_p (in)
1	1	1.6	Fresno	4/8/26	1.4	51	0.878
2	1	1.1	San Francisco	3/5/12	1.0	51	0.878
3	20	5.4	Orland	2/10-11/25	4.3[a]	49	0.795
4	22	6.2	Willows	2/11-12/25	4.9[a]	49	0.795
5	24	7.4	Colusa	1/2-3/16	5.6[b]	48	0.756
6	24	6.0	Gardena	1/25-26/56	6.5[c]	55	1.076
7	24	5.8	Marysville	1/2-3/16	4.4[a]	48	0.756
8	24	4.7	Lodi	12/11/06	4.1[a]	51	0.878
9	24	4.7	Corning	3/31/06	4.6[a]	53	0.972
10	24	4.6	Willows	12/29/33	3.8[a]	50	0.836
11	24	4.3	Davis	12/18-19/55	4.4	54	1.023
12	24	4.0	Davis	1/20-21/43	4.1	54	1.023
13	48	7.8	Colusa	1/2-3/16	5.9	48	0.756
14	48	7.6	Los Angeles	12/31/33-1/1/34	8.2[d]	55	1.076

a Maximum 24-hr amount estimated for non-recorder station by mass curves.
b Some doubtful aspects to time distribution.
c Reduced from total of 7.1 inches for possible orographic effect.
d Total rain amount may contain orographic effect.

FIG. 4-7.   MAXIMUM P/M RATIOS (WITH OROGRAPHIC STORM)
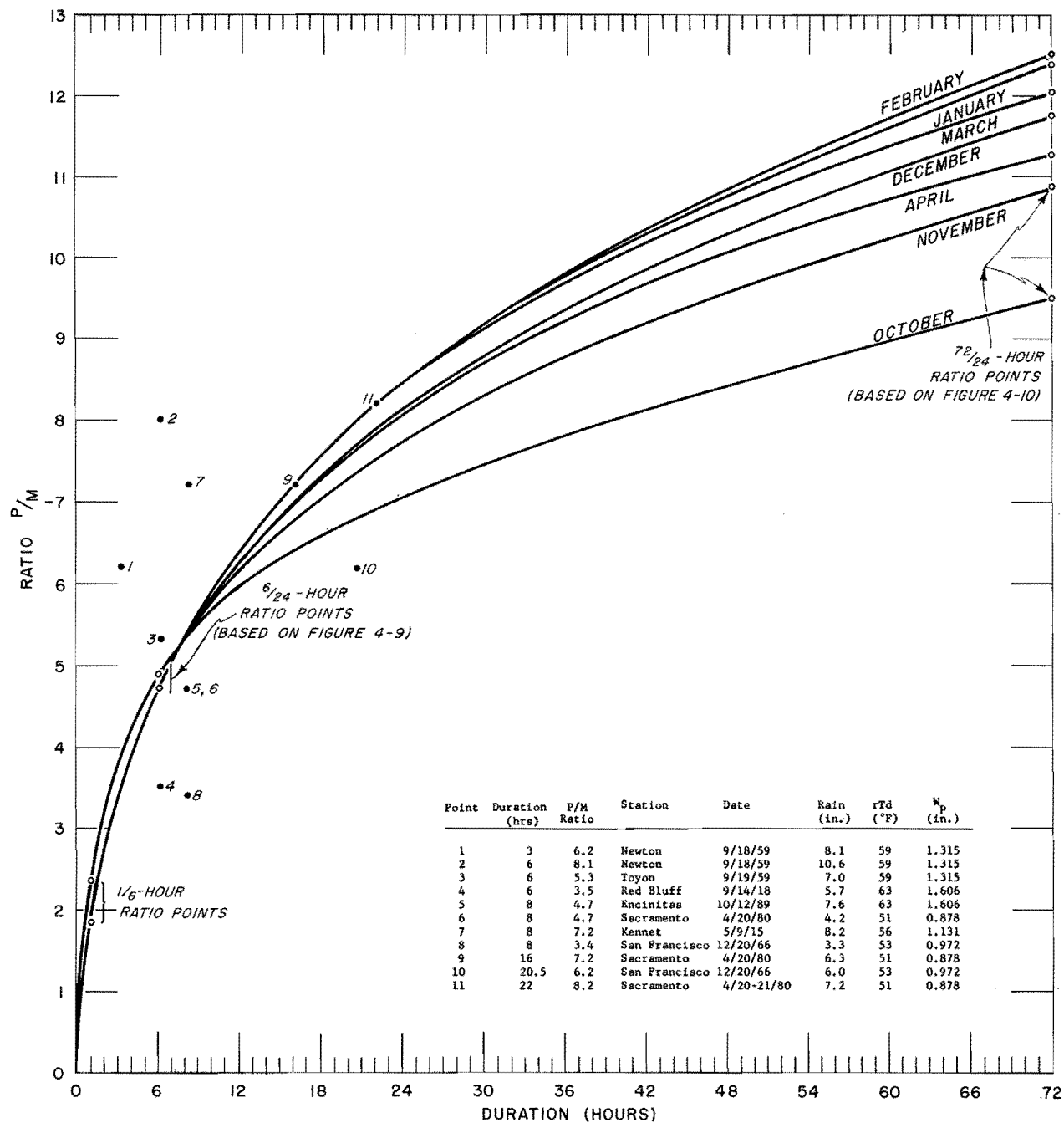
FIG. 4-8. MAXIMUM P/M RATIOS (CONVERGENCE-ONLY STORM)

Point	Duration (hrs)	P/M Ratio	Station	Date	Rain (in.)	rTd (°F)	W_p (in.)
1	3	6.2	Newton	9/18/59	8.1	59	1.315
2	6	8.1	Newton	9/18/59	10.6	59	1.315
3	6	5.3	Toyon	9/19/59	7.0	59	1.315
4	6	3.5	Red Bluff	9/14/18	5.7	63	1.606
5	8	4.7	Encinitas	10/12/89	7.6	63	1.606
6	8	4.7	Sacramento	4/20/80	4.2	51	0.878
7	8	7.2	Kennet	5/9/15	8.2	56	1.131
8	8	3.4	San Francisco	12/20/66	3.3	53	0.972
9	16	7.2	Sacramento	4/20/80	6.3	51	0.878
10	20.5	6.2	San Francisco	12/20/66	6.0	53	0.972
11	22	8.2	Sacramento	4/20-21/80	7.2	51	0.878

FIG. 4-9.   RATIO OF 6- TO 24-HOUR PRECIPITATION.
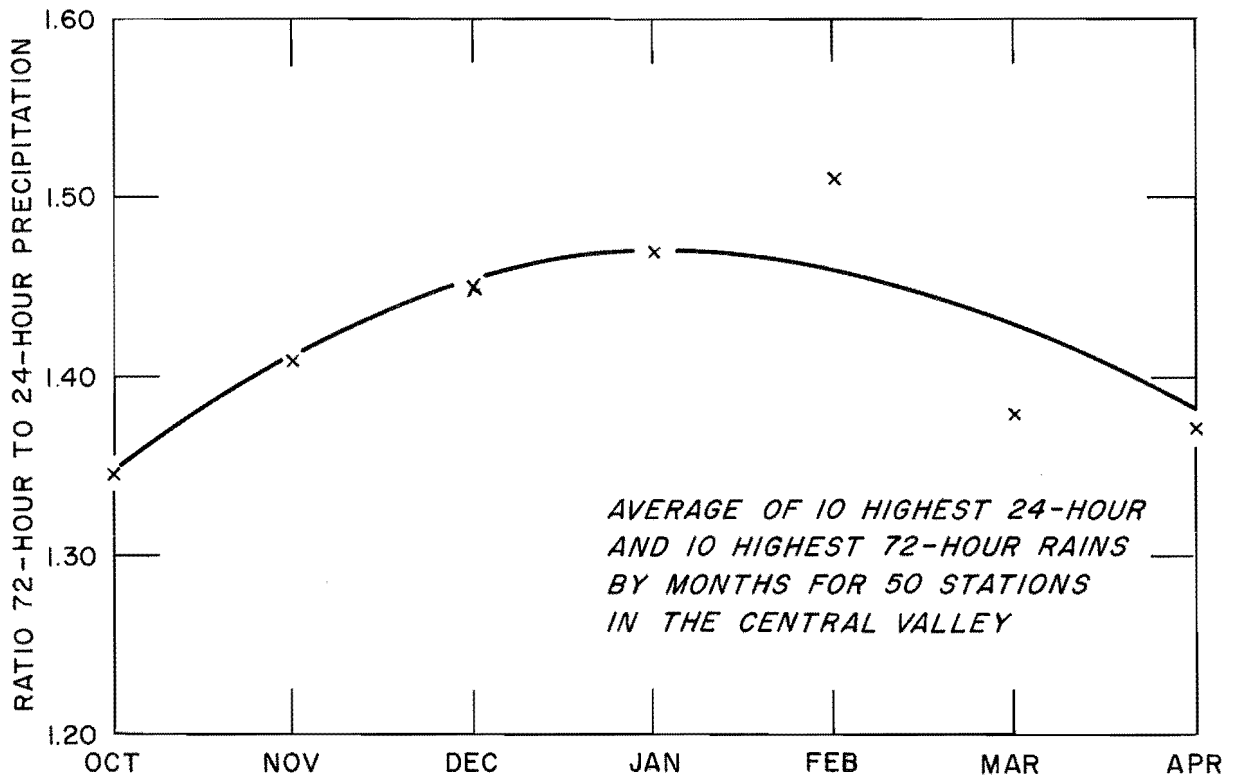
FIG. 4-10.   RATIO OF 72- TO 24-HOUR PRECIPITATION
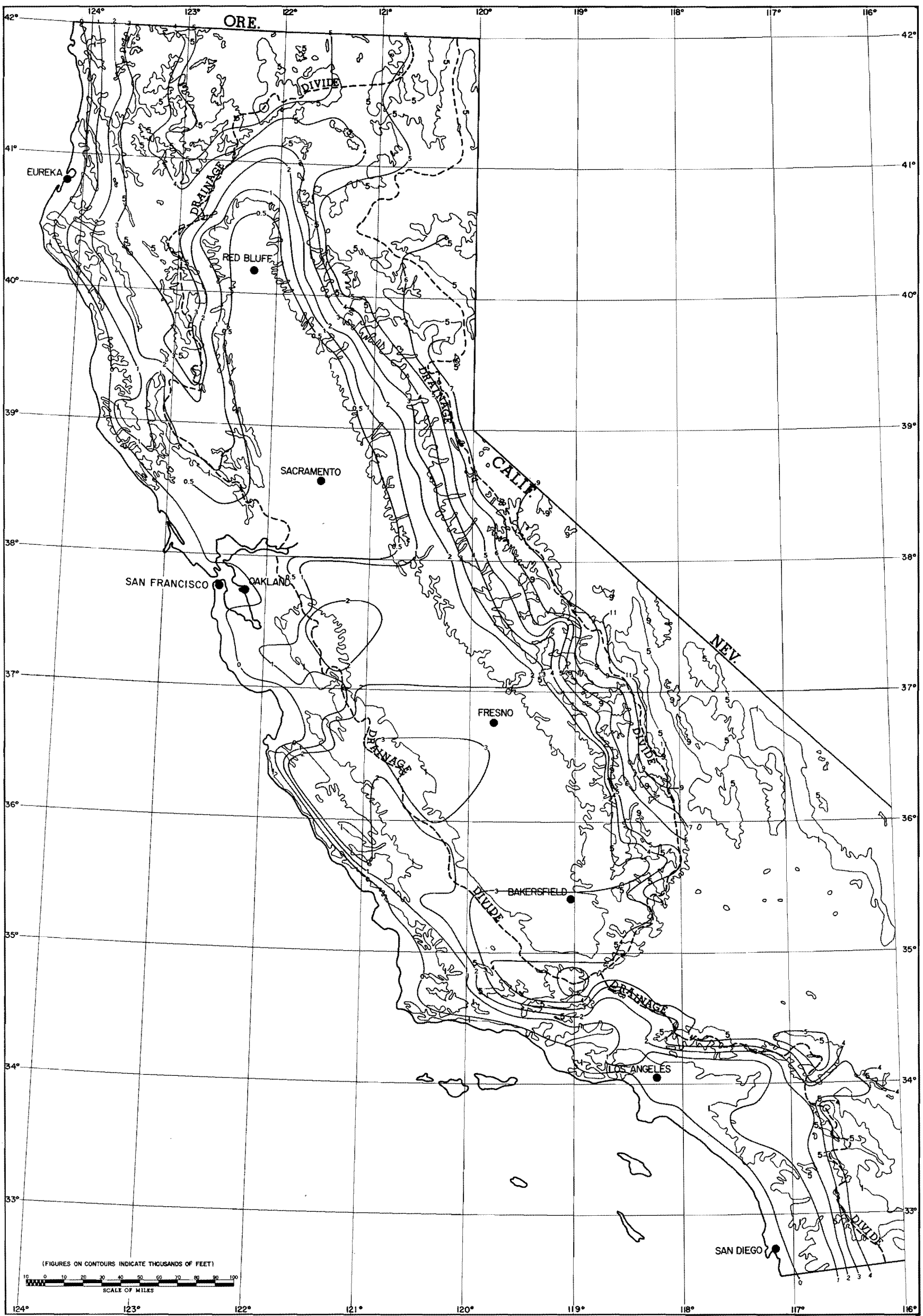
FIG. 4-11. EFFECTIVE ELEVATION AND BARRIER HEIGHTS
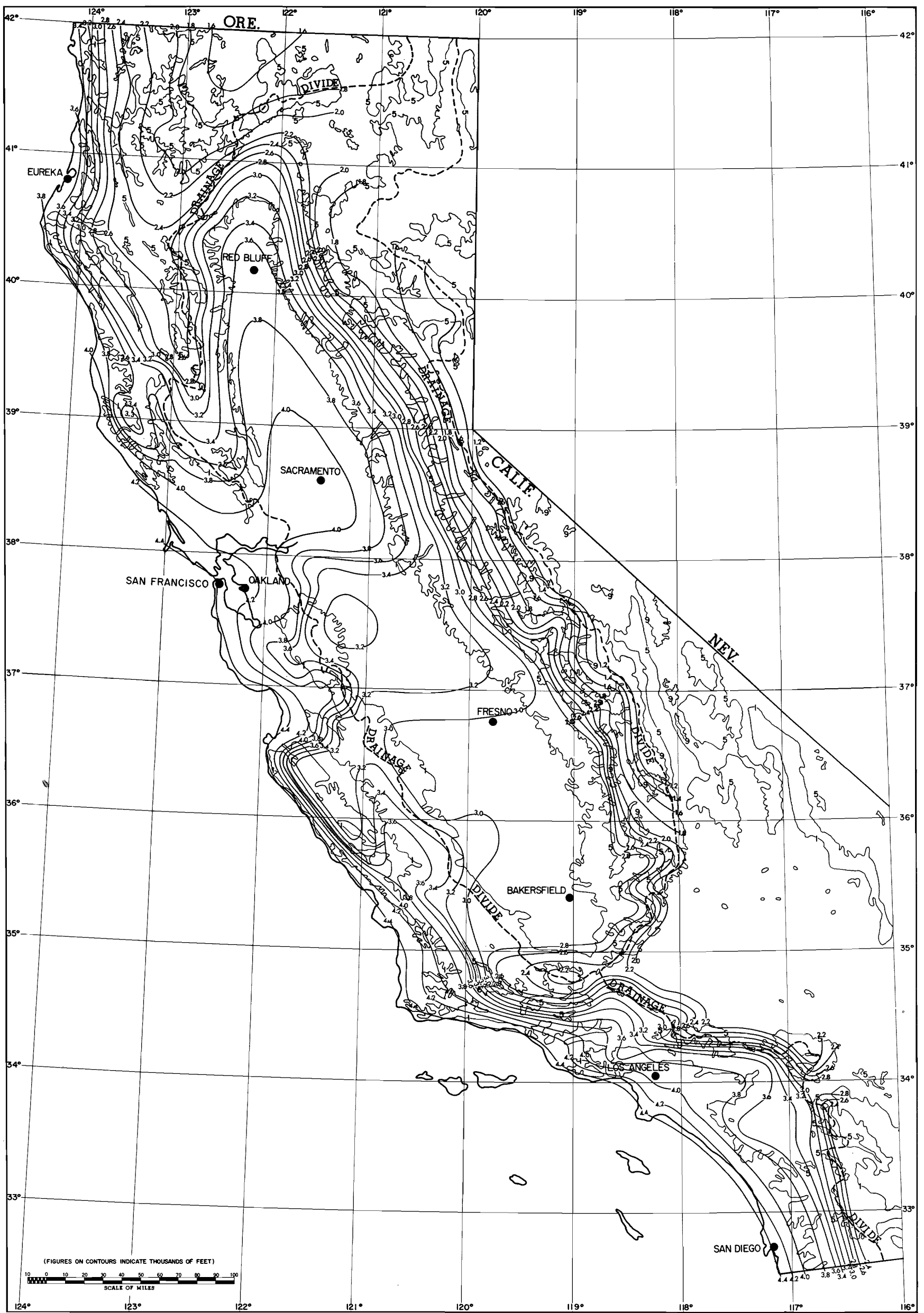
FIG. 4-12. CONVERGENCE PMP INDEX. 6-HR 200-SQ MI
JANUARY (inches)

OCTOBER

PERCENTS FOR OTHER 6-HOUR PERIODS

6-HR. PERIOD	5	6	7	8	9	10	11	12
PERCENT	14	12	11	10	9	9	8	8

NOVEMBER

PERCENTS FOR OTHER 6-HOUR PERIODS

6-HR. PERIOD	5	6	7	8	9	10	11	12
PERCENT	16	14	13	11	10	10	10	10
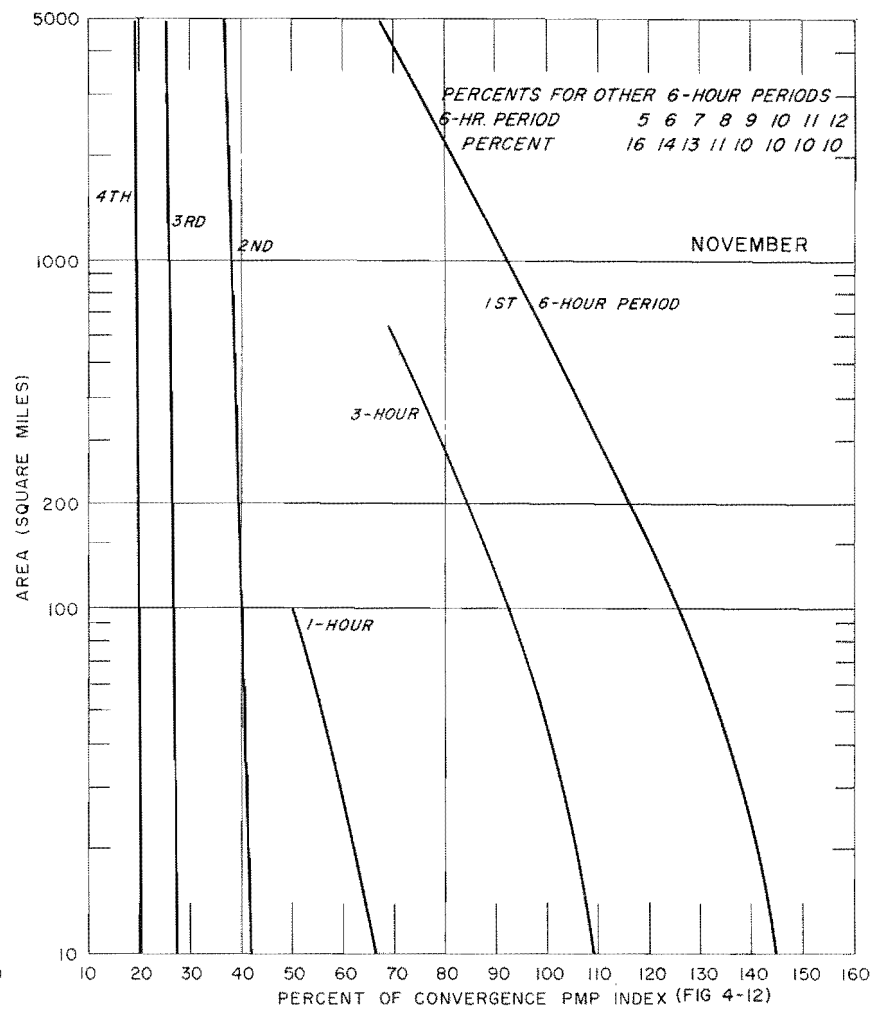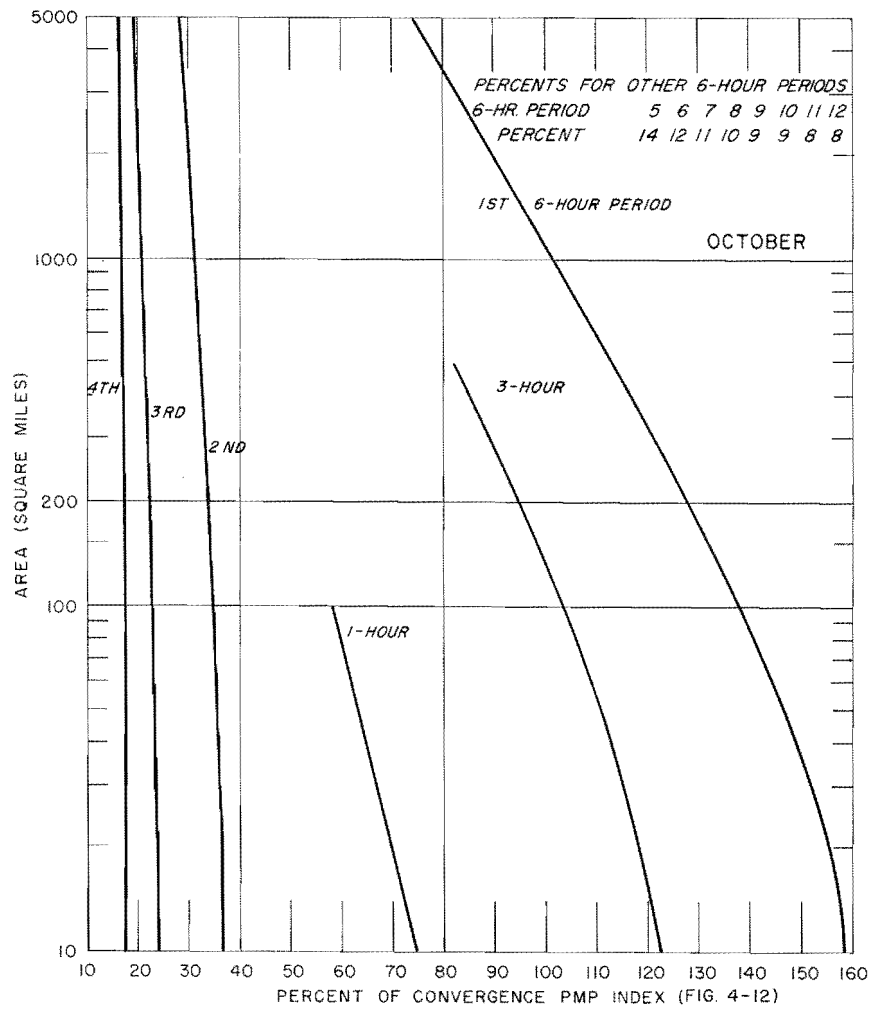
FIG. 4-13a. VARIATION OF CONVERGENCE PMP WITH BASIN SIZE AND DURATION

151
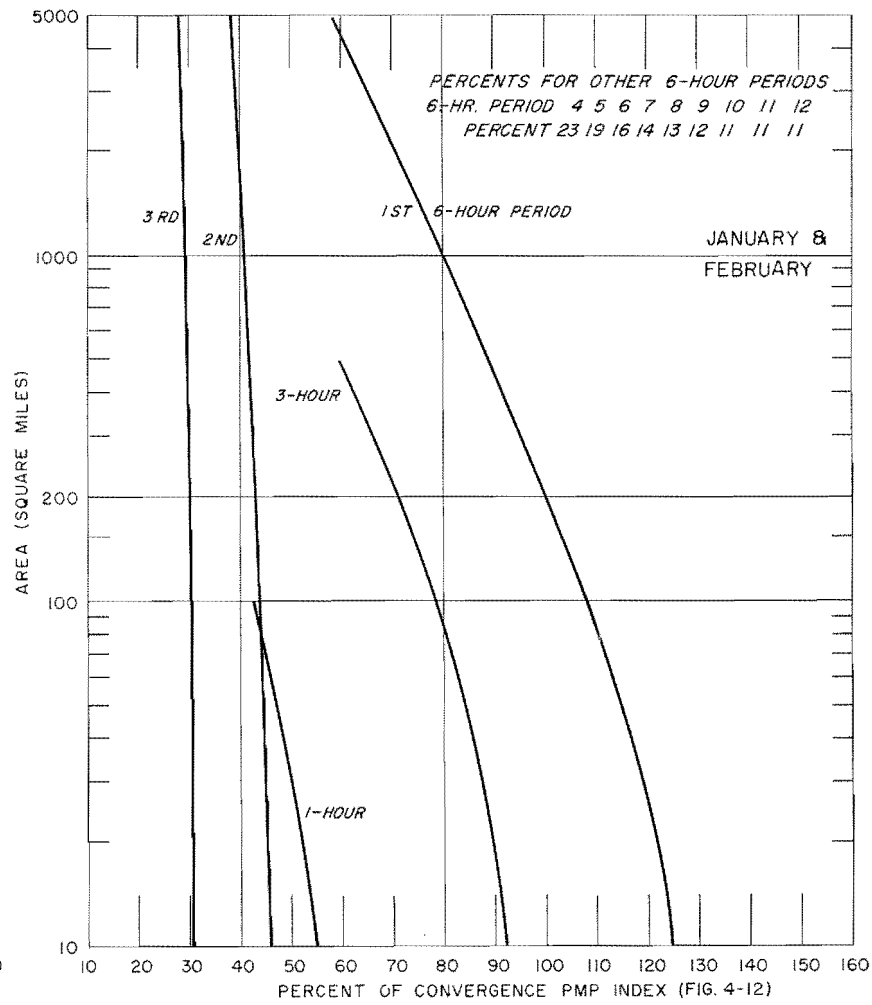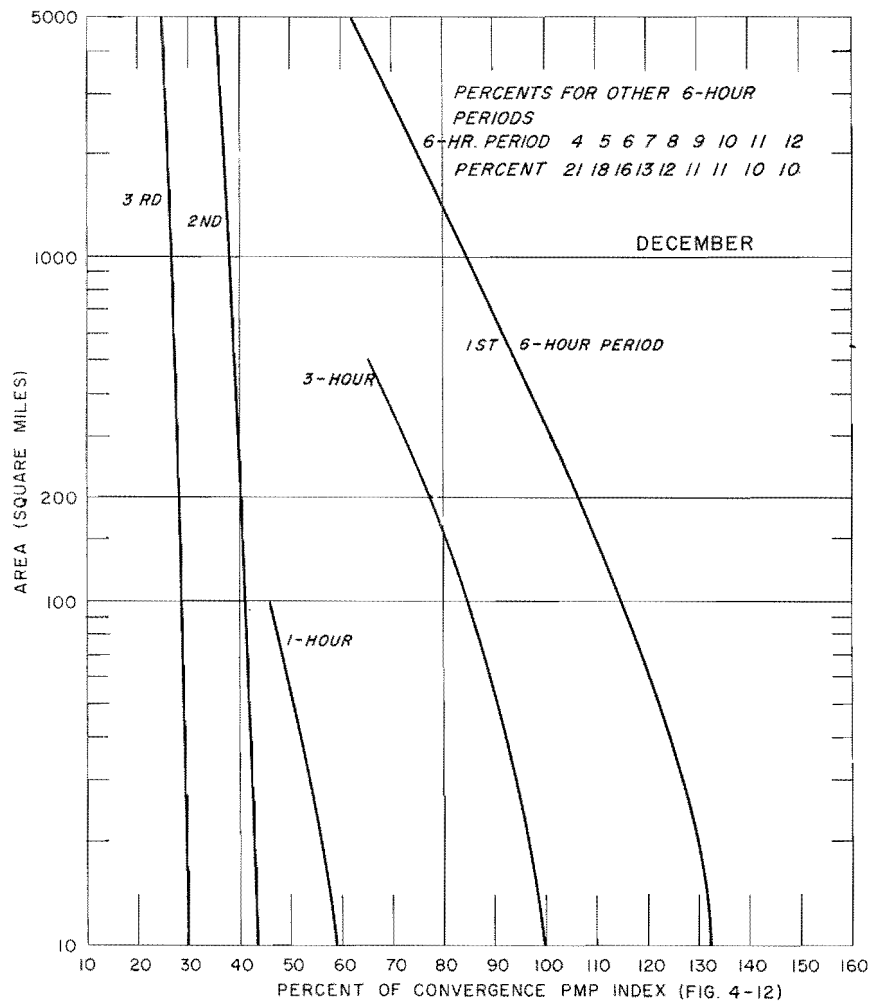
FIG. 4-13b. VARIATION OF CONVERGENCE PMP WITH BASIN SIZE AND DURATION (Cont'd)
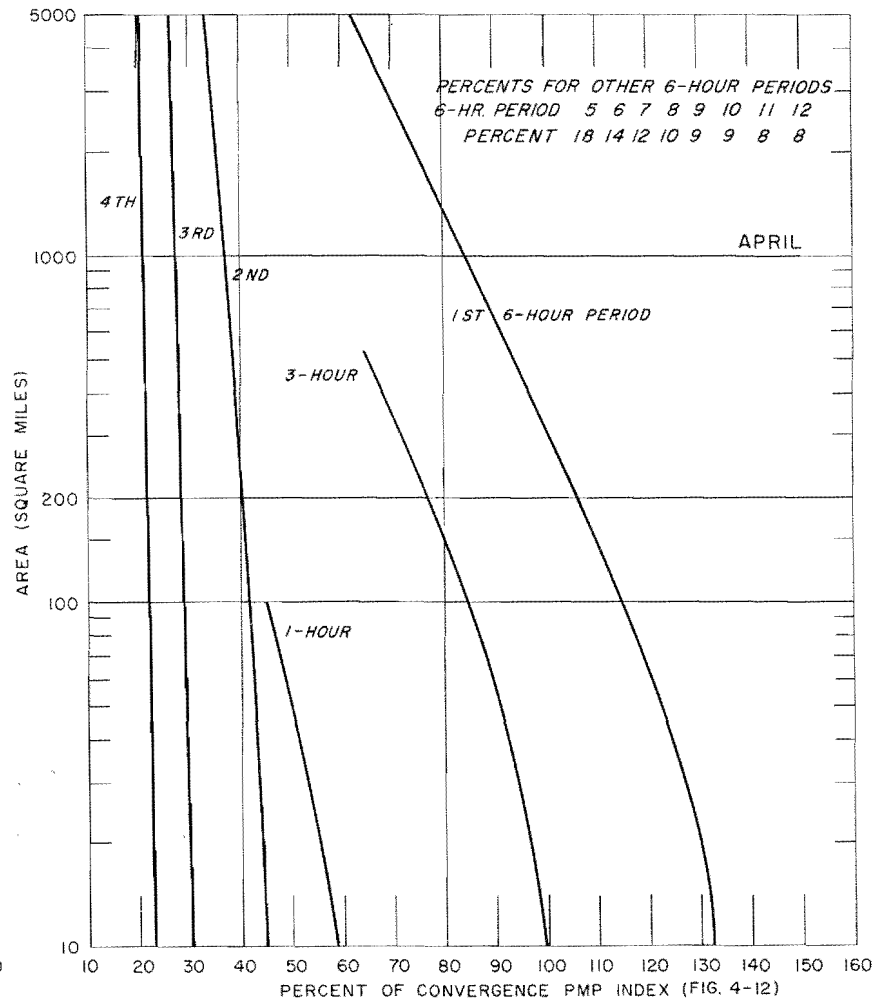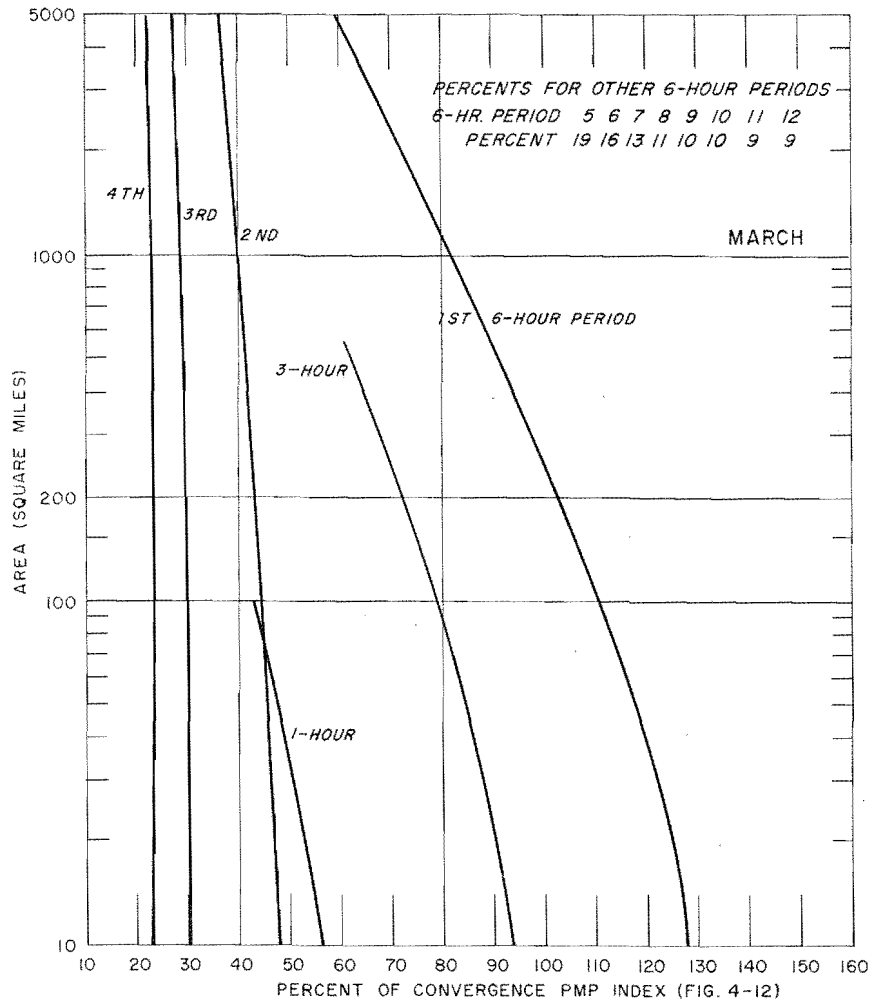
FIG. 4-13c.   VARIATION OF CONVERGENCE PMP WITH BASIN SIZE AND DURATION (Cont'd)
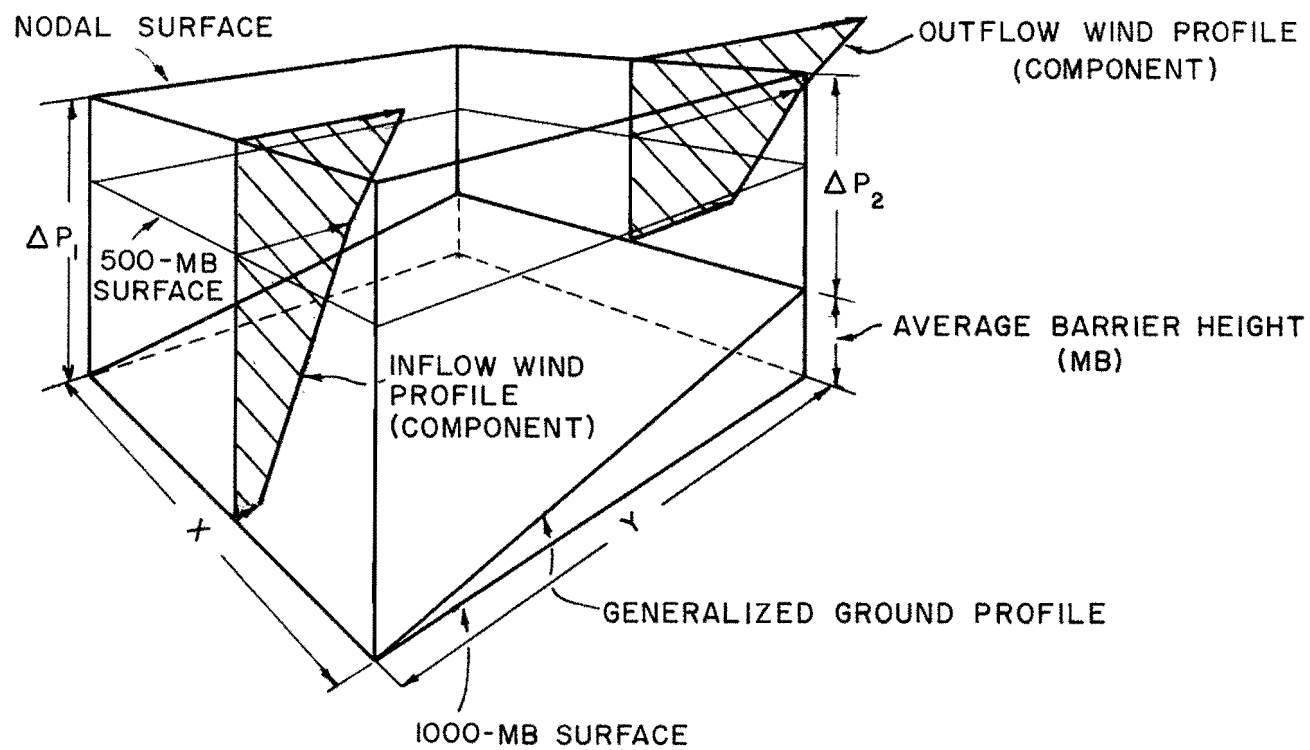
FIG. 5-1. SCHEMATIC INFLOW AND OUTFLOW WIND PROFILES OVER MOUNTAIN BARRIER
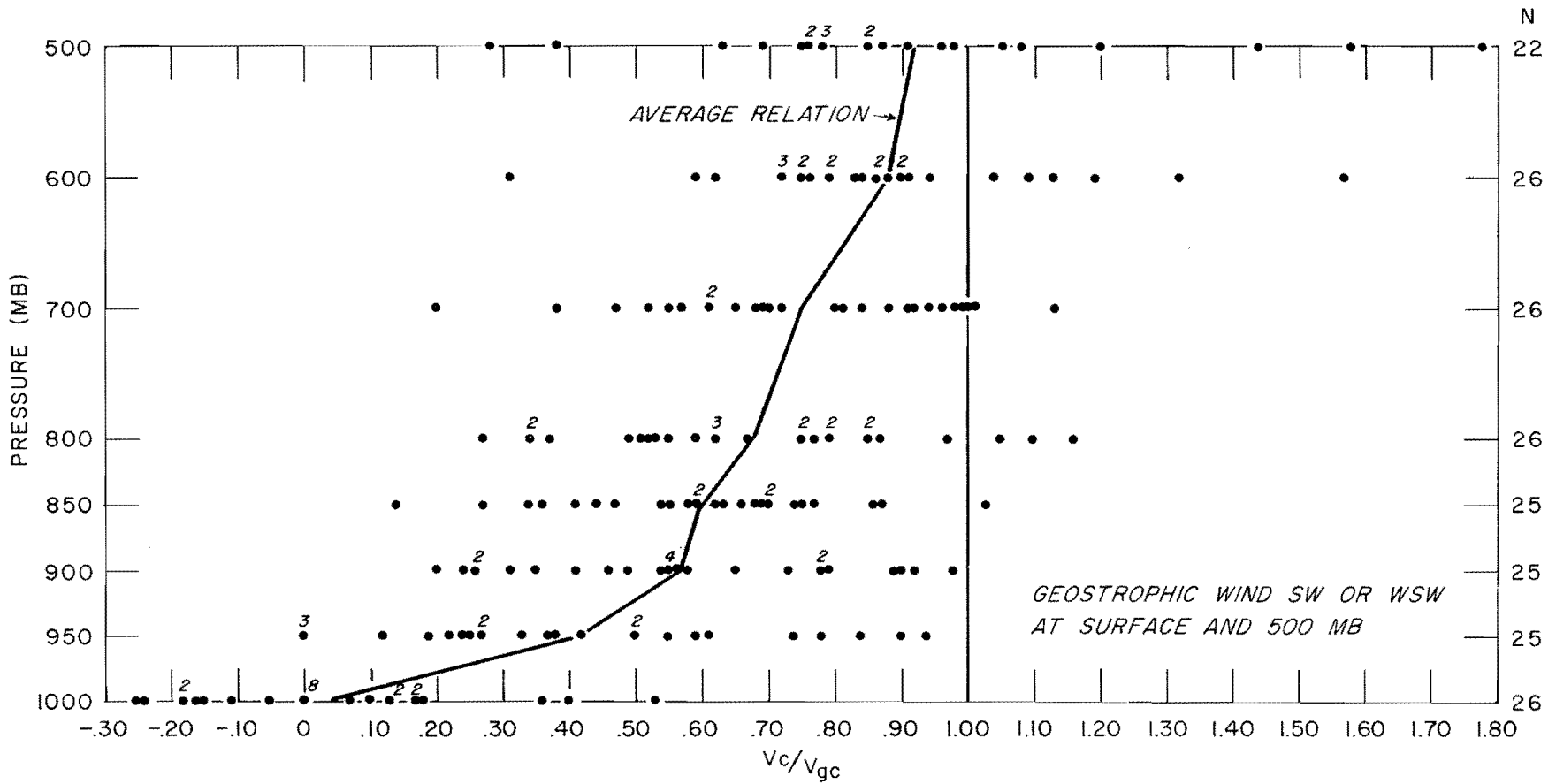
FIG. 5-2. AVERAGE RATIO OF OBSERVED, V_c, TO GEOSTROPHIC WIND COMPONENT, V_{gc}, OAKLAND, CALIFORNIA

156
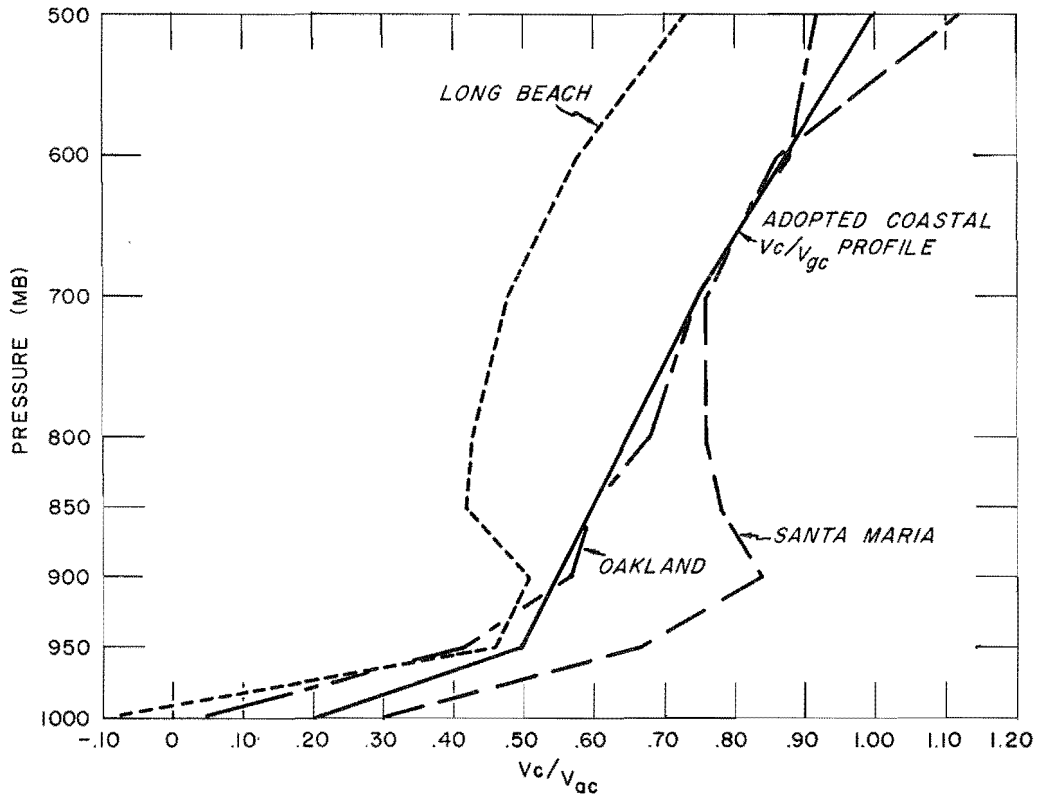
FIG. 5-3. COASTAL V_c/V_{gc} PROFILES
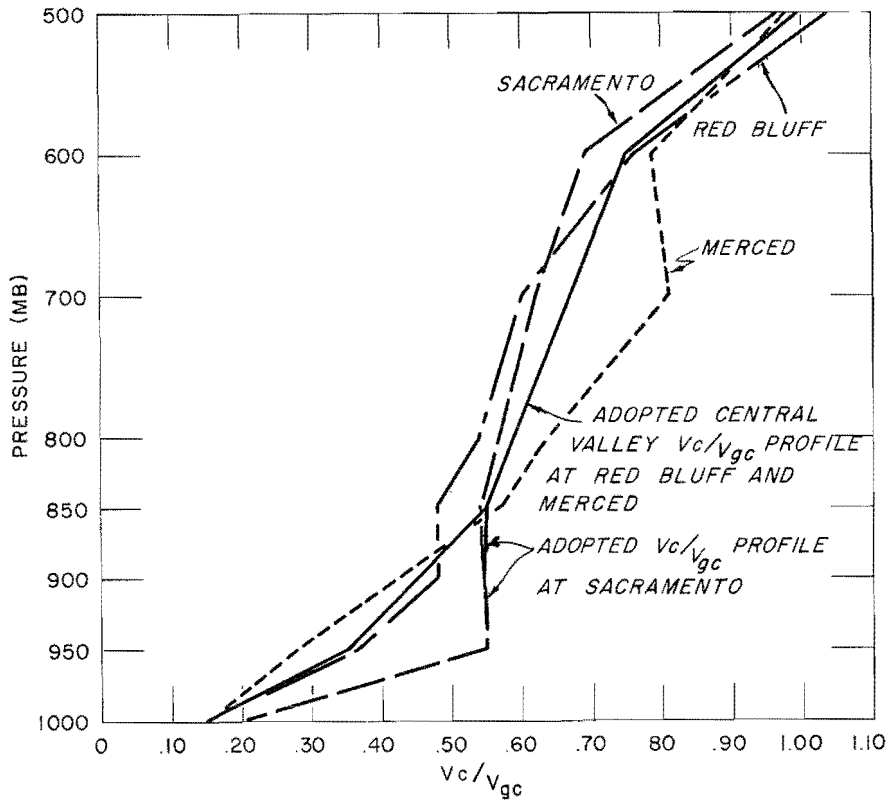
FIG. 5-4. CENTRAL VALLEY V_c/V_{gc} PROFILES
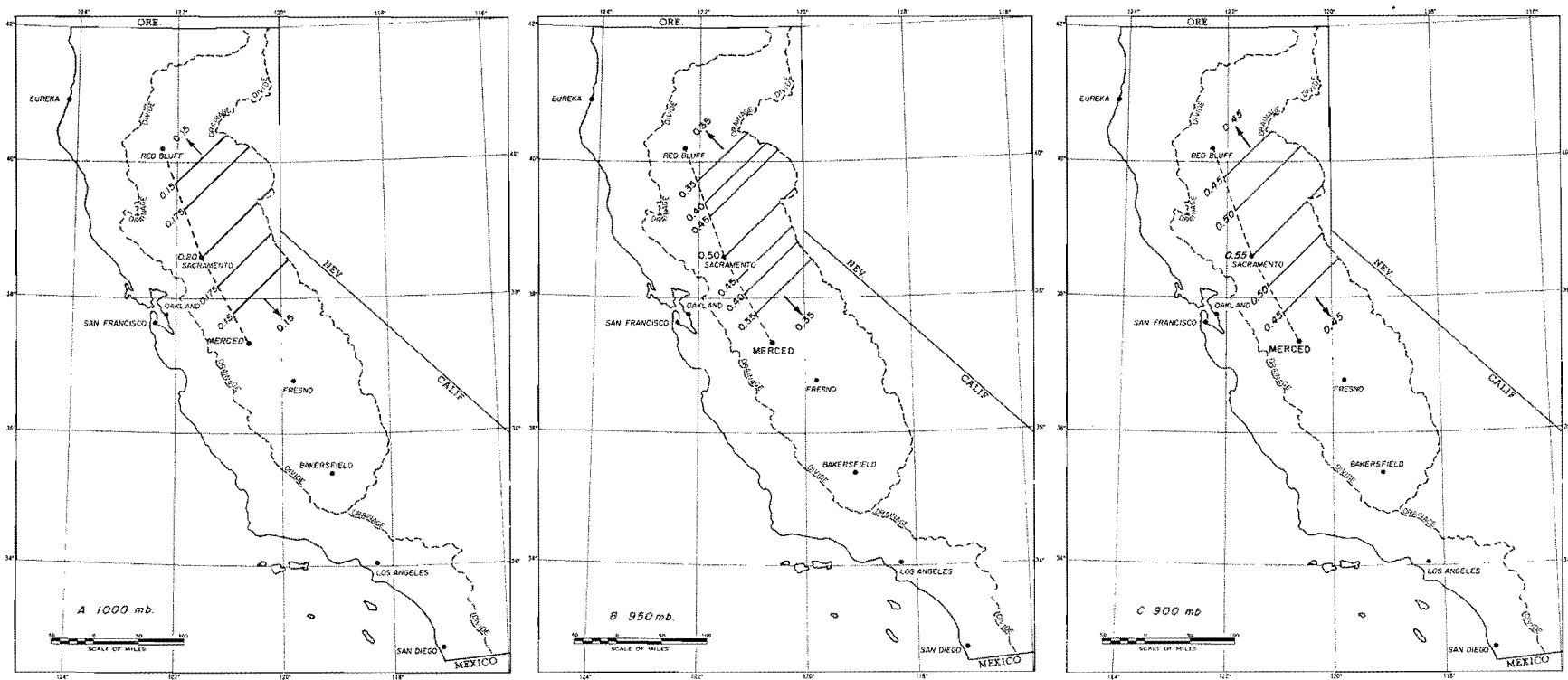
FIG. 5-5. CENTRAL VALLEY AREAL VARIATION OF V_c/V_{gc}, (A) 1000 MB, (B) 950 MB, (C) 900 MB

158
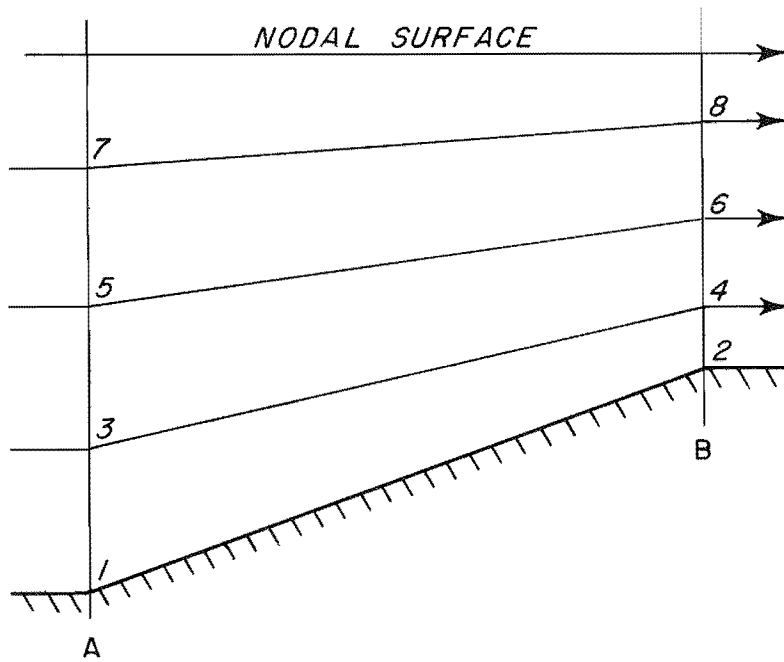
FIG. 5-6. SCHEMATIC AIR STREAMLINES IN OROGRAPHIC STORM
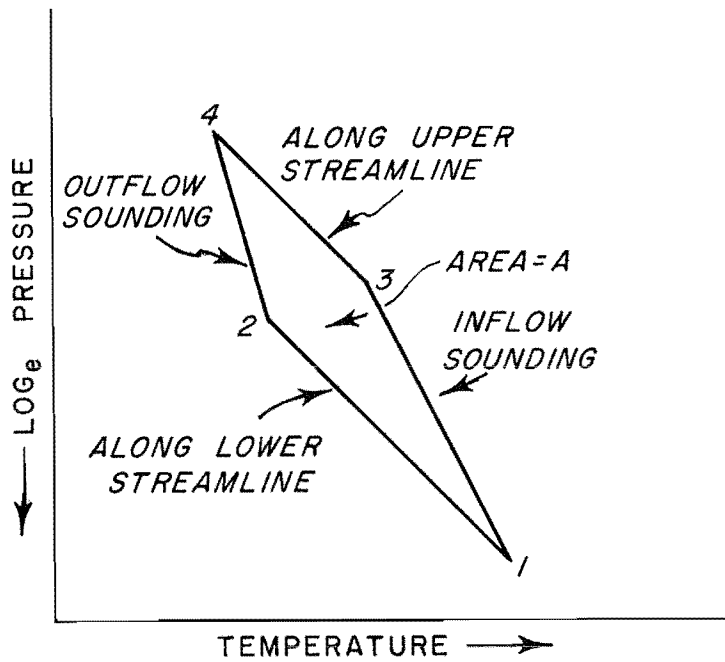
FIG. 5-7. SCHEMATIC PLOT OF TEMPERATURES AND PRESSURES
IN OROGRAPHIC STORM ON THERMODYNAMIC DIAGRAM
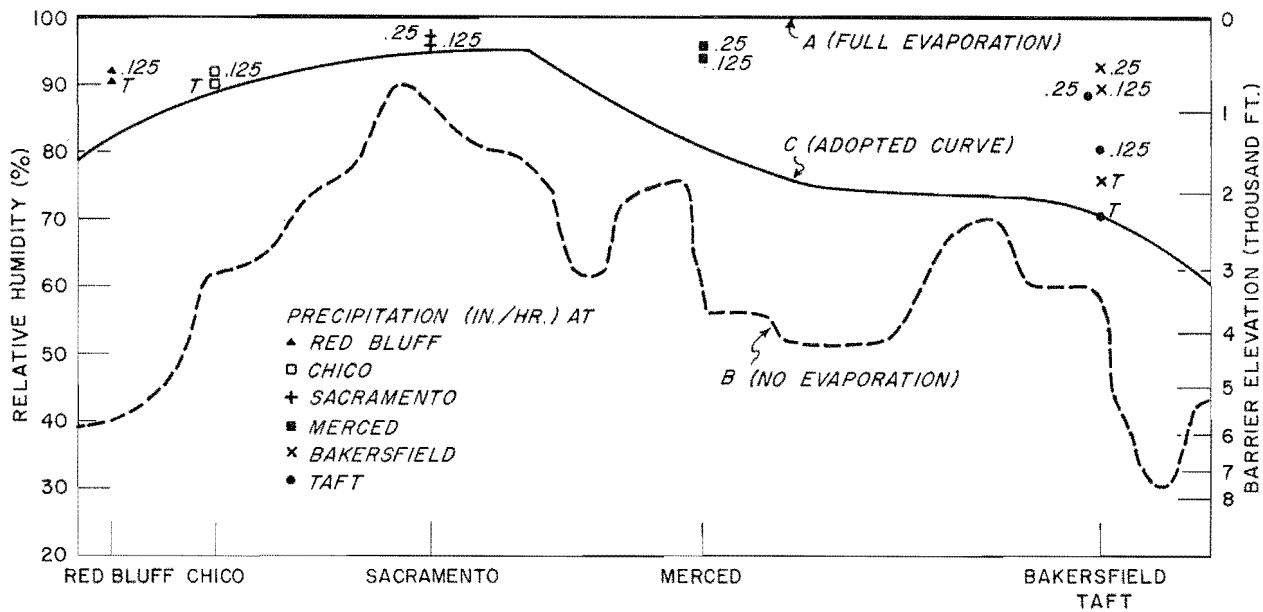
FIG. 5-8. CENTRAL VALLEY DEGREE-OF-SATURATION FOR PMP CONDITIONS
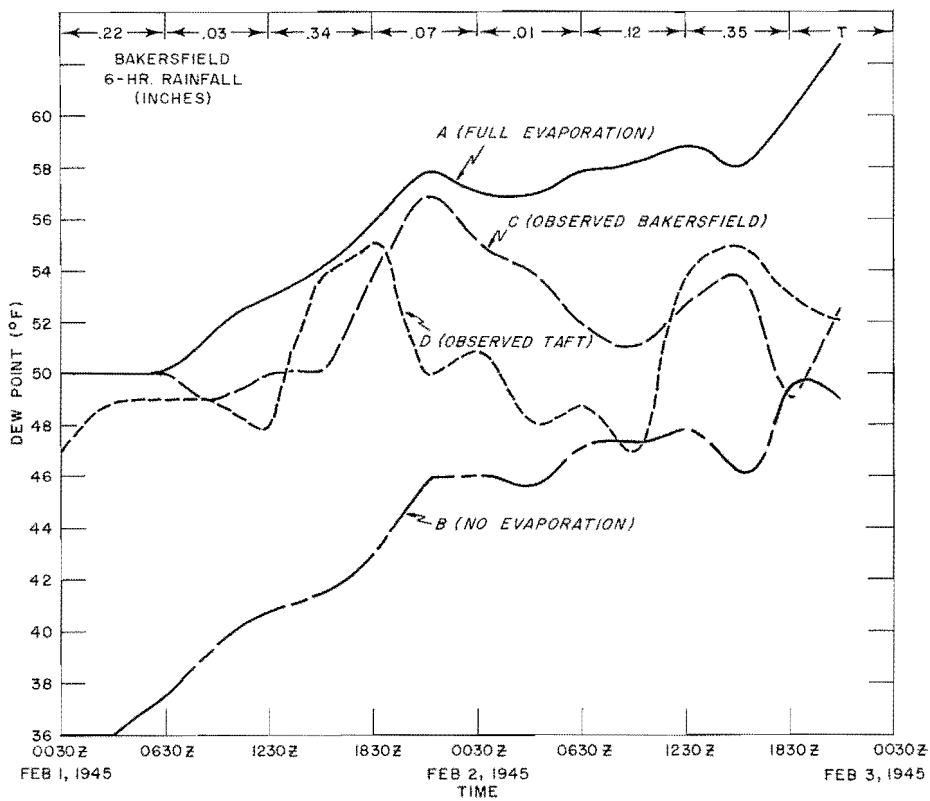
FIG. 5-9. SAN JOAQUIN VALLEY DEW-POINT VARIATIONS
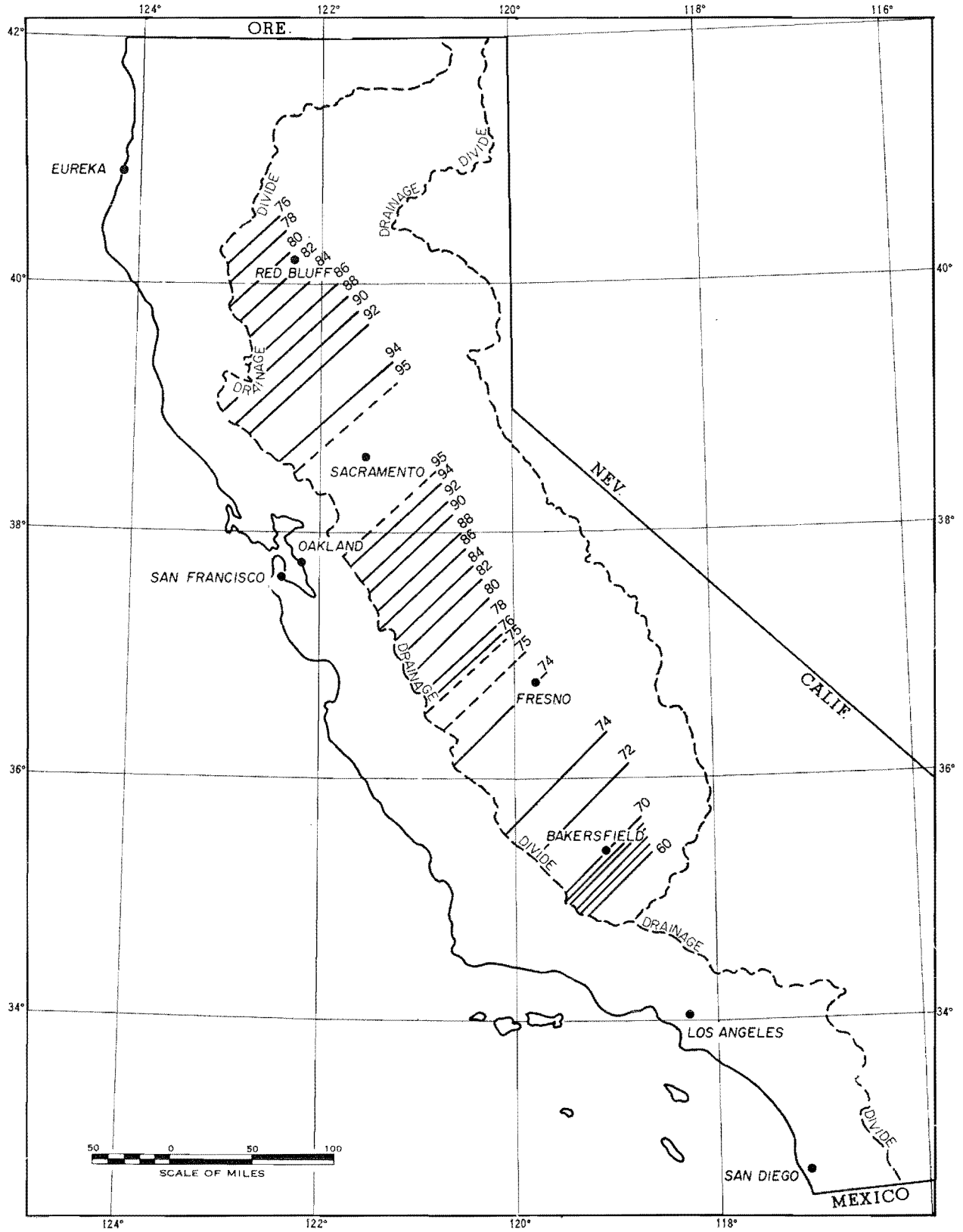
FIG. 5-10. CENTRAL VALLEY SURFACE-RELATIVE-HUMIDITY FOR PMP CONDITIONS
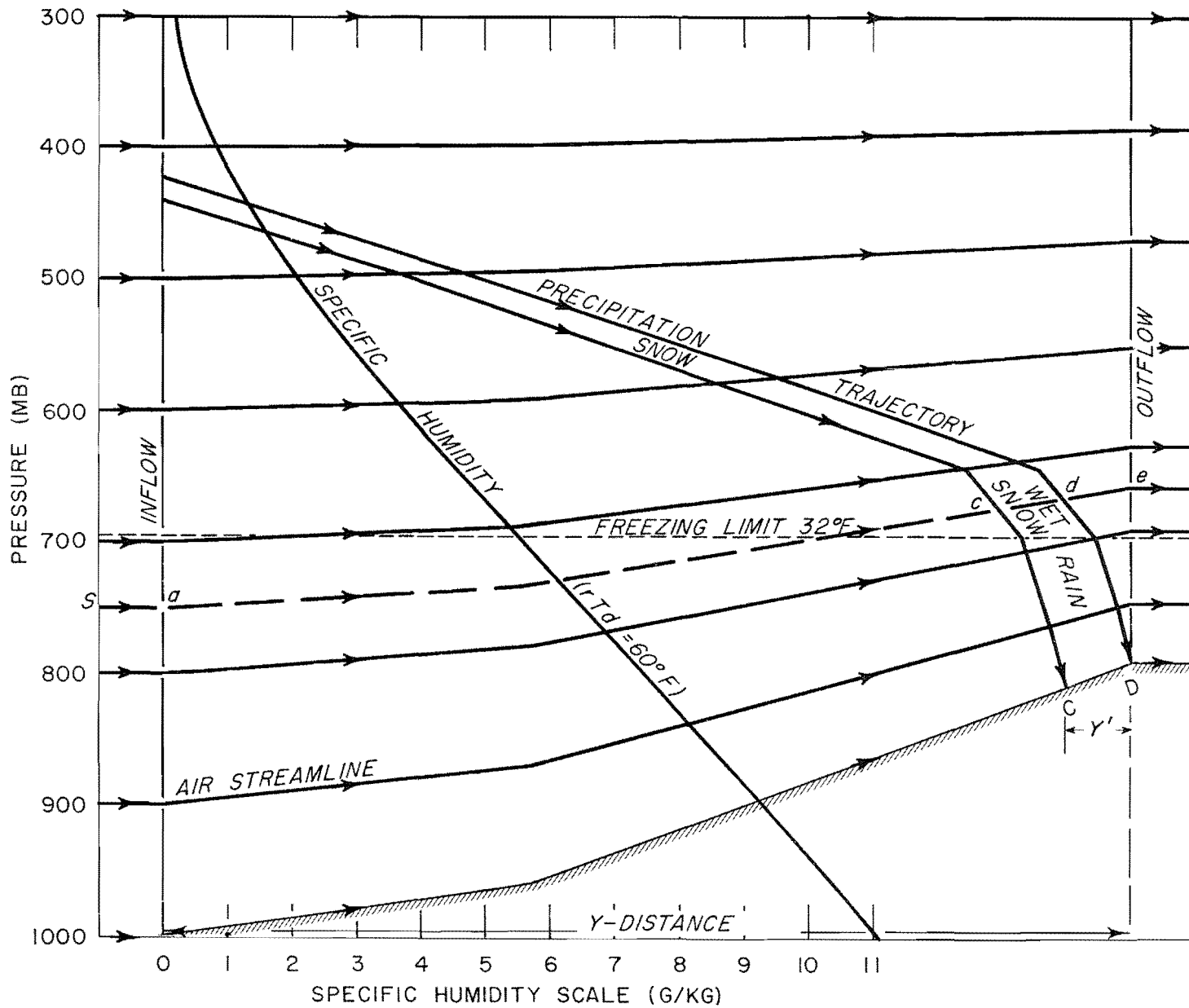
FIG. 5-11.   SCHEMATIC DIAGRAM OF OROGRAPHIC MODEL
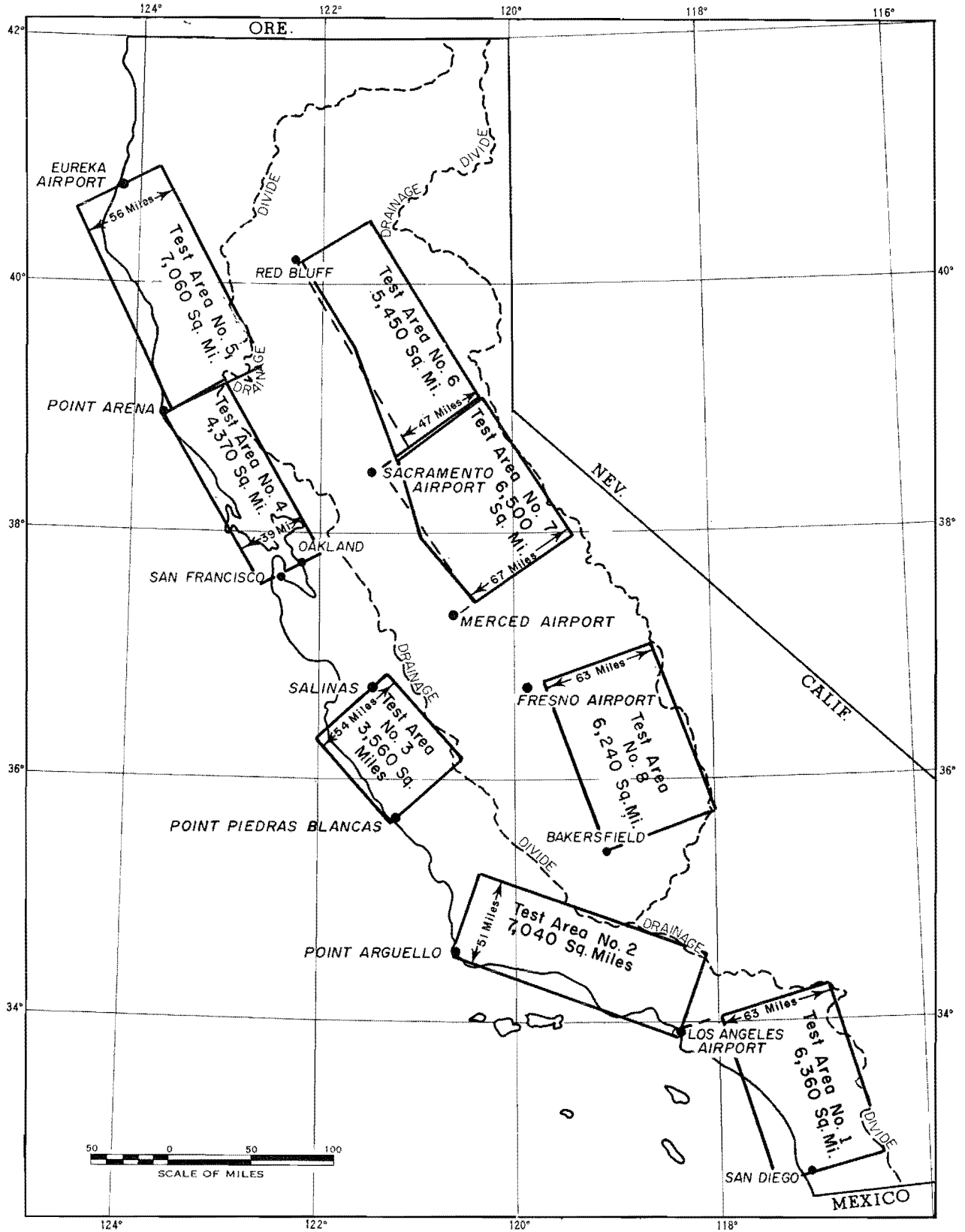
FIG. 5-12. STORM CALIBRATION AREAS
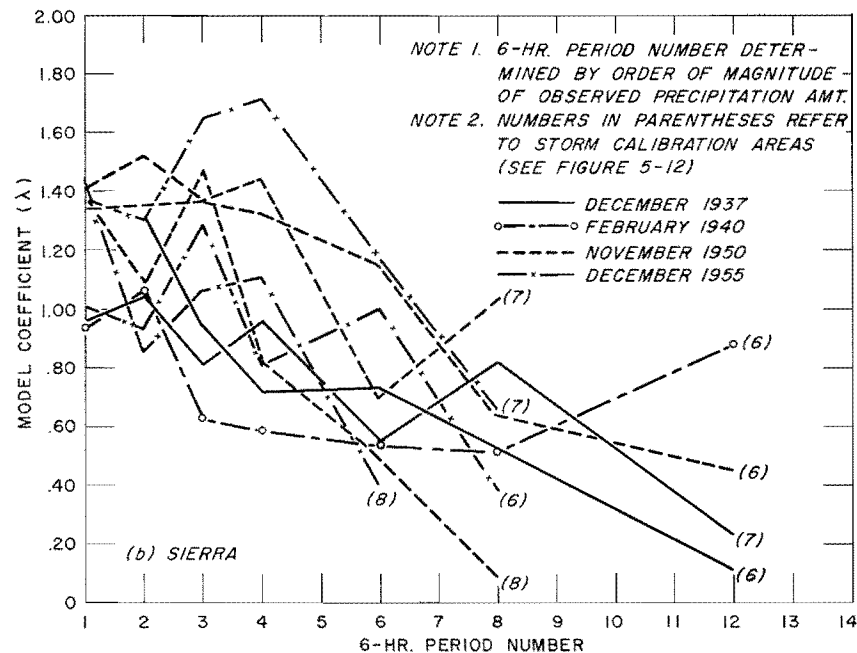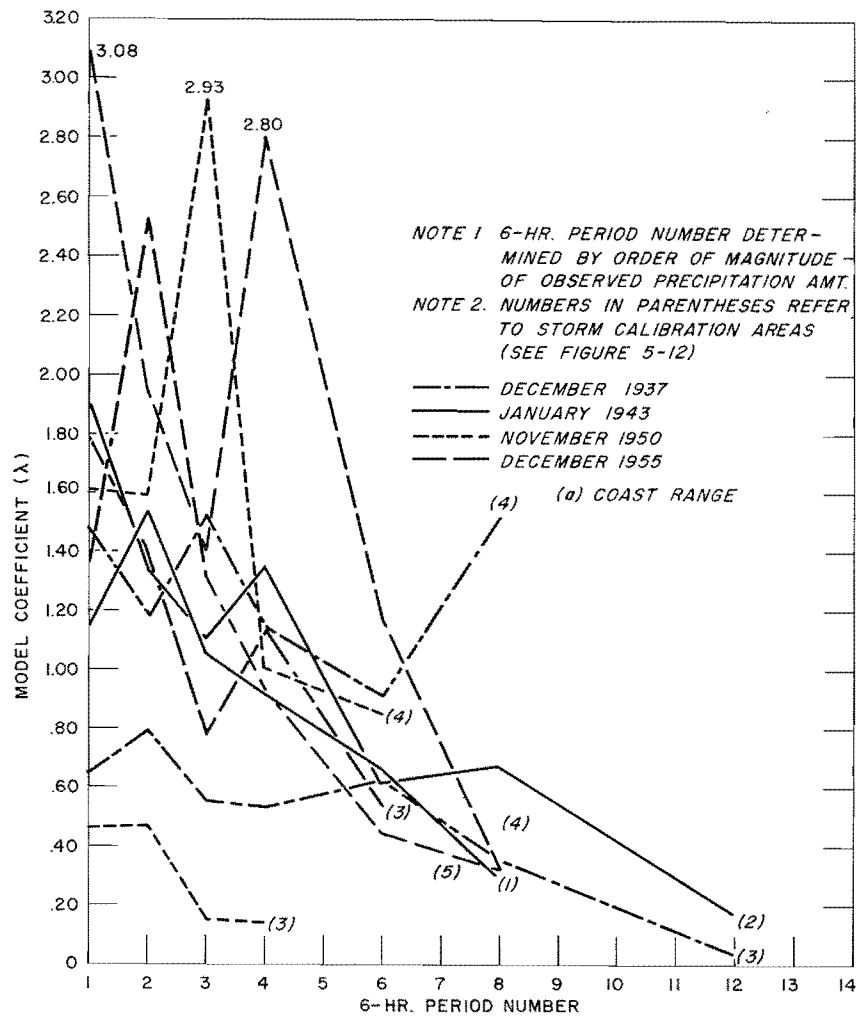
FIG. 5-13. MODEL COEFFICIENT, λ, (a) COASTAL RANGE, (b) SIERRAS
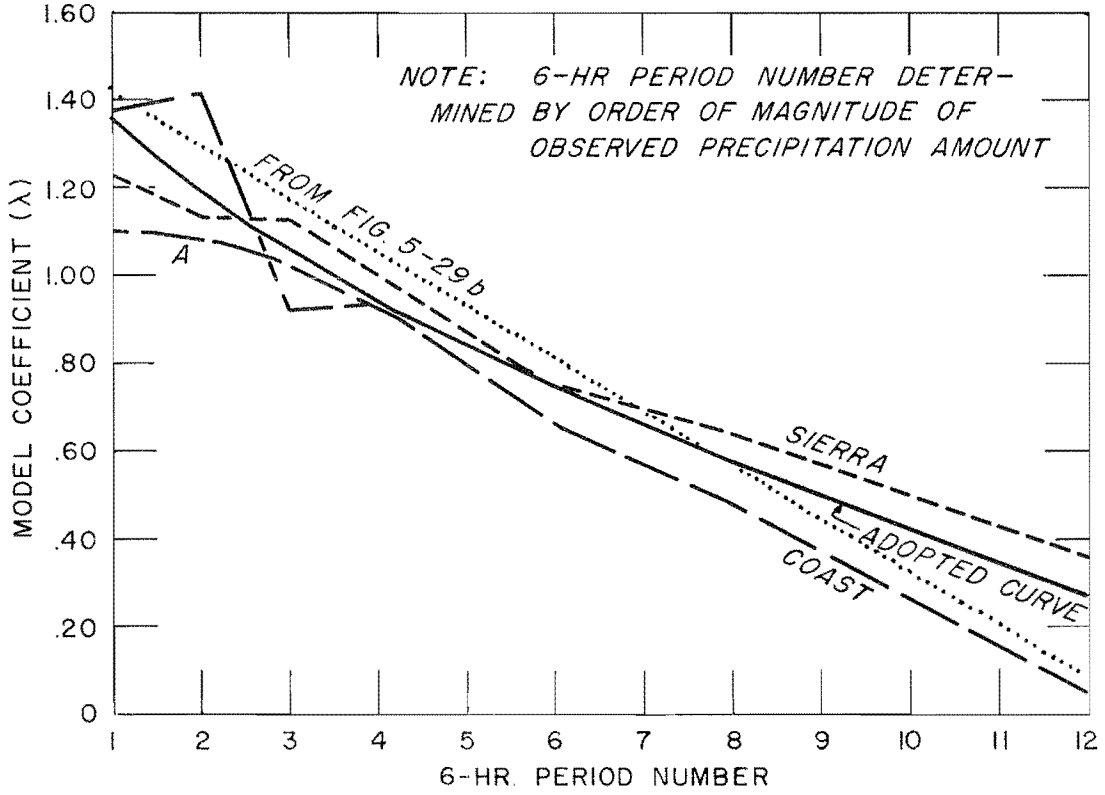
FIG. 5-14. AVERAGE MODEL COEFFICIENT, λ
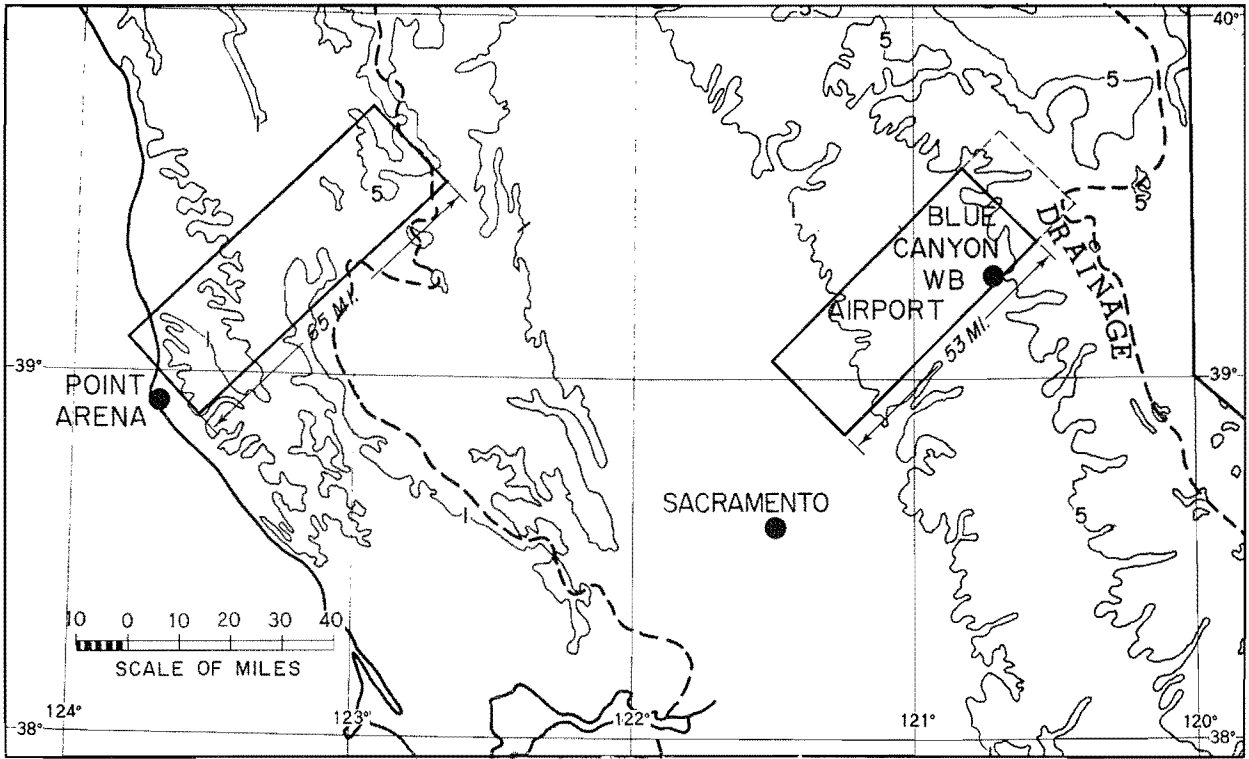
FIG. 5-15. PRECIPITATION-DISTRIBUTION TEST AREAS
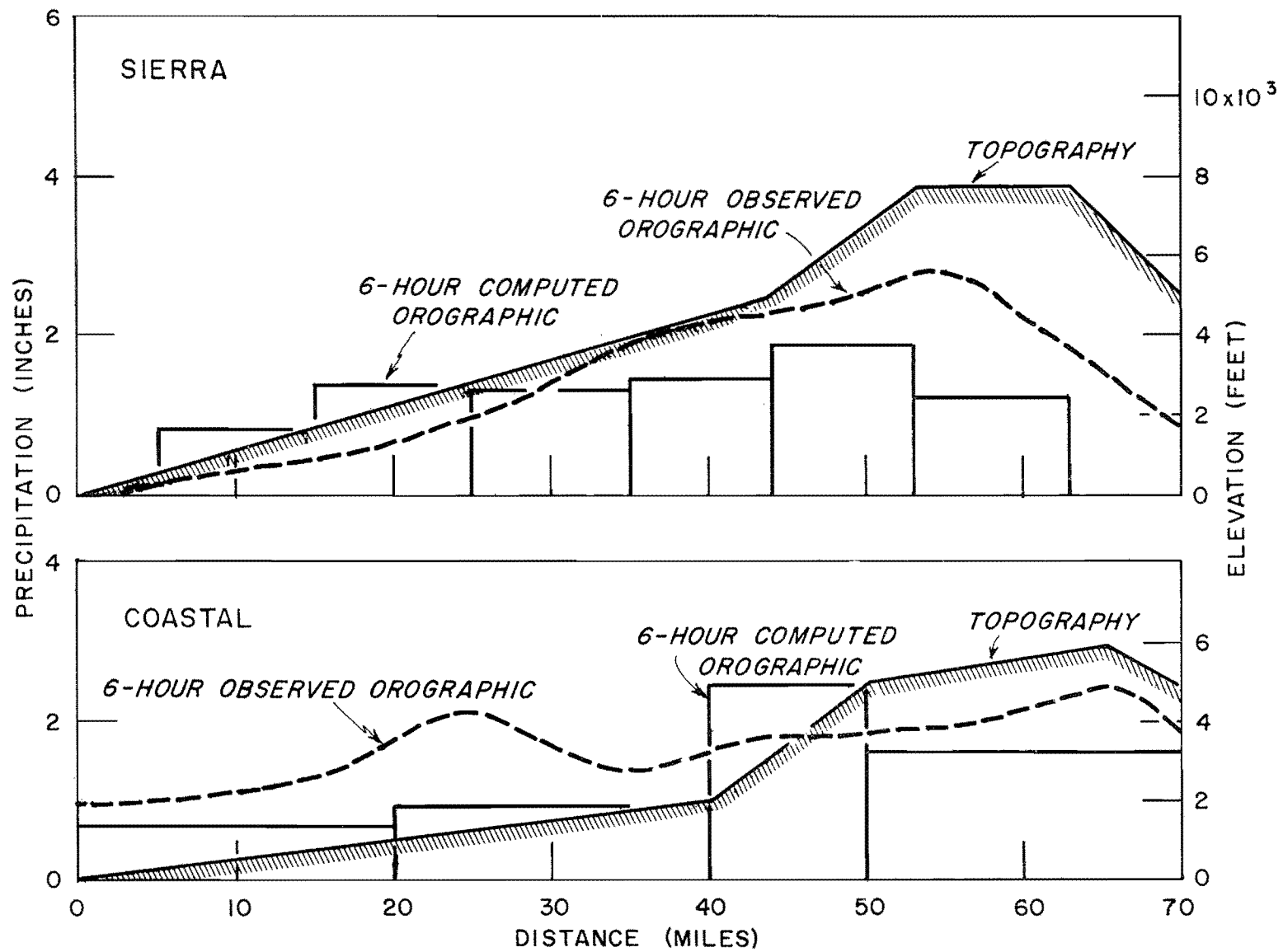
FIG. 5-16. COMPARATIVE PRECIPITATION PROFILES
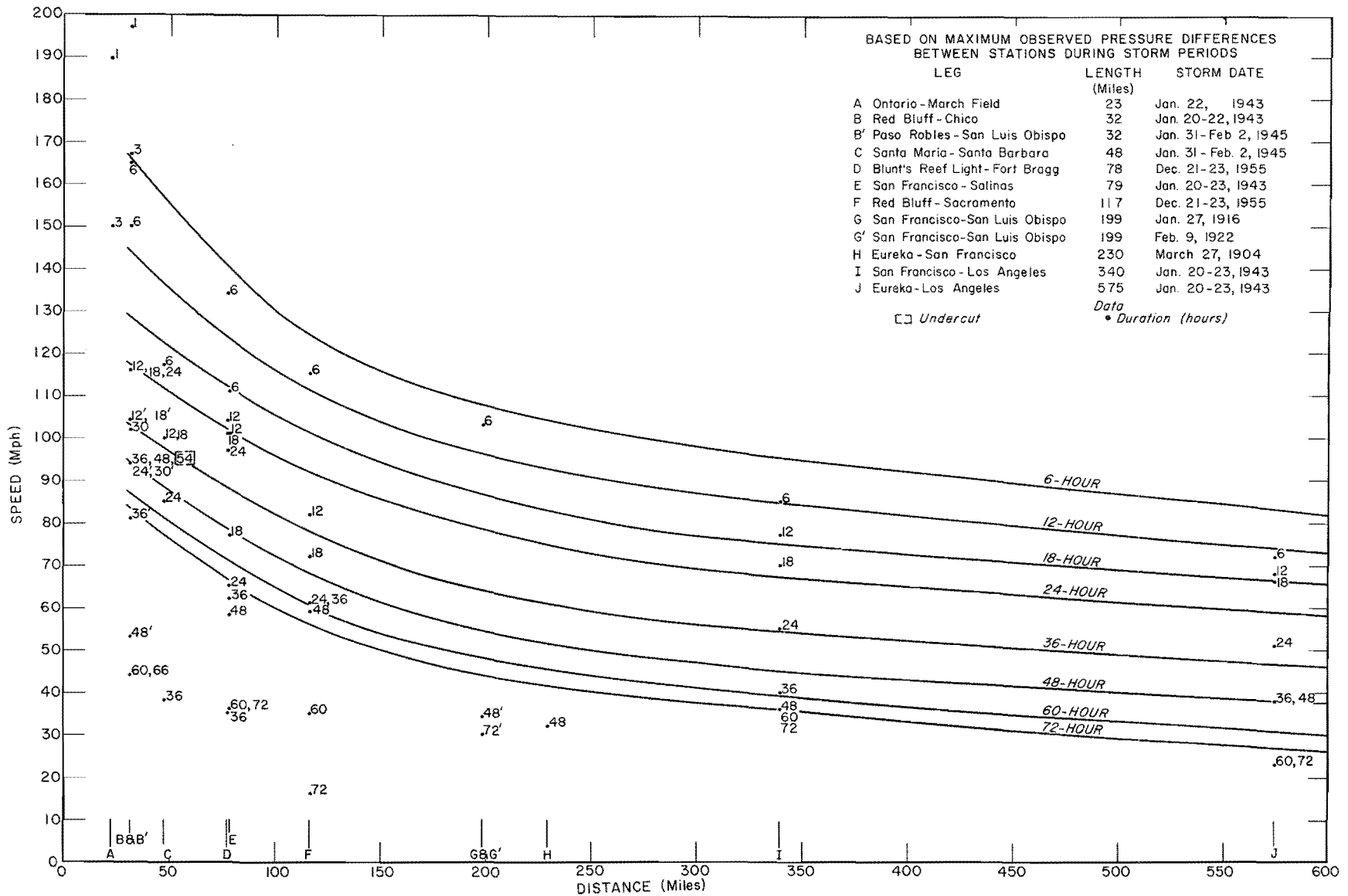
FIG. 5-17. MAXIMUM SEA-LEVEL GEOSTROPHIC WINDS
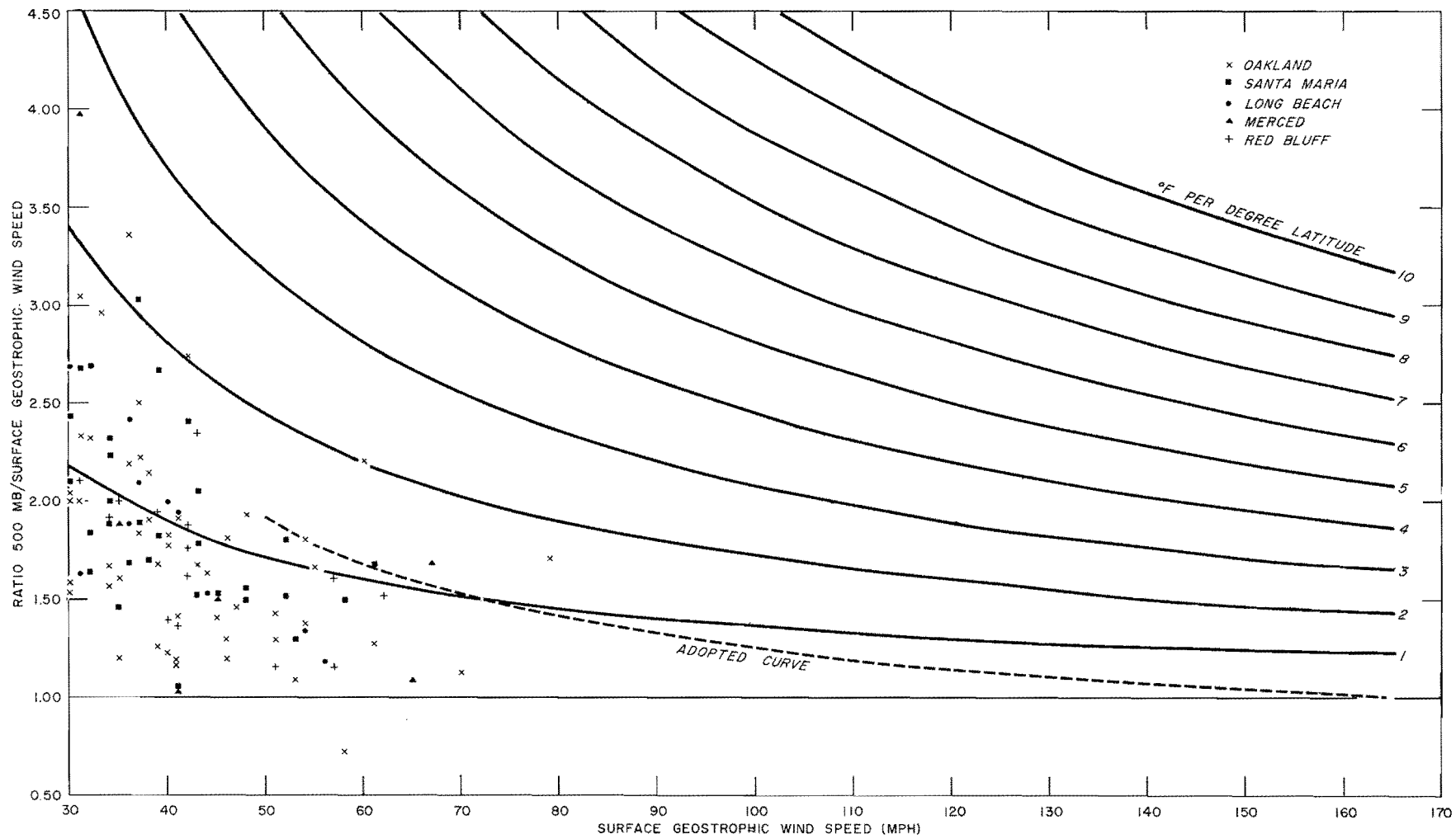
FIG. 5-18. RATIO OF 500-MB TO SURFACE GEOSTROPHIC WIND
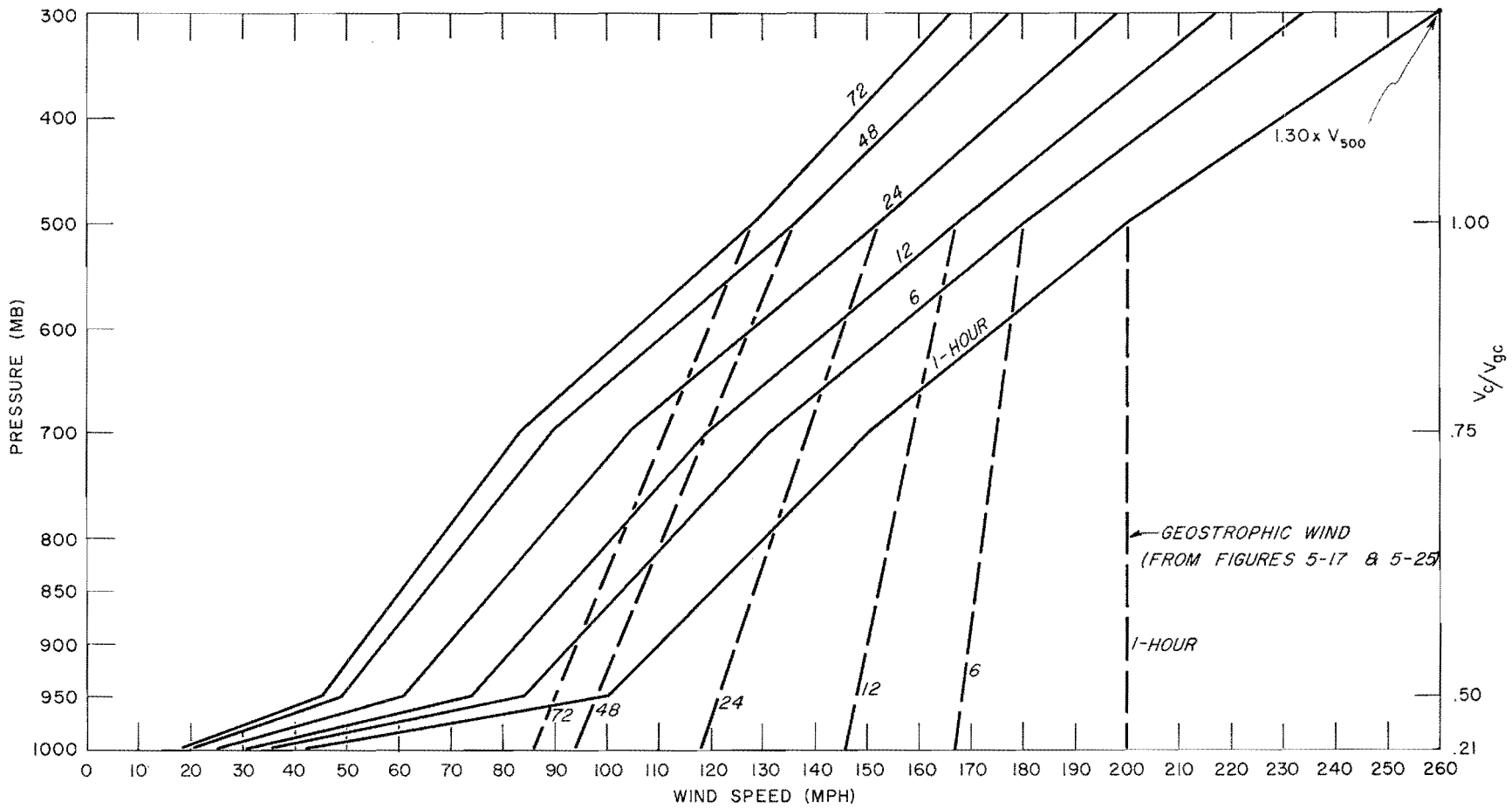
FIG. 5-19. GEOSTROPHICALLY-DERIVED MAXIMUM WINDS, COASTAL
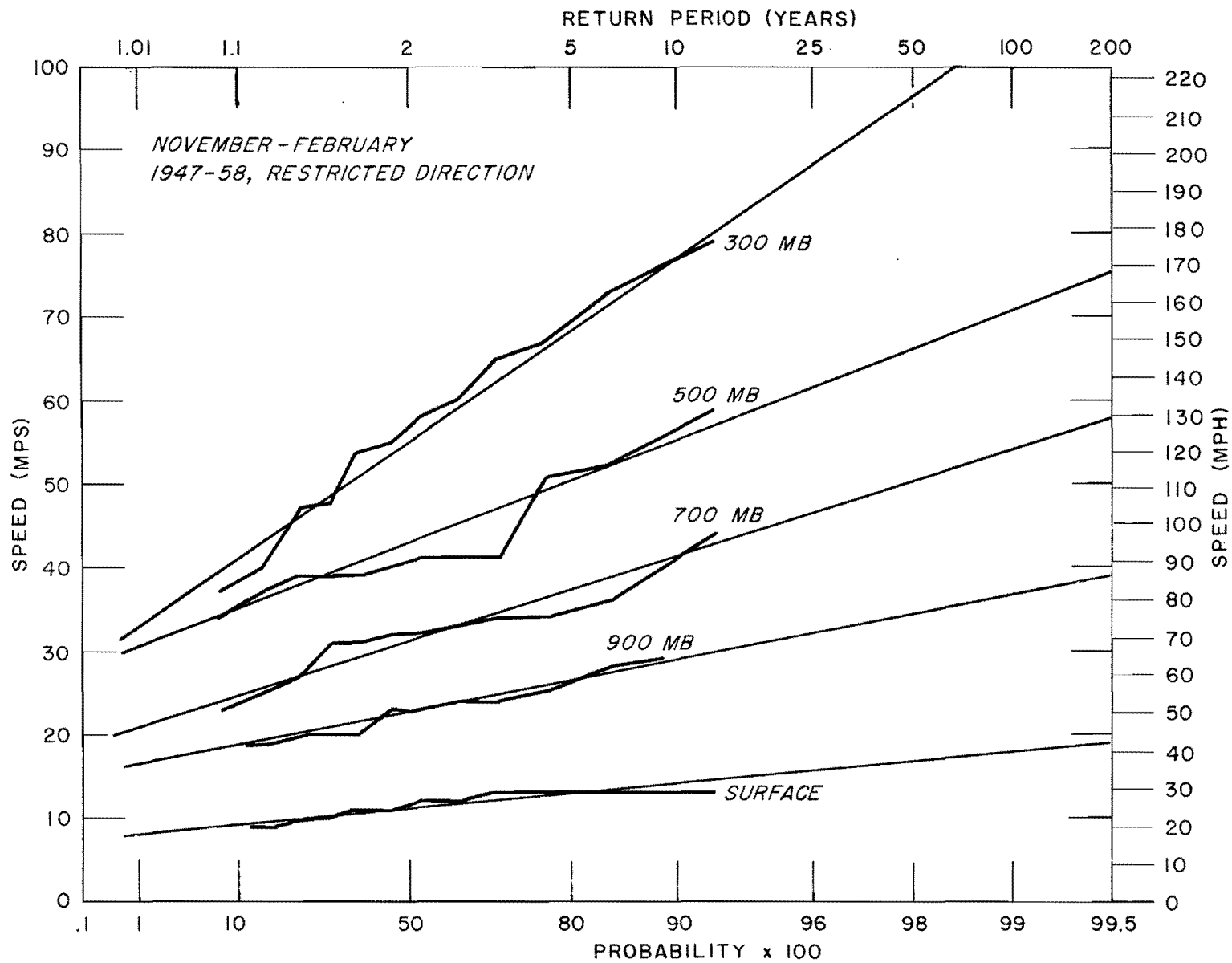
FIG. 5-20. MAXIMUM WINDS ALOFT, OAKLAND, CALIFORNIA
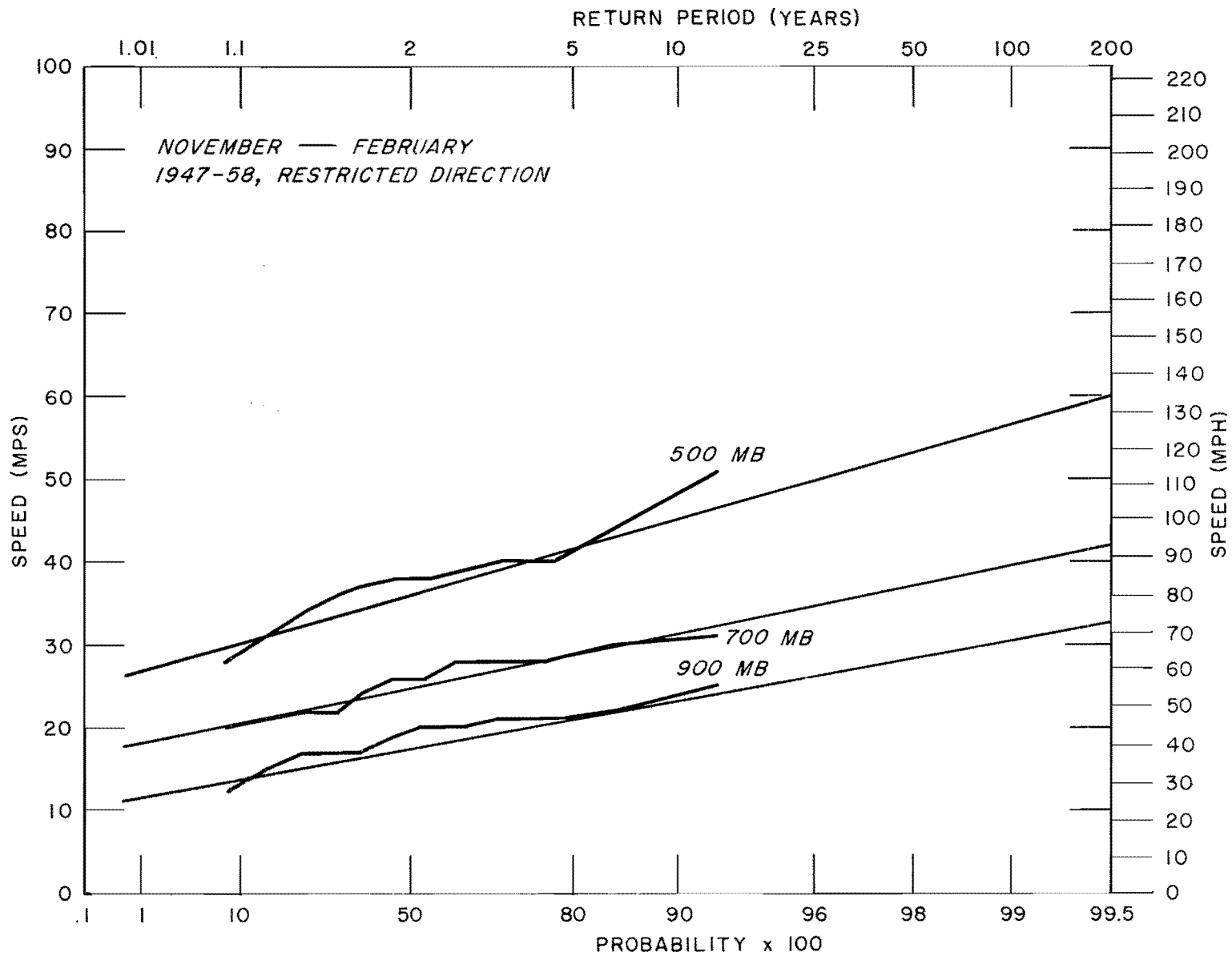
FIG. 5-21. MAXIMUM WINDS ALOFT, SANTA MARIA, CALIFORNIA
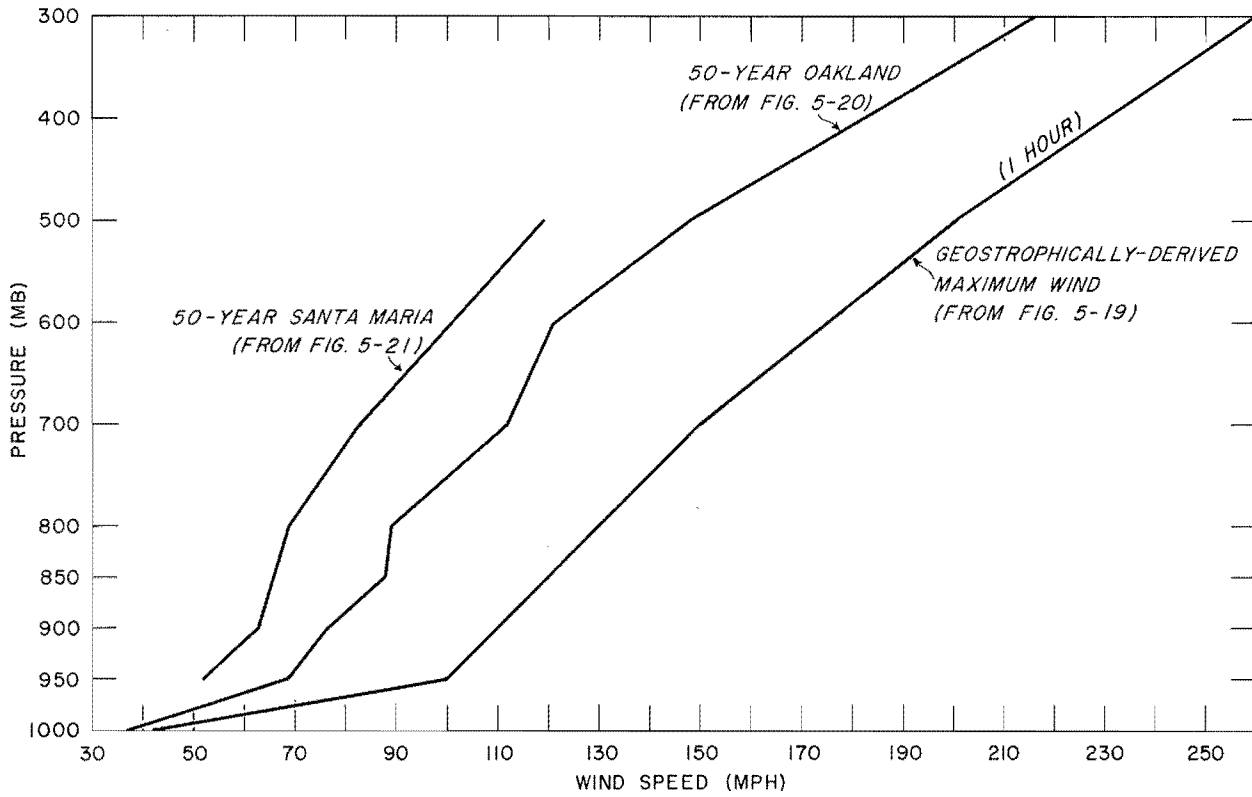
FIG. 5-22. COMPARISON OF STATISTICAL WITH GEOSTROPHICALLY-DERIVED MAXIMUM WINDS, COASTAL
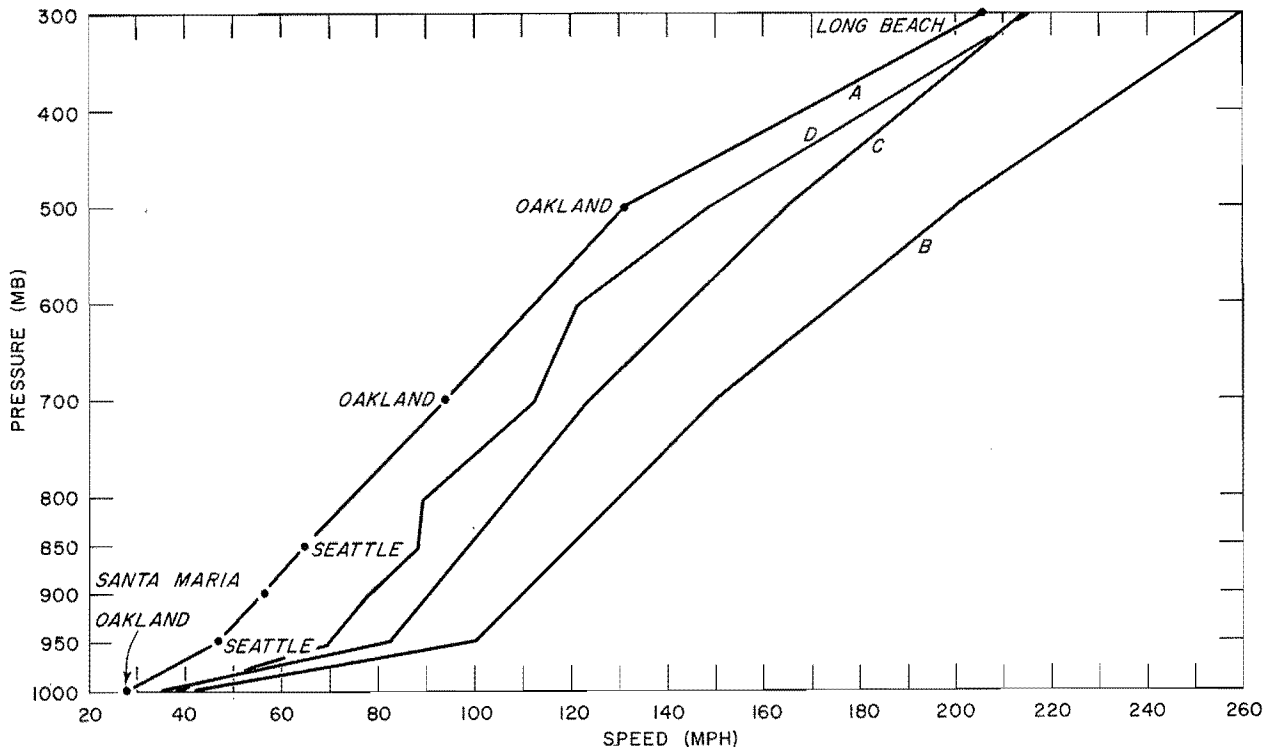
FIG. 5-23. ADOPTED MAXIMUM 1-HOUR WINDS AND SUPPORTING DATA, COASTAL
(A) COMPOSITE, (B) GEOSTROPHICALLY-DERIVED, (C) ADOPTED,
(D) 50-YEAR, OAKLAND

172
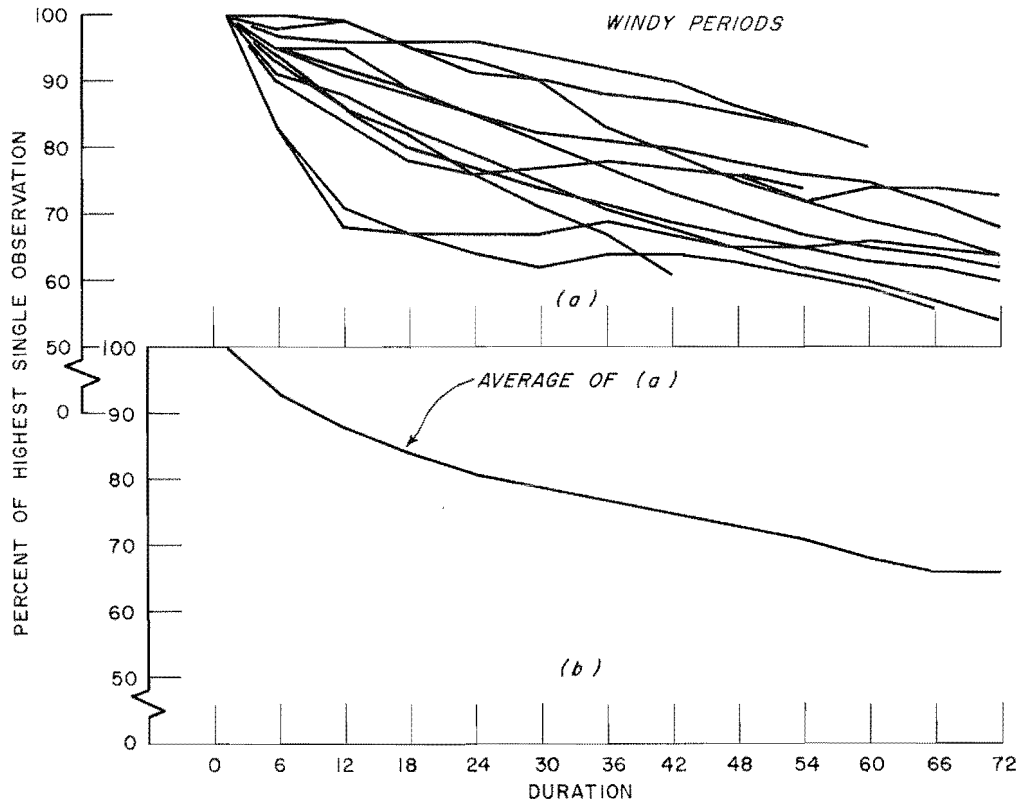
FIG. 5-24. VARIATION OF 900-MB WINDSPEED, OAKLAND
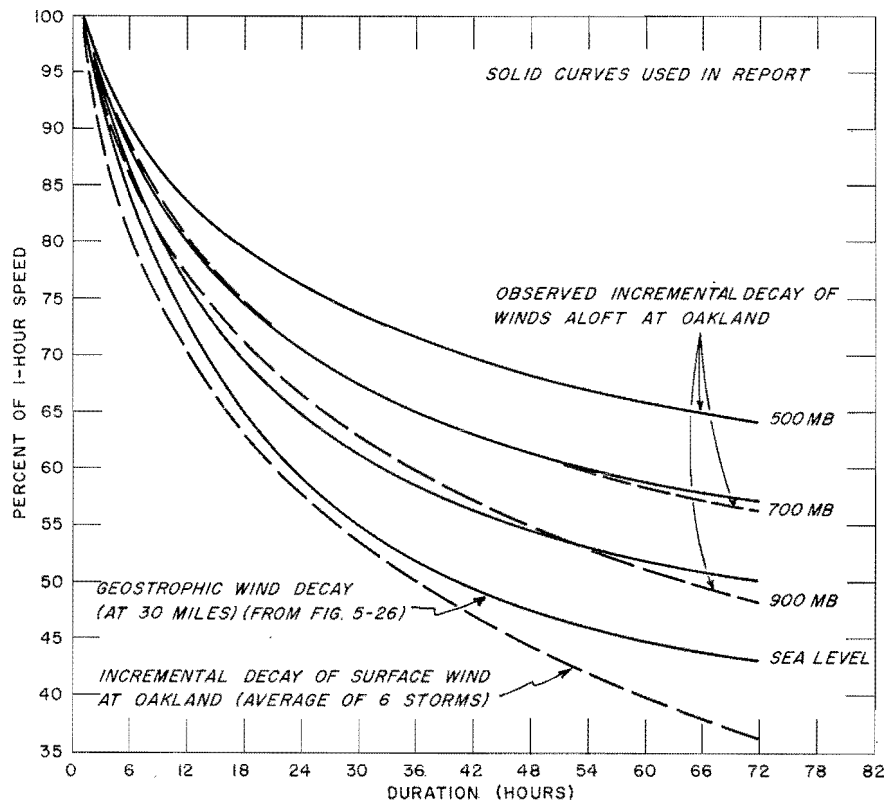
FIG. 5-25. ADOPTED VARIATION OF WINDSPEED WITH DURATION

FIG. 5-26. ADOPTED MAXIMUM WINDS NORMAL TO COAST RANGE
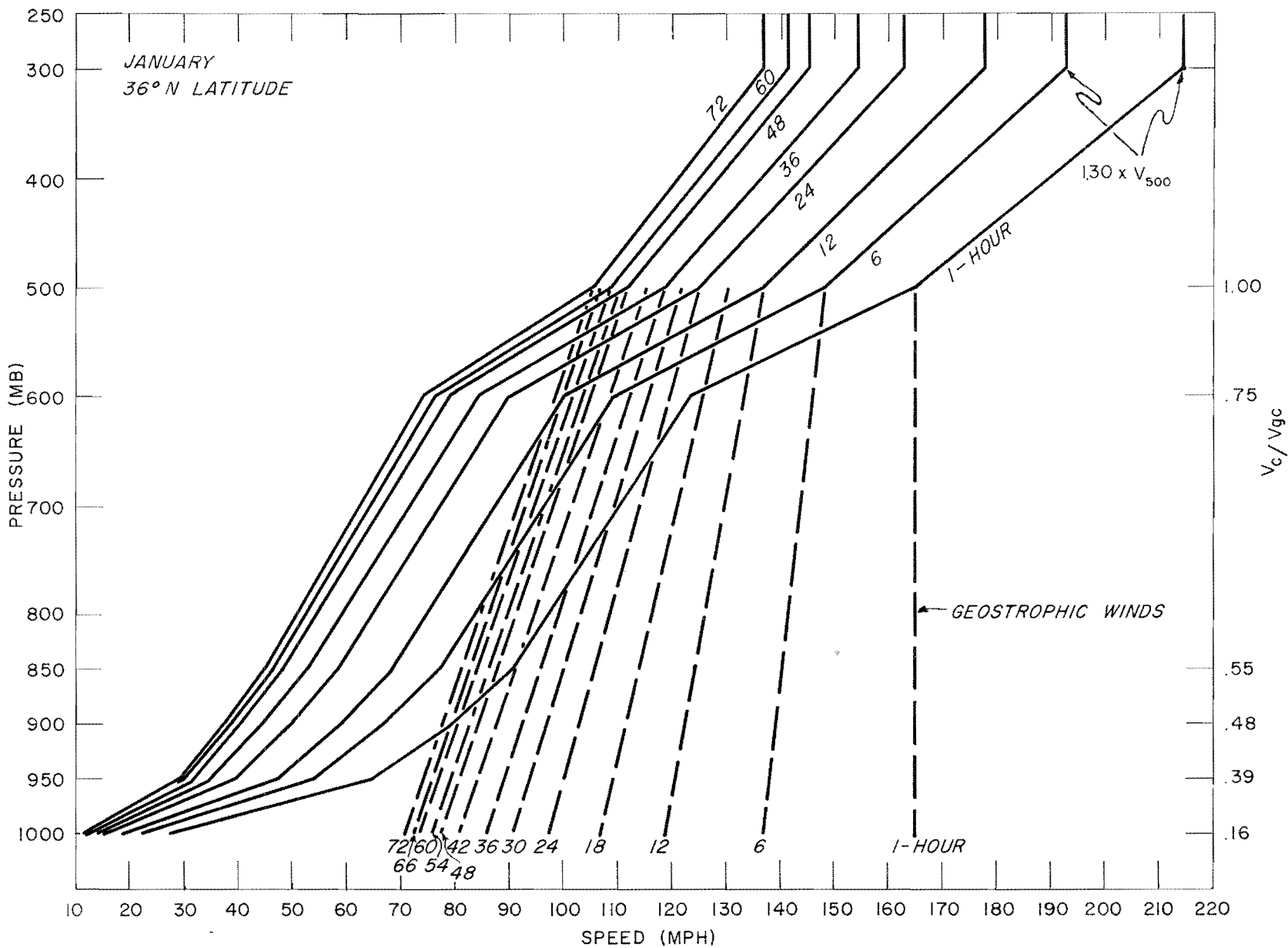
FIG. 5-27. ADOPTED MAXIMUM WINDS NORMAL TO SIERRAS
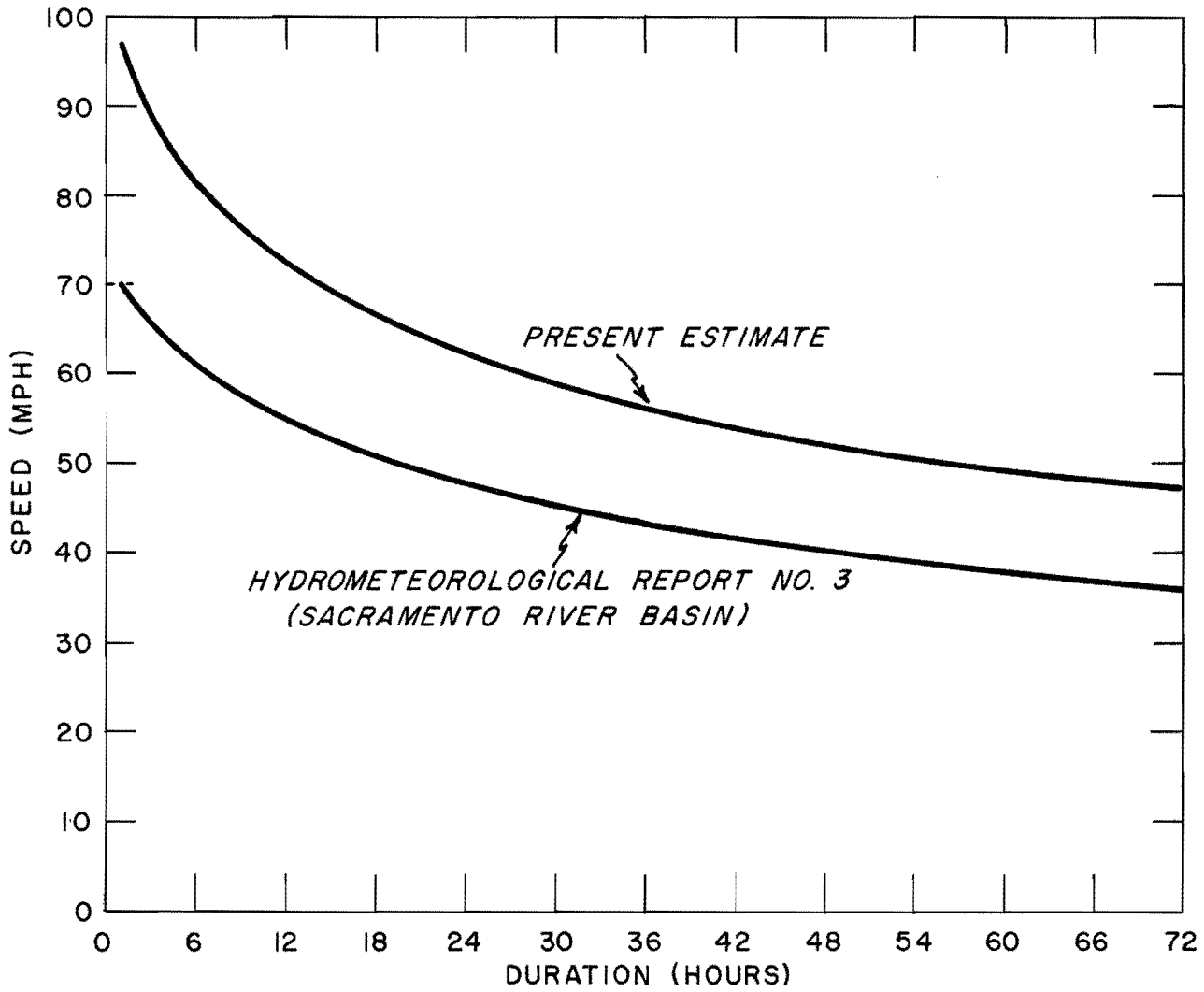
5-28. MAXIMUM 4000-FOOT WINDSPEED COMPARISON, COASTAL
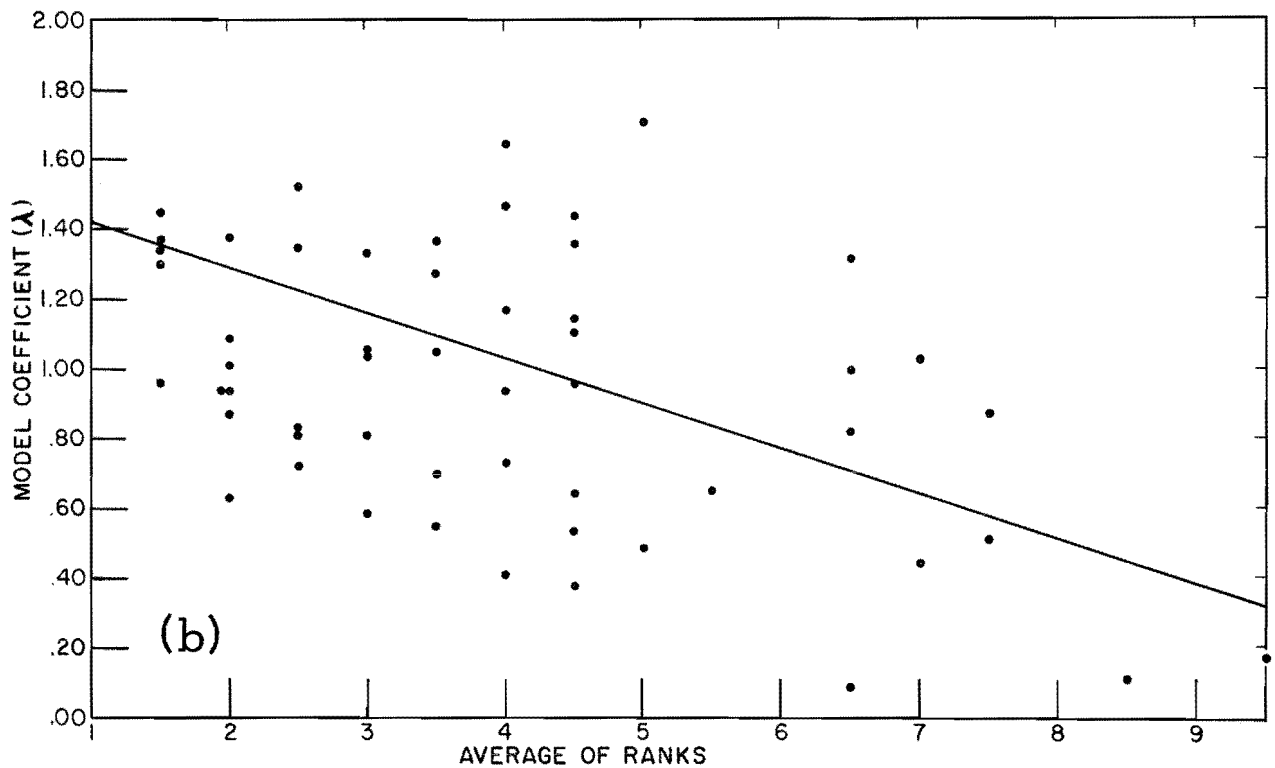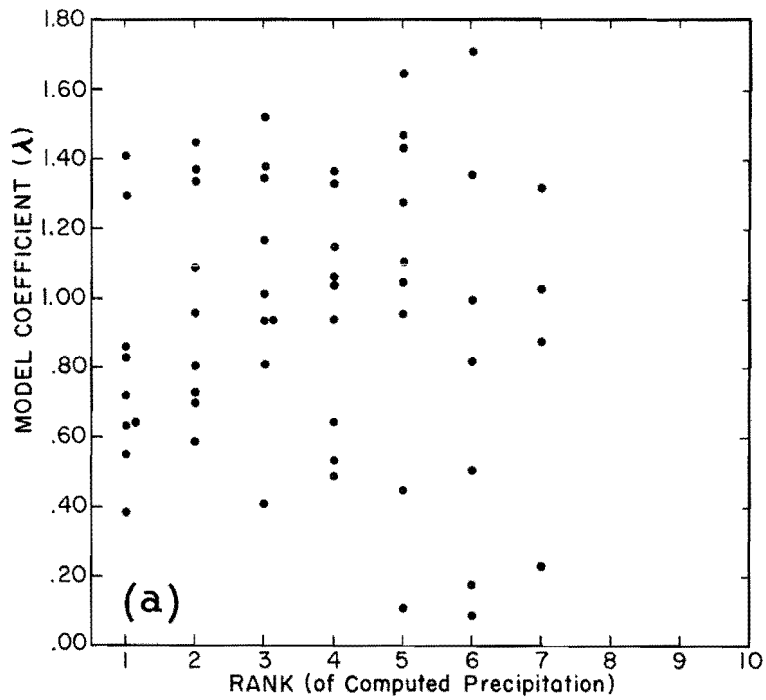
FIG. 5-29. MODEL-COEFFICIENT-VARIATION TESTS (a) λ VS. RANK OF COMPUTED
PRECIPITATION, (b) λ VS. RANK OF AVERAGE OF COMPUTED AND
OBSERVED PRECIPITATION

FIG. 5-30. OROGRAPHIC PMP COMPUTATION AREAS
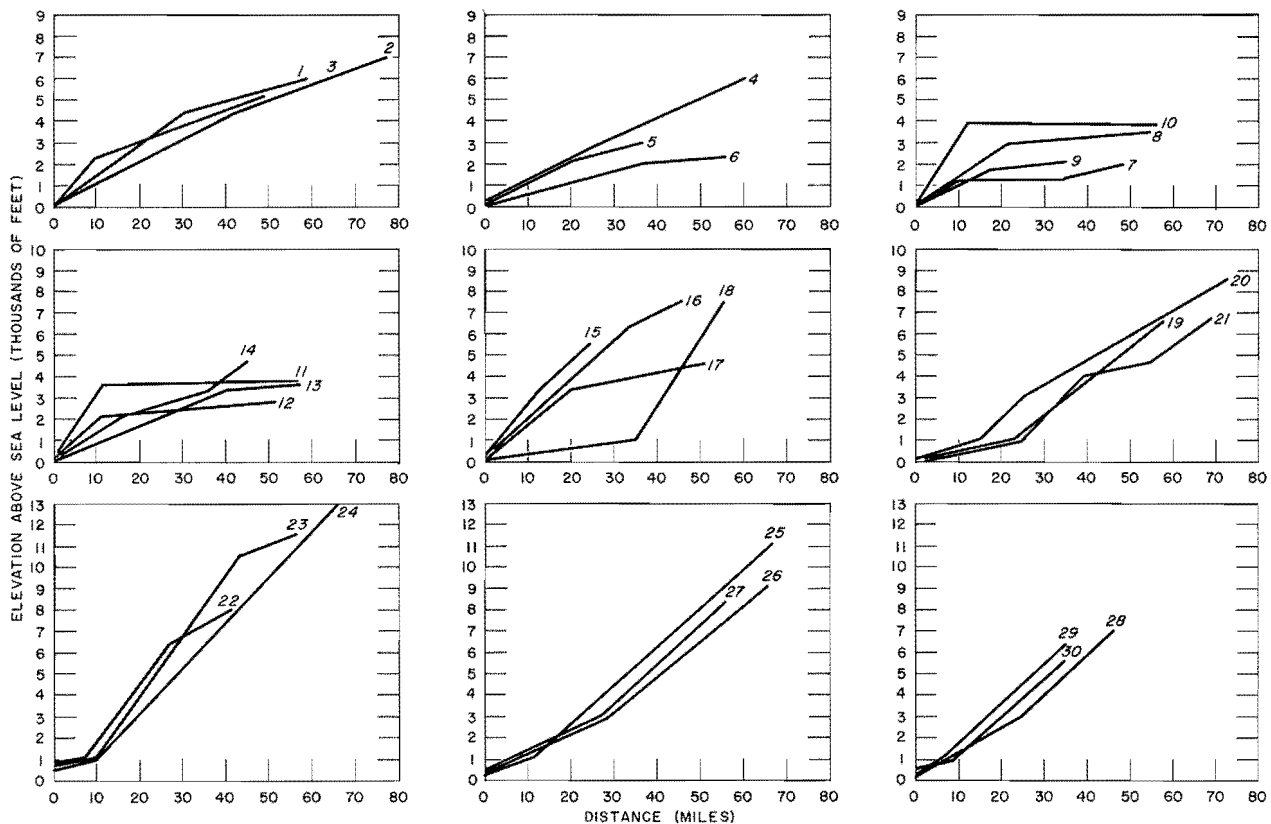
FIG. 5-31. ADOPTED GROUND PROFILES (PMP AREAS NUMBERED, SEE FIG. 5-30)
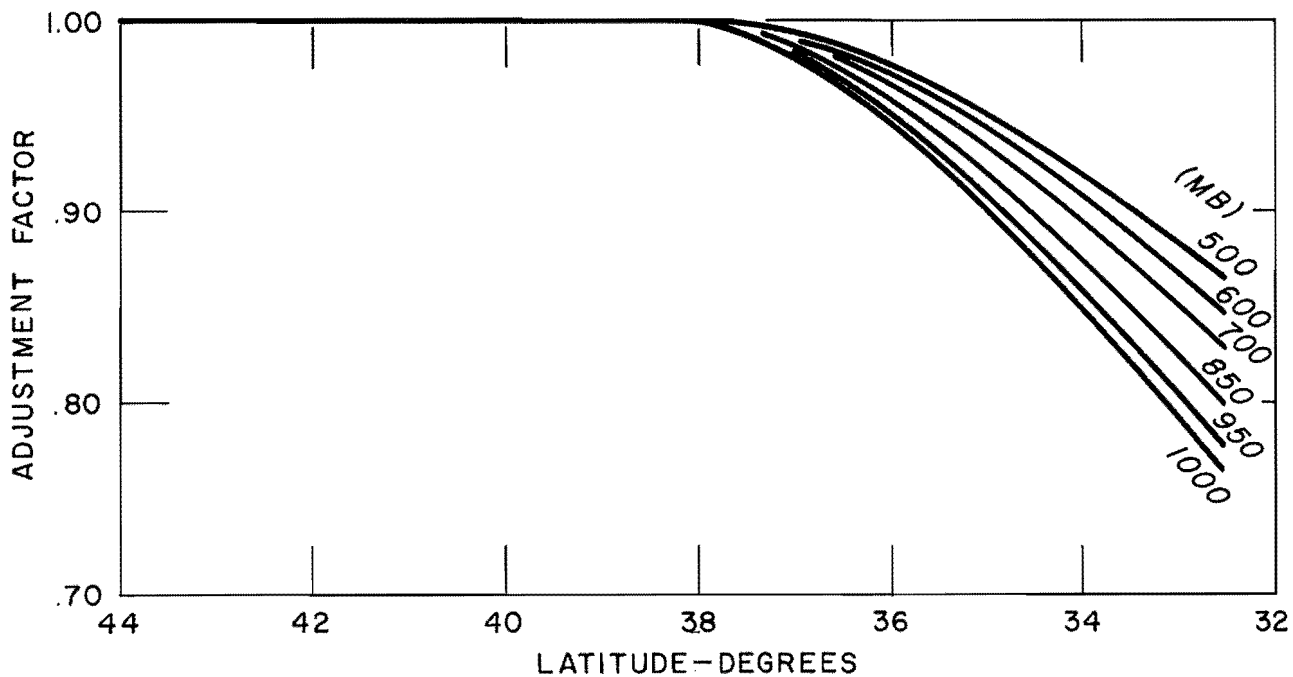
FIG. 5-32. LATITUDINAL VARIATION OF MAXIMUM WINDS
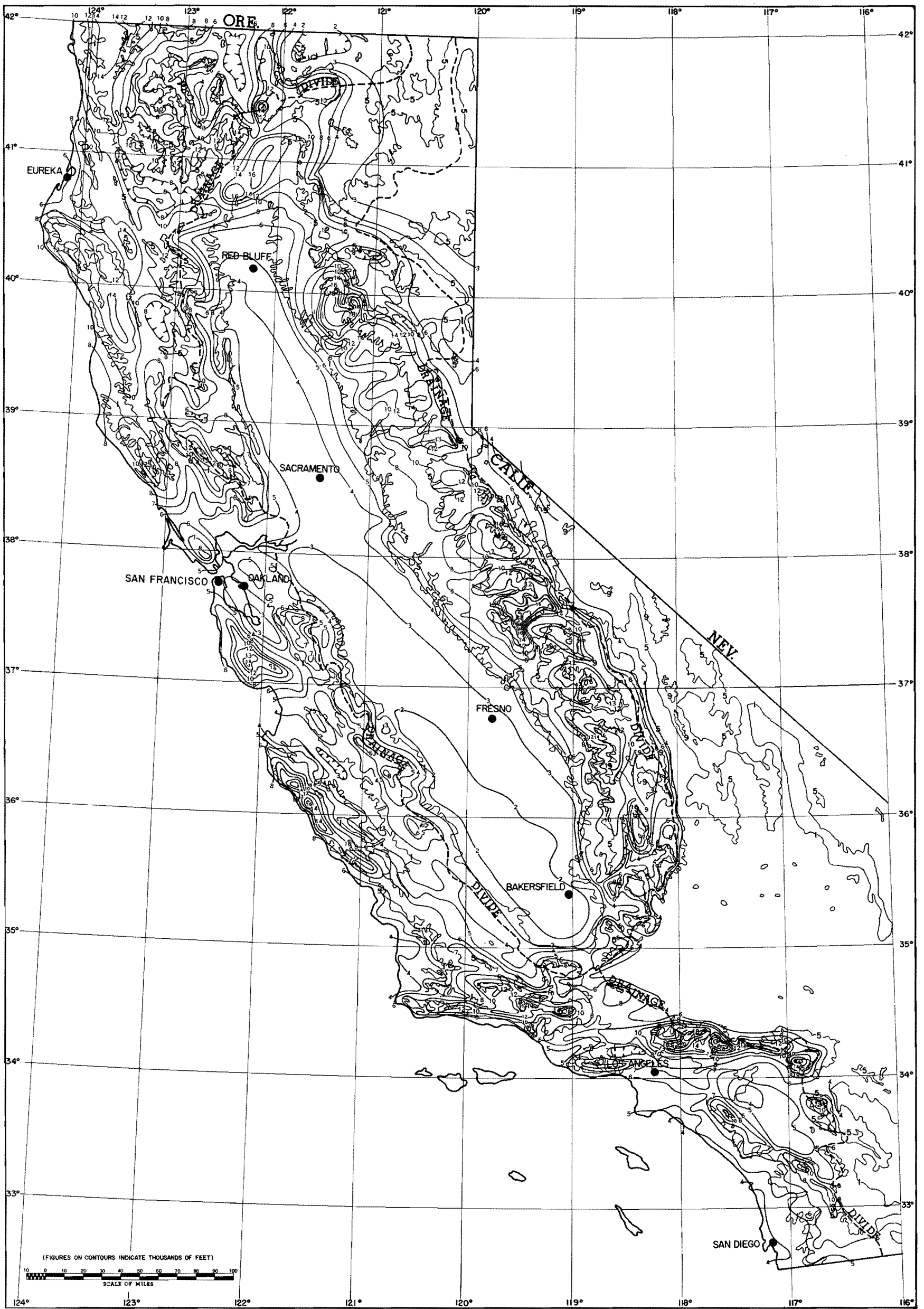
FIG. 5-33A. 10-YEAR 3-DAY POINT PRECIPITATION (inches)
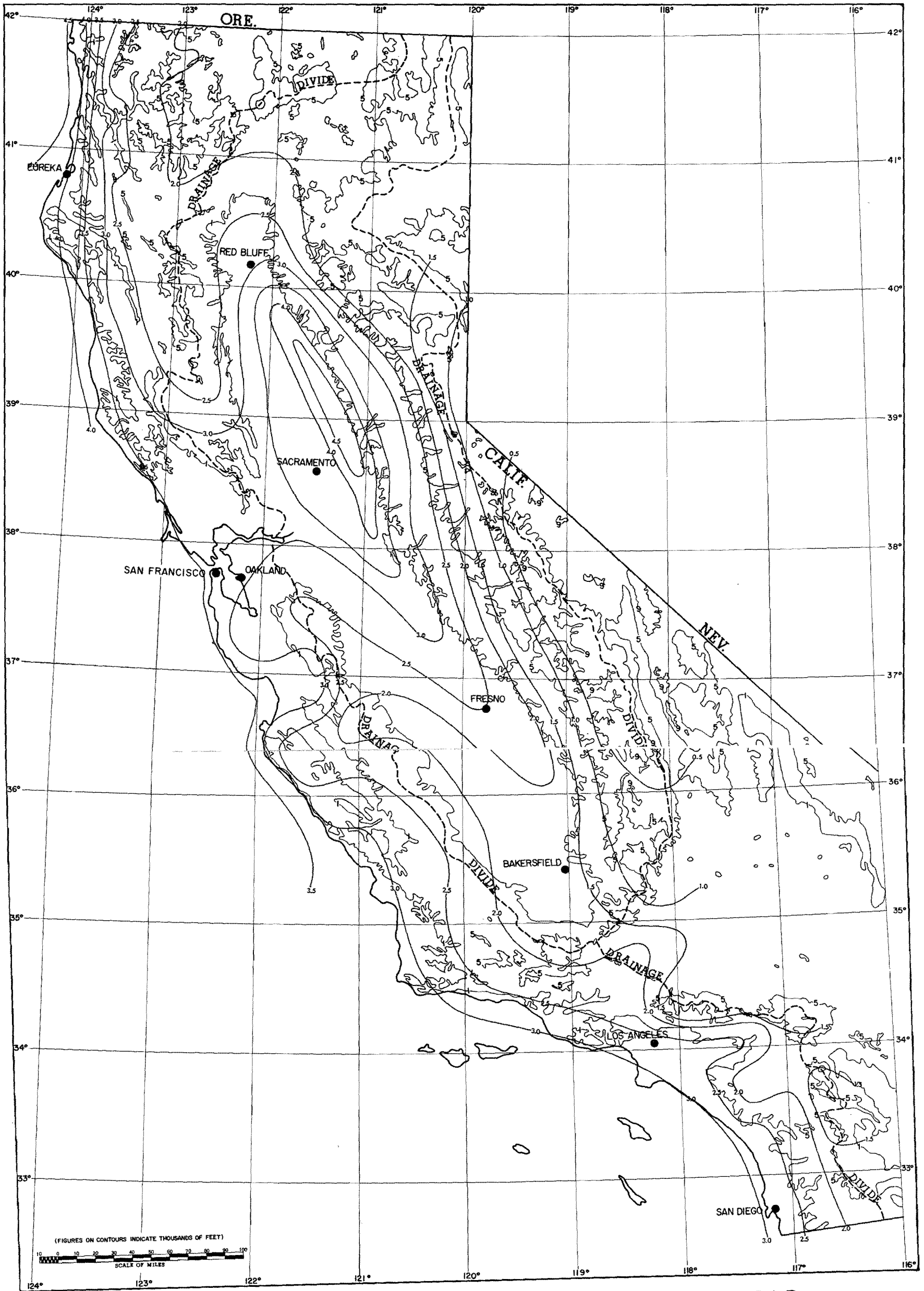
FIG. 5-33B. CONVERGENCE COMPONENT 10-YEAR
3-DAY POINT PRECIPITATION (inches)
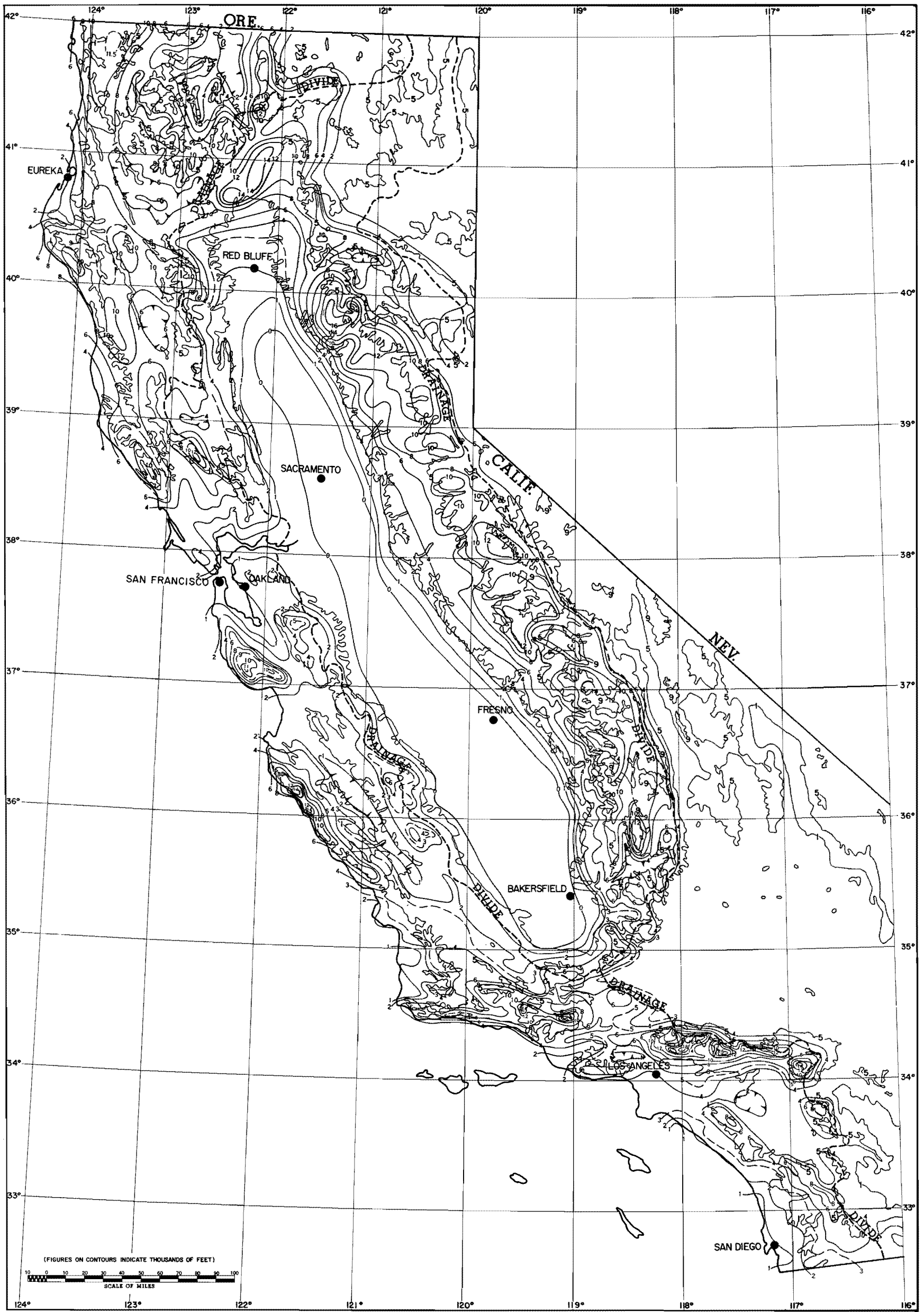
FIG. 5-33C. OROGRAPHIC COMPONENT 10-YR 3-DAY POINT
PRECIPITATION (inches)
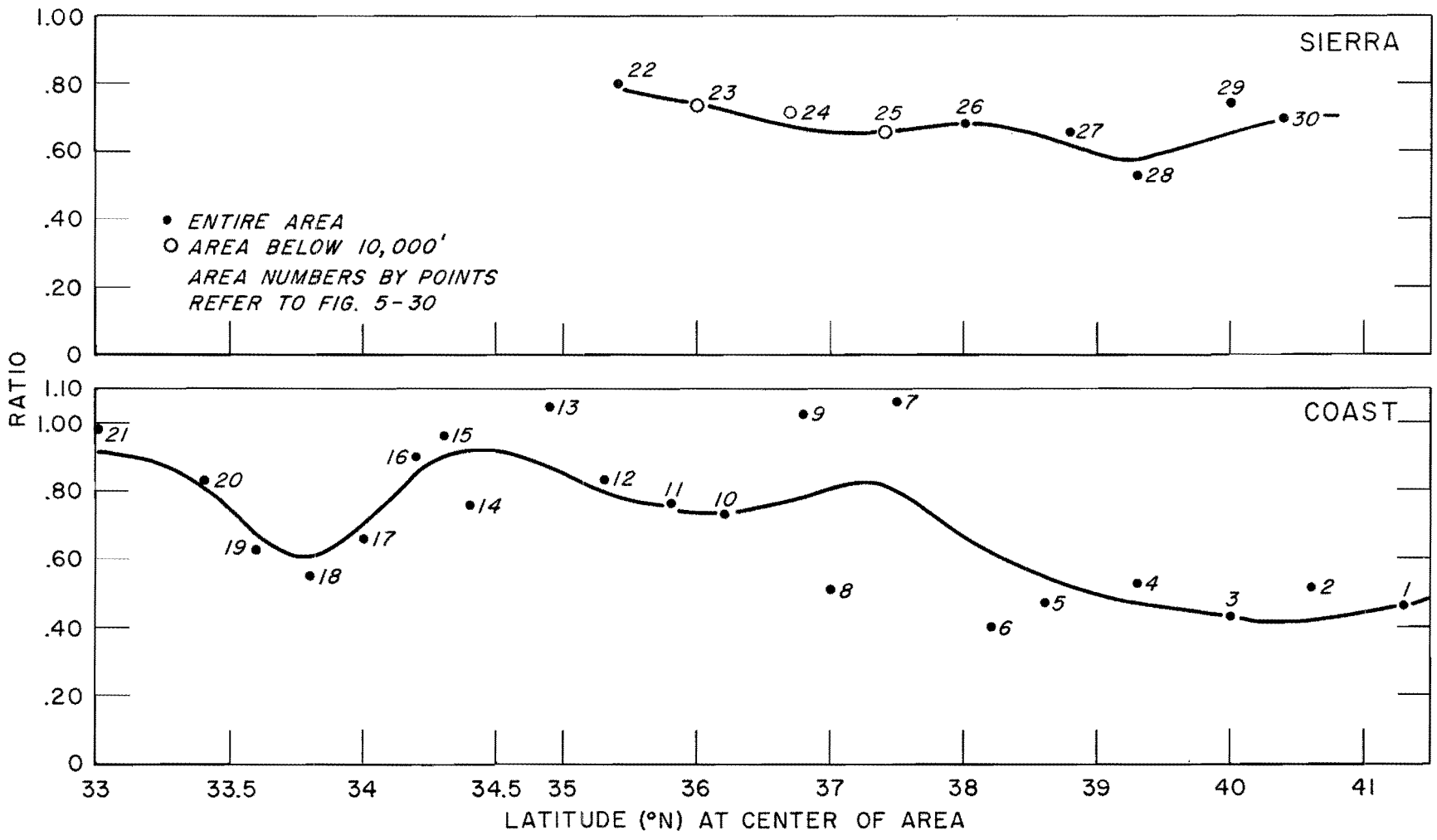
FIG. 5-34. RATIO OF 6-HOUR JANUARY OROGRAPHIC PMP TO OROGRAPHIC COMPONENT OF 10-YEAR 3-DAY PRECIPITATION

(FIGURES ON CONTOURS INDICATE THOUSANDS OF FEET)

SCALE OF MILES
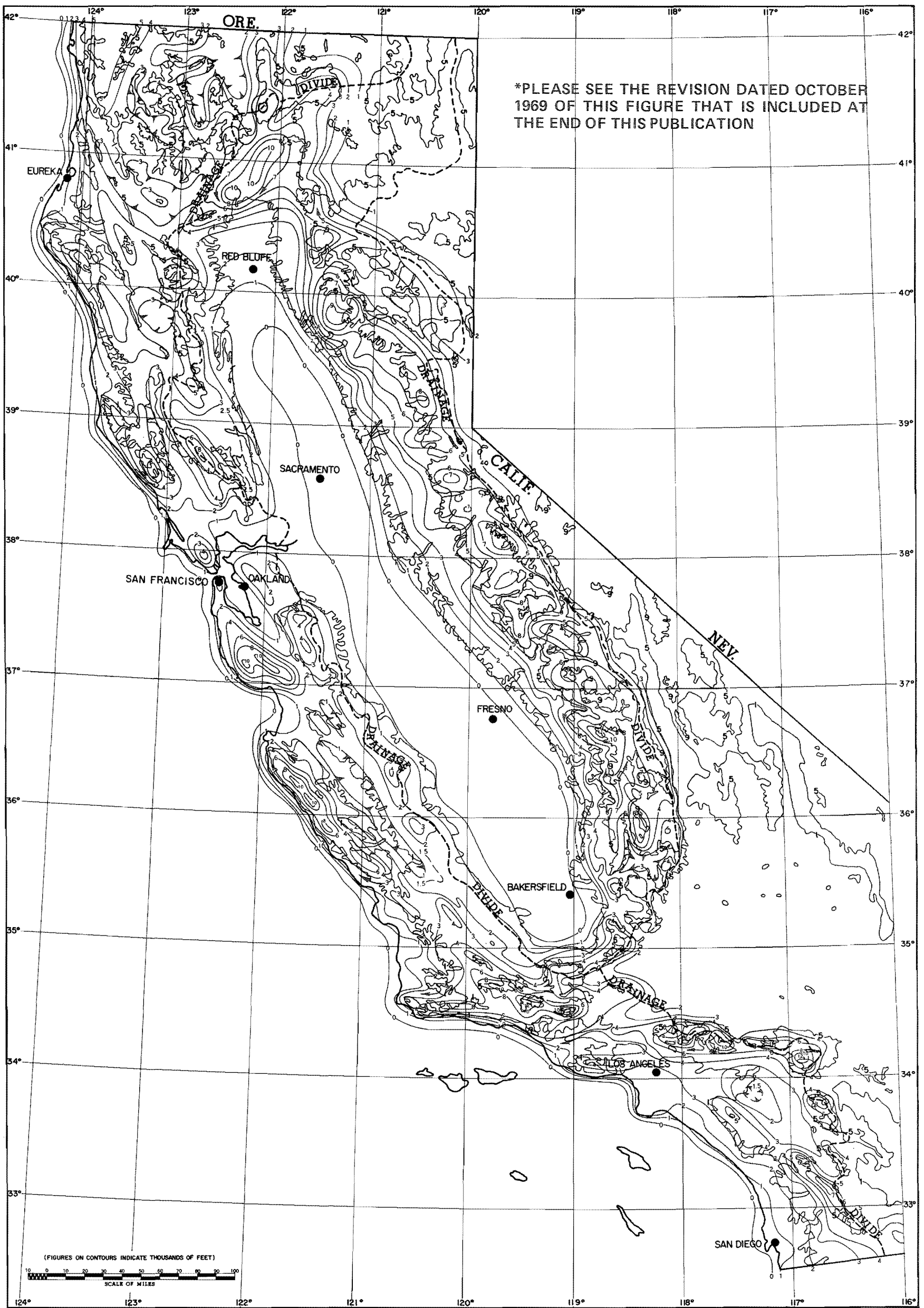
FIG. 5-35. OROGRAPHIC PMP INDEX. 6-HR JANUARY (inches)
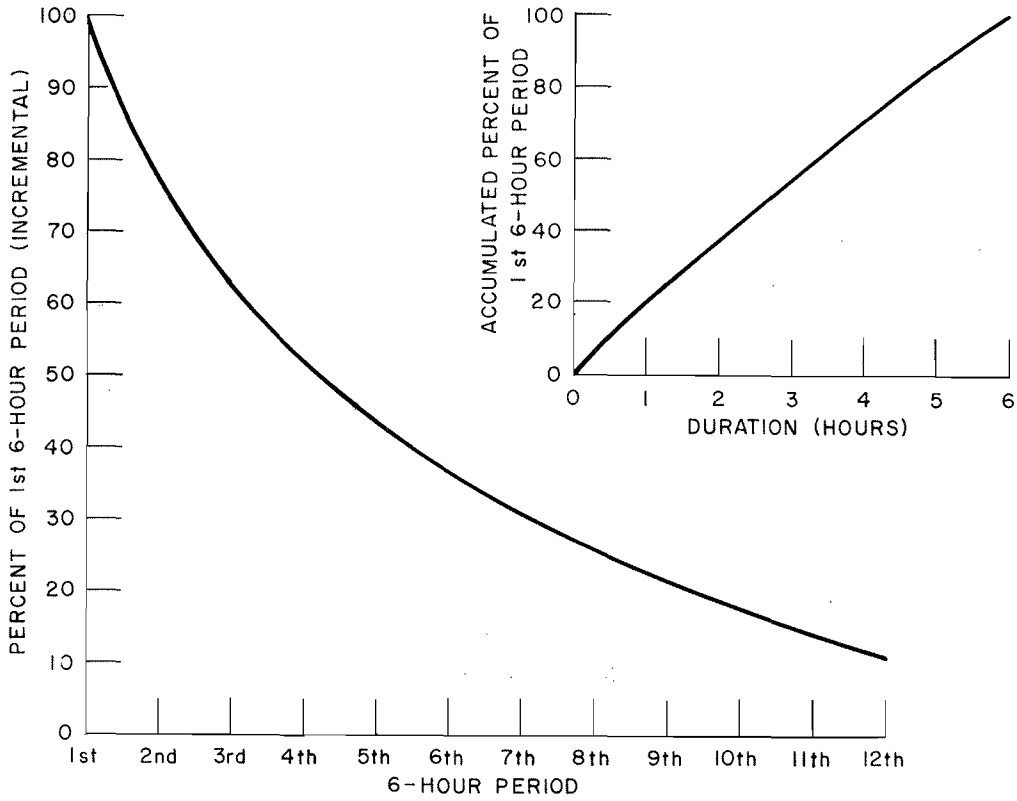
FIG. 5-36. VARIATION OF OROGRAPHIC PMP WITH DURATION
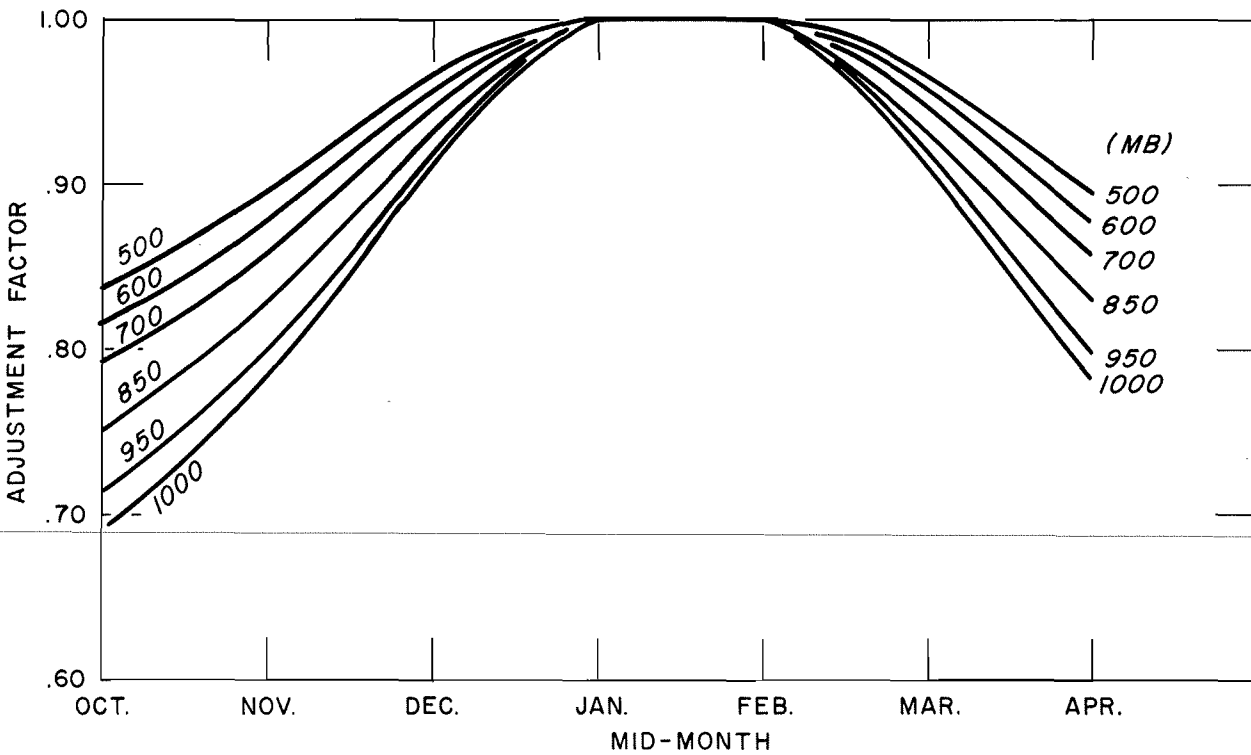
FIG. 5-37. SEASONAL VARIATION OF MAXIMUM WINDS
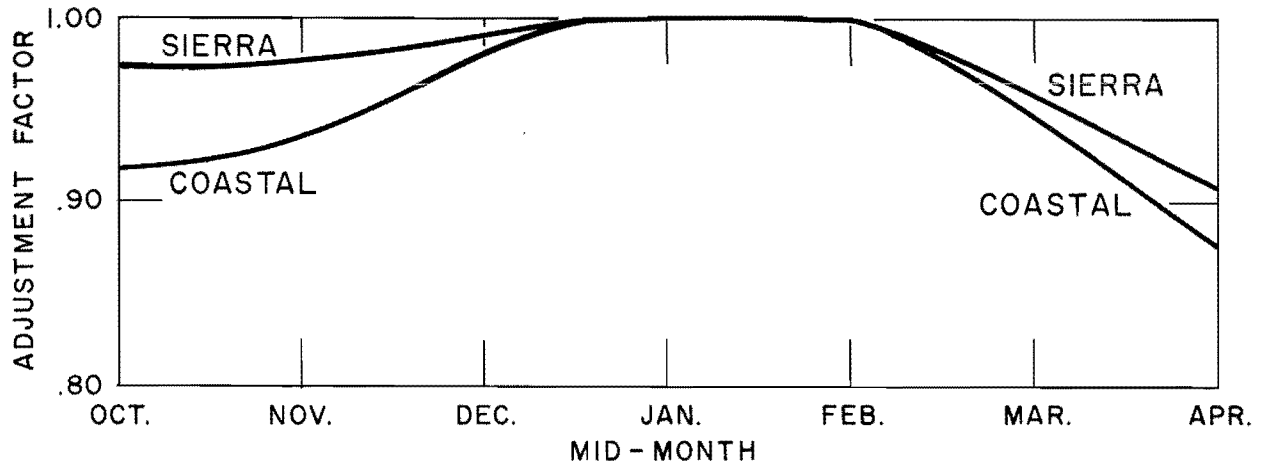
FIG. 5-38. SEASONAL VARIATION OF OROGRAPHIC PMP
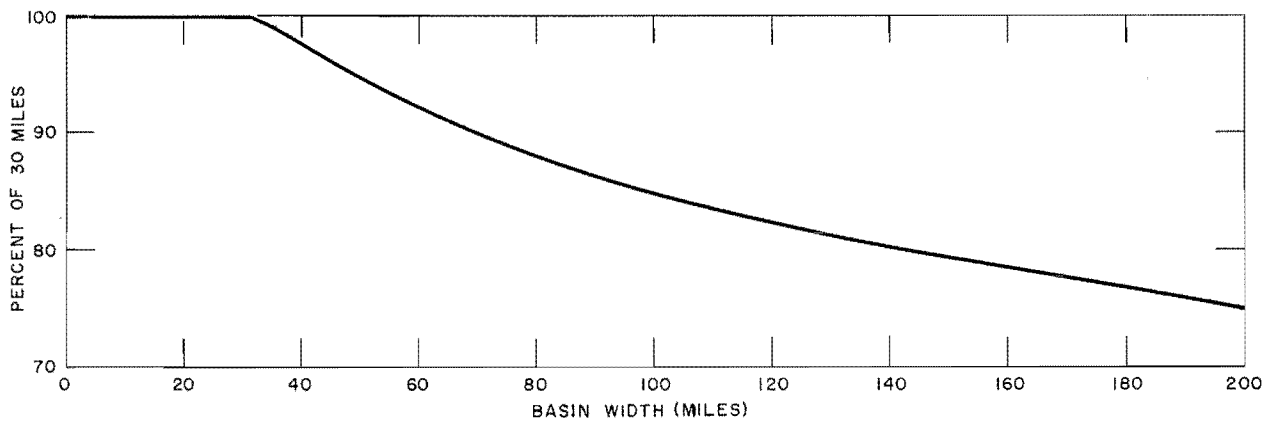
FIG. 5-39. BASIN-WIDTH VARIATION
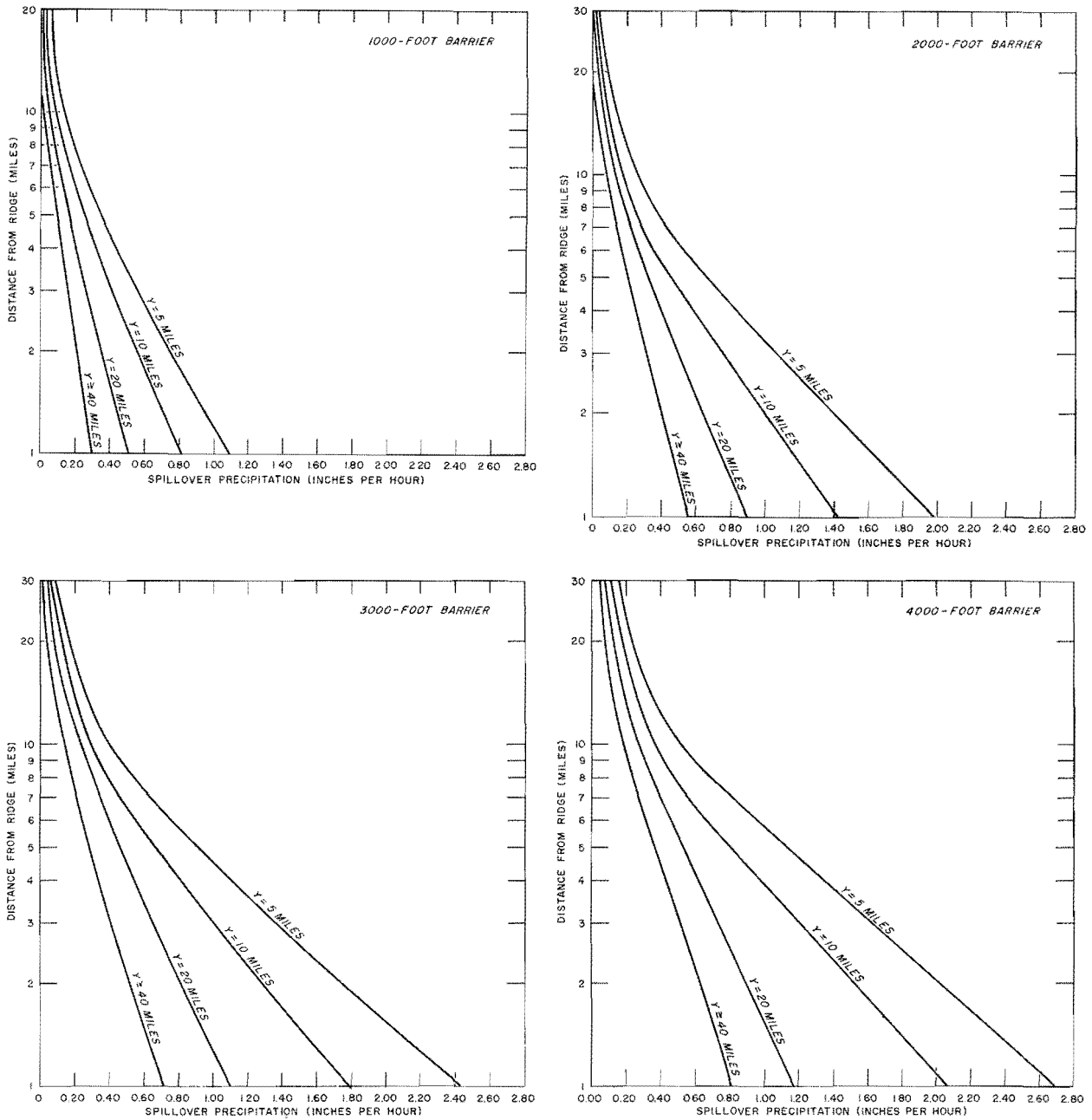
FIG. 6-1. OROGRAPHIC PLATEAU SPILLOVER

182
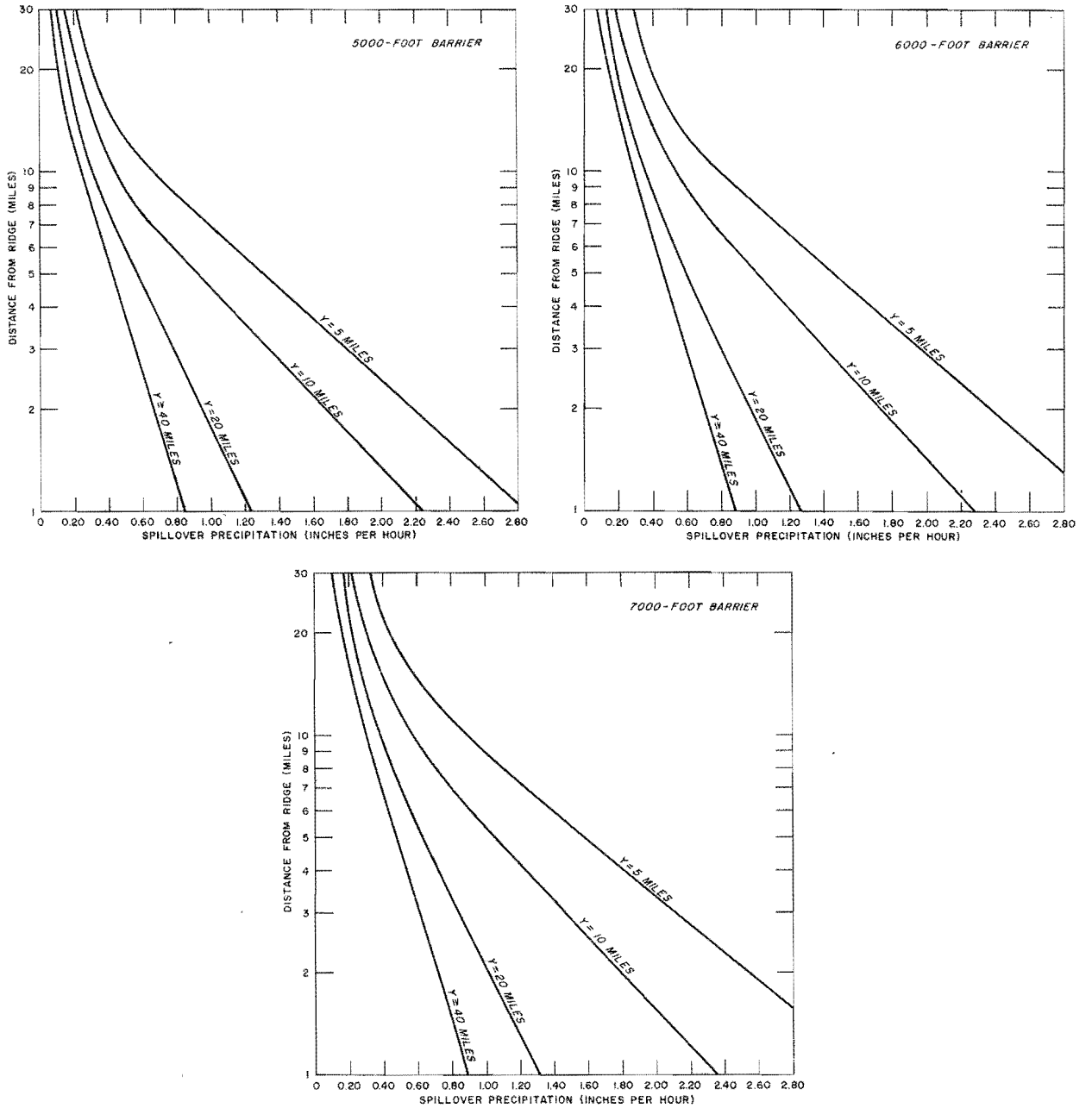
FIG. 6-2. OROGRAPHIC PLATEAU SPILLOVER (CONT'D)
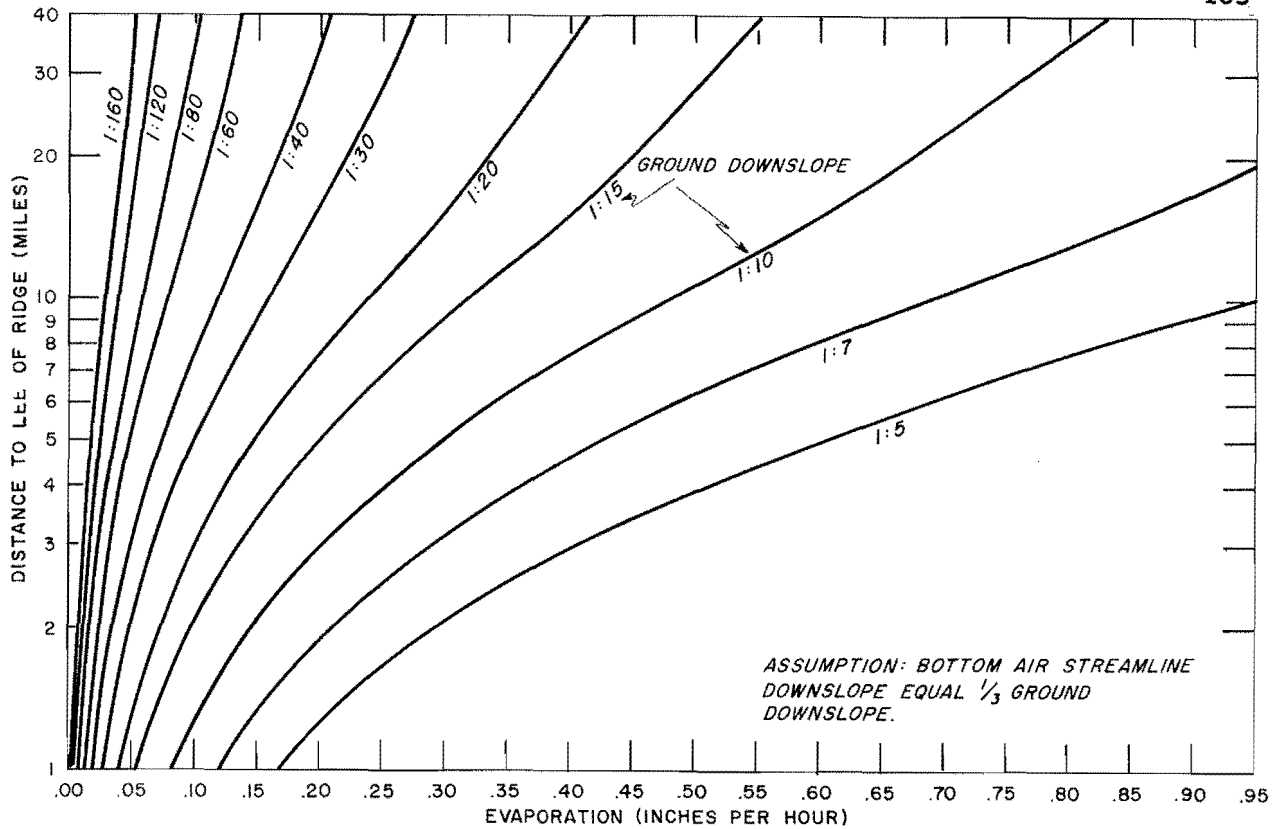
FIG. 6-3. LEEWARD EVAPORATION
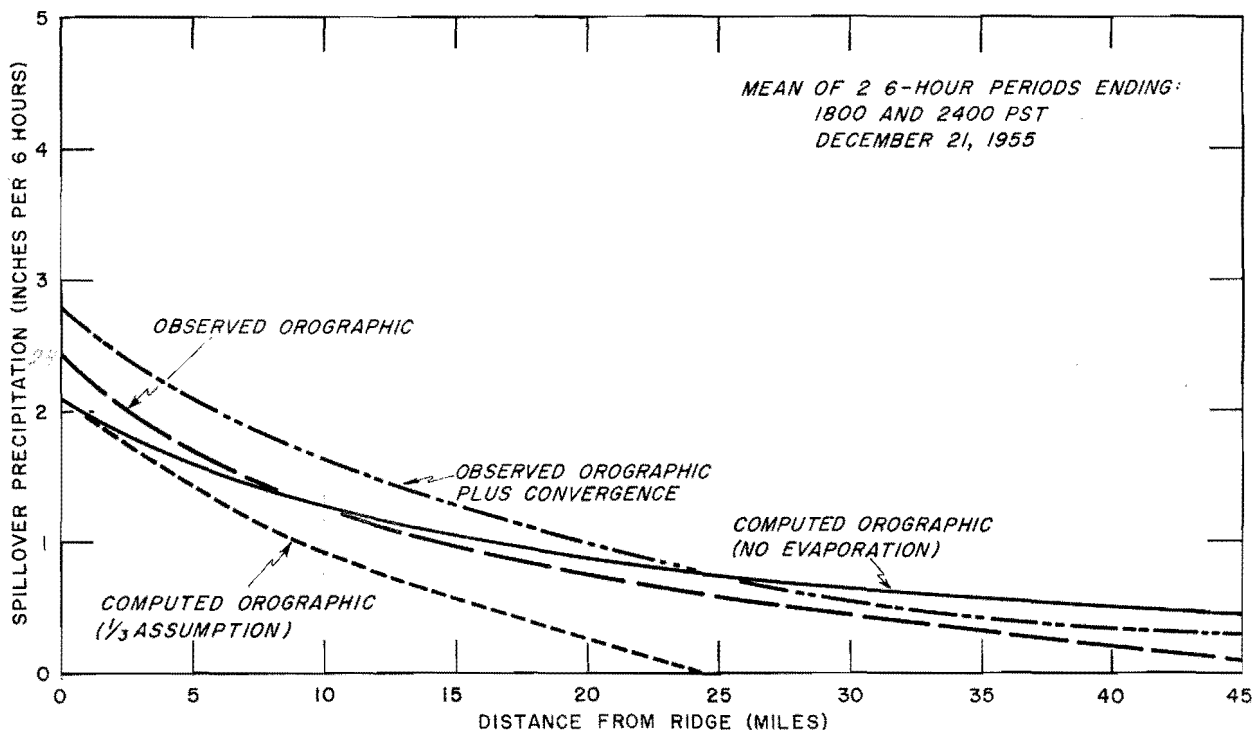
FIG. 6-4. SPILLOVER COMPARISON — COASTAL (See figure 5-15)
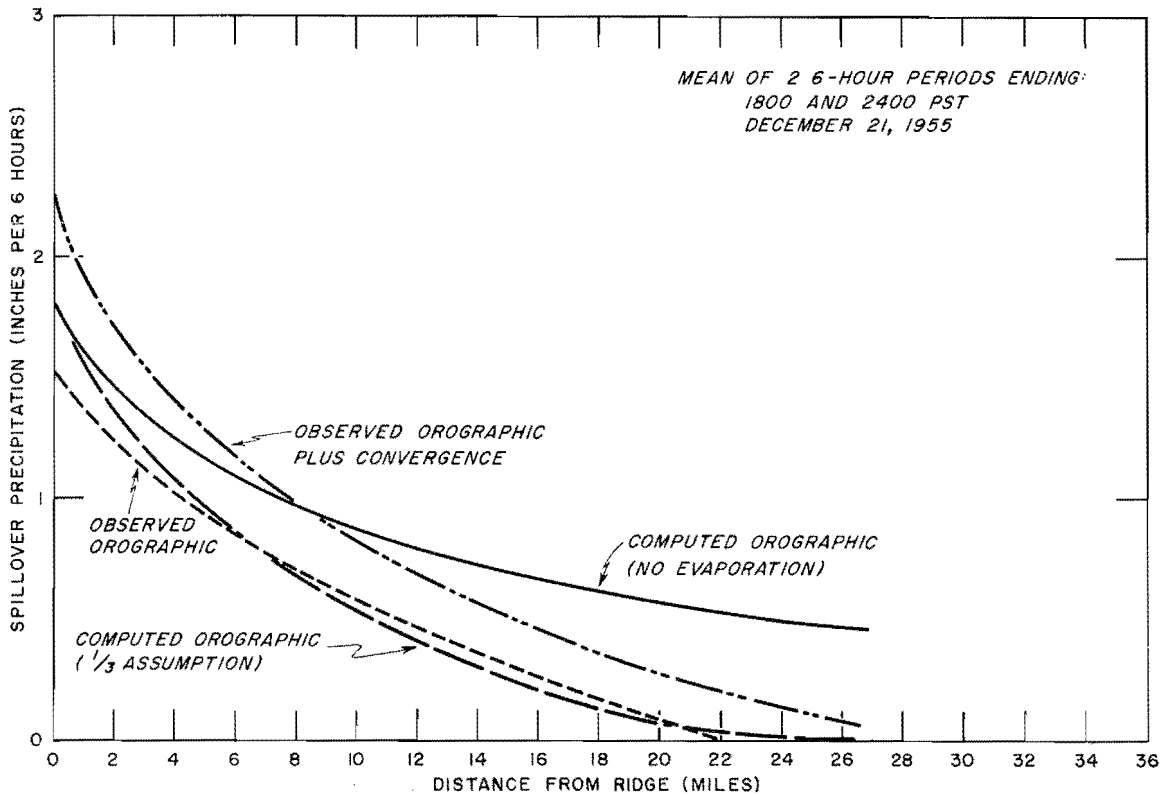
FIG. 6-5. SPILLOVER COMPARISON — SIERRA (See figure 5-15)
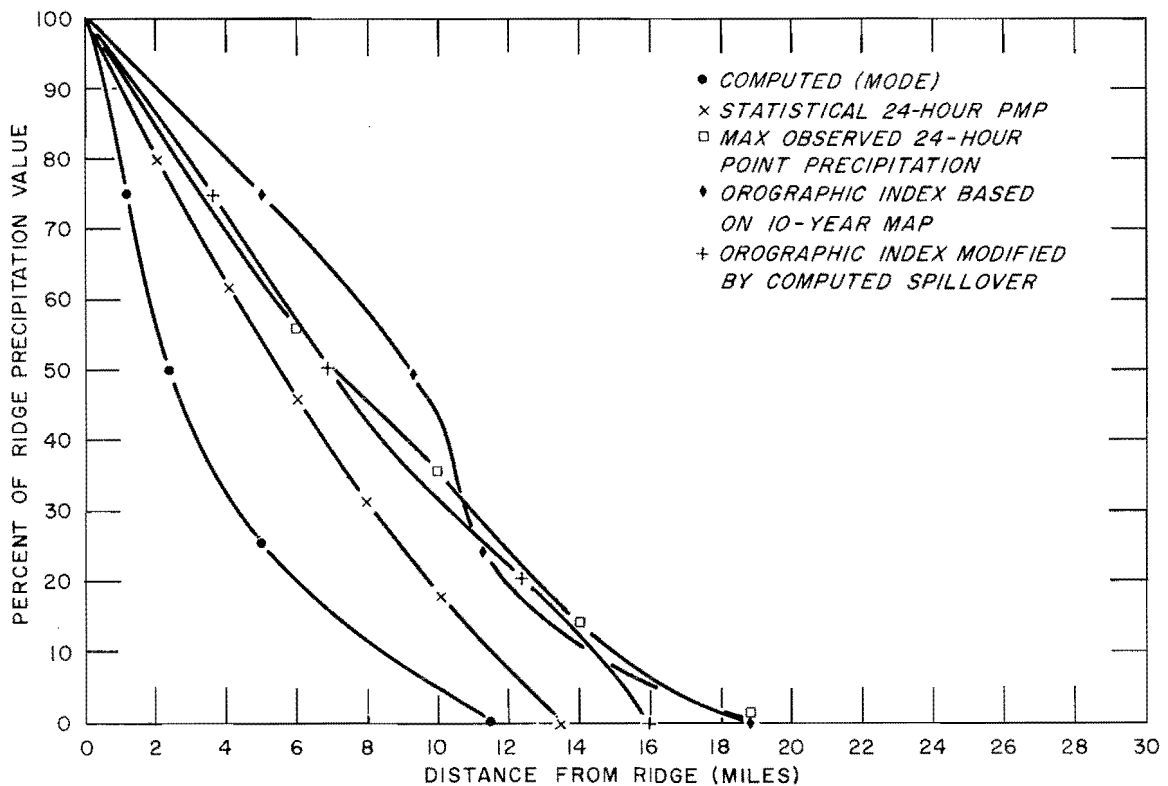
FIG. 6-6. SPILLOVER COMPARISON — PMP AND MAXIMUM OBSERVED PRECIPITATION
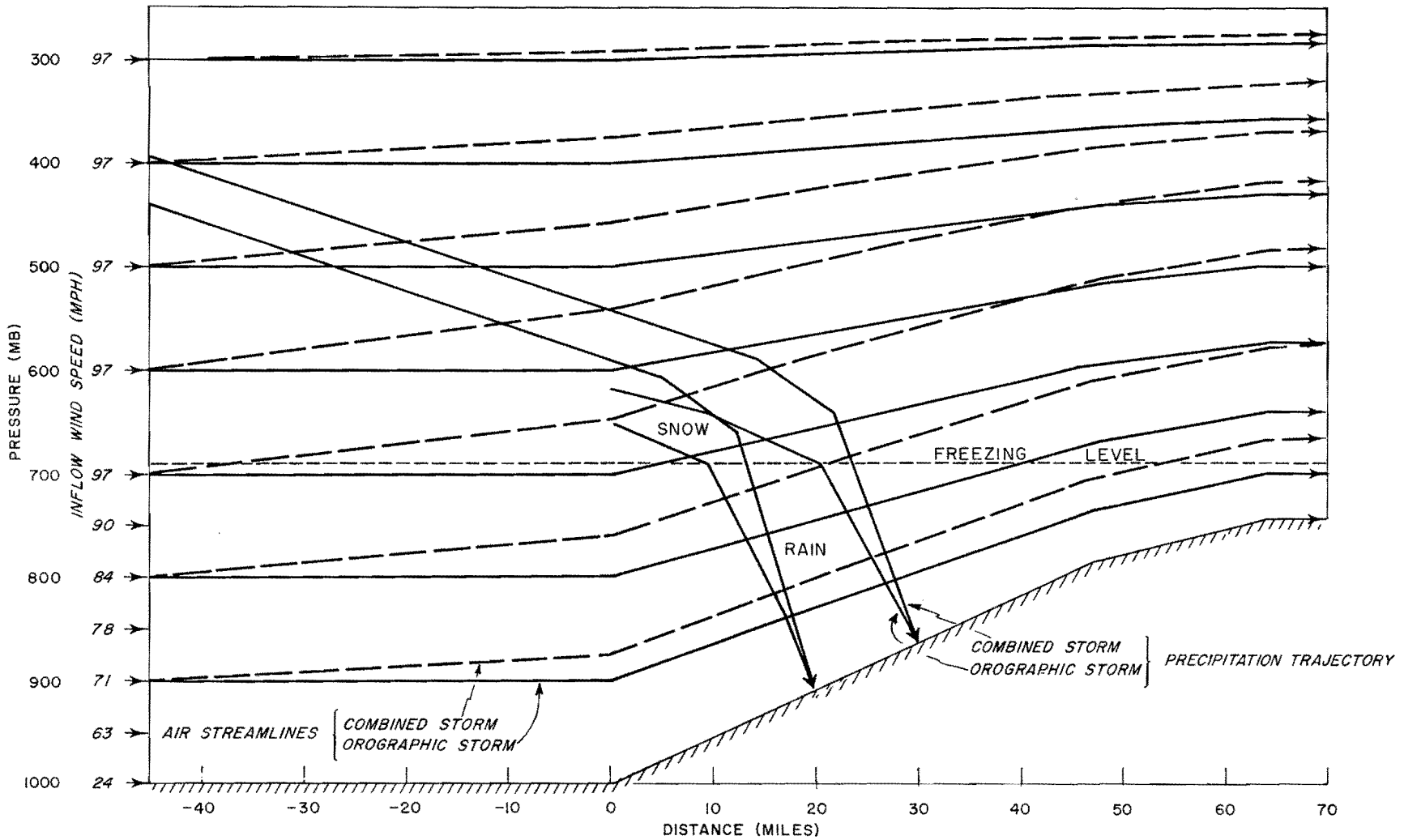
FIG. 7-1. SCHEMATIC COMPARISON OF SOME FEATURES OF OROGRAPHIC STORM AND COMBINED STORM
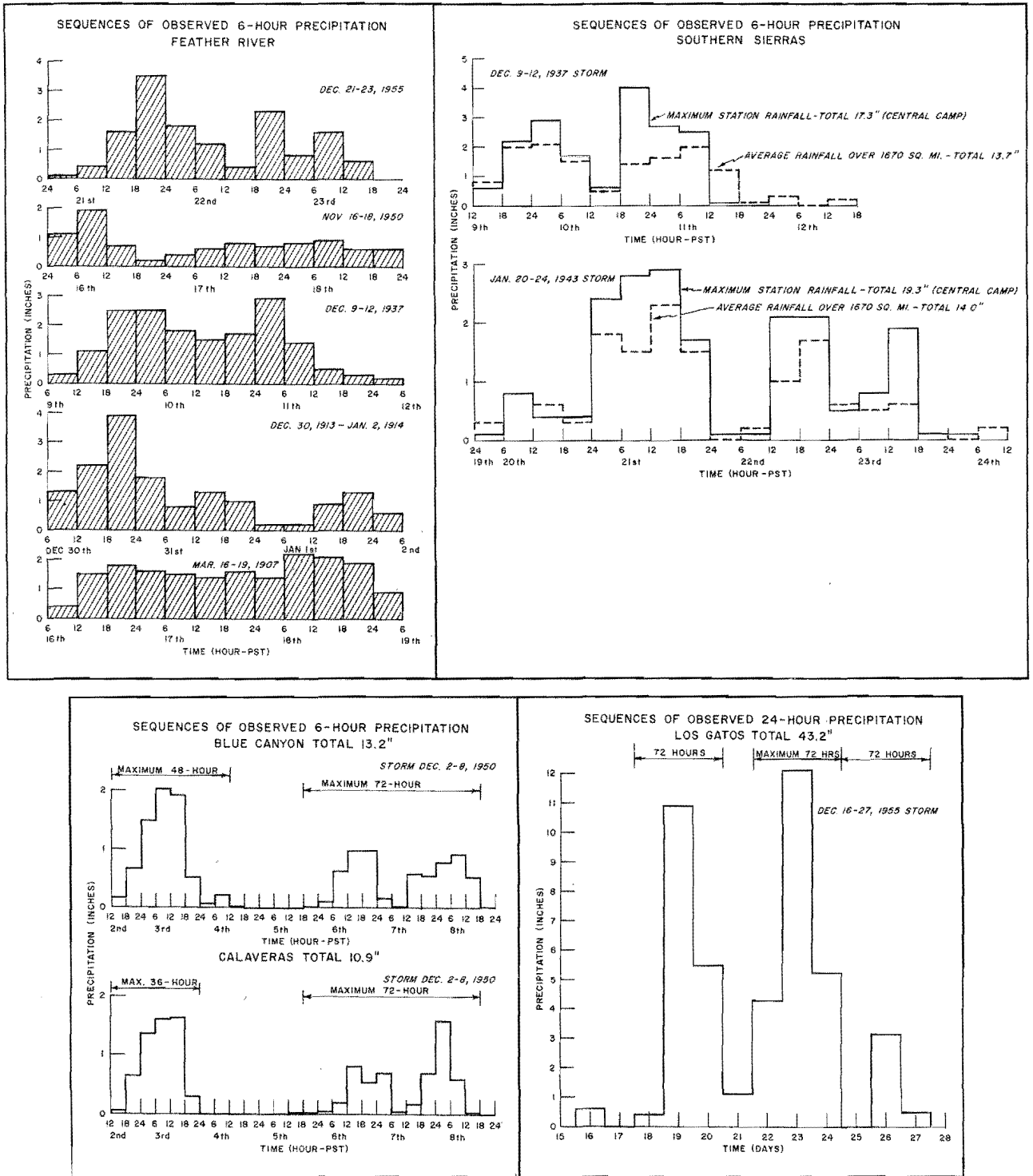
FIG. 7-2.   SEQUENCES OF OBSERVED PRECIPITATION
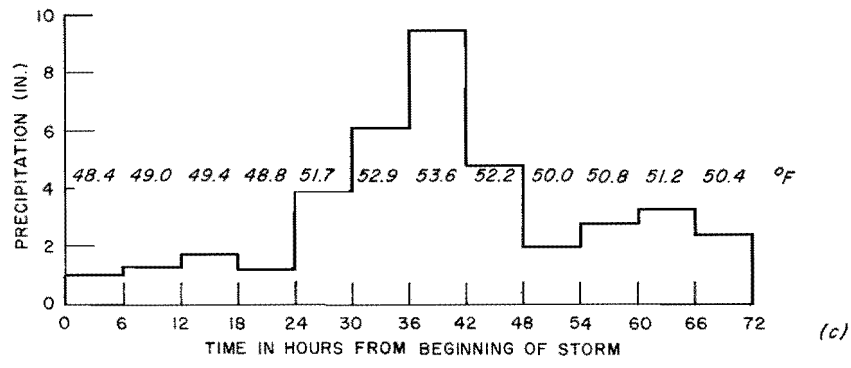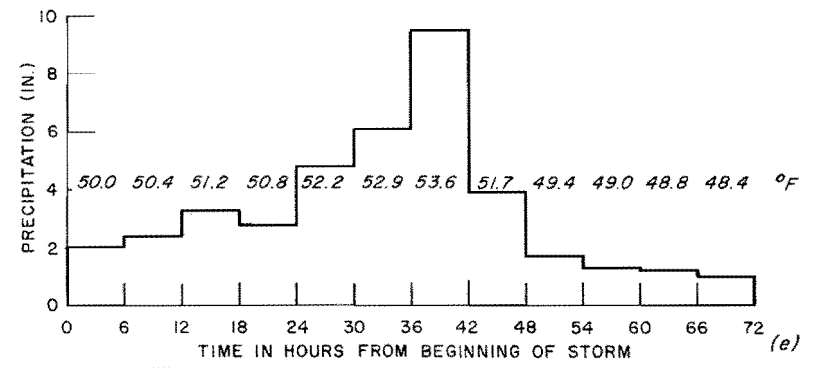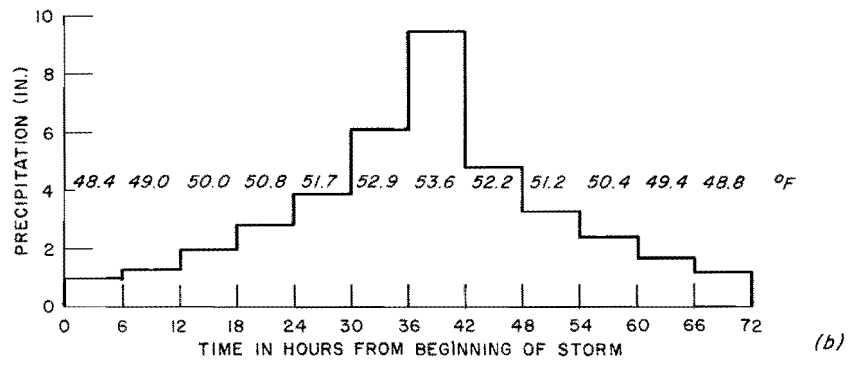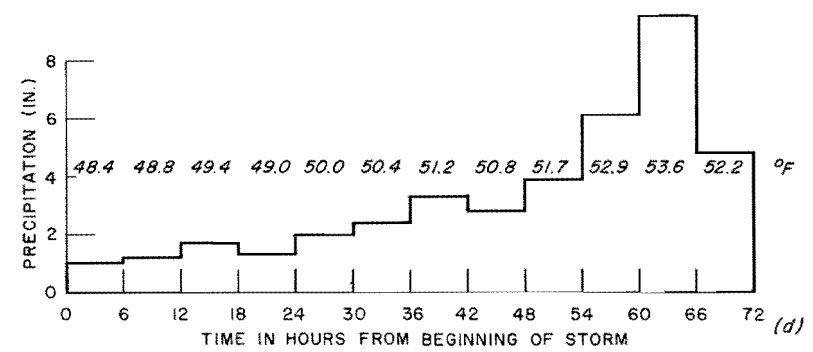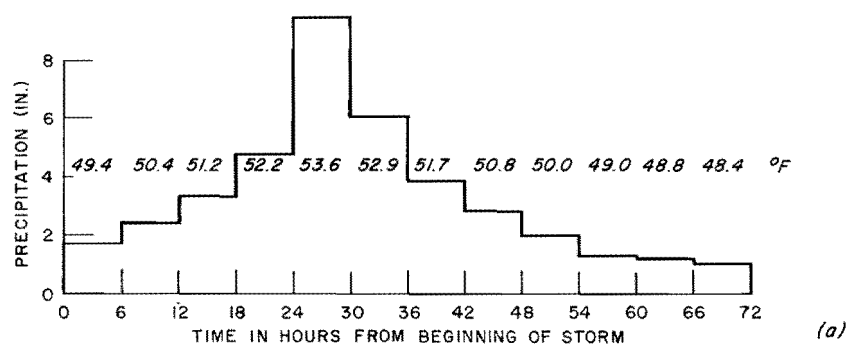
FIG. 7-3.   SAMPLE PMP TIME-SEQUENCES
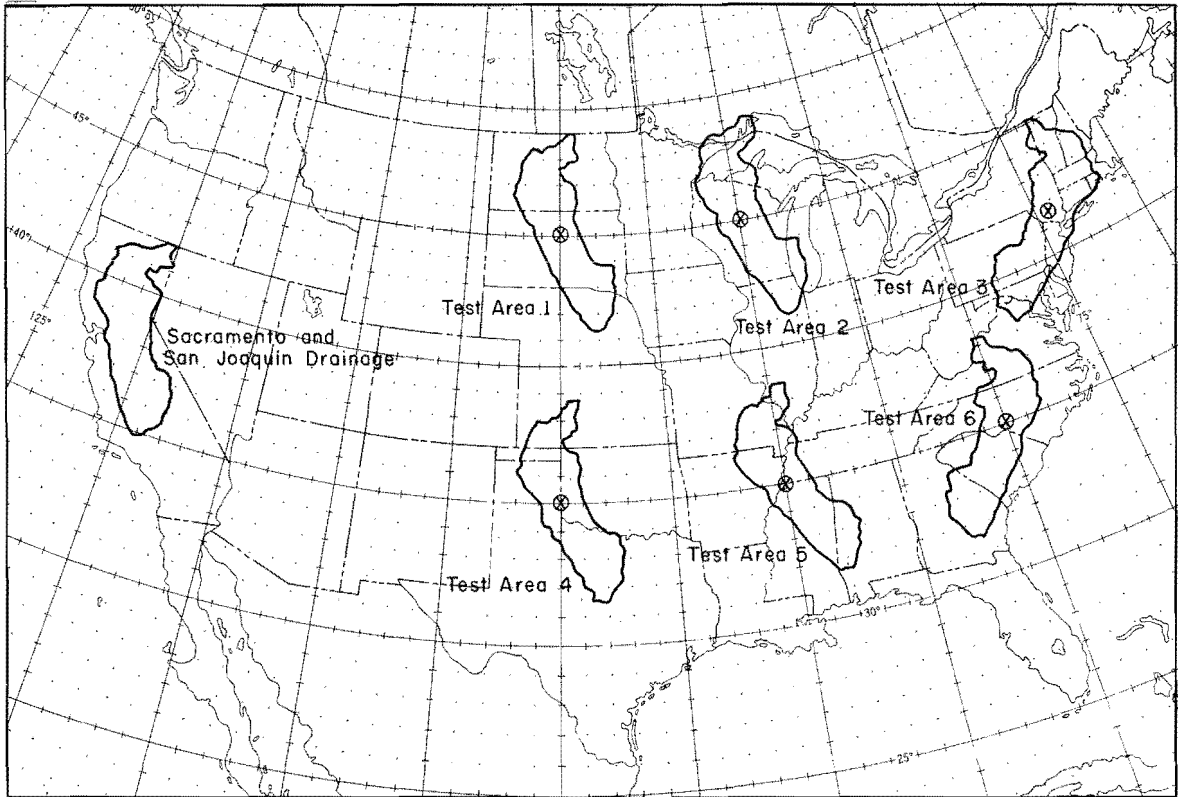
FIG. 8-1.   TEST AREAS FOR COMPARISON OF STORM VALUES WITH PMP
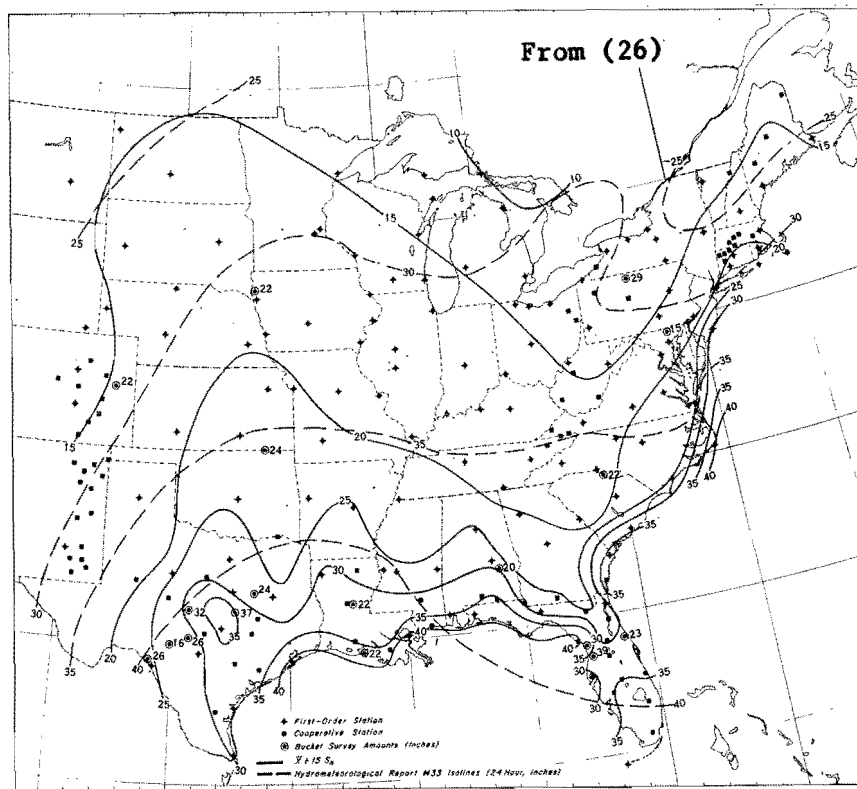
FIG. 8-2.   COMPARISON OF PMP FROM HYDROMETEOROLOGICAL REPORT NO. 33 WITH
STATISTICAL PMP FOR 24 HOURS AND 10 SQUARE MILES
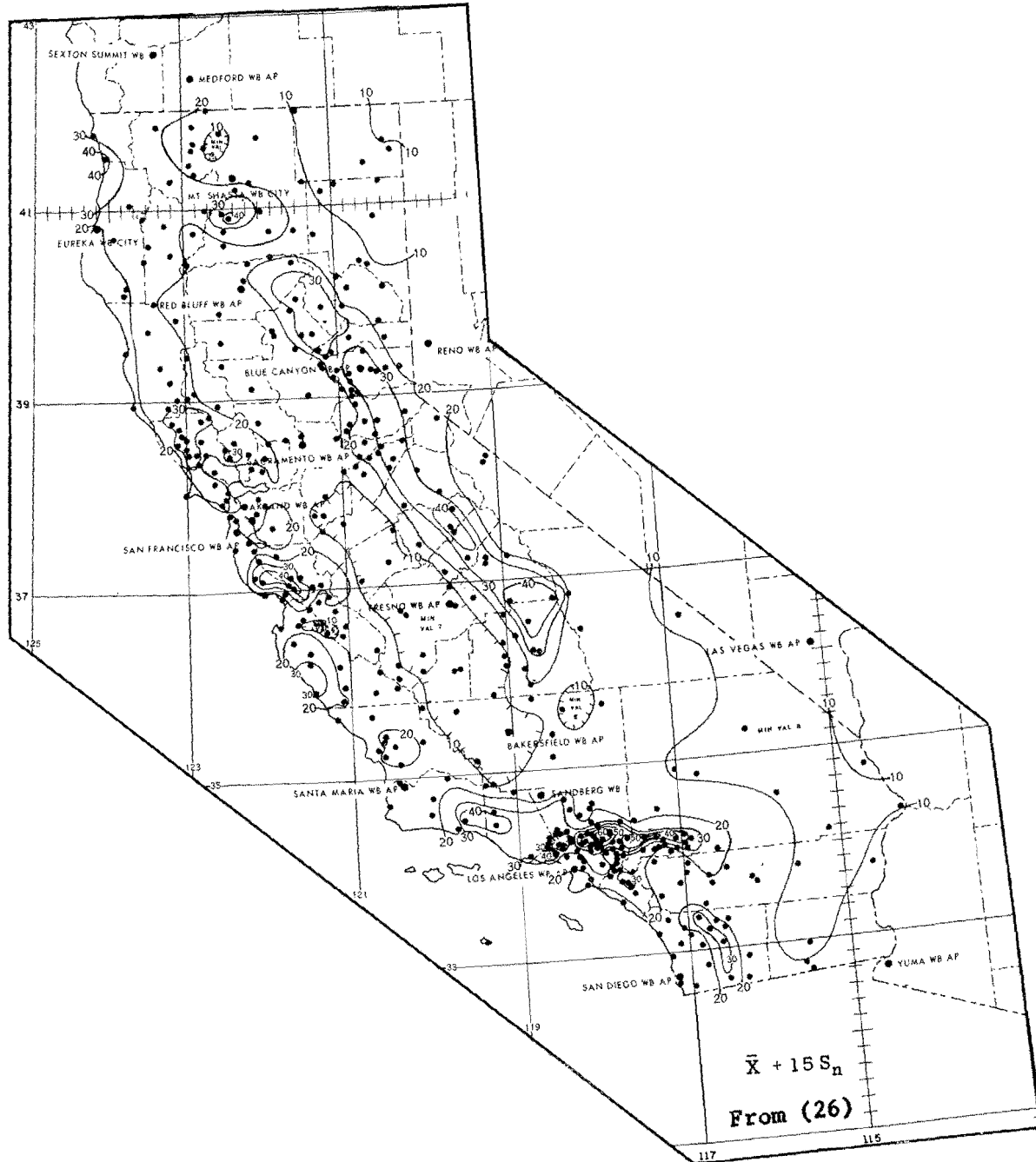
FIG. 8-3. STATISTICAL PMP FOR 24 HOURS AT A POINT, CALIFORNIA
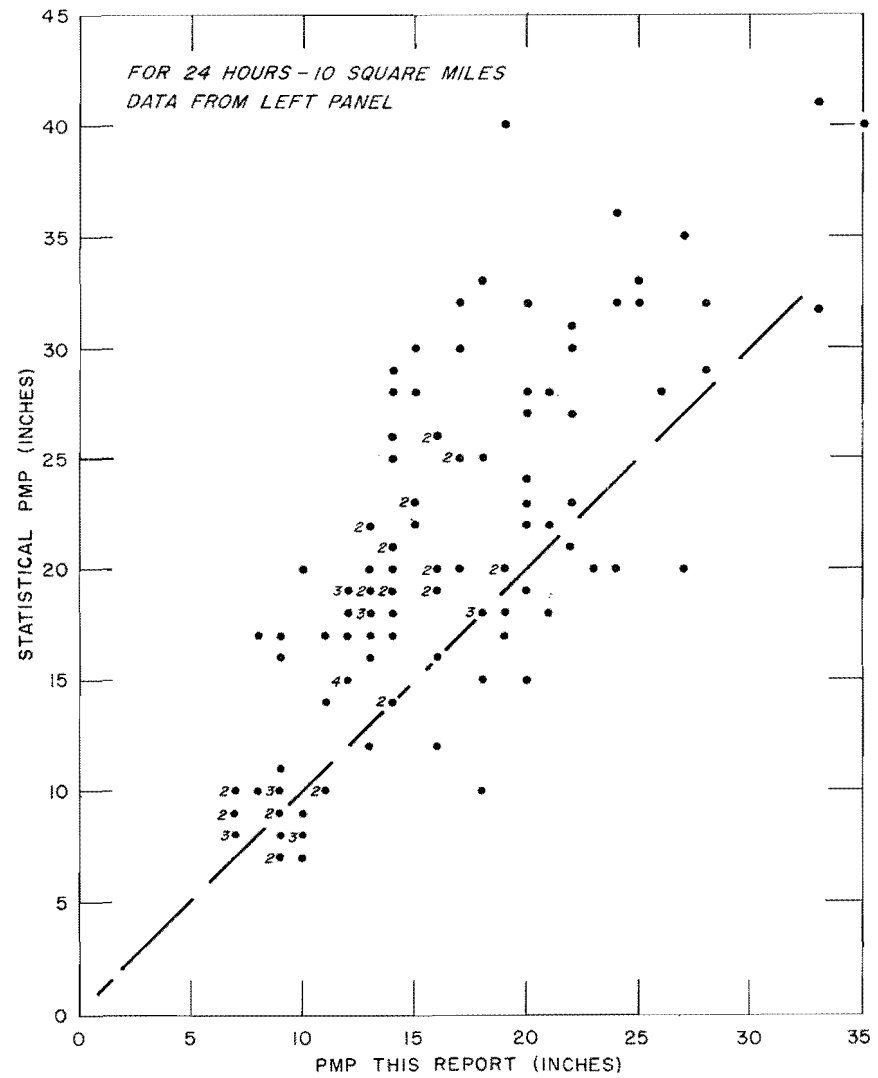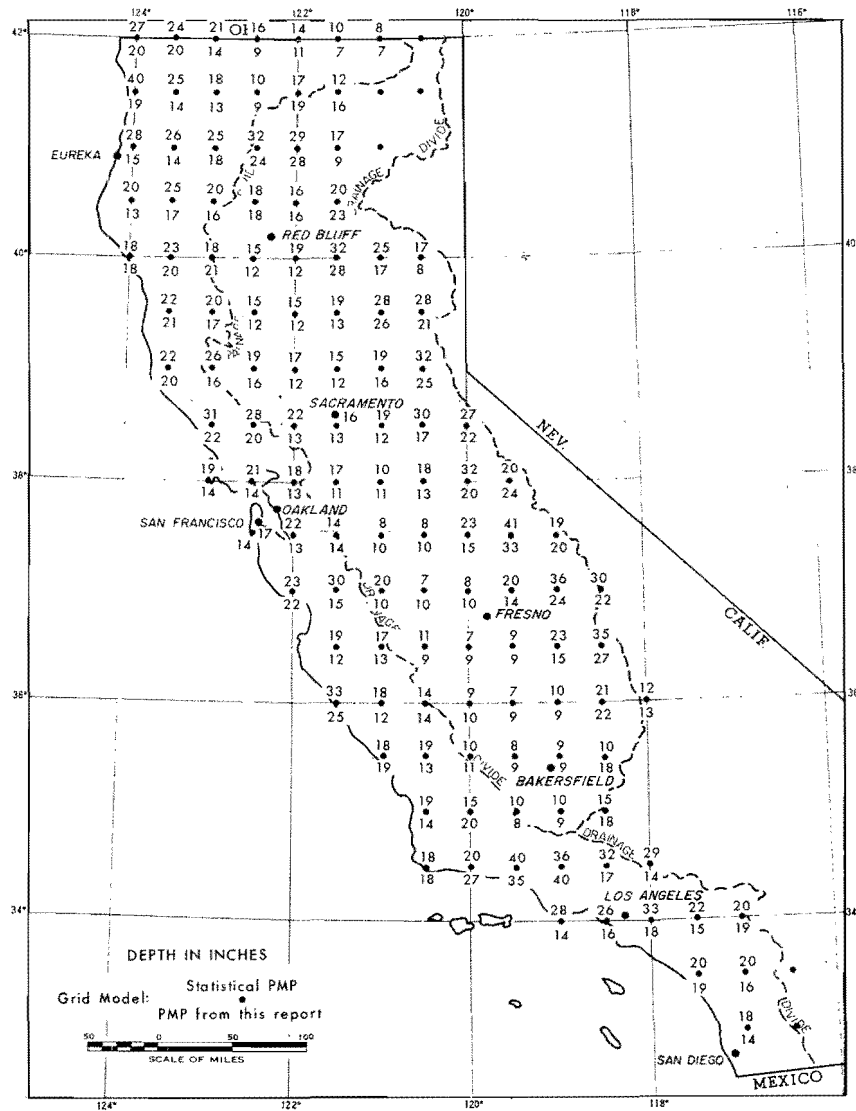
FIG. 8-4. COMPARISON OF STATISTICAL PMP WITH PMP FROM THIS REPORT FOR 24 HOURS AND 10 SQUARE MILES
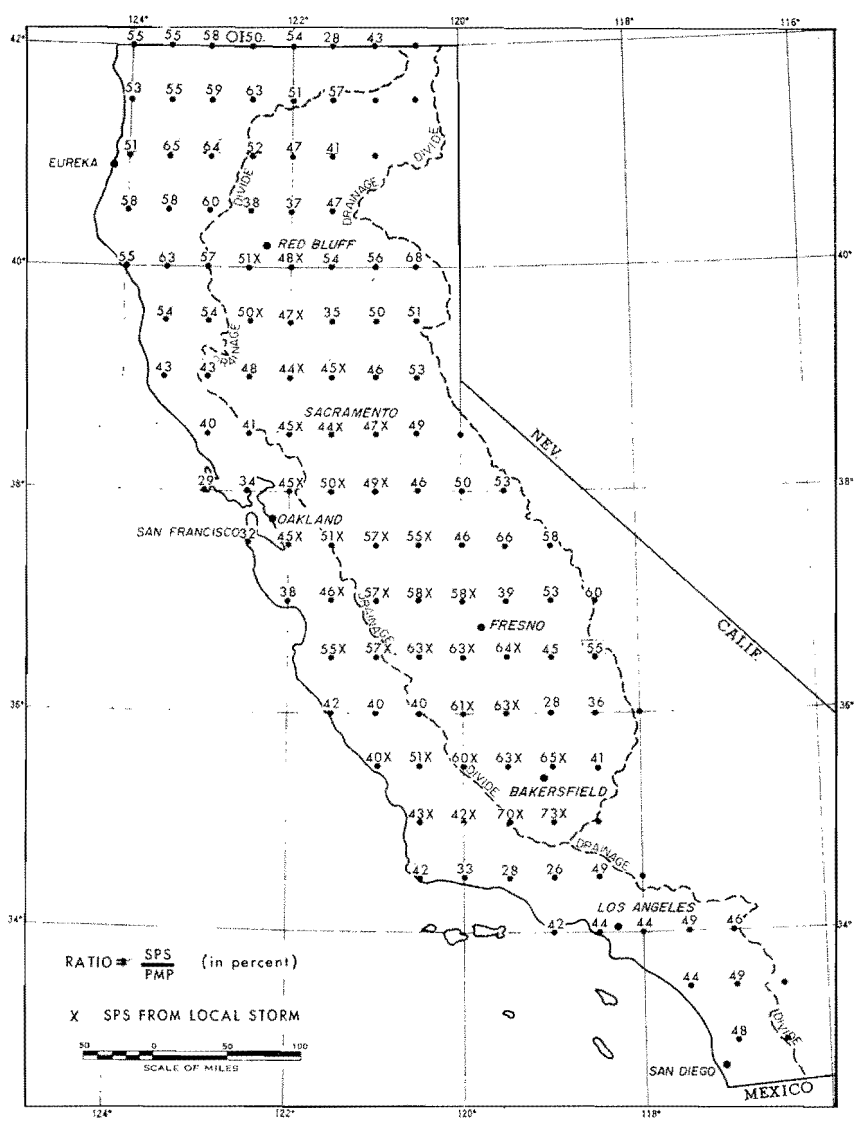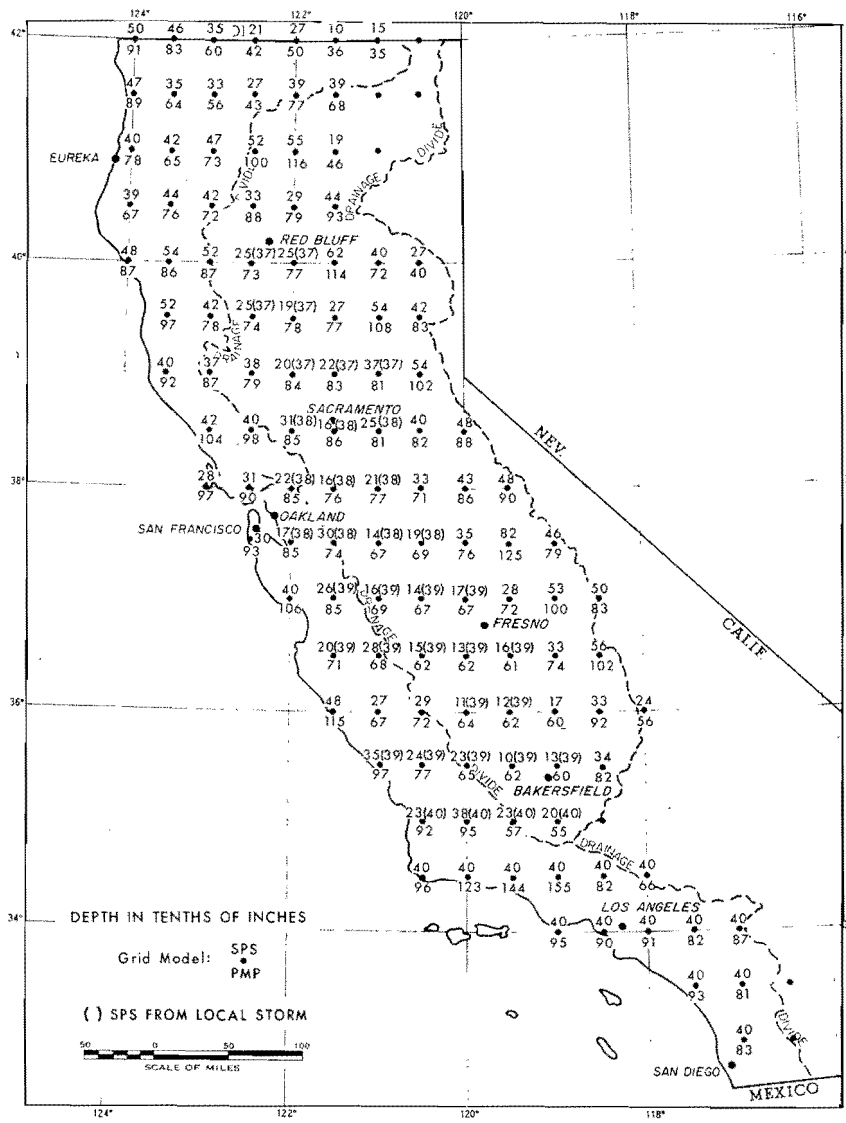
FIG. 8-5. COMPARISON OF SPS AND PMP FOR 6 HOURS AND 10 SQUARE MILES
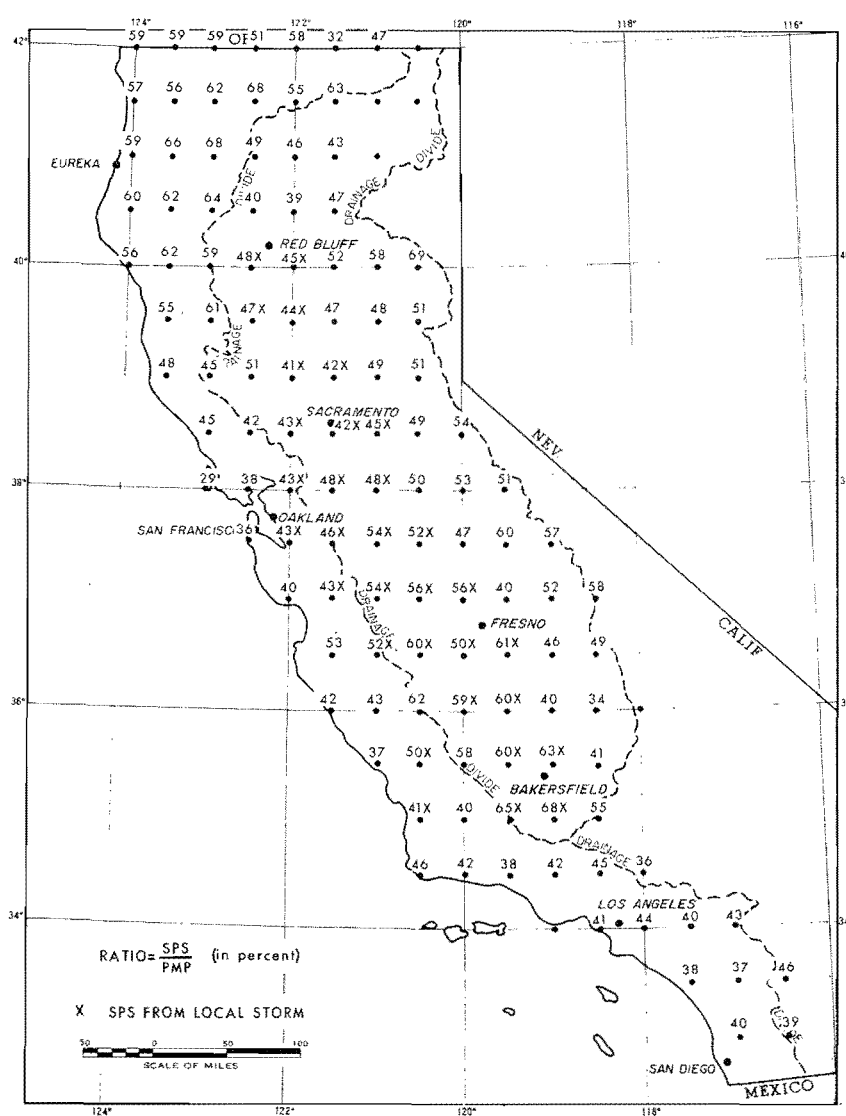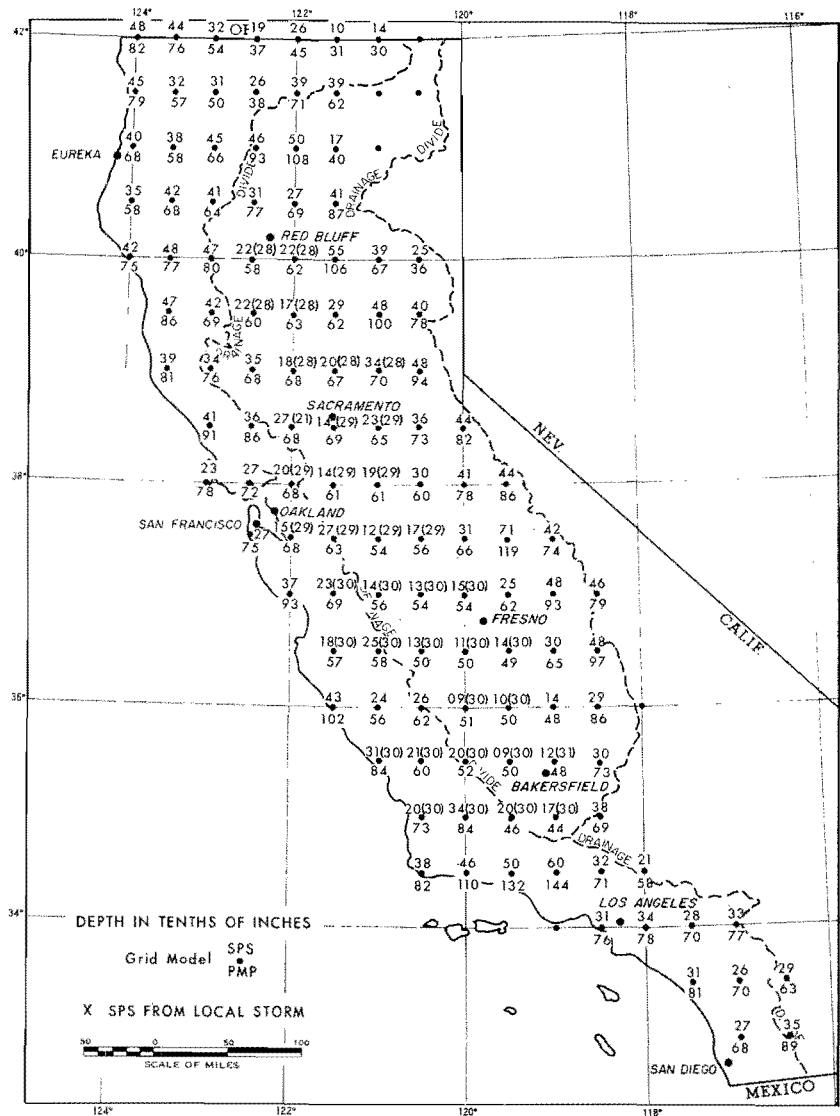
FIG. 8-6. COMPARISON OF SPS AND PMP FOR 6 HOURS AND 200 SQUARE MILES
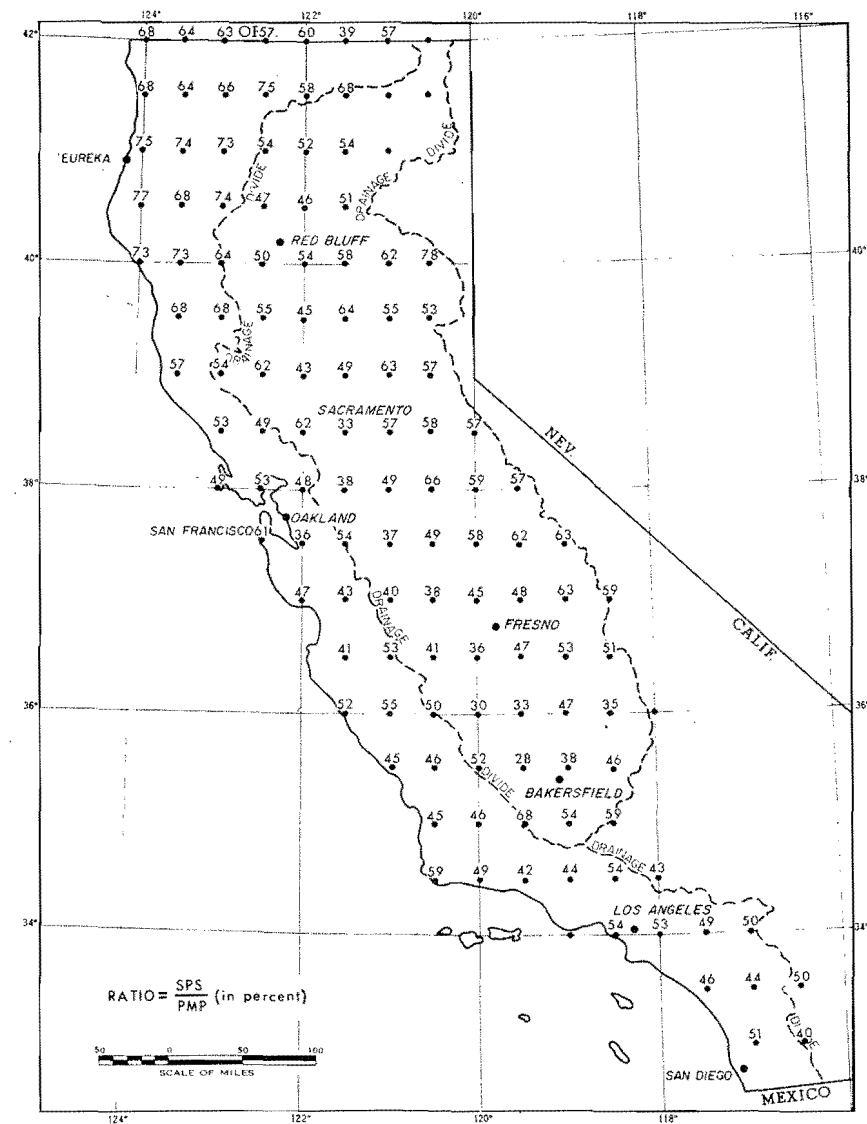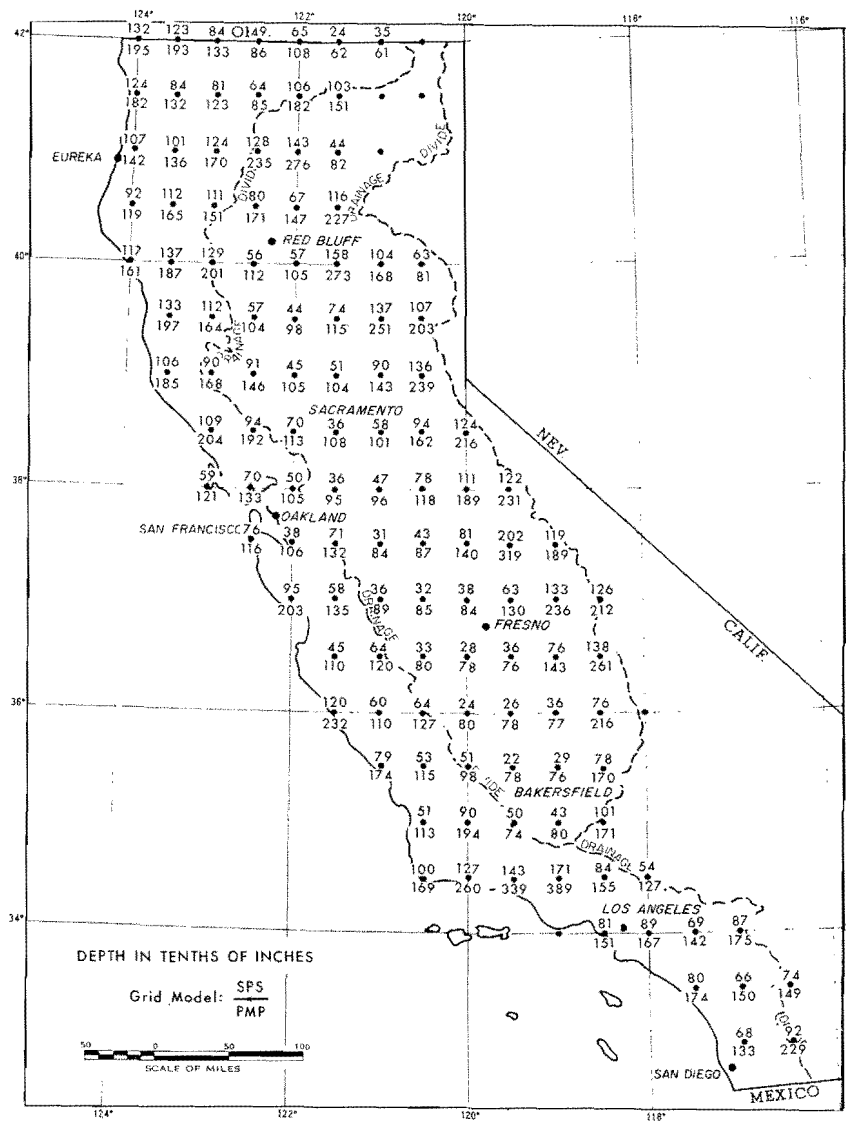
FIG. 8-7. COMPARISON OF SPS AND PMP FOR 24 HOURS AND 200 SQUARE MILES
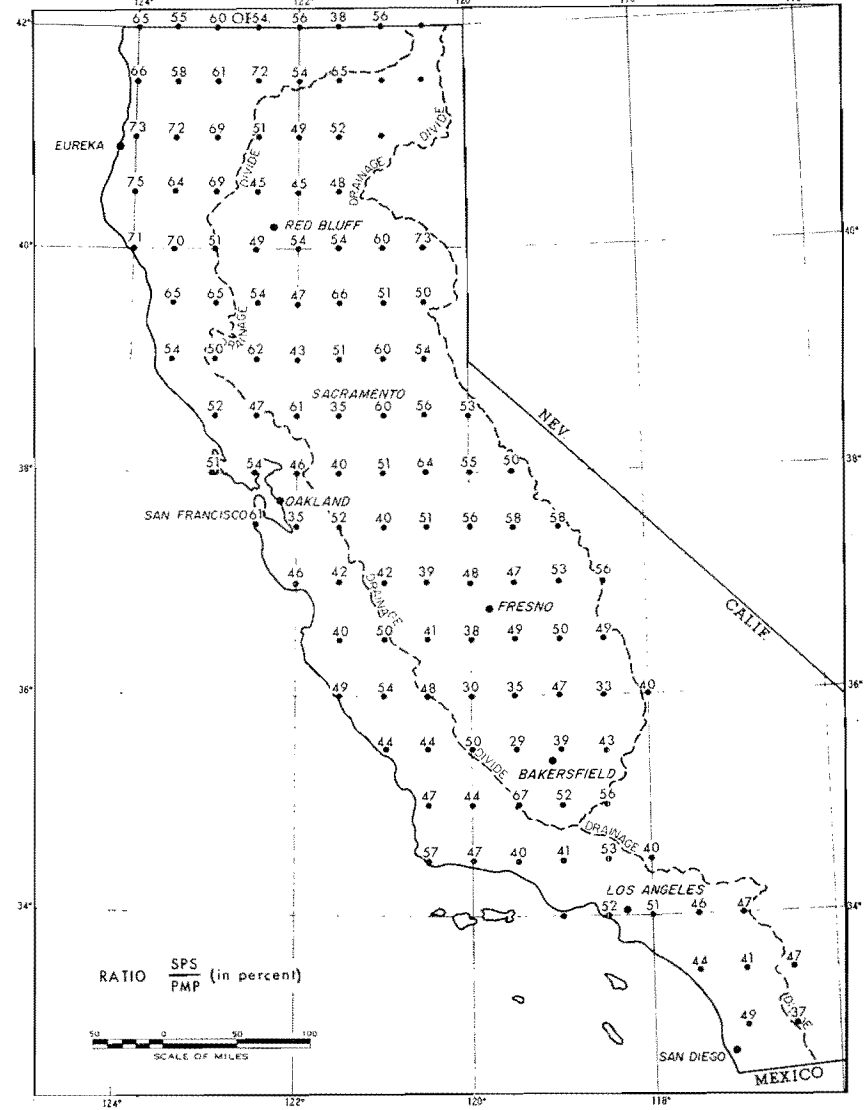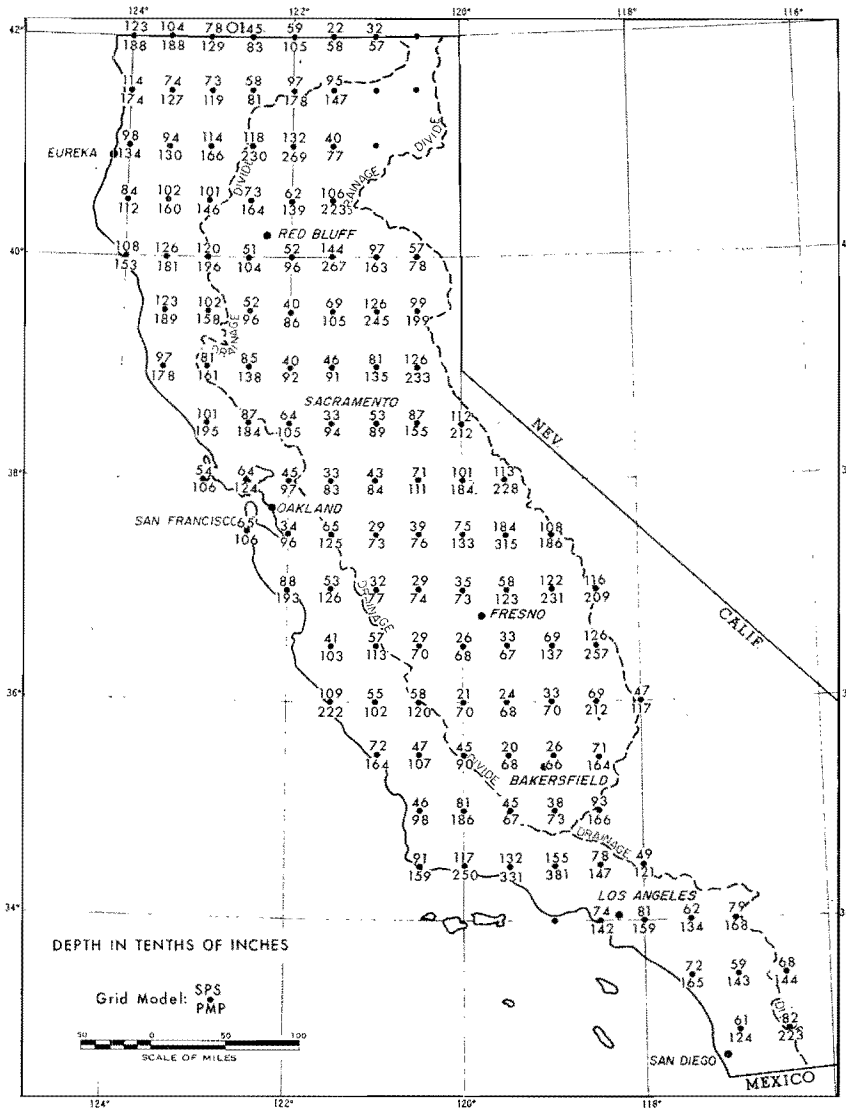
FIG. 8-8. COMPARISON OF SPS AND PMP FOR 24 HOURS AND 1000 SQUARE MILES
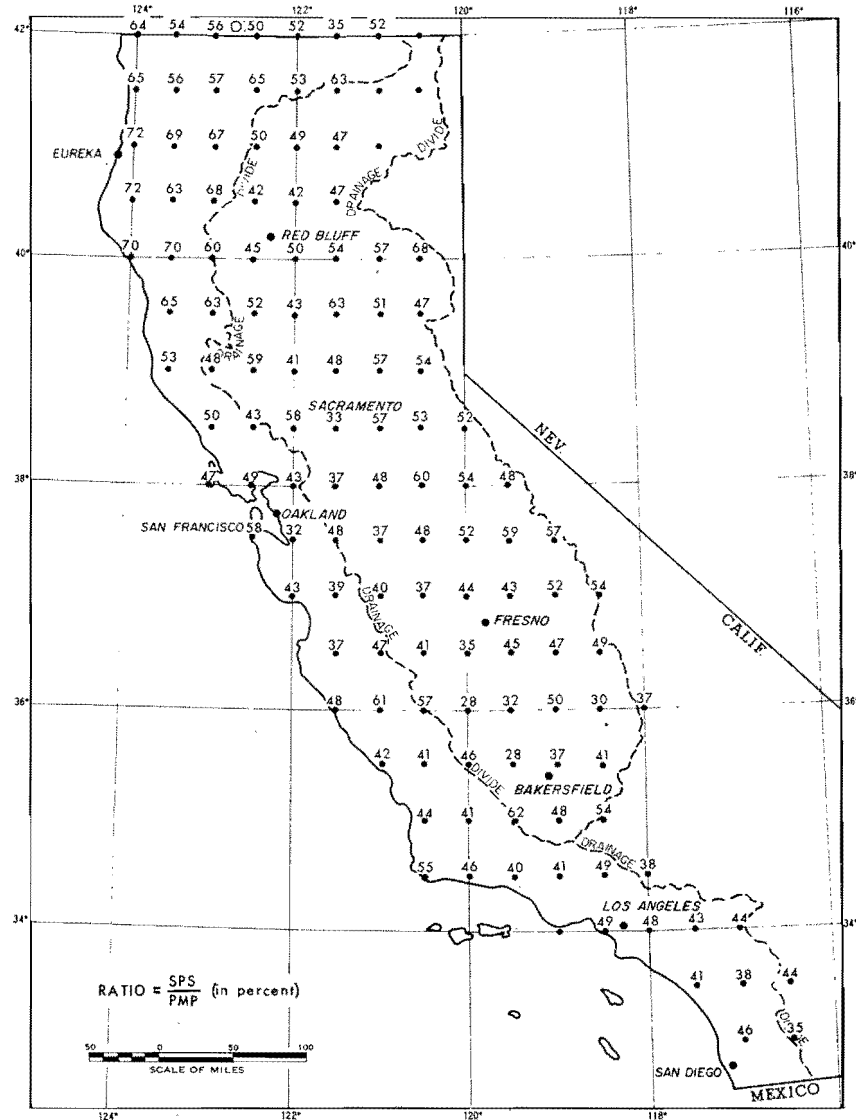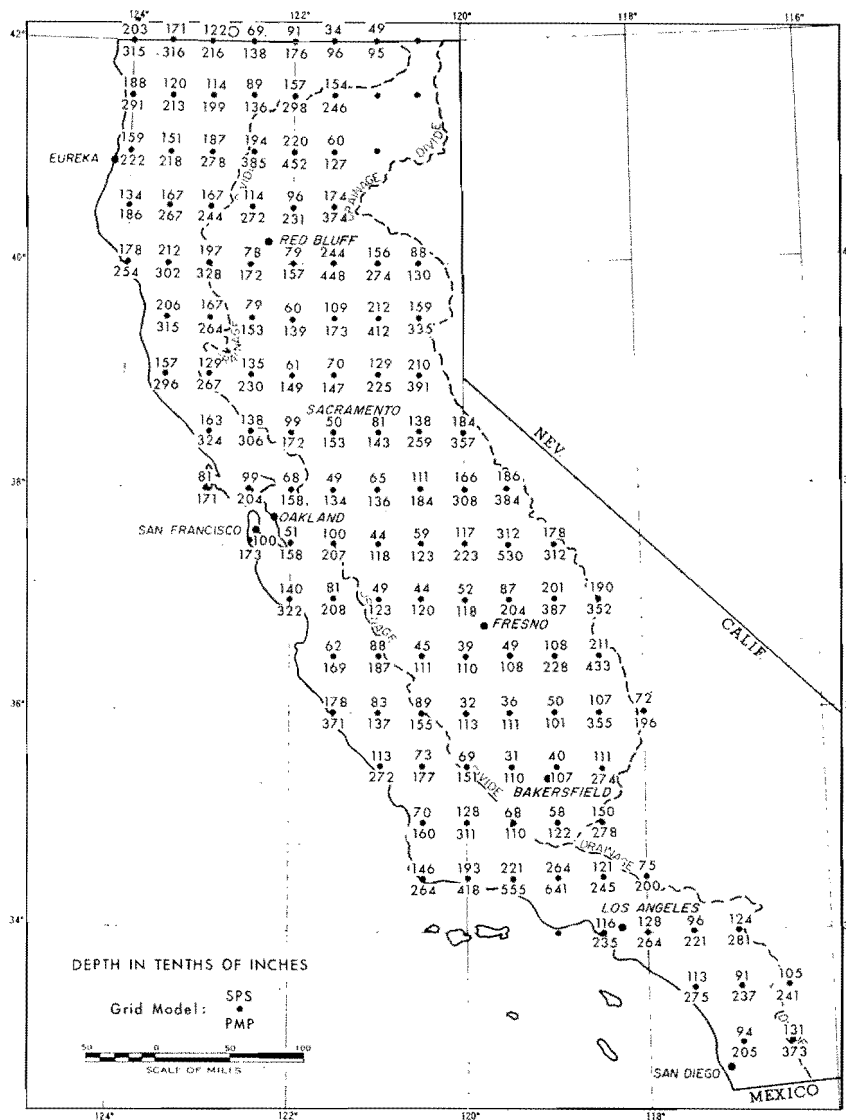
FIG. 8-9. COMPARISON OF SPS AND PMP FOR 72 HOURS AND 1000 SQUARE MILES
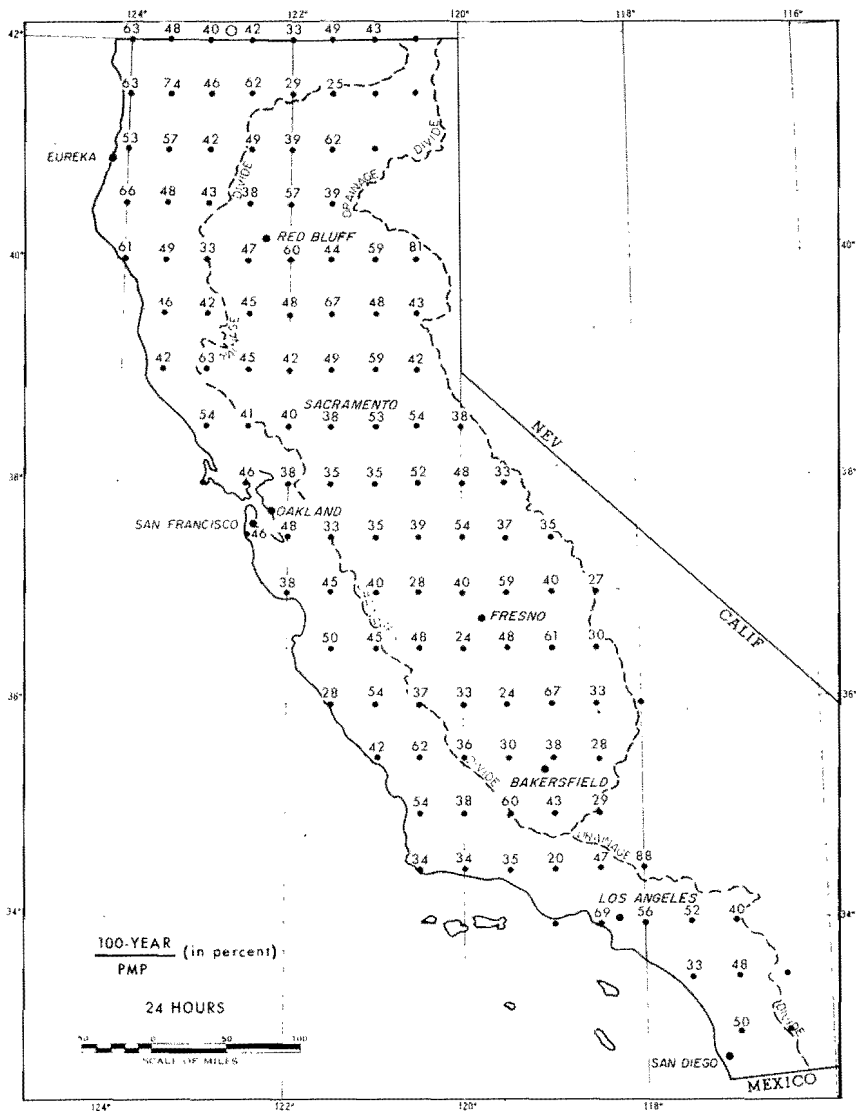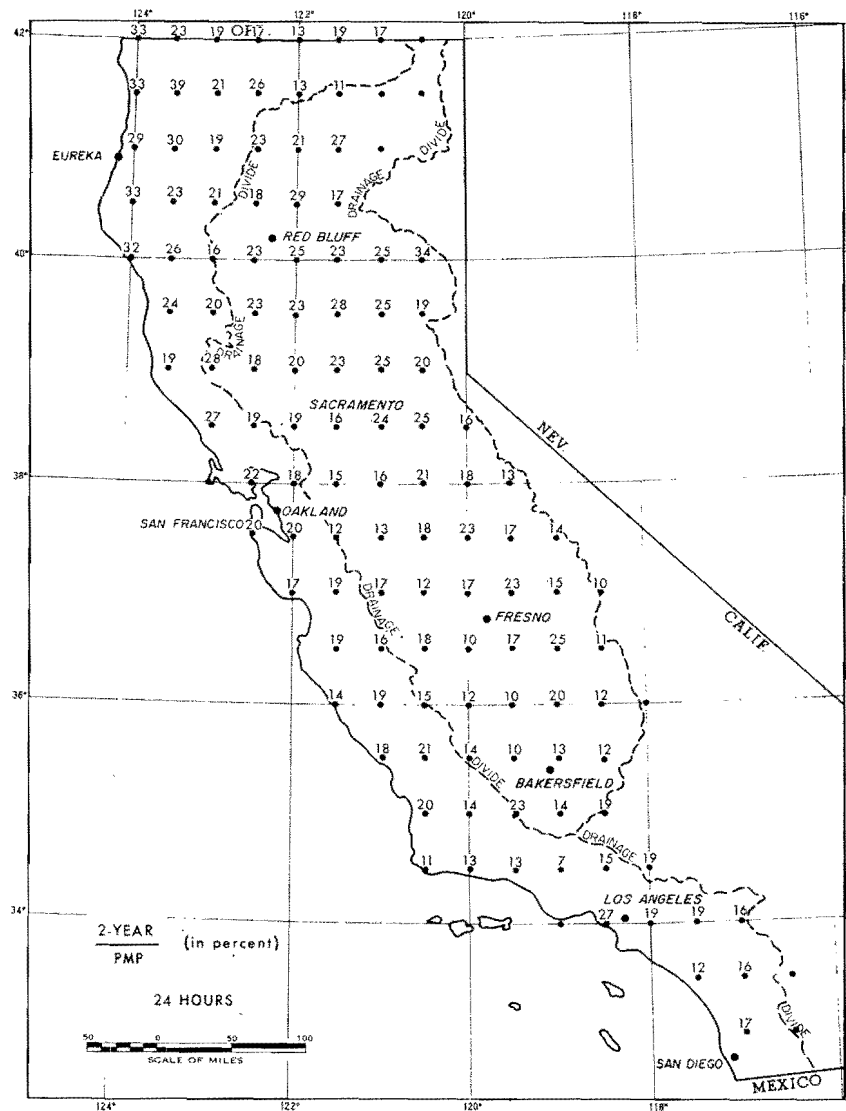
FIG. 8-10. RATIO OF 2-YEAR AND 100-YEAR 24-HOUR PRECIPITATION TO 10-SQUARE-MILE 24-HOUR PMP
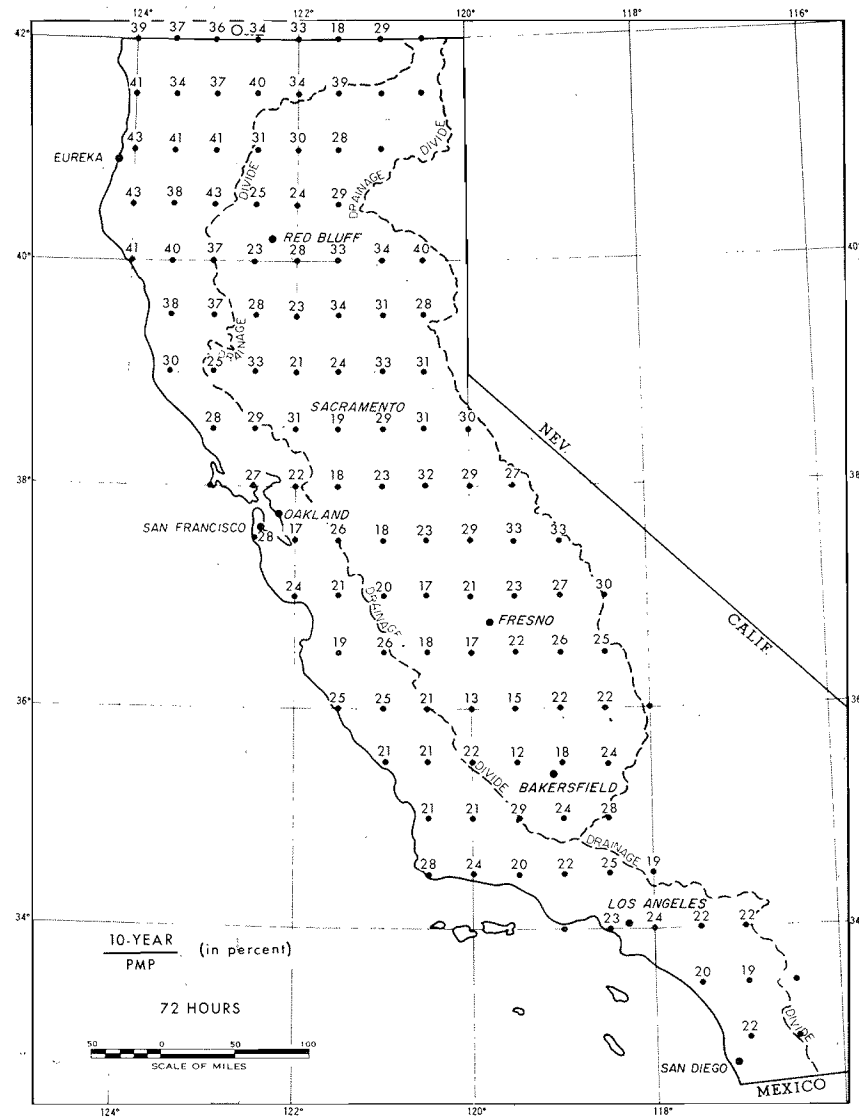
FIG. 8-11. RATIO OF 10-YEAR 72-HOUR PRECIPITATION TO 10-SQUARE-MILE 72-HOUR PMP
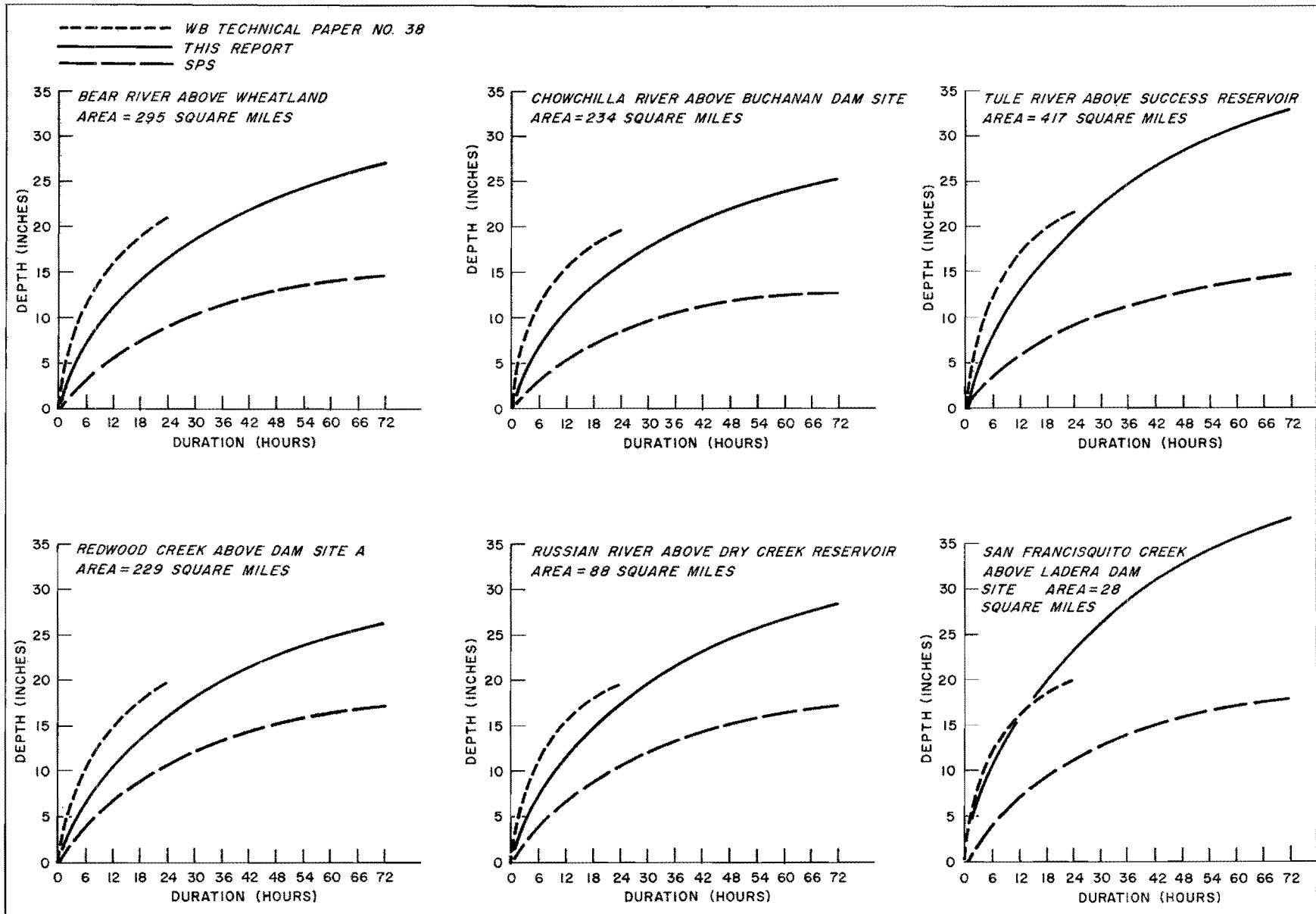
FIG. 8-12. COMPARISON OF PMP FROM W. B. TECHNICAL PAPER NO. 38 WITH PMP FROM THIS REPORT AND STANDARD PROJECT STORM (SPS), FOR SELECTED BASINS

Left Map

EUREKA

RED BLUFF

SACRAMENTO

SAN FRANCISCO OAKLAND

FRESNO

BAKERSFIELD

LOS ANGELES

SAN DIEGO

NEV CALIF MEXICO

DEPTH IN TENTHS OF INCHES

Grid Model: W.B.T.P. No. 38 / this report

SCALE OF MILES

Right Map

EUREKA

RED BLUFF

SACRAMENTO

SAN FRANCISCO OAKLAND

FRESNO

BAKERSFIELD

LOS ANGELES

SAN DIEGO

NEV CALIF MEXICO

PMP FROM THIS REPORT MINUS PMP FROM
W.B. TECHNICAL PAPER NO. 38 (INCHES)

( ) High spot from orographic index map this report

[ ] High spot from index map of Tech. Paper NO.38

SCALE OF MILES

FIG. 8-13. COMPARISON OF PMP FROM W.B. TECHNICAL PAPER NO. 38 WITH THIS REPORT
FOR 24 HOURS AND 200 SQUARE MILES
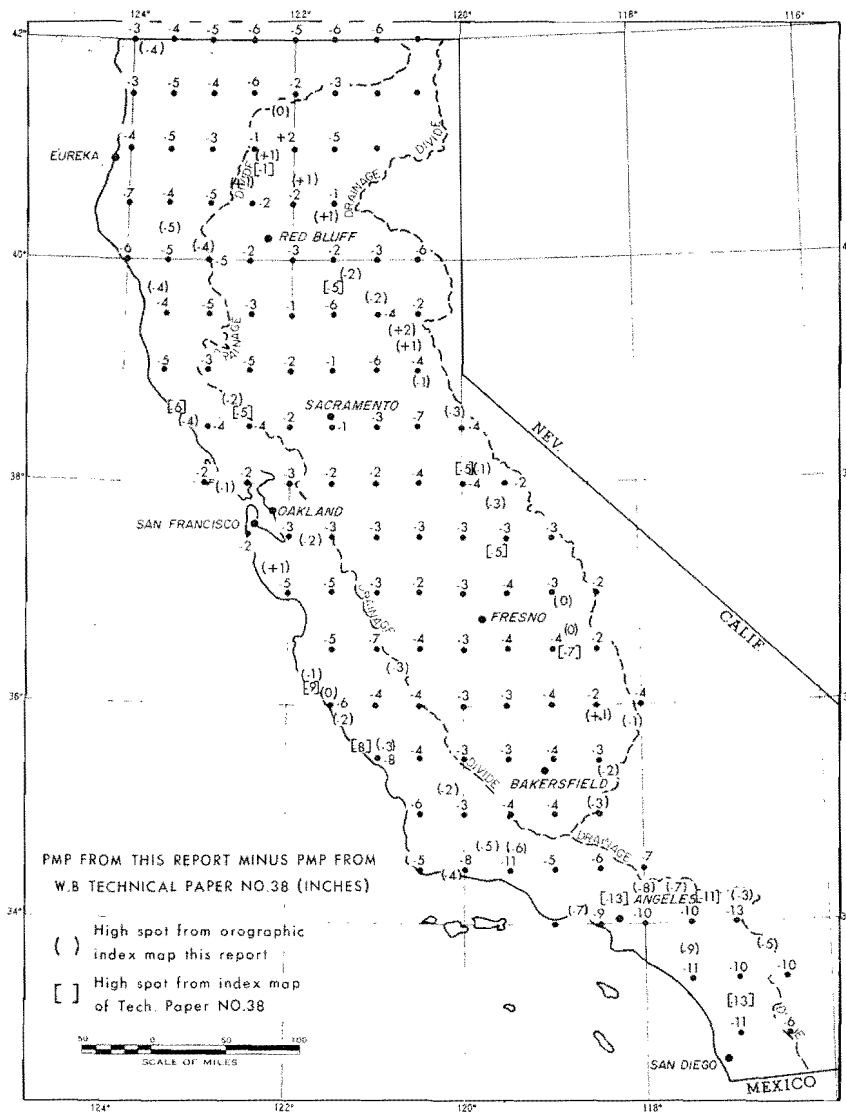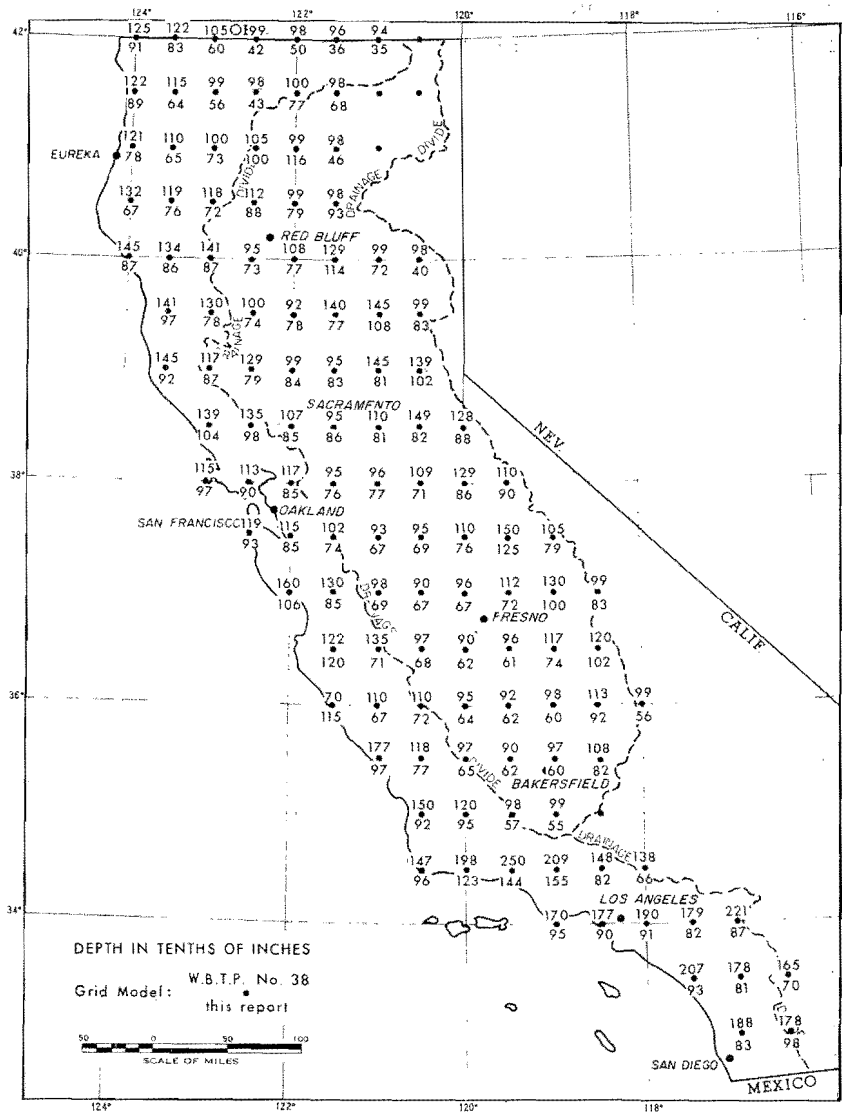
FIG. 8-14. COMPARISON OF PMP FROM W. B. TECHNICAL PAPER NO. 38 WITH THIS REPORT
FOR 6 HOURS AND 10 SQUARE MILES
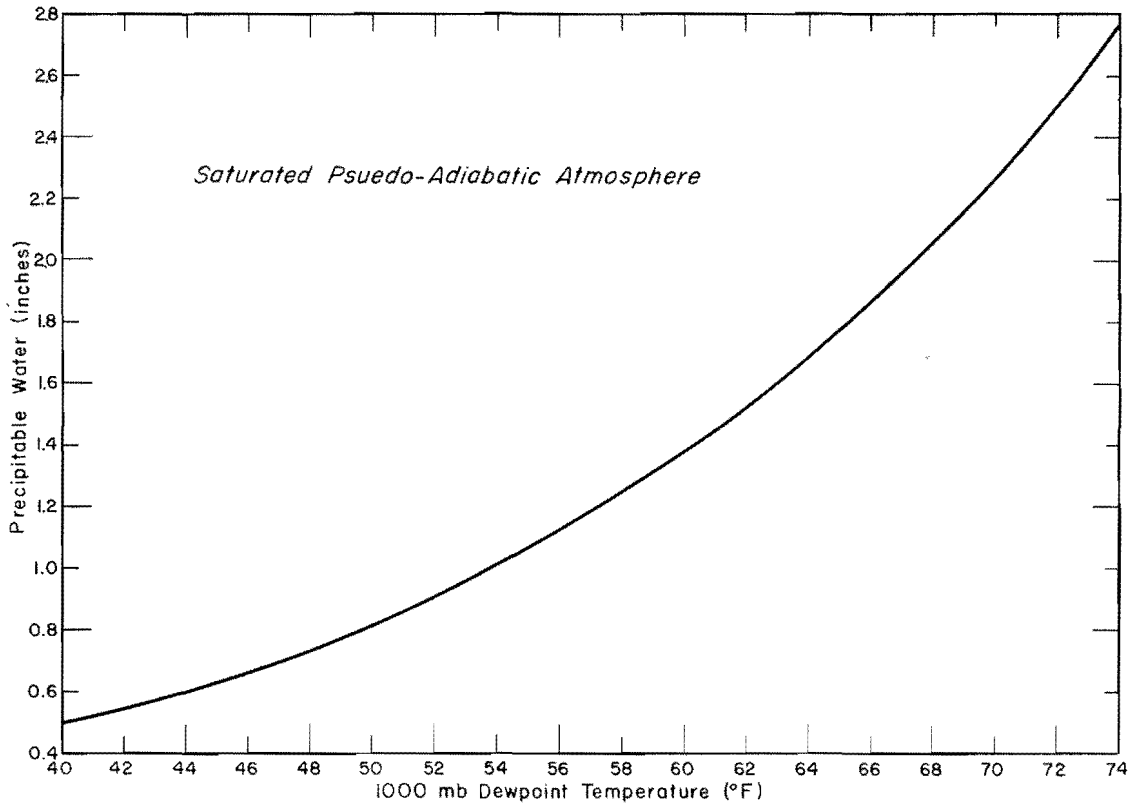
FIG. 10-1. VARIATION OF PRECIPITABLE WATER WITH 1000-MB DEW POINT TEMPERATURE
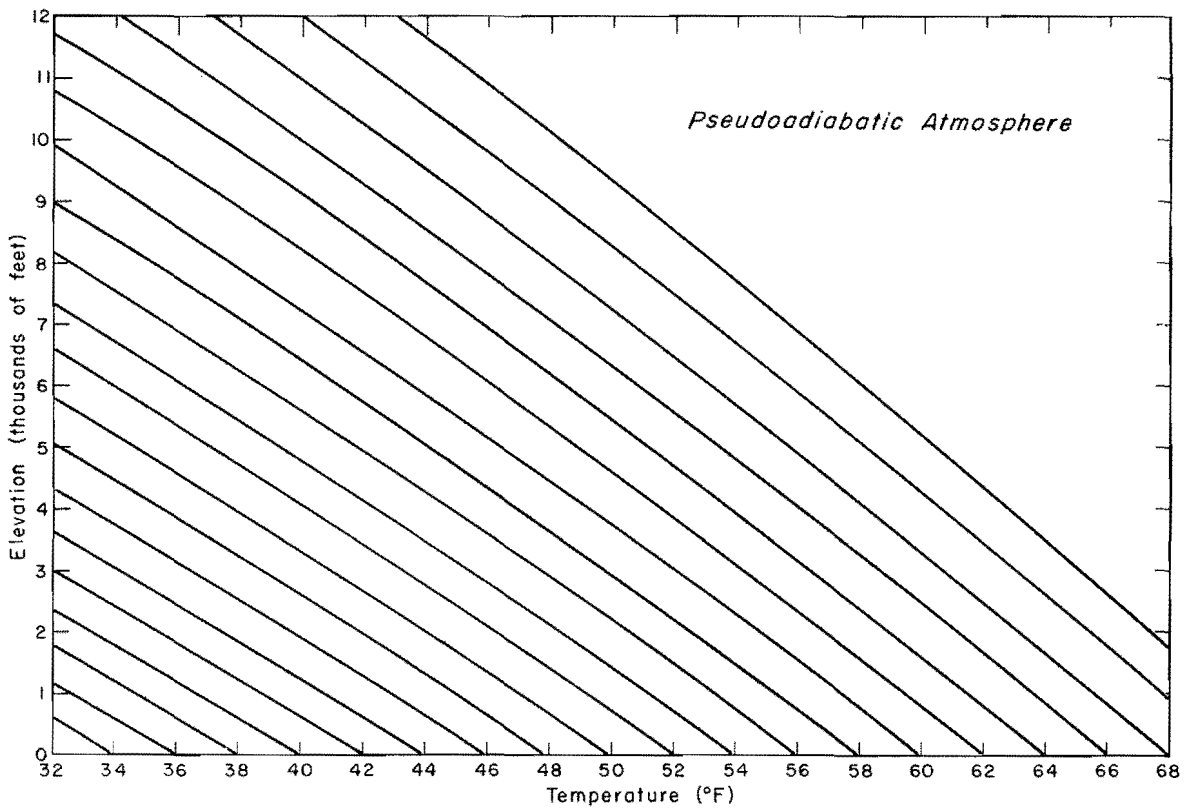
FIG. 10-2. DECREASE OF TEMPERATURE WITH ELEVATION
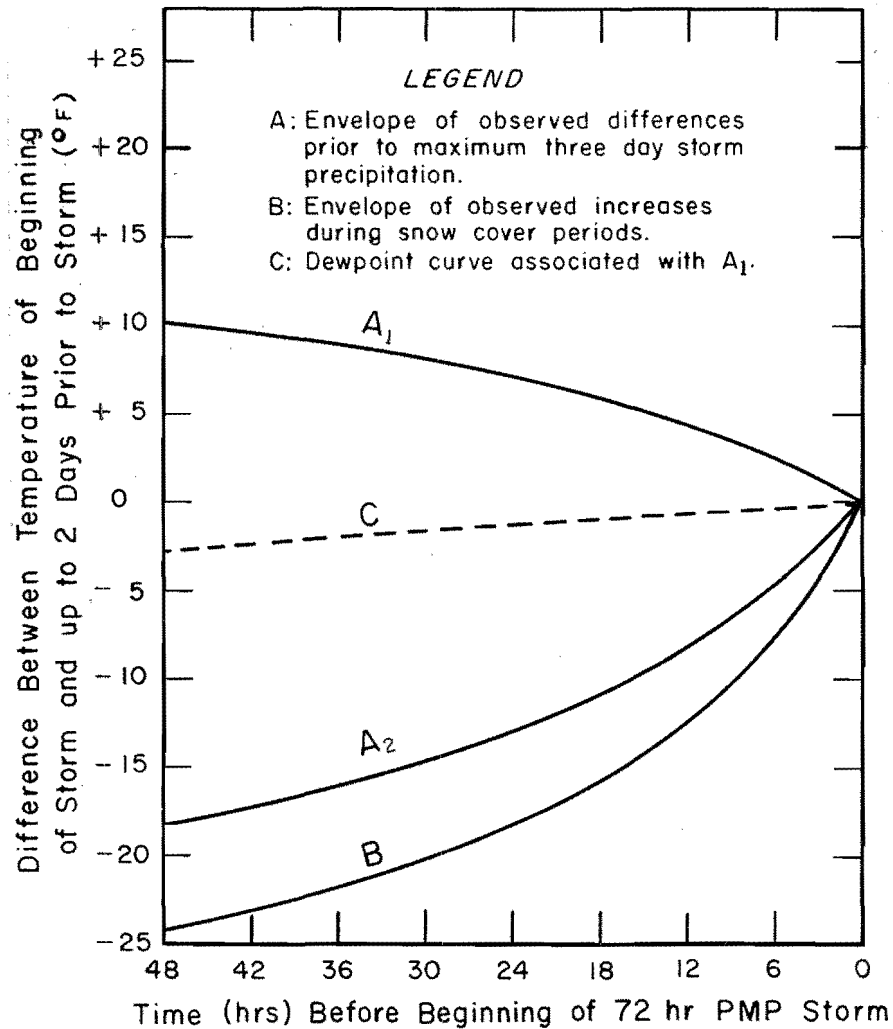
FIG. 10-3. TEMPERATURES PRIOR TO A PMP STORM
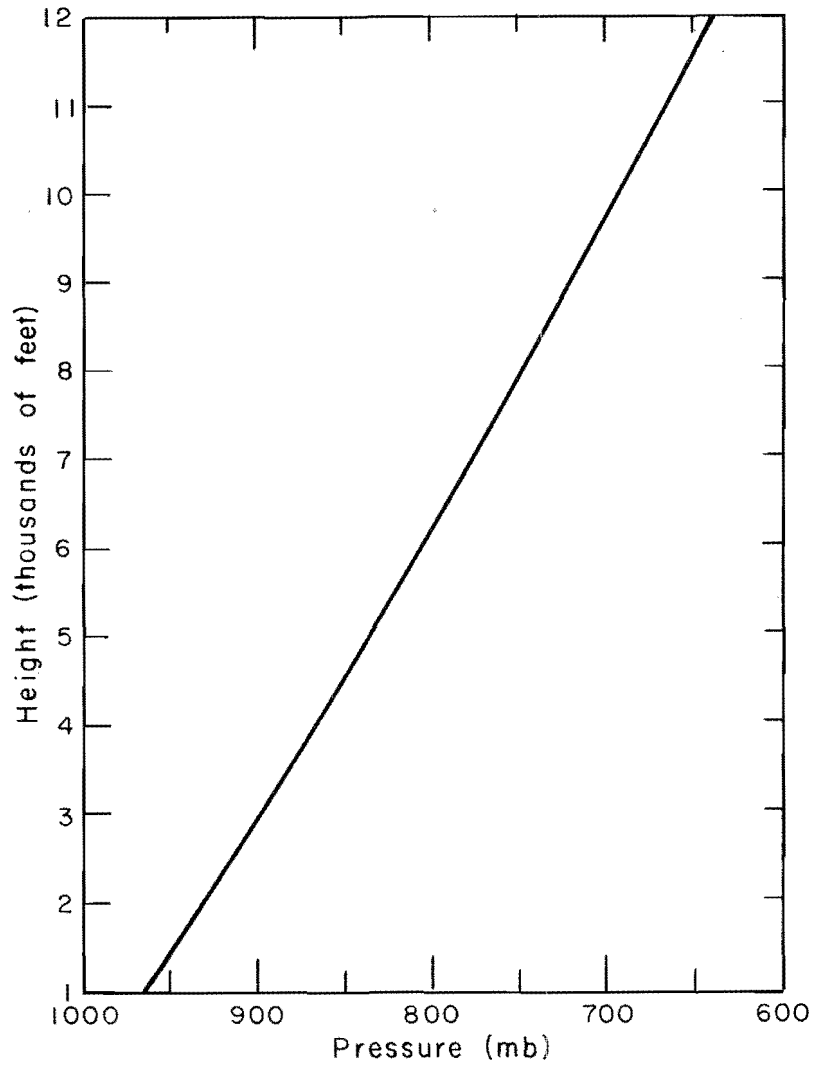
FIG. 10-4. PRESSURE-HEIGHT RELATION

Revisions of October 1969 to

Hydrometeorological Report No. 36

INTERIM REPORT - PROBABLE MAXIMUM PRECIPITATION IN CALIFORNIA

For distribution to all users of
Hydrometeorological Report No. 36

Prepared by

Hydrometeorological Branch
Office of Hydrology

October 1969

INTERIM REPORT - PROBABLE MAXIMUM PRECIPITATION IN CALIFORNIA

Revisions of October 1969

Introduction

The "Interim Report - Probable Maximum Precipitation in California," Hydrometeorological Report No. 36, was published in 1961. It provides estimates of probable maximum precipitation for storm durations up to 72 hours for basin areas up to several thousand square miles throughout the Pacific drainage of California by months through the primary precipitation season of October to April. Small-basin criteria that might depend on warm-season thunderstorms are excluded.

Upon completion of the California report a similar study was made of the Pacific Coast drainages of Oregon and Washington and of the Columbia Basin. This culminated in a report, "Probable Maximum Precipitation - Northwest States," Hydrometeorological Report No. 43, published in 1966. While the methods and approach were basically the same as in the California study there were numerous refinements. Not long after the completion of this work a review of the California criteria was initiated, making use of new experience in techniques gained in the Northwest study, and also new storm data. There were important storms in Southern California in 1962 and 1965, on the North Coast in 1960, 1964, and 1966 and in the Northern Sierras in 1962, 1963, and 1964, all subsequent to the original work on Hydrometeorological Report No. 36. The use of the word "interim" in the title of the report indicates the realization by the Weather Bureau authors of the report and their sponsors, the Corps of Engineers, that revisions might ultimately be expected. This note provides the revisions for calculating PMP in California that are now recommended.

Revised orographic index map (Fig. 5-35)

In the method of Hydrometeorological Reports Nos. 36 and 43, the orographic part of PMP, due to mountain effects, and the convergence part, due to storm processes not directly related to the mountains, are calculated separately, then added together. An index map provides the 6-hour orographic part of the PMP in January for small basin sizes. Nomograms and tables provide adjustments for other durations, basin sizes, and months.

A modified orographic index map, figure 5-35 revised, is provided here and is to be used in substitution of figure 5-35 of the original report. This is based on numerous tests with a more refined orographic flow model than in the original report, using both old and new storm data. Values are lowered by 26 percent in the Sierra Nevada (partly compensated by larger durational factors - see below), remain about the same in the Coast Range except for modest increases in the vicinity of Eureka, and some adjustments downward near San Francisco. A transition zone to lower values is provided on the lee side of the Coast Range.

Revised durational factors for orographic PMP

The same durational variation of orographic PMP is used throughout
the study area in Hydrometeorological Report No. 36, table 5-5. There
is now enough information available to take into account the tendency for
storms to be more intense at longer durations in the north. A new table
of durational factors (percentage of first 6 hours of PMP) has been
developed in which latitude is an argument. The values blend into
Hydrometeorological Report No. 43 values at the California-Oregon border.
The new table is table 5-6 of this note.

Seasonal variation

No change is made in the percentage seasonal variation of orographic
PMP. However the seasonal variation is now presented separately, table 5-7
of this note, instead of being amalgamated with the durational variation
(table 5-5 of Hydrometeorological Report No. 36).

Revised steps in determining orographic PMP

The steps in determining orographic PMP in section 9.02 on page 117
of the original report are revised as follows:

1. Determine average probable maximum precipitation index within basin
outline from figure 5-35, revised. (A grid average is adequate.)

2. Determine the basin representative width perpendicular to the optimum
inflow direction. This is measured perpendicular to the sides of the
appropriate orographic PMP computation area shown on figure 5-30. (Narrow
extensions of the basin perpendicular to the inflow would not be con-
sidered in determining the basin representative width.)

3. Determine basin-width adjustment factor from figure 5-39.

4. Multiply the basin-average probable maximum orographic precipitation
index from step 1, by the basin-width adjustment factor. This will give
the January 6-hour maximum orographic PMP.

5. To obtain the seasonal variation of the maximum or first 6-hour oro-
graphic PMP, use the monthly percentages given in table 5-7. If the basin
is in the Sierra Range east of a line through the middle of the Central
Valley, multiply the width-adjusted basin-average probable maximum oro-
graphic precipitation index from step 4 by the Sierra Range percentages.
For a basin in any other area, use the Coastal Range percentages.

6. To obtain 6-hour orographic PMP amounts adjusted for latitude, for the
first 12 6-hour periods, multiply the result from step 5 by the percentages
shown in table 5-6 corresponding to the mean latitude of the basin. Use
the upper part of the table for incremental values and the lower part for
cumulative amounts.

October 1969

7. For small basins, the 1- and 3-hour duration orographic PMP values are 20 and 54 percent respectively (see section 5.50) of the 1st (maximum) 6-hour orographic PMP.

Other criteria

No changes are made in convergence PMP criteria or in snowmelt winds and temperatures. The steps in the examples of chapter IX of the original report may be followed, using the modifications presented here.

Table 5-6

DURATIONAL VARIATION OF OROGRAPHIC PMP

6-hr. period

		1	2	3	4	5	6	7	8	9	10	11	12
		Incremental by 6-hr. period (percent of first 6-hr. period)											
Lat. (°N.)	42	100	89	80	71	63	56	50	44	39	34	30	26
	39	100	87	78	69	61	54	48	42	37	33	29	25
	38	100	86	76	66	58	51	45	39	34	30	26	23
	37	100	85	74	63	54	47	41	36	31	27	23	20
	36	100	83	70	59	50	43	37	32	28	24	21	18
	35	100	80	66	55	46	39	33	28	24	21	18	15
	34	100	77	61	50	42	35	30	25	21	18	15	13
	33	100	74	58	47	39	32	27	22	18	15	13	12
	32	100	72	56	45	36	29	24	20	16	13	11	10
		Cumulative by 6-hr. period (percent of first 6-hr. period)											
Lat. (°N.)	42	100	189	269	340	403	459	509	553	592	626	656	682
	39	100	187	265	334	395	449	497	539	576	609	638	663
	38	100	186	262	328	386	437	482	521	555	585	611	634
	37	100	185	259	322	376	423	464	500	531	558	581	601
	36	100	183	253	312	362	405	442	474	502	526	547	565
	35	100	180	246	301	347	386	419	447	471	492	510	525
	34	100	177	238	288	330	365	395	420	441	459	474	487
	33	100	174	232	279	318	350	377	399	417	432	445	457
	32	100	172	228	273	309	338	362	382	398	411	422	432

Table 5-7

SEASONAL VARIATION OF OROGRAPHIC PMP

(In percent of basin-average orographic PMP index)

	Oct.	Nov.	Dec.	Jan.-Feb.	Mar.	Apr.
Coastal Range	92	94	98	100	95	87
Sierra Range	97	98	99	100	96	90

The Sierra percentages are to be used for any basin to the east of a line through the middle of the Central Valley between Redding and Bakersfield. Coastal percentages apply to the remaining areas of interest in California.
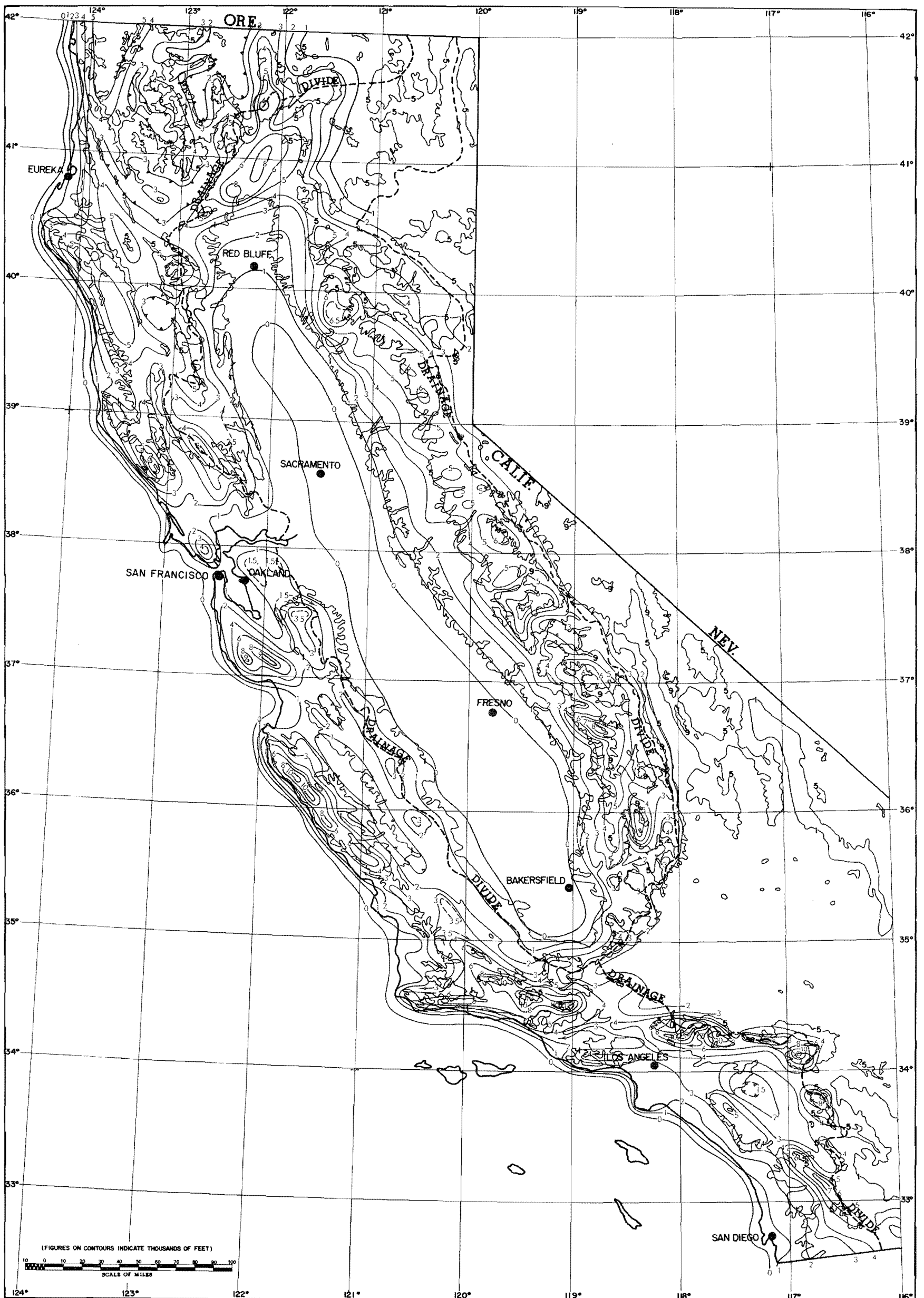
FIG. 5-35 REV. OROGRAPHIC PMP INDEX. 6-HR JANUARY (inches)